Developing Bioactive Composite Scaffolds for Bone Tissue Engineering

by

Chen Yun

A Thesis Submitted for the Degree of
Doctor of Philosophy
in Biomedical Engineering

Department of Health Technology and Informatics
The Hong Kong Polytechnic University

Oct 2006

CERTIFICATE OF ORIGINALITY

I Hereby declare that this thesis is my own work and that, to the best of my knowledge and belief, it reproduces no material previously published or written, nor material that has been accepted for the award of any other degree or diploma, except where due acknowledgment has been made in the text.

_____ (Signed)

Chen Yun (Name of student)

Abstract of Thesis entitled

Developing Bioactive Composite Scaffolds for Bone Tissue engineering

submitted by

Chen Yun

for the degree of Doctor of Philosophy

at The Hong Kong Polytechnic University

in Oct 2006

Poly(L-lactic acid) (PLLA) films were fabricated using the method of dissolving and evaporation. PLLA scaffold was prepared by solid-liquid phase separation of polymer solutions and subsequent sublimation of solvent.

Bonelike apatite coating was formed on PLLA films, PLLA scaffolds and poly(glycolic acid) (PGA) scaffolds in 24 hours through an accelerated biomimetic process. The ion concentrations in the simulated body fluid (SBF) were nearly 5 times of those in human blood plasma. The apatite formed was characterized using scanning electron microscopy (SEM), energy dispersive X-ray spectroscopy (EDX), X-ray diffraction (XRD), and Fourier transform infrared spectroscopy (FTIR). The apatite formed in 5SBF was similar in morphology and composition to that formed in the classical biomimetic process employing SBF or 1.5SBF, and similar to that of natural bone. This indicated that the biomimetic apatite coating process could be accelerated by using concentrated simulated body fluid at 37^{o}C. Besides saving time, the accelerated biomimetic process is particularly significant to biodegradable polymers.

Some polymers which degrade too fast to be coated with apatite by a classical biomimetic process, for example PGA, could be coated with bone-like apatite in an accelerated biomimetic process.

Collagen and apatite were co-precipitated as a composite coating on poly(L-lactic acid) (PLLA) in an accelerated biomimetic process. The incubation solution contained collagen (1g/L) and simulated body fluid (SBF) with 5 times inorganic ionic concentrations as human blood plasma. The coating formed on PLLA films and scaffolds after 24 hours incubation was characterized using EDX, XRD, FTIR, and SEM. It was shown that the coating contained carbonated bone-like apatite and collagen, the primary constituents of natural bone. SEM showed a complex composite coating of submicron bone-like apatite particulates combined with collagen fibrils. This work provided an efficient process to obtain bone-like apatite/collagen composite coating.

Saos-2 osteoblast-like cells were used to evaluate the cellular behaviors on these biomimetic coatings. Cell morphologies on the surfaces of PLLA films and scaffolds, PLLA films and scaffolds with apatite coating, and PLLA films and scaffolds with apatite/collagen composite coating were studied by SEM. Cell viability was assessed by the 3-(4,5-dimethylthiazol-2-yl)-2,5-diphenyltetrasodium bromide (MTT) assay. In addition, differentiated cell function was assessed by measuring alkaline phosphatase activity. These results suggested that the apatite coating and apatite/collagen composite coating fabricated through the accelerated biomimetic processes could improve the interactions between osteoblasts and PLLA. The composite coating was more effective than apatite coating in improving such interactions. PLLA scaffolds coated with submicron collagen fibrils and submicron

apatite paticulates are expected to be one of the promising 3D substrates for bone tissue engineering.

To facilitate coating into scaffolds, the flowing condition was introduced into the accelerated biomimetic process. The apatite formed in the different sites in the scaffold was characterized using SEM. It was found that the accelerated biomimetic process performed in the flowing condition yielded more uniform spatial distribution of apatite particles than that in the regular shaking condition. This work provides a novel condition for obtaining uniform spatial distribution of bone-like apatite within the scaffolds in a timely manner, which is expected to facilitate uniform distribution of attached cells within the scaffolds *in vitro* or *in vivo*.

Referred journal articles:

Chen Y, Mak AFT, Li J, Wang M, Shum A. Formation of apatite on poly(α-hydroxy acid) in an accelerated biomimetic process. J Biomed Mater Res (Part B). 2005; 73B(1) : 68-76.

Chen Y, Mak AFT, Wang M, Li J. Composite Coating of Bone-like Apatite Particles and Collagen Fibers on Poly L-lactic Acid Formed through an Accelerated Biomimetic Coprecipitation Process. J Biomed Mater Res (Part B). 2006; 77B(2) : 315-322

Chen Y, Mak AFT, Wang M, Li J, and Wong MS. PLLA scaffolds with biomimetic apatite coating and biomimetic apatite/collagen composite coating to enhance osteoblast-like cells attachment and activity. Surface and Coatings Technology. 2006; 201(3-4): 575-580

Li J, Beaussart A, Chen Y, Mak AFT. Transfer of apatite coating from porogens to scaffolds: Uniform apatite coating within porous poly(DL-lactic-co-glycolic acid) scaffold in vitro. J Biomed Mater Res (Part A). Accepted. 2005.

Conference presentation:

Chen Y, Mak AFT, Wang M. Formation of Apatite on Poly(α-hydroxy acid) in an Accelerated Biomimetic Process. Biomedical Engineering Conference (BME) Sep 23-25 2004. Hong Kong, China.

Chen Y, Mak AFT, Wang M, Li J. Biomimetic coating of apatite/collagen composite on Poly L-lactic Acid facilitates cell seeding. 27th Annual International Conference of the IEEE Engineering In Medicine and Biology Society (EMBS). Sep 1-4 2005. Shanghai, China.

Acknowledgements

I would like to express my deepest appreciation to my supervisor, Prof. Arthur Mak, for his inspiration, guidance and support. His foresight and encouragement have given me a very rewarding and lasting experience in the whole period of the research work at The Hong Kong Polytechnic University.

I would also like to acknowledge my co-supervisor, Dr. Min Wang in Hong Kong University, for his stimulating comments and valuable suggestions in research. I also wish to express my gratitude to Dr. Jiashen Li for his assistance in the experiments and discussion of my research study.

I would like to thank Dr. M. S. Wong in the Department of Applied Biology & Chemical Technology for teaching me the basic techniques of cell seeding. I also wish to express my appreciation for the help provided by all my colleagues. The assistance provided by Mr. M. N. Yeung at the Materials Research Center in conducting materials analyses is highly appreciated.

The financial support provided by the Research Committee of the Hong Kong Polytechnic University is gratefully acknowledged.

A very special appreciation is due to my wife Laura and my parents not only for their constant support and encouragement but also for their patience and understanding throughout. This thesis is dedicated to my family.

Table of Contents

Acronyms

5SBF	5 times simulated body fluid
5SBFC	5SBF with collagen
ALP	Alkaline phosphatase
DMEM	Dulbecco’s modified Eagle’s medium
EDX	Energy dispersive X-ray spectroscopy
FBS	Fetal bovine serum
FTIR	Fourier transform infrared spectroscopy
PGA	Poly(glycolic acid)
PLLA	Poly(L-lactic acid)
SBF	Simulated body fluid
SEM	Scanning electron microscopy
XRD	X-ray diffraction

List of Tables

List of Figures

CHAPTER 1

Introduction

1.1 Motivation and Objectives of Research

The need of new bone to replace or restore the function of lost or damaged bone is a major clinical and socioeconomical demand. Bone tissue loss as a result of injury or disease compromises mobility, function and quality of life of those affected (Chapekar, 2000).

Traditional therapies for bone defects include autografts, allografts, and xenografts. However, all of these methods have specific problems and limitations. Bone tissue engineering provides alternative solutions for bone regeneration.

Bone tissue engineering involves the use of three-dimensional porous scaffolds implanted at the sites of tissue defects. The scaffold serves as a transitional template for bone regeneration. It is difficult for a single biomaterial to satisfy all the specified requirements as a scaffold for bone tissue engineering. Poly(α-hydroxy acids), including poly(lactic acid)(PLA), poly(glycolic acid) (PGA), and poly(D,L-lactic acid-co-glycolic acid) (PLGA), with the approval of US Food and Drug Administrations (FDA) for specific human clinical uses, have long drawn much interest. They have been fabricated into scaffolds for tissue engineering purposes (Mikos *et al.*, 1994; Ma and Langer, 1998; Karp *et al.*, 2003).

The objective of this research is to develop three-dimensional and highly porous bioactive, biodegradable composite scaffolds with suitable surface for bone cell attachment, proliferation, and differentiation. In this research, we chose to work with the FDA approved poly(α-hydroxy acids) as the scaffold material. As poly(α-hydroxy acid)-based matrices are known to have poor cell-material interactions because of their hydrophobic nature and lack of cell recognition signals, the focus of this research is to modify the surface properties of such biomaterials to improve their capacity for cell attachment, proliferation, and differentiation.

1.2 Scope and Outline of Thesis

This research work consists of three main parts, namely:

- Fabrication of PLLA films and scaffolds.
- Surface modification of PLLA films and scaffolds.
- Cell seeding on PLLA films and scaffolds to evaluate the efficiency of surface modification.

The second part, surface modification of PLLA films and scaffolds, is composed of three sections, namely:

- Biomimetic apatite coating using an accelerated biomimetic process.
- Biomimetic apatite coating formed in the flowing condition.
- Biomimetic apatite/collagen composite coating.

The thesis is divided into six chapters. Chapter 1 provides an overview of the thesis, particularly its objectives and scope. Chapter 2 provides the background information related to this research study. Literatures related to bone tissue

engineering in general, candidate materials for bone tissue engineering, fabrication techniques of polymer-based scaffolds, surface modification of biomaterials, etc were reviewed.

Chapter 3 describes the fabrication procedures of PLLA films and scaffolds, the accelerated biomimetic processes to form apatite in the regular shaking and flowing condition, the procedures of the formation of apatite/collagen composite coating, the procedures of cell seeding on PLLA films and scaffolds with and without coating. Chapter 3 also presents the characterization methods for the coatings and cellular behaviors.

Chapter 4 presents the results of the characterizations of the coatings and cell seeding, including the microstructure and composition of the coatings, the spatial distribution of the coatings, and cell morphology, proliferation and viability, and so on.

Chapter 5 discusses the results of the coatings formed and cell seeding in the context of existing literatures. It also reflects on the limitations of the current study and their implications.

Chapter 6 summarizes the important findings of the current study, along with recommendations for future works.

1.3 Original Contributions

The original contributions reported in this present research work are:

(1) The accelerated biomimetic process has been reported earlier to be successful on metal substrate (Barrere *et al.,* 2002a&b; Chou *et al.,* 2004). We applied this process on polymeric substrate. Because of the shortened immersion time in the simulated body fluid, PGA scaffolds were successfully coated with the biomimetic apatite, which is impossible to be obtained in the traditional biomimetic process due to the fast degradation rate of PGA.

(2) With the use of a perfusion bioreactor, the flowing condition was introduced into the biomimetic process to achieve an apatite coating with a more uniform spatial distribution inside a scaffold.

(3) Collagen was incorporated into the accelerated biomimetic process and a novel complex coating composed of submicron bone-like apatite particulates and collagen fibrils was obtained. Results suggested that not only collagen but other organic components also, such as, RGD, growth factors, etc., may be included in the biomimetic process to form a complex inorganic/organic composite with potential benefits for bone tissue engineering.

CHAPTER 2

LITERATURE REVIEW

2.1 Bone and bone replacement and regeneration

2.1.1 Bone structure

In the microscopic level, bone could be classified into woven bone and lamellar bone. The collagen fibres in woven bone are interlaced and randomly dispersed with hydroxyapatite crystals deposited in a disorderly manner. In lamellar bone, hydroxyapatite crystals are deposited parallel to the collagen fibers.

Based on shape, bone can be divided into different groups (Sikavitsas *et al,* 2001; Baron, 1993): long bones (femur and tibia), short bones (wrist and ankle), and flat bones (skull vault and irregular bones). Based on the architectural forms, bone could be grouped into two kinds (Sikavitsas *et al,* 2001; Hill and Orth, 1998 ; Baron, 1993): trabecular (also called cancelous or spongy bone) and cortical (also called compact bone). The comparison of trabecular bone and cortical bone is in Table 2.1

Because of the higher porosity of trabecular bone, the modulus and ultimate compressive strength of trabecular bone is around 20 times lower than that of cortical bone (Sikavitsas *et al,* 2001; Temenoff *et al.,* 1999).

Table 2.1 Two architechtural forms of bone

Architectural form	Trabecular bone	Cortical bone
Porosity	50-90%	<30%
Architecture	Network of connecting plates and rods	Solid with voids
Mass	20% of the total skeleton	80% of the total skeleton

Trabecular bone is typically found in the ends of long bones covered with a thin protective layer of cortical bone, and in flat bones between two layers of cortical bone (Shipman *et al.,* 1985). The macrostructure and microstructure of a long bone is shown in Figure 2.1. The bone apatite reinforced collagen form individual lamella at the nm to mm scale. Lamella is deposited concentrically around blood vessels to form haversian systems. Trabecular bone consists primarily of lamellar bone, arranged in packets that make up an interconnected irregular array of plates and rods, called trabeculae. The space between trabeculae is filled with bone marrow.

2.1.2 Bone composition

The main organic component of bone is collagen. And most of the collagen is Type I (Black and Hastings, 1998). Collagen's basic components are amino acids, linked together into peptides. The main inorganic component of bone is biological apatites, usually with low Ca/P ratios and containing substantial amounts of other ions such as CO_3^{2-}, Mg^{+}, and Na^{+} (Hench and Wilson, 1993).

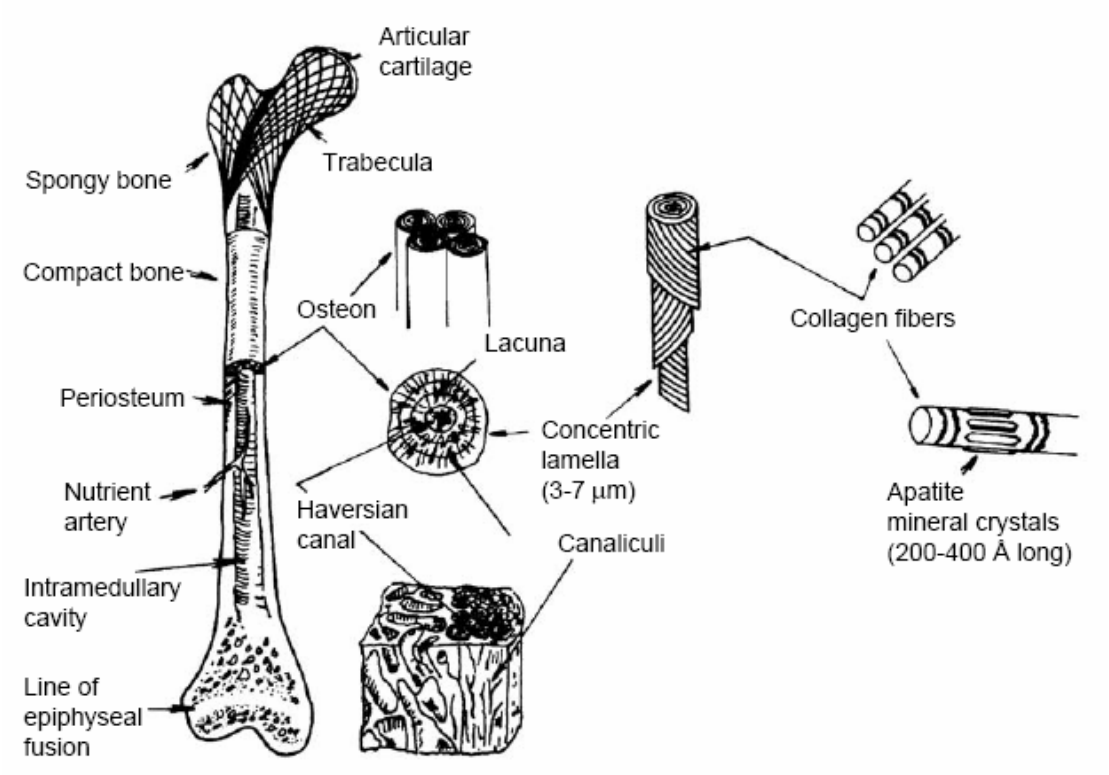

Figure 2.1 *Structural organization of a human long bone (Park and Lakes, 1992)*

2.1.3 Current approaches for bone replacement and regeneration

Traditional reconstruction for bone defects are mostly based on autologous bone grafts, autogenous bone grafts, or alternatively metals and ceramics (Yaszemski *et al.*, 1994; Spitzer *et al.*, 2002; Simon *et al.*, 2002; Rose *et al.*, 2002; Petite *et al.*, 2000) .

Autologous bone graft refers to bone taken from another part of the patient's own body. Autologous bone provides osteogenic cells as well as essential osteoinductive factors needed for bone healing and regeneration (Rose *et al.*, 2002; Asahina *et al.*, 1999). It presents relatively better chance of success. However, the fact that only limited amount of autograft tissues are available restricts the application of

autologous bone graft (Yaszemski *et al.,* 1994; Spitzer *et al.,* 2002; Simon *et al.,* 2002; Rose *et al.,* 2002; Petite *et al.,* 2000).

Allograft refers to tissues taken from somebody else's body. Allograft bone may introduce the risks of immunological rejection and of pathogen transmission from donor to host (Yaszemski *et al.,* 1994; Spitzer *et al.,* 2002; Simon *et al.,* 2002; Rose *et al.,* 2002; Petite *et al.,* 2000; Williams, 1999). The rate of host incorporation of allograft usually is lower than that of autograft.

Biomaterials, such as metals and ceramics, could be alternatives to bone grafts (Yaszemski *et al.,* 1994). Metals could provide immediate mechanical support at the site of the defect. However, metals exhibit poor overall integration with the host tissue, and may fail because of infection or fatigue loading (Yaszemski *et al.,* 1994). Ceramics also have disadvantages. Ceramics are brittle and have low tensile strength. They cannot be used in locations of significant torsion, bending, or shear stress (Yaszemski *et al.,* 1994).

Bone tissue engineering provides a potential solution to regenerate bone in a reliable, economical and physiologically acceptable manner. Bone tissue engineering has emerged as an alternative to bone-grafting procedures and been developed intensively in the past decades.

2.2 Bone tissue engneering

2.2.1 Overview of tissue engineering

Tissue engineering could be considered as the science of inducing the body to regenerate or repair tissues that fail to regenerate or heal spontaneously (Agrawal and Ray, 2001). It includes the design, generation, modification and growth of living tissues using biomaterials, cells and other biochemical/biophysical factors, alone or in combination (Langer and Vacanti, 1993; Sittinger et al., 1996). The ultimate goal of tissue engineering is usually to generate grafts. Sometimes, the goal could be to yield non-implantable structures to be used as external organ support devices when a compatible donor is not readily available (Mazariegos *et al.*, 2002). These tissue constructs could be obtained by growing isolated cells on scaffolds using various *in vitro* tissue culture bioreactors.

In tissue engineering, the tissue construct could be classified into two main types, closed systems and open systems (Langer and Vacanti, 1993). The closed systems [Figure 2.2] could be implanted or used as external organ support devices.

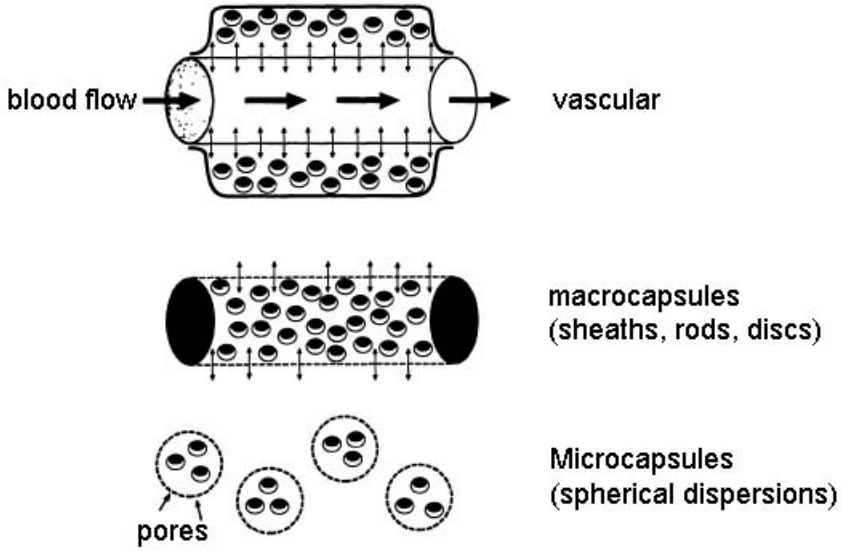

Figure 2.2 *Three common closed-system configurations for cell transplant devices (Langer and Vacanti, 1993). In vascular devices, the cells are placed in an extra-cellular compartment surrounding a tubular membrane(diameter ~1mm) through which blood can flow. In macrocapsule systems, the cells are placed in sheaths, rods, or disks (diameter 0.5 to 1mm). In microcapsule systems, the cells are place in injectable spherical beads (diameter<0.5mm).*

In open systems, scaffolds with attached cells are implanted into the body. The scaffold is three-dimensional (3D) and highly porous with an interconnected pore network. It serves as a transitional template for tissue regeneration. The typical approach is shown in Figure 2.3. A small tissue biopsy was taken from the patient. Cells were isolated from the biopsy, expanded *in vitro*, and seeded into a scaffold. This cell-scaffold construct, incorporated with signalling molecules in some strategies, was cultured in the bioreactor until a suitably developed graft was produced. Finally, the 3D culture was implanted into the patient (Temenoff and Mikos, 2000).

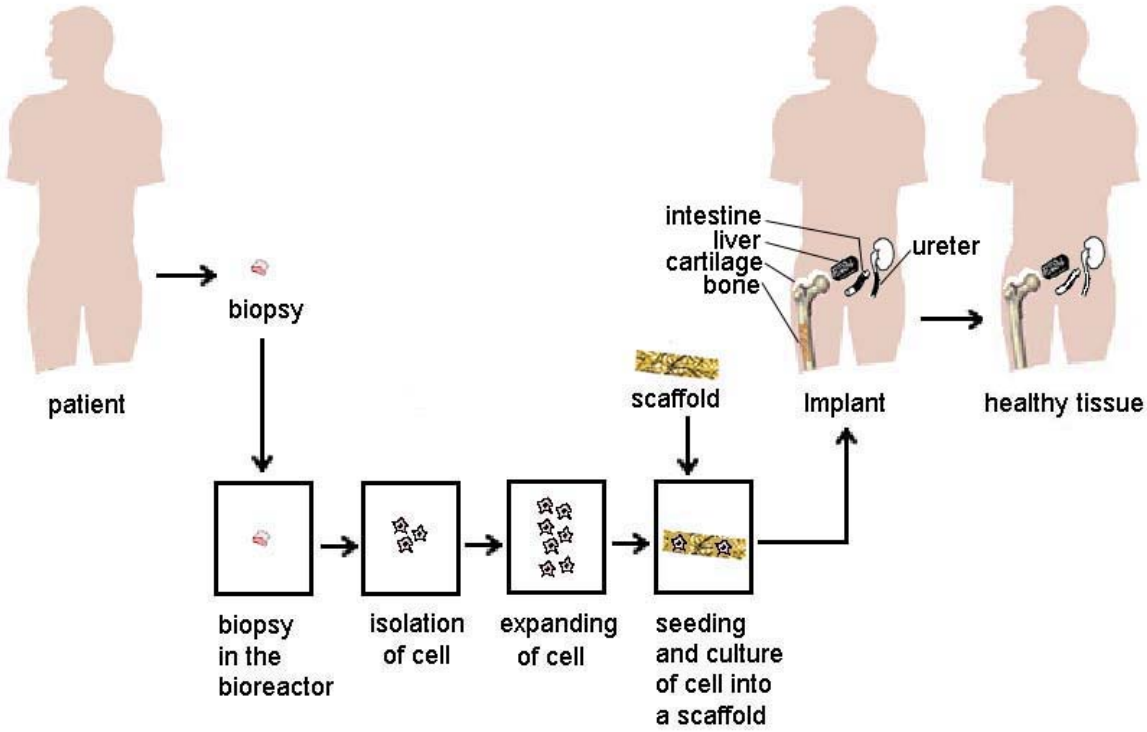

Figure 2.3 *The usual strategy for tissue engineering*

Other approaches include implanting an un-seeded polymer into the defect, the scaffold is subsequently infiltrated with cells from the surrounding tissue or cells are injected after a few days, using the body as a natural bioreactor (Cohen *et al.*, 1993).

Among the many tissues in the body, bone has the highest potential for regeneration. The accumulating knowledge in tissue engineering will lead to the design of bone with predetermined shapes for orthopaedic surgery applications. Hutmacher (2000) classified the research program for bone tissue engineering into six phases: (i) Fabrication of bioresorbable scaffold, (ii) Seeding of the osteoblasts population into the polymeric scaffold in a static culture (petri dish), (iii) Growth of premature tissue in a dynamic environment (spinner flask), (iv) Growth of mature tissue in a physiologic environment (bioreactor), (v) Surgical transplantation, (vi) Tissue-engineered transplant assimilation/remodeling.

2.2.2 Scaffolds for bone tissue engineering

In bone tissue engineering, the scaffold serves as a reservoir of water, nutrients, cytokines, growth factors. It is a transitional template for bone regeneration.

Many researchers (Hutmacher, 2000; Zhang and Ma, 1999b) gave the necessary characteristics of an ideal scaffold, in the following four categories: surface, architecture, mechanical property, and degradation property.

2.2.2.1 Surface of scaffolds

Surface should be suitable for cell attachment, proliferation, and differentiation. The surface properties can be changed by either bulk modification or surface modification. To polymer, bulk modification is usually applied before scaffold fabrication (Hubbell 1999; Cook *et al.*, 1997; Barrera *et al.*, 1993). Surface modification can be realized after a porous scaffold has been fabricated. Bulk modification usually changes the mechanical and processing properties of the polymers. Surface modification usually changes only the surface properties and was more frequently used in bone tissue engineering. This latter part is the focus of this study and will be discussed in more detail in Section 2.3.

2.2.2.2 Architecture of scaffolds

Scaffolds should be three-dimensional and highly porous with an interconnected pore network and appropriate pore size for cell migration and proper

transport of nutrients and metabolic wastes. The architectural characteristics, such as pore size and porosity, are often dependent on the fabrication method.

The appropriate range of porosity and pore size of scaffold for bone tissue engineering can be quite wide apparently. There have been a number of investigations showing that pore size ranging from 100 to 900 μm may be viable for bone tisuue engineering (Spector *et al.,* 1978; Yang S *et al.,* 2001; Maquet and Jerome, 1997; Burg *et al.,* 2000; Baksh and Davies, 2000).

Usually, big pore size will facilitate cell, tissue and blood vessels in-growth. However, big pore size usually reduces the mechanical properties. The value of porosity and pore size should be balanced with the biomechanical roles of the particular tissue to be replaced. Fisher and coworkers (2002) reported that in a rabbit cranial defect model scaffold porosity (ranging from 57% to 75%) and pore size (either 300 - 500 μm or 600 - 800 μm) did not significantly affect the result of bone formation. Another study found that pore size less than or equal to 350 μm produced the most bone ingrowth (Robinson *et al.,* 1995).

Scaffold porosity and pore size are traditionally measured by mercury porosimetry using intrusion or adsorption techniques. In such measurement, the porous volume of a scaffold under vacuum is filled with mercury. The total porous volume of the scaffold is determined by the volume of intruded mercury; Porosity (the percent of porous volume when compared to total volume) can then be calculated with knowledge of the materials mass and density. Furthermore, the intruded volume as a function of pressure can provide information on pore size. One advantage of this

mercury intrusion method is that only pores that are connected to the surface were calculated and thus pore interconnectivity could be derived.

Imaging techniques also could be used to determine scaffold porosity (Behravesh *et al.,* 2002). Micro-computed tomography (uCT) could be used to create a three dimensional image of the entire scaffold, from which not only porosity, but also other architecture information may be determined.

2.2.2.3 Mechanical property of scaffolds

Scaffolds should have a transitional structure with adequate mechanical properties to allow the transfer of an appropriate amount of biomechanical stress to the growing tissues. Furthermore, the mechanical properties of the implanted scaffold construct should ideally match those of surrounding host tissues, promote healing and the formation of bone tissue (Hutmacher, 2000; Agrawal and Ray, 2001; Leong *et al.,* 2003). For degradable polymer-based bone substitute, it should possess sufficient strength and stiffness until *in vivo* tissue ingrowth has replaced the slowly vanishing substitute.

It is obvious that too low mechanical properties are not appropriate because it could not bear the in-situ loading. Too high mechanical properties are also not suitable. According to the principle of load sharing for composites (Hull and Clyne, 1996), a stiff material implanted into bone could shield the host tissues from the normal physiological loading, and consequently bone will resorb (Park and Lakes, 1992).

It is reasonable to use natural bone as the template for making new materials for bone substitute. The mechanical properties of bone have been investigated and documented extensively (Fung, 1994). This may be a benchmark against which the mechanical performances of bone analogue materials can be evaluated.

Bone is anisotropic, non-linear, and viscoelastic. The tensile strength of cortical bone varies from 100 to 300MPa, the modulus varies from several to more than 20GPa, and the strain at failure is 1 to 2% (Cowin, 1989). Figure 2.4 illustrates a typical stress-strain behavior for cortical bone. It could be seen that the stress-strain curve is strain-rate dependent. At higher strain rates the curve shifts to the left.

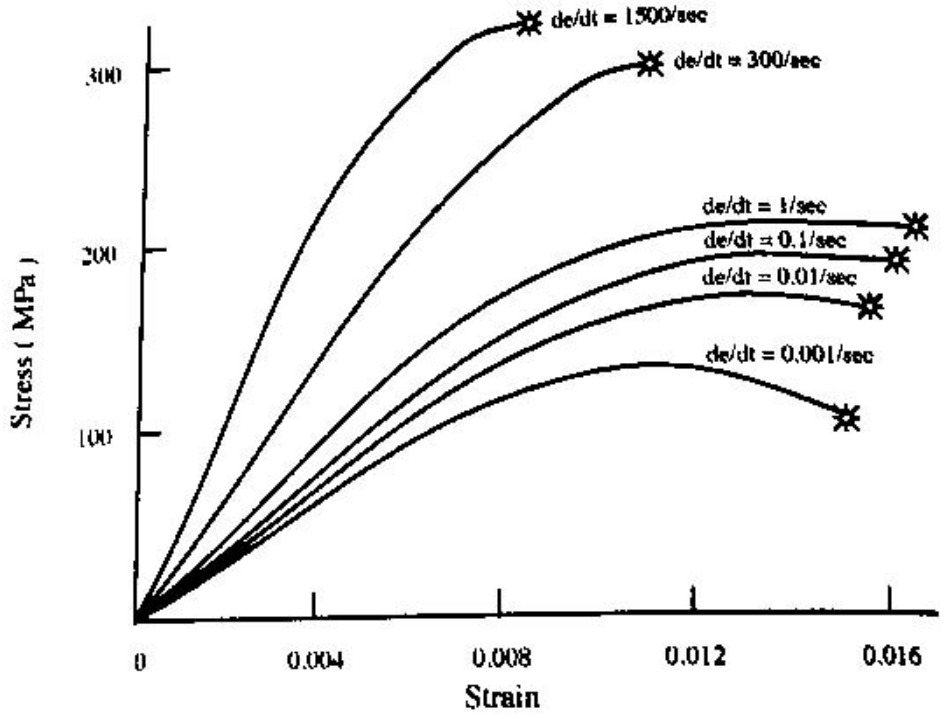

Figure 2.4 *Strain-rate dependence of stress-strain curve for bone*
Source: Ref. (Cowin, 1989)

The strength and stiffness of spongy bone is much lower than that of cortical bone. The exact mechanical properties of cancellous bone depend on its density and

porosity. Typically, the modulus of human trabecular bone is in the range of 0.01 to 2GPa. Tensile strength varies from 0.1 to 30Mpa (Black and Hastings, 1998).

Most polymeric scaffolds for bone tissue engineering exhibits poor mechanical properties. This results from their porous architecture. Even when a bulk material may possess significant mechanical properties, these properties are often lost when the material is formed into a porous scaffold. How to enhance the mechanical properties of polymer-based scaffolds is an important challenge in bone tissue engineering.

2.2.2.4 Biocompatibility and degradability of scaffolds

Scaffolds should be biocompatible, which means that scaffolds could be integrated in the host tissue without eliciting an immune response. Furthermore, scaffolds should be bioresorbable with a controllable degradation rate to match the rate of bone regeneration, with degradation products being nontoxic and easily excretable.

The biocompatibility of a scaffold is largely determined by the material. If the material is novel, initial work should involve cytotoxicity studies. Furthermore, the process of scaffold fabrication is also a concern. It should involve as few species as possible in the fabrication of a scaffold without the use of chemical reactions to reduce the likelihood of toxicity problems.

Scaffold degradation could be studied either *in vitro* or *in vivo*. For hydrolytically degrading polymers, *in vitro* studies are typically conducted with the

scaffold immersed in phosphate buffered saline (pH 7.4) at 37°C. For enzymatically degrading polymers, the functional enzyme would be added to the saline. Most degrading polymers are polyesters and the reaction of water with the ester bonds is catalyzed by acidic conditions. Thus the acidic degradation products may catalyze the degradation of the scaffold. Thus the buffer solution is usually changed hourly in the beginning and less frequently (daily to weekly) later to make sure that the system does not significantly deviate from neutrality. Results from *in vitro* studies could provide a baseline to infer the *in vivo* properties. For *in vivo* study, scaffolds are implanted into a suitable animal model and then retrieved at predetermined time points.

2.2.3 Candidate materials for scaffolds in bone tissue engineering

Polymers and inorganic materials are the primary materials for scaffolds in bone tissue engineering research. The first requirement of materials used in bone tissue engineering is that they can form robust porous structures to serve as 3D scaffolds and generally do not dissolve in aqueous conditions. Other requirements such as biodegradability, biocompatibility, surface properties, and mechanical properties are also important.

2.2.3.1 Naturally derived degradable polymer

Natural polymers, such as polysaccharides and proteins, have been used for bone tissue engineering.

I. Collagen

Collagen is a fibrous protein and one of the two primary components of extracellular bone matrix, so has biological properties suitable for tissue engineering applications. On the other hand, collagen has some disadvantages for bone tissue engineering application, such as poor mechanical properties and less controllable biodegradability. Rocha and coworkers (2002) obtained anionic collagen scaffolds by means of an alkaline treatment. The histological results of implantation into surgically created bone defects in rat tibias showed a low inflammatory response and bone formation within a short period of time.

Collagen-glycosaminoglycan (collagen-GAG) copolymers (Mueller et al., 1999) and denatured collagen (gelatin) (Choi *et al.*, 1999) were also fabricated into scaffolds for tissue engineering. Mueller and coworkers (1999) seeded calf meniscus cells in type I and type II collagen–glycosaminoglycan (GAG) copolymers. The type II matrix demonstrated higher GAG synthesis and resistance to cell-mediated contracture, compared with the type I matrix.

II. Polysaccharides

Polysaccharides, for example, alginate, chitosan, and hyaluronate, are another class of natural polymers used in tissue engineering. Shapiro and Cohen (1997) prepared a three-dimensional, porous sponge made from the marine polysaccharide alginate with the pore size of 70-300um. They seeded fibroblasts within the scaffold and found that the alginate scaffold seemed to be able to provide an excellent support for cell transplantation. Chitosan is a partially deacetylated derivative of chitin.

Madihally and Matthew (1999) fabricated chitosan porous scaffolds using freezing and lyophilization of chitosan solutions and gels. Mean pore diameters could be controlled within the range 1-250um, by varying the freezing conditions. A hyaluronan-based scaffolds were implanted into 4-month-old rabbits and appeared to be able to invoke some natural responses and to facilitate integration with the adjacent host tissue (Solchaga *et al.,* 2002).

2.2.3.2 Synthetic degradable polymer

It has been lasting for several decades to search for an ideal biocompatible biodegradable synthetic polymer (Schneider, 1955; Lowe, 1954). Some of those degradable polymers that have been investigated are based on an ester polymer backbone, such as poly(L-lactic acid) (PLA), poly(glycolic acid) (PGA), poly(D,L-lactic acid-co-glycolic acid) (PLGA), poly(3-hydroxybutyrate) (PHB), poly (propylene fumarate), and poly(caprolactone). Water reacts with polyesters to break, or degrade, the polymers.

Other degradable polymers, such as polyanhydrides and polycarbonates, have been also studied for use in bone tissue engineering applications. These polymers have been shown to be biocompatible and nonimmunogenic.

I. Poly(a-hydroxyacids)

With the approval of US Food and Drug Administrations (FDA) for specific human clinical uses, Poly(lactic acid) (PLA), poly(glycolic acid) (PGA), and their copolymers poly(lactic acid-co-glycolic acid) (PLGA) have drawn much interest as candidate for tissue engineering scaffolds.

These polymers satisfy many of the material requirements for bone tissue engineering and already have been fabricated into scaffolds for tissue engineering (Mikos *et al.*, 1994; Ikada *et al.*, 1996; Shinoka *et al.*, 1996; Ma and Langer, 1998; Andriano *et al.*, 1999; Thomson *et al.*, 1999; Zhang and Ma, 1999b; Ma *et al.*, 2001; Partridge *et al.*, 2002; Yang Y *et al.*, 2002; Chen *et al.*, 2003; Karp *et al.*, 2003; Karp *et al.*, 2003). They are biocompatible and non-toxic polymers and can be easily processed into various shapes. They possess predictable resorption rates and controllable mechanical properties. Their degradation periods can also be manipulated by controlling the crystallinity, molecular weight, etc. of the polymers. However, they also have disadvantages. The main disadvantage is that synthetic poly(α-hydroxy acids) have poor cell–material interactions because of their hydrophobic nature and lack of cell recognition signals.

PLA is more hydrophobic than PGA because PLA have the extra methyl group. The hydrophobic properties of PLLA also lead to a slower hydrolysis or degradation rate. It usually takes several months or even years for PLA scaffolds to lose their mechanical integrity *in vitro* or *in vivo* (Yuan *et al.*, 2002). Compared with PLA, PGA is more hydrophilic and degrades rapidly in aqueous condition. It could lose its mechanical integrity in several weeks (Shum and Mak, 2003). The degradation rates of PLGA are somewhere between that of PLA and PGA and could be tailored using various lactic to glycolic acid ratios.

Because poly(L-lactic acid) (PLLA) has the advantages demonstrated above and has been approved by FDA for specific human clinical uses, in this research

PLLA was chosen as the substrate material. A major focus of this research is to modify the surface of poly(α-hydroxy acids) to improve the capacity for cell attachment, proliferation, differentiation, and tissue matrix synthesis.

II. Poly(3-hydroxybutyrate) (PHB)

Poly(hydroxyalkonate)s (PHA) are biodegradable, biocompatible thermoplastic polyesters produced by various microorganisms such as *Bacillus megaterium*, soil bacteria, estuarine microflora, blue-green algae, and also by genetically modified plants (Williams *et al.*, 1999; Pouton and Akhtar, 1996). Among PHA, the poly(3-hydroxybutyrate) (PHB) is the most extensively studied one and can be produced in high yield. PHB degrades *in vivo* to D-3-hydroxybutyrate, a normal constituent of human blood, thus it has low toxicity (Reusch *et al.*, 1995).

The general structure for PHBV is given below:

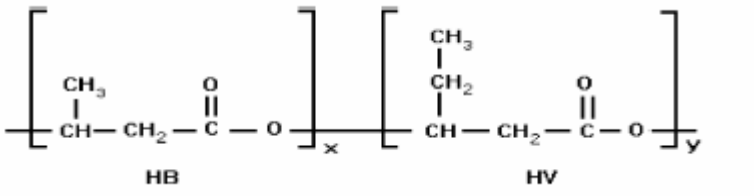

Degradation rate of PHBV can be adjusted by changing the copolymer composition (Juni and Nakano, 1987). The more crystalline PHBV have a lower degradation rate in aqueous media. PHB and PHBV matrices lose their mass slower than poly(lactide-co-glycolide) systems (El-Hadi *et al.*, 2002).

Rivard et al. (Rivard *et al.*, 1996) reported that PHBV (9%) sustained a fibroblast proliferation rate similar to that observed in collagen scaffolds for at least 35 days. Moreover, the total protein production in the PHBV scaffold after 4 weeks

was found to be twice as high as in the collagen scaffold. PHB and PHBV could be suitable substrate for cell culture in bone tissue engineering.

III. Polyanhydride

Polyanhydrides are highly sensitive to hydrolysis and degrade rapidly by surface erosion. Polyanhydrides such as poly(methacrylated sebacic anhydride) and poly(methacrylated 1,6-bis(carboxyphenoxy) hexane) have been shown to be well suited for bone tissue engineering applications (Burkersroda *et al.,* 2002; Katti *et al.,* 2002; Muggli *et al.,* 1999).

Ibim and coworkers (1998a&b) demonstrated that poly(anhydride-co-imide) polymers could support endosteal and cortical bone regeneration. Their study suggested that poly(anhydride-co-imides) are promising polymers that may be suitable for use as implants in bone surgery, especially in weight-bearing areas because of good mechanical properties and tissue compatibility.

IV. Polycarbonate

Polycarbonates, and especially tyrosine derived polycarbonates, have been extensively studied for bone tissue engineering applications (Choueka *et al.,* 1996; Tangpasuthadol *et al.,* 2000a&b).

Poly(BPA-carbonate) is a commercially available polycarbonate. This polycarbonate is processable, mechanically strong, and nondegradable (Goodman and Rhys, 1965). The carbonyl oxygen of poly(BPA-carbonate) could be replaced by the imino group (Kohn and Langer, 1986). This modification could increase the

hydrolytic ability of poly(BPA-carbonate) without compromising its strength.

To lessen the possibility of potential toxicity, tyrosine-derived iminocarbonateamide copolymers were produced (Li and Kohn, 1989; Pulapura *et al.*, 1990). Their mechanical strength was similar to poly(BPA-carbonates). Meanwhile, they possess the biocompatibility of amino acids. Choueka and coworkers (1996) found that from a degradation-biocompatibility perspective, the tyrosine-derived polycarbonates appear to be comparable to PLA in a canine bone chamber model.

V. Poly(propylene fumarate) (PPF)

Poly(propylene fumarate) (PPF) has also been investigated for tissue engineering (Behravesh *et al.,* 1999; Fisher *et al.,* 2002 ; Shin *et al.,* 2002; Cooke *et al.,* 2003). PPF is an unsaturated polyester consisting of alternating propylene glycol and fumaric acids. Its main degradation products are fumaric acid and propylene glycol. Peter and coworkers (1997) studied PPF for use in filling skeletal defects and reported its mechanical properties to be similar to that of trabecular bone.

2.2.3.3 Bioactive ceramics

Besides the various polymeric materials, certain inorganic ceramics have also been used for bone tissue engineering research. Bioceramics could be classified as “calcium phosphate ceramics” or “bioactive glasses” with the difference in chemical composition, specific surface area, crystal structure, porosity, etc. (Ducheyne *et al.,* 1994; Hench, 1993). Bioceramics exhibit biocompatible and bioactive behavior and have often been used as coatings on metals for orthopedic/dental implants. In host bone tissue, they could physiochemically bond to bone and promote new bone

formation (Ducheyne *et al.,* 1994; Hench, 1993).

I. Calcium phosphates (HA and TCP)

The most widely studied calcium phosphate ceramics in bone tissue engineering are β-tricalcium phosphate (β-TCP, $Ca_3(PO_4)_2$), hydroxyapatite (HA) ($Ca_{10}(PO_4)_6(OH)_2$), its derivatives, and their combinations (Hollinger and Battistone, 1986; Friedman *et al.,* 1998; Boo *et al.,* 2002; Kruyt *et al.,* 2003; Li S *et al.,* 2003). Macroporous calcium phosphates have achieved considerable success as cancellous bone graft substitutes (Tancred *et al.,* 1998).

The mineral part of bone is made of a crystalline form of calcium phosphate similar to HA. These calcium phosphates are biocompatible and have the advantages of minimal immunologic reactions, foreign body reactions, and systemic toxicity (Hollinger and Battistone, 1986; Hammerle *et al.,* 1997). Furthermore, they possess osteoconductive capacity (Akao *et al.,* 1993; Puleo *et al.,* 1991) as their surface properties support the adhesion, growth, and differentiation of osteoblastic cells, and osteoinductive capacity as they could bind bone morphogenetic proteins (BMPs) *in vivo* (LeGeros, 2002). These calcium phosphates also possess a remarkable ability to bind directly to bone (Hollinger and Battistone, 1986; Hammerle *et al.,* 1997).

Young's modulus values of bulk HA are 80-120GPa. Bending strength and compressive strength are in the range of 103 ～ 113MPa and 462 ～ 509MPa, respectively (Hench and Wilson, 1993). HA has relatively poor mechanical toughness (Suchanek and Yoshimura, 1998).

II. Bioactive glass (BG)

Bioactive glasses and glass-ceramics have been used to repair or replace parts of some long bones (Teófilo *et al.*, 2004). They could form a stable, mechanically strong interface with bone. Bioglass® is a family of bioactive glasses that contain SiO_2, Na_2O, CaO and P_2O_5 in specific proportions. The bending strength of most bioglass® is in the range of 40-60Mpa. A-W glass-ceramic(AW-GC) is made from the parent glass by heat treatment to get superior mechanical properties.

The limitation of ceramic on clinical application is their inappropriate mechanical properties, such as high Young's modulus and low toughness. Coating of bioactive ceramic on organic polymer substrate and/or forming composite of bioactive ceramic with organic polymer were sttempted to achieve a mechanical performance comparable to that of natural bone (Zhang and Ma, 1999b; Kikuchi *et al.*, 1997).

2.2.3.4 Composites

Composite materials are solids containing two or more distinct constituent materials or phases on a scale larger than the atomic (Park and Bronzino, 2003). Most engineering composites are developed aiming at unique mechanical properties. Mechanical properties are also the most important cause for researchers to investigate composite biomaterials as bone substitutes. Composite materials usually exhibit controllable mechanical properties such as strength, stiffness, toughness, etc. Ceramic/polymer composites integrate the best characteristics of each constituent, such as the toughness of polymer and stiffness of ceramic. Natural bone is a collagen/apatite composite. Artificial ceramic/polymer composites are usually produced as analogue biomaterials for bone substitute.

Kikuchi and coworkers (1997) fabricated TCP/CPLA (β-tricalicum phosphate/copoly-L-lactide) composites with a maximum bending strength of 54Mpa, nearly equal to that of CPLA and about half that of cortical bone. And Young's modulus was 8.2 Gpa, which is the same as cortical bone. Young's modulus for TCP/CPLA composites was especially enhanced in comparison to the original CPLA. Peter and coworkers (1998) reported a method in which poly(lactide-co-glycolide) were crushed and then compression molded with hydroxyapatite (HA) to obtain an improved compressive yield strength

Zhang and Ma (1999b) prepared PLLA/HA and PLGA/HA composite scaffolds using phase separation technique, and demonstrated a significant improvement in mechanical properties over pure polymer scaffolds. They (Zhang *et al.*, 2002) also prepared porous poly(L-lactide)/bioactive glass (PLLA/BG) composite scaffolds by phase separation. Mechanical results showed that the elastic modulus of the composites was increased with the increase in glass content.

Zhao and coworkers (2002) fabricated the biodegradable hydroxyapatite/chitosan-gelatin network (HA/CS-Gel) composite scaffold by phase separation method for bone tissue engineering. They reported that the osteoblasts successfully attached to and proliferated on the scaffolds, and that extracellular matrices including collagen I and proteoglycan-like substrate were synthesized, with osteoid and bone-like tissue formed during the culture period. Zhang and coworkers (2003) also fabricated macroporous calcium phosphate–chitosan composite scaffolds and evaluated them for use in bone tissue engineering. The results of human

osteoblast-like MG63 cells cultured on the scaffolds indicated that the hydroxyapatite–matrix composite scaffolds could enhance the phenotype expression of MG63 cells, in comparison with chitosan–matrix scaffolds. They also mentioned that soluble calcium phosphate glasses added to the scaffolds could prevent chitosan from fast degradation that may affect the differentiation of osteoblast cells.

Marra and coworkers (1999) made a blend scaffold of poly(caprolactone)/poly(D,L-lactic-co-glycolic acid)/hydroxyapatite for applications in bone tissue engineering. Their cell incubation study showed that this composite polymer/ceramic scaffold supported cell growth throughout the scaffold for 8 weeks.

Lee and coworkers (2006) fabricated a synthetic polymer/naturally derived polymer composite scaffold composed of poly(D,L-lactide-co-glycolide) (PLGA) and collagen. They evaluated the biological activities of the composite scaffolds for use in bone tissue regeneration and reported that the composite scaffolds are able to promote cellular interactions.

It could be appreciated that there are a number of biodegradable polymers and ceramic available for bone tissue engineering. Each material has its own properties. No single material has been shown to be able to meet the requirements for bone tissue engineering. Composites, as suggested by nature, seem to be the most promising way forward.

2.2.4 Fabrication techniques of polymer-based scaffolds

After the selection of suitable biomaterials, scaffolds could be fabricated using processing techniques. A variety of fabrication techniques have been developed for producing scaffolds. Solid implants, such as plates, rods, and screws used as fracture fixation systems, are often fabricated using extrusion or injection molding techniques (Gibbons *et al.,* 1992). For the fabrication of scaffolds, such approaches were not used because of the need to create high porosity. It is better for the fabrication process to avoid the use of high temperatures, which may present difficulties if proteins or other bioactive molecules are to be included during the process.

2.2.4.1 Solvent casting/particulate leaching

The most straightforward strategy to fabricate a porous scaffold is to include the casting of a polymer/porogen composite followed by aqueous washing out of the incorporated porogen. (Mikos *et al.,* 1993&1994; Fisher *et al.,* 2001; Yoon and Park, 2001; Murphy *et al.,* 2002). The volume that was once filled by the porogen is then left void, forming pores within the material. This method is most easily accomplished by utilizing a water soluble porogen, such as salt, sugar, or gelatin particles, which can be removed by aqueous washing. In the casting of a polymer/porogen composite, enough porogen must be incorporated so that the individual pores are in contact with each another, leading to an interconnected pore structure. This method could be used to control pore sizes by changing the size of porogen. However, it is easy for porogen, such as salts, to remain in the scaffolds. The interconnected structure is poor usually because it is not easy to control the inter-pore openings.

Mikos and coworkers (1993) described this process. Firstly, PLGA were dissolved in chloroform. Sodium chloride particles were mixed with these solutions with the salt/polymer ratio of 9:1. Then the chloroform was evaporated and extracted. Finally the sodium chloride particles were leached out by immersion in water at 25°C for 48 hous.

2.2.4.2 Gas foaming

Another general strategy to form a porous scaffold is to use a gas to form pores within the material (Mooney *et al.,* 1996; Harris *et al.,*1998; Partridge *et al.,* 2002; Hutmacher, 2000; Yang S *et al.,* 2001&2002). Conventionally, gases such as nitrogen or carbon dioxide are incorporated into the bulk material either by purging the material with the gas or by forming gas as a product of a chemical reaction. Sufficient gas volume was necessary to form an interconnected pore structure. In this technique, highly porous sponges could be produced without the use of toxic organic solvents, traces of which may remain in the scaffold after the fabrication. However, the preparation of the starting dense substrate may involve the use of heat or solvents.

Mooney and coworkers (1996) subjected solid disks of PLGA to high pressure CO_2 gas (5.5 MPa) for 72 hous at room temperature, then the gas pressure was reduced to atmospheric levels. The solubility of the CO_2 gas in PLGA disks was then rapidly decreased, inducing the nucleation and growth of pores within the PLGA matrix. PLGA scaffolds with pore size of ~100 um and porosities of up to 93% were obtained.

Harris and coworkers (1998) presented a method combining the high-pressure gas foaming and particulate leaching technique. Firstly, The mixtures of PLGA and NaCl were loaded into a die and compressed at 1500 psi for 1 min to yield solid disks. The samples then were exposed to high pressure CO_2 gas (800 psi) for 48 h to saturate the polymer with gas. The gas pressure was decreased to ambient pressure, resulting in a porous structure composed of the continuous PLGA matrix and NaCl particles. The NaCl particles finally were removed from the matrices by leaching the matrices to yield macro-pores.

2.2.4.3 Phase separation and freeze-drying

Phase separation and freeze-drying were also used in the fabrication of porous scaffolds (Lo *et al.*, 1995 & 1996; Whang *et al.*,1995; Schugens *et al.*, 1996). The thermally induced phase separation technique is based on the principle that a single homogeneous polymer solution made at elevated temperature, under cooling conditions, becomes thermodynamically unstable and tends to separate into two phase composed of a polymer-rich phase and a polymer-lean phase in order to lower the system free energy (van de Witte *et al.*, 1996; Bansil and Liao, 1997). The quenched polymer solution is subsequently freeze-dried to remove the solvent, leaving a highly porous polymer network. Freeze-drying under vacuum usually lasts for several days to insure complete solvent sublimation.

In this method, thermodynamic and kinetic parameters influence the porous structures. Figure 2.5 shows a schematic temperature-composition phase diagram for a binary polymer/solvent system. Above the binodal curve, the solution exists as a single polymer solution phase. Below the curve, polymer-rich and polymer-lean

phases are separated. If the system is quenched into the metastable region between bimodal curve and spinodal curve, phase separation occurs, forming an isolated cellular structure. At lower temperatures beneath the spinodal curve, the system goes into the unstable region where the phase separation takes place via a spinodal decomposition mechanism, forming a bicontinuous structure (both the polymer-lean and polymer-rich phases are continuous). After the removal of the solvent, the system will form a scaffold with an open-pore interconnected structure (Song and Torkelson, 1994). So spinodal decomposition could increase the number of interconnected pores.

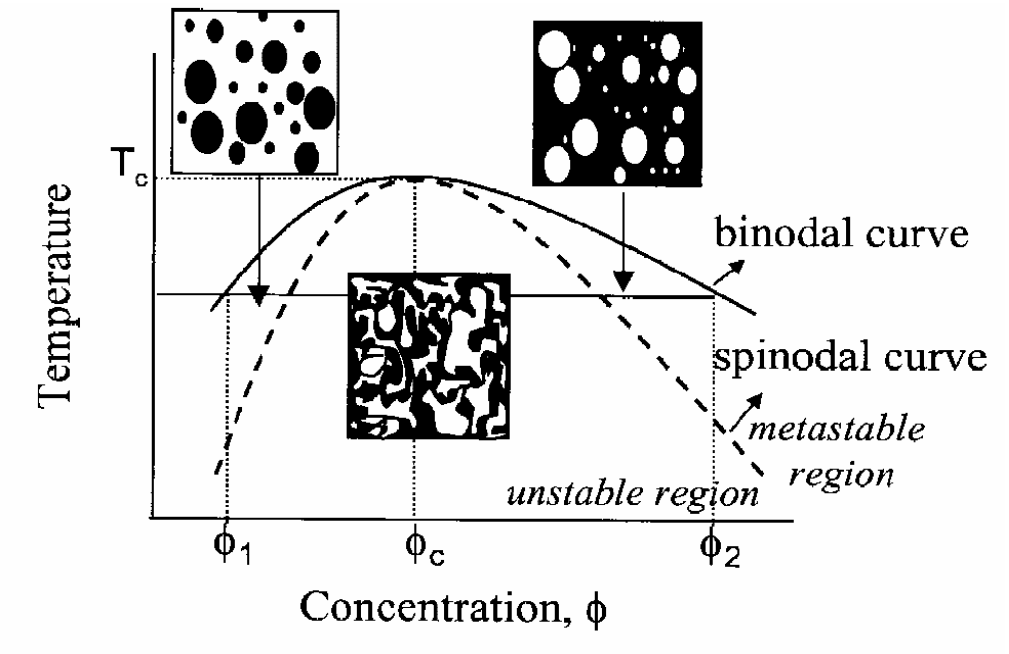

Figure 2.5 *Temperature-composition phase diagram of polymer solution.* (Nam and Park, 1999a) *Tc: upper critical solution temperature (UCST); Φc: the concentration under Tc.*

Besides the quenching temperature, various other parameters, such as solvent/nonsolvent ratio, cooling method and time, polymer concentration, and the presence of surfactants, could influence the resulting structure. Surfactants could

increase interconnectivity and pore size by reducing the interfacial tension between phases (Nam and Park, 1999a&b). Ma and Zhang (1999) fabricate a fibrous scaffold with an interconnected fibrous network with a fiber diameter ranging from 50 to 500 nm using a procedure involving thermally induced gelation, solvent exchange, and freeze-drying. It was demonstrated that at a high gelation temperature, a platelet-like structure was formed, and at a low gelation temperature the nano-fibrous structure was formed. The porosity decreased with polymer concentration. The mechanical properties (Young's modulus and tensile strength) increased with polymer concentration. Under the conditions for nano-fibrous matrix formation, the average fiber diameter (160–170 nm) did not change statistically with polymer concentration or gelation temperature. Ma and Zhang (2001) also fabricated scaffolds with an oriented array of open microtubules by growing oriented rod-shaped crystals from a polymer solution followed with the removal of these rods.

Both PLGA and PLLA scaffolds have been fabricated using this technique (Schugens *et al.*, 1996; Lo *et al.*, 1995 & 1996; Nam and Park, 1999a&b). PLLA or PLGA are dissolved in a solvent with a low melting point, such as 1,4-dioxane or naphthalene, which is easy to sublime. Nam and Park (1999a) fabricated scaffolds with 90% porosity and pores of approximately 100μm using this technique. In this thesis study, we also used the method of phase separation to fabricate PLLA scaffolds.

The disadvantage of this fabrication method is that organic solvents may be residual in the scaffolds, which may affect the cells after cell seeding. The advantage is that it is flexible to tailor porosity and pore size for specific applications by changing various processing parameters. In this thesis, the method of phase separation

and gas sublimation was used to fabricate scaffolds. This is a relatively mature technique and the porosity and pore size could be controlled. As the focus of this thesis is on surface modification, we decided to go with a more established method for scaffold fabrication.

Zhang and Ma (2000) combined particulate leaching and phase separation technique to prepare nano-fibrous matrices with particulate macropores. Polymer solutions were cast over the porogen assemblies in a mold, and were then thermally phase-separated to form nanofibrous matrices. Lastly, the porogen materials were leached out with water. The created matrices have interconnected open pore structure and nano-fibrous pore walls. The macropores were a few hundred micrometers in size determined by the size of the porogen used. The interfiber distance was in the microns level determined by the polymer concentration used. The fiber diameter ranged from 50 to 500 nm.

2.2.4.4 Rapid prototyping

With the methods above, a random architecture will been achieved. The methods of creating scaffolds of precisely defined architecture involve rapid prototyping techniques (Park *et al.*,1998).

Rapid prototyping Technologies (RP) also called Solid Free Form fabrication (SFF) methods are defined as a set of manufacturing processes that are capable of producing complex-free form parts directly from a computer-aided design (CAD) model of an object without specific tooling or knowledge (Beaman, 1997). Both 3-D

printing (3-DP) and fused deposition modeling (FDM) are rapid prototyping technologies. Three-dimensional printing developed at the Massachusetts Institute of Technology (Sachs *et al.,* 1992) has been used to process bioresorbable scaffolds for tissue engineering applications (Cima *et al.,* 1991; Giordano *et al.,* 1996; Park *et al.,* 1998). 3-D printing is a solid free-form fabrication process.

The FDM process forms 3-D objects from a CAD file as well as digital data produced by an imaging source such as computer tomography (CT) or magnetic resonance imaging (MRI) (Agarwala *et al.,* 1996).

2.2.5 Cells for bone tissue engineering

After the fabrication of a porous scaffold, cells could be seeded onto it and be expected to expand into high numbers. An ideal cell source should be easily expandable to higher passages, non-immunogenic and have a protein expression pattern similar to the tissue to be regenerated (Heath, 2000).

2.2.5.1 Osteoblasts

The isolation of osteoblasts from biopsies taken from the patients (autologous cells) appears to be a direct choice. These cells have the advantages of being non-immunogenic. However, relatively few cells are available after the dissociation of the tissue and their expansion rates are relatively low.

Another choice is cells obtained from non-human donors (xenogeneic cells), which could provide enough cell numbers. However, these cells have the limitations

due to immunogenicity, and the possibilities of the transmission of infectious agents such as virus also increased.

Because the potential application of this research is bone tissue engineering, the osteoblast-like cells, Saos-2 cells, was used in this research. Saos-2 is an immortalized cell line with an osteoblastic phenotype (Murry *et al.*, 1978) and has been used in the research of bone tissue engineering(Gao *et al.*, 2001; Mayr-Wohlfart *et al.*, 2001; Rea *et al.*, 2004). Mayr-Wohlfart and coworkers (2001) investigated the influence of four bone substitutes on the cell growth behavior using Saos-2. To better understand glass-ceramic apatite-wollastonite (A-W)/high-density polyethylene composite (AWPEX) properties, Rea and coworkers (2004) examined the effects of surface finish and ceramic filler size and content on Saos-2 cell attachment, proliferation, and differentiation.

2.2.5.2 Stem cells

Stem cells are undifferentiated cells with a high proliferation capability, being able of self-renewal, multilineage differentiation and therefore the regeneration of tissues (Blau *et al.*, 2001). Stem cells biology provides a promising solution.

In the bone tissue engineering field, mesenchymal stem cells (MSC), stem cells located in the bone marrow, have drawn much interest. Caplan (1994) described that these cells, when placed in adequate culture conditions, could differentiate into cells of mesenchymal origin and generate bone. MSCs have been used in clinical trials for applications in bone tissue engineering (Pittenger, 2001; Weinand *et al.*, 2006).

Furthermore, the muscle-derived stem cells could be used to improve bone healing. Sun and coworkers (2005) reported that the muscle-derived stem cells were capable of inducing and participating in bone formation.

2.2.6 Growth Factors for bone tissue engineering

Growth factors are cytokines that are secreted by many cell types and function as signaling molecules (Rose and Oreffo, 2002). These molecules are essential for tissue formation and play an important role in tissue engineering. Growth factors have a stimulating effect on bone defect healing by inducing chemotaxis, proliferation, and differentiation of osteoblasts and their precursors (Bostrom *et al.*, 1999; Reddi, 1998b). A number of growth factors, such as bone morphogenetic proteins (BMPs), transforming growth factor beta (TGFb), vascular endothelial growth factor (VEGF), fibroblast growth factors (FGFs), insulin growth factor I and II (IGF I/II), and platelet derived growth factor (PDGF), have been found to be involved in bone tissue engineering.

Growth Factors could be incorporated into the scaffolds either during the fabrication of scaffolds or after the fabrication by subsequent surface modification. For example, Murphy and coworkers (2000) fabricated three-dimensional, porous poly(lactide-co-glycolide)/VEGF scaffolds by including the growth factor into a gas foaming/particulate leaching process. Section 2.3.4.3 presents a more detailed review on growth factors as surface modifiers.

2.2.6.1 Bone morphogenetic proteins (BMPs)

Bone morphogenetic protein (BMP) is a family of proteins originally purified from bone matrix and is responsible for a variety of events in embryogenesis and in the postnatal skeleton (Croteau *et al.,* 1999; Ripamonti and Duneas, 1998). BMPs play a critical role in embryological bone formation, osteoinduction, and bone repair (Bostrom *et al.,* 1995; Ripamonti and Duneas, 1998; Johnson *et al.*, 1988; Yasko *et al.*, 1992; Bostrom and Camacho, 1998; Sampath *et al.,* 1992; Takagi and Urist, 1982).

Fifteen BMPs have been characterized and cloned (Croteau *et al.,* 1999; Rengachary, 2002). These BMPs are not identical in their osteoinductive potential. Among these BMPs, the report on BMP-2 is much more than the others. The primary activity of recombinant human BMP-2 (rhBMP-2) is to induce formation of new bone. In this process, rhBMP-2 induces endochondral ossification by stimulating proliferation and differentiation of mesenchymal cells into chondroblasts and osteoblasts and by stimulating production and maturation of cartilage in bone matrix (Lovell *et al.,* 1989). BMP-7 also has strong osteoinductivity (Yeh *et al.,* 2002). The BMPs used in bone-fracture healing have mainly been BMP-2 and BMP-7. It was demonstrated that recombinant human BMP (rhBMP) -2 and -7 are capable of inducing bone formation (Sampath *et al.,* 1992; Wang EA *et al.,* 1990). Bostrom and Camacho (1998) reported that the healing of fractures in rats could be accelerated with the percutaneous injection of rhBMP-2. Lu and coworkers (2003) evaluated the ability of BMP-7 to induce the differentiation of cells derived from rabbit skeletal muscle into osteoblast-like cells and subsequently form mineralized tissue. Results confirmed that BMP-7 released from PLGA induced the muscle-derived cells to

increase bone marker expression and form mineralized cultures.

BMP-3 could also induce the formation of bone tissue (Chen *et al.,* 1995). BMP-4 is similar to BMP-2 not only in structure but also in function. However, its osteoinductive potential is weaker than BMP-2 (Ma WH, 2001). The osteoinductivity of BMP-5 is apparently weaker than that of BMP-2 with an apparent delay in its effective time (Ma WH, 2001). BMP-6 is used mainly in cartilage engineering. *In vivo*, BMP-6 could induce chondrogenesis and the growth of the cartilage tissue (Gitelman *et al.,* 1994). BMP-9 alone apparently did not show much of an effect of stimulating bone formation. Li and coworkers (2003a) reported that a helper-dependent adenoviral vector containing the BMP-9 and green fluorescent protein (GFP) genes has significant osteoinductive activity in both athymic nude and immune competent rats.

Because BMP alone easily diffuses and disappears, the practical use of BMP is dependent on a carrier substrate which may act to protect **B**MP from nonspecific proteases. A number of materials could reportedly serve as the carrier of BMP. An ideal carrier system would allow a gradual release of the BMPs.

I. BMP/naturally derived polymers system

Collagen was reported to be a carrier for BMP (Levine *et al.,* 1997), and was demonstrated to be superior as a drug-releasing matrix compared to HA, TCP, glass beads, and polymethylmethacrylate (Reddi, 1998a). Nishizaki and coworkers (2003) investigated whether bone morphogenetic protein-2 (BMP-2)/collagen composites are potential obliteration materials for use in the mastoid cavity using an animal model.

The histological examination demonstrated that the BMP-2/collagen composites was stable and persisted in the rat mastoid.

II BMP/synthetic polymers system

Synthetic polymers could be used as vehicles to delivery BMPs. Kirker-Head and coworkers (1998) combined rhBMP 2 with poly-D,L-lactide-co-glycolide (PDLGA) particles to heal defects in sheep femora. Miyamoto and coworkers (1993) used prepared polylactic acid-polyethylene glycol block copolymer (PLA/PEG) as the carrier for BMP. The complex composite induced bone formation and the formation of haematopoietic marrow three weeks after implantation into rat muscle bellies. Murakami and coworkers (2003) combined human BMP-2 with a synthetic biodegradable polymer, poly-D,L-lactic–acid-paradioxanone-polyethyleneglycol block co-polymer (PLA-DX-PEG). Twelve weeks after implantation in a canine model, the original bone defects were repaired.

The properties of carrier materials, such as molecular weight, could influence the BMP delivery. Miyamoto and coworkers (1992) evaluated PLAs of differing molecular weights for their potential use as a carrier for BMP. They determined that only PLA with a molecular weight of 650 daltons allowed BMP to reproducibly induce bone formation at ectopic sites.

III. BMP/ceramics system

Koempel and coworkers (1998) reported that the addition of BMP to a porous HA with a porosity of 40% and noninterconnected pore sizes ranging from 100 to 300 mm would augment the ingrowth of host bone. Takahashi and coworkers (1999) used

porous HA and rhBMP 2 in the anterior multilevel cervical spine arthrodesis in goats, and the results showed 100% fusion in 14 goats. Reddi (1998a) demonstrated that the geometry of HA could affect the BMP delivery. BMP was loaded on beads and discs of HA, and the results showed that the beads were inactive.

IV. BMP/composite system

Ceramic/polymer composites have also been used as carriers of BMP. Laurencin and coworkers (2001) demonstrated that *in vivo* poly(lactide-co-glycolide)/hydroxyapatite composite scaffolds successfully functioned as a delivery vehicle for bioactive BMP-2. A HA/collagen/bovine BMP composite was fabricated and placed into mandibular defects in a primate model, demonstrating superior bone induction in comparison to controls (Asahina *et al.*, 1997). Yang and coworkers (2005) fabricated a tricalcium phosphate and glutaraldehyde crosslinked gelatin (GTG) scaffold, with bone morphogenetic proteins (BMPs) incorporated for bone tissue engineering. They reported that alkaline phosphatase (ALP) activity and gla-type osteocalcin (Gla-OC) activity of the GTG-BMP samples were not greater than that of the GTG samples in the second and third weeks, but it continued increasing and became significantly greater than that of the GTG samples by the fourth week.

Kokubo and coworkers (2003) used PLGA-coated gelatin scaffold as the carrier of recombinant human bone morphogenetic protein (rhBMP)-2. The results showed that bone defect in rabbits treated with rhBMP-2 were radiographically repaired. Mechanical properties of regenerated bones were restored in a dose-dependent manner. These results suggest that PLGA-coated gelatin scaffold is a promising carrier for rhBMP-2. From the view of the surface modification, the results

show that rhBMP-2 is a good surface modification choice for PLGA-coated gelatin scaffold.

2.2.6.2 Other growth factors

Besides BMPs, other growth factors also have the potential to be used in bone tissue engineering.

Transforming growth factor beta (TGF-β) has been shown to stimulate cellular proliferation *in vitro* (Govinden and Bhoola, 2003). Malafaya and coworkers demonstrated that TGF-β stimulated osteoblast-like cells to proliferate and promoted collagen production *in vitro* (Malafaya *et al.,* 2002).

Vascular endothelial growth factor (VEGF) is commonly found in bone fracture healing sites. VEGF regulates vascularization and plays an important role in the regulation of the interaction between osteogenesis and angiogenesis (Jadlowiec *et al.,* 2003; Furumatsu *et al.,* 2003). Murphy and coworkers (Murphy *et al.,* 2000) used the scaffolds of the copolymer 85 : 15 poly(lactide-co-glycolide) as the carrier of VEGF. Sustained release of VEGF from the scaffolds was achieved, and the VEGF released from the scaffolds was over 70% active for up to 12 days.

Fibroblast growth factors (FGFs, namely FGF-2) is believed to be involved in the regulation of the maintenance of the balance between bone forming cells and bone resorbing cells (Mackay *et al.,* 1998). It is also believed that FGFs promotes the development of new blood vessels (Jadlowiec *et al.,* 2003) and has a role in the stimulation of the osteogenic phenotype (Franceschi and Xiao, 2003).

It was reported that insulin growth factor (IGF) stimulated type I collagen synthesis, increased matrix apposition rates, and maintained collagen integrity in the bone microenvironment (Jadlowiec *et al.*, 2003, Canalis and Agnusdei, 1996). When compared with each other, IGF I was apparently more potent than IGF II (Canalis and Agnusdei, 1996).

PDGF is produced by osteoblasts, platelets and monocytes/macrophages, and is believed to affect the migration of mesenchymal stem cells (MSCs) to the wound healing sites (Rasubala *et al.*, 2003).

2.2.7 Bioreactors for bone tissue engineering

Bioreactors are generally defined as devices in which biological and/or biochemical processes develop under closely monitored and tightly controlled environmental and operating conditions (Martin *et al.*, 2004). Bioreactors are classically used in industrial fermentation processing, food processing, wastewater treatment, and production of pharmaceuticals. In tissue engineering, bioreactors are used to provide environments mimicking the *in vivo* body. The bioreactor provides the chemical and physical cues to guide cell differentiation and assembly into the 3D constructs.

The overall requirement of tissue engineering bioreactor is to facilitate the cell seeding and culture. Seeding into 3D scaffolds needs to be of (a) spatially uniform distribution of cells, (b) high kinetic rate to minimize the time in culture medium for shear-sensitive cells, and (c) high yield to maximize the utilization of donor cells

(Vunjak-Novakovic *et al.,* 1998). A bioreactor should facilitate the uniform mixing of culture medium and control of mass transport. The condition parameters (such as concentration of nutrient, pH, temperature) should be controlled readily and properly, and the gradient of these condition parameters should be as little as possible. Cell damage by shear stresses due to mixing should be as low as possible. For cells of load-bearing tissues, mechanical stimulation is also fabricated in the bioreactors sometimes.

In general, a structural and functional tissue equivalent can be regenerated *in vitro* only if the bioreactor provides a proper culture environment for tissue growth. Typical bioreactors for tissue engineering are discussed in the following.

2.2.7.1 Petri dish (static or shaking)

Among the various cell seeding and culture techniques, the simplest method is static seeding in Petri dish [Figure 2.6 (a)]. In this method, a highly concentrated cell suspension is statically loaded onto the scaffold surface. Due to its relative simplicity, static seeding has been used quite widely and was perceived as effective in some studies.

(a) (b)

Figure 2.6 *Cell seeding and culture in Petri dish under (a) static and (b) shaking condition.*

Petri-dish could also be placed on an orbital shaker [Figure 2.6 (b)] for enhanced mixing. This has also been used widely (Carrier *et al.,* 1999; Martin *et al.,* 1998). Wiesmann and coworkers (2003) cultured constructs of bone tissue in Petri dishes. Under the shaking condition, metabolic parameters could be maintained in physiological ranges, indicative of more aerobic metabolism.

2.2.7.2 Spinner-flask bioreactor

In the spinner-flask bioreactor [Figure 2.7], scaffolds are attached to needles suspended from the mouth of the flask. The magnetic stirrer at the bottom generates considerable convective forces, inducing relative velocity between the scaffolds and the culture medium together with the cells, thus transporting cells into the scaffolds and continuously transferring fresh media to the scaffolds. One potential drawback associated with the spinner-flask bioreactor is related to the turbulent eddies induced by stirring. The stresses so generated could be detrimental to the cells in the scaffolds.

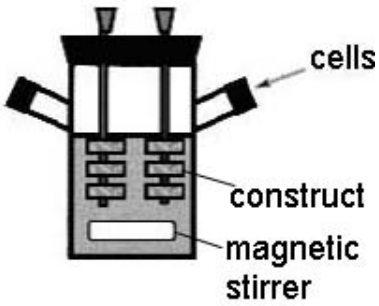

Figure 2.7 *A typical spinner-flask bioreactor* (Sikavitsas *et al.,* 2002)

Spinner-flask bioreactors have been used for the cell seeding and culture on scaffolds for bone (Goldstein *et al.,* 2001) tissue engineering.

2.2.7.3 Rotating-wall vessel bioreactor

Rotating wall vessel (RWV) bioreactor consists of two concentric cylinders [Figure 2.8]. The inner cylinder is composed of semi-permeable membrane, allowing gas exchange, whereas the outer cylinder is impermeable. The scaffolds are placed in the annular space.

Rotating wall vessel bioreactor was originally designed to simulate a microgravity environment (Schwarz *et al.*, 1992; Unsworth and Lelkes, 1998). The inner cylinder is stationary and the outer cylinder rotates at a controlled rate. The centrifugal force due to the rotation of the outer cylinder and net gravitational force of scaffolds could be balanced by controlling the rotation rate, thus establishing a microgravity environment. That is, the rotation rate can be adjusted so as to suspend the tissue constructs at certain positions (Obradovic *et al.*, 2000).

Clearly, the rotating wall vessel bioreactor does not actually cancel gravity, but only maintains an appropriate microgravity condition similar to the simulation of space microgravity on earth. This provides the scaffolds with high mass-transfer rates in low shear condition. To minimize shear and turbulence, usually the terminal velocity of the constructs is minimized by matching the density of the scaffolds and the culture media (Lappa, 2003).

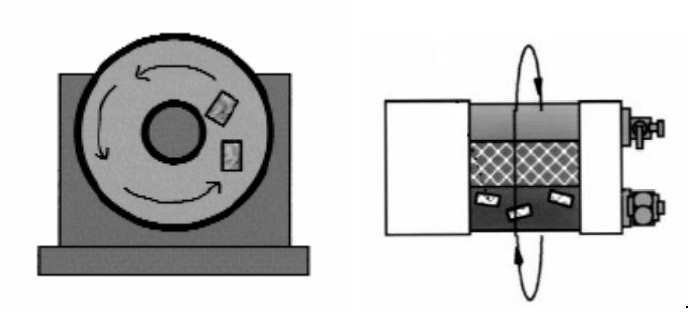

Figure 2.8 *A typical rotating wall vessel bioreactor* (Sikavitsas *et al.*, 2002; Freed and Vunjak-Novakovic, 1998)

Rotating wall vessel bioreactors have been used for the cell seeding and culture into microcarriers or scaffolds for bone tissue engineering (Qiu *et al.,* 1999; Botchwey *et al.,* 2001). Rotating wall vessel bioreactors have been used to investigate the factors influencing tissue culture *in vitro*. Obradovic et al (Obradovic *et al.,* 1999) seeded primary chondrocytes onto PGA scaffolds and cultured the constructs *in vitro* for 5 weeks in rotating bioreactors under different gas exchange conditions. Gas exchange was found to be an important factor for tissue cultivation in the bioreactor. Efficient gas transport could stimulate rapid tissue growth, while cultivation in low oxygen tension suppressed chondrogenesis in 3D tissue constructs.

2.2.7.4 Perfusion bioreactor

Perfusion bioreactor [Figure 2.9] is another example of convective transport of cells for scaffold seeding and culture. In this kind of bioreactor, cell suspensions flow directly through the pores of 3D scaffolds, yielding a highly uniform cell distribution and high mass transfer not only at the periphery but also through internal porosity of the scaffolds (Wendt *et al.*, 2003).

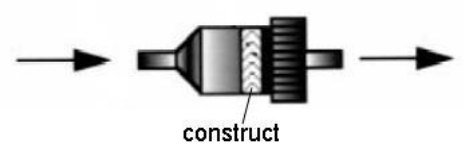

Figure 2.9 *A typical perfusion bioreactor* (Freed and Vunjak-Novakovic, 1998)

Another advantage of perfusion bioreactors over the former three types of bioreactors is maintenance of the concentrations of the chemical species under the flowing condition. Steady perfusion more closely approximates the *in vivo* cell and tissue homeostasis than the step-changes in medium composition during the scheduled medium change in operation of batch-based bioreactors.

Perfusion bioreactor could be achieved by many ways. Li and coworkers (2001) employed a depth-filtration seeding method [Figure 2.10]. Wendt and coworkers developed an automated perfusion bioreactor using a U-tube configuration [Figure 2.11] for 3D scaffold seeding. Higher seeding efficiencies, more uniform cell distributions, and more homogeneously sized cell clusters were achieved compared with seeding in either the static or shaking condition (Wendt *et al.,* 2003).

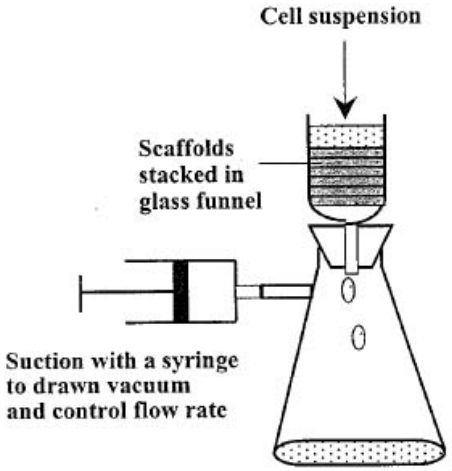

Figure 2.10 *Perfusion bioreactors using depth-filtration* (Li *et al.*, 2001).

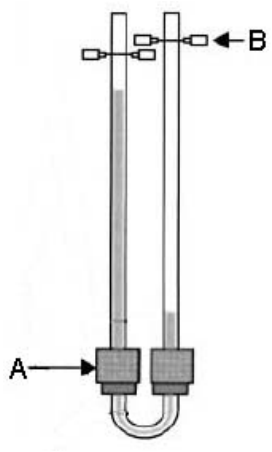

Figure 2.11 *Perfusion bioreactor using U-tube. Scaffolds were placed in chambers (A). Flow of the cell suspension in the tube was induced with the use of a vacuum pump. The direction of flow was reversed when the fluid level in one column reached an optical sensor (B) placed near the top of each glass column* (Wendt *et al.*, 2003).

These typical bioreactors might be combined to form new ones. For example, the rotating-wall perfused-vessel (RWPV) bioreactor proposed by Begley and Kleis (Begley and Kleis, 2000) could be considered as a combination of the rotating-wall vessel (RWV) bioreactor and perfusion bioreactor. Like the RWV bioreactor, the RWPV vessel had a concentric cylinder arrangement [Figure 2.12]. The inner cylinder was porous, with a filter covering the exit for extracting fluid into the external perfusion flow loop. Both the inner and outer cylinders can be independently rotated. The fluid flew in through the inlet, entering the high shear region and flew out through the porous inner cylinder.

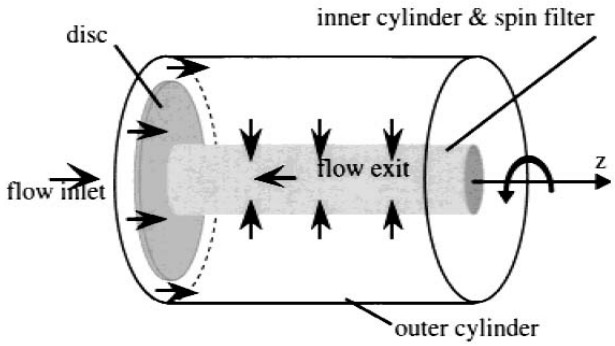

Figure 2.12 *Rotating-wall perfused-vessel bioreactor* (Begley and Kleis, 2000)

2.3 Surface modification for bone tissue engineering

It is rare that a biomaterial with good bulk properties also possesses the surface characteristics suitable for bone tissue engineering. It is often necessary to modify the surface properties without changing the bulk attributes.

The interactions between the biological environment and biomaterials used in tissue engineering take place on the material surfaces. It has been described (Kasemo and Lausmaa, 1986) that biological tissues interact with mainly the outermost atomic layers of an implant. These primary interactions scope is generally about 0.1-1 nm (Zhao *et al.,* 1999, Ong and Lucas, 1998). Consequently, it is promising to modify the above biomaterial surface to achieve the desired biological responses. Surface modification of biomaterials is one of the key issues in the development of tissue engineering.

The biological response of living tissues to these extrinsic biomaterials depends on the surface properties, such as, chemical composition, surface energy,

semiconductor properties, surface charge and wettability (Liefeith *et al.*, 1998; Zhao *et al.,* 1999). Surface free energy could influence the cell attachment, spreading, and growth. Usually, the surface with a higher surface free energy facilitate the cell attachment and spreading. Schakenraad and coworkers (1986) reported that cells could not spread well until the surface free energy reaches 57×10^{-7} J • cm^{-2}.

There are many methods and technology applied to surface modification. Szabo and coworkers (Szabo *et al.,* 1999) grouped surface modification methods into three general categories: adding materials, removing materials, and changing materials. Adding materials usually means coating the surface with a material having a different chemical composition. Etching would involve removing materials. Changing materials would be to chemically or physically alter the atoms, compounds, or molecules on the surface.

With respect to polymeric biomaterials, the surface modification methods can be physicochemical or biochemical. In the physicochemical methods, such as plasma treatment and apatite coating, physicochemical characteristics of surface, such as energy, charge and composition, could be altered. In the biochemical methods, some critical organic components, such as growth factors, peptides, collagen, polysaccharides and so on, were immobilized on biomaterials for the purpose of inducing specific cell and tissue responses. These methods will be discussed as follows.

2.3.1 Glow discharge gas plasma treatment

Glow discharge gas plasma treatment is an effective and widely used physicochemical method for modifying the surface of polymeric substrate. In 1975, glow discharge gas plasma-induced surface modification was reported to enhance cell adhesion, growth, and differentiation on polymer surfaces (Amstein and Hartman, 1975). The glow discharge process produces a high energy gas glow, which could increase surface free energy of solid surfaces without affecting the underlying bulk properties of the polymer substrate (Hesby *et al.,* 1997, Baier and Meyer, 1988). Furthermore, these nonpolymerizing gases could create reactive sites such as hydroxyl (Curtis et al., 1983; Curtis and McMurray, 1986) and carboxyl group (Ramsey *et al.,* 1984), amine groups (Hollahan *et al.,* 1969), and sulfonic acid groups (Inagaki *et al.,* 1989) on the surfaces of polymers (i.e. surface functionalization). Such plasma surface modification could be applied to modify synthetic polymeric biomaterials, for example poly(a-hydroxyacids), which have poor properties for cell attachment because of their hydrophobic property.

Anhydrous ammonia plasma treatment has been used to increase the hydrophilicity of polylactide (PLA) and to improve its cell adhesion (Yang J *et al.,* 2002a). Wan and coworkers reported that the adhesive force and affinity of mouse 3T3 fibroblasts on PLLA films and scaffolds treated by ammonia plasma were greatly enhanced (Wan *et al.,* 2003). Chim and coworkers (Chim *et al.,* 2003) demonstrated that gas plasma surface modification of three-dimensional poly (d,l-lactide) scaffolds enhance osteoblast-like cell adhesion, proliferation, and differentiation over 10 days in culture using human embryonic palatal mesenchyme cells. The roughness of treated

surfaces was also reported to increase, which may contribute to increased cell adhesion.

The treatment parameters could influence the resultant surface and thus affect the subsequent cell adhesion activities. Wan and coworkers (2004) treated poly (lactide-co-glycolide) (PLGA) films by oxygen plasma. The results showed that cells stretched well and the ability to endure the shear stress was also improved greatly after the PLGA was modified under the condition of 50W for 2 or 10 min. When the treatment time was increased to 20 min, the percentage of adherent cells on the surface decreased because the content of polar groups incorporated onto the surface decreased.

Other advantages of plasma treatment include sterilization of the treated material, its ability to treat complex shapes including two-dimension films and three-dimension scaffolds (Chim *et al.*, 2003), and easy preparation.

2.3.2 Ion irradiation

Ion irradiation is also a tool to modify the physicochemical structure of polymeric surface. The irradiation could induce compositional and chemical modification and surface free energy modification of the polymeric surfaces. Pignataro and coworkers (Pignataro *et al.,* 1997) reported that a very strong improvement of the cell adhesion, spreading and proliferation was observed for ion beam irradiated surfaces of polyethersulphones and polyurethane.

2.3.3 Bonelike apatite coating

Calcium phosphate coatings (Dhert, 1994; Varma *et al.,* 1999) and apatite coatings (Zhang and Ma, 1999a; Yuan *et al.,* 2001) have been extensively investigated because of their chemical similarity to bone mineral. They should provide a good environment for osteoblasts and osteoprogenitor cells to attach and proliferate.

As one of the primary components of extracellular bone matrix, apatite exhibits unique advantages when used in bone reconstruction. Apatite has demonstrated good osteoconductivity (Hench, 1991), high affinity to living cells (Rizzi *et al.,* 2001) and an ability to adsorb protein (Tiselius *et al.,* 1956). Apatite can reduce fibrous encapsulation (Nagano *et al.,* 1996), promote bone ingrowth, enhance direct bone contact (Yan *et al.,* 1997; Li P, 2003; Barrere *et al.,* 2003), and has been shown to promote differentiation of bone marrow stromal cells along osteogenic lineage (Ohgushi and Caplan, 1999). However, by itself alone, the mechanical properties of apatite are quite limiting in many applications. Coating apatite on suitable substrates provides an attractive alternative to utilize its advantages in skeletal reconstruction for load bearing purposes.

2.3.3.1 The biomimetic process

Formation of an apatite layer has been shown to be an important phenomenon leading to direct bone bonding onto bioactive ceramic surfaces *in vivo* (Hench, 1991). Kokubo and coworkers (Tanahashi *et al.,* 1994b&1995b; Miyaji *et al.,* 1999; Fujibayashi *et al.,* 2003) demonstrated that a material's *in vivo* bioactivity could be

directly related to the rate at which the material forms apatite *in vitro* when immersed in simulated body fluids (SBF).

Since Kokubo and coworkers first used a biomimetic process to form carbonated apatite coating on a substrate in 1990 (Abe *et al.,* 1990), apatite coating has attracted much attention over the last decade. Formation of apatite coating on many types of substrates (Abe *et al.,* 1990; Tanahashi *et al.,* 1994b; Barrere *et al.,* 2001; Murphy *et al.,* 1999; Rhee and Tanaka, 1998; Yokogawa *et al.,* 1999; Yuan *et al.,* 2001; Zhang and Ma, 1999a) using biomimetic processes has been reported.

The biomimetic method has advantages compared with other apatite coating methods, such as plasma spraying (Clemens *et al.,* 1999; Kweh *et al.,* 2000) and ion assisted deposition (Ong *et al.,* 1995). It could prepare bonelike apatite layer on a substrate without using special equipments and extremely high processing temperatures. Hence, it is possible to coat heat-sensitive materials such as polymers using this technique. Furthermore, for the porous 3-D scaffold, the surface is not just the outside surface, but also the internal pore surfaces. Other apatite coating methods, such as plasma spraying, is difficult to affect the internal pore surfaces. The simulated body fluid in the biomimetic method could go into the interconnected pore and introduce bone-like apatite into the internal three-dimension surfaces (Zhang and Ma, 1999a&2004).

However, a long coating period is often necessary in the biomimetic process. The classical biomimetic process usually involves immersion of substrate in simulated

body fluid (SBF) or 1.5 times simulated body fluid (1.5SBF), with the fluid being refreshed every other day for about 1-4 weeks.

Maeda and coworkers (Maeda *et al.,* 2005) coated bonelike apatite on the vaterite/PLA scaffold using the biomimetic processing, and cultured human osteoblasts on it for 7 days. The result showed that the apaitite on the composite has excellent bioresorbability.

2.3.3.2 The accelerated biomimetic process

Many factors, such as temperature and ion concentration, could influence the growth rate of the apatite layer. As reported by Kokubo (Kokubo, 1996), the growth rate of apatite layer increased with increasing temperature (range: 10^{o}C-60^{o}C) or with increasing the ion concentration of the solution (range: 0.2SBF-2SBF).

Recently, several studies have made efforts in shortening the coating process by using higher ion concentration than 2SBF. It has been reported that apatite was formed on some metal substrate in one day using supersaturated SBF (5 times SBF) (Barrere *et al.,* 2002a&b; Chou *et al.,* 2004). Barrere and coworkers illustrated systematically the interdependence of ionic strength, pH, carbonate concentration, and their collective influence on the formation of the resultant apatite.

But no reports could be found on forming apatite layer on polymer substrate by this accelerated biomimetic process. Shortening immersion period should be particularly significant to degradable biopolymer because some polymers could degrade significantly during the long incubation period. It would therefore be very

useful to coat apatite on degradable polymer in a short time in 5SBF without compromising the properties of the substrate. In this thesis research, we applied the accelerated biomimetic process on the polymeric matrix.

2.3.4 Immobilization of bioactive organic components

Biochemical surface modification for modulating tissue responses to biomaterials has received increasing consideration for bone-implant applications.

2.3.4.1 Collagen

Collagen, as one of the two primary components of extracellular bone matrix, has demonstrated good osteoconductivity (Chen *et al.*, 2000; Yang *et al.*, 2002&2003) because it contains specific amino acid receptors that allow them to bind directly to cell-surface receptors (Hubbell, 1997). Collagen has been coated on various biomaterials, such as metals (Morra *et al.*, 2003; Geissler *et al.*, 2000) and polymers (Suh *et al.*, 2001; Ma *et al.*, 2002; Chen *et al.*, 2000), to promote cell adhesion and bone integration.

Suh and coworkers immobilized collagen on ozone oxidized PLLA films and demonstrated that the type I atelocollagen provided a favorable matrix for cell migration (Suh *et al.*, 2001). The process for collagen coating usually involved immersing the substrates into collagen-containing solution for 2-24 hours. To render the substrate surfaces favorable for collagen adsorption, some reactive groups, such as hydroxyl (–OH), carboxyl (–COOH) and amino group ($–NH_2$), were usually pre-

introduced to the substrate surfaces using physical and chemical treatments, such as plasma treatment (Yang *et al.,* 2002), ozone oxidization (Suh *et al.,* 2001), and graft polymerization (Ma *et al.,* 2002; Bisson *et al.,* 2002; van Wachem *et al.,* 2002).

Denatured collagen (gelatin) has also been processed on the materials surface for bone tissue repair. Liu and coworkers (2005) incorporated gelatin onto the surface of nano-fibrous PLLA scaffolds using the electrostatic layer-by-layer self-assembly technique. They reported that the cell number on the surface-modified PLLA film was significantly higher than that on the control 4 h and 24 h after cell seeding. Furthermore, the osteoblasts proliferated at a higher rate and were more evenly distributed on surface-modified PLLA scaffolds than on the control scaffolds.

2.3.4.2 RGD

The RGD (Arg-Gly-Asp) tripeptide is recognized as the active sequence of adhesive proteins of the extracellular matrix (ECM) (Ruoslahti, 1996). The RGD motif actively promotes cellular adhesion through binding to integrin receptors. Accordingly, RGD-containing peptides have been deposited on biomaterials surface to improve the cell growth and differentiation (Hu *et al.,* 2003; Marchand-Brynaert *et al.,* 1999; Quirk *et al.,* 2001; Jeschke *et al.,* 2002; Neff *et al.,* 1999).

Hu and coworkers (2003) seeded osteogenic precursor cell (OPC) on PLA films and scaffolds modified with amino group ($-NH_2$), poly(L-lysine) (PLL), or RGD in tissue culture media. After 24 h of incubation, the results showed that the PLA film surface-modified with RGD showed better OPC cell attachment than the other films. The cells on the PLA scaffolds surface-modified with RGD also exhibited an increase

in alkaline phosphatase activity and calcium levels in comparison with those on other scaffolds.

Robin and coworkers (Quirk *et al.,* 2001) attached Gly-Arg-Gly-Asp-Ser (GRGDS) to poly(L-lysine) (PLL) and coated PLL-GRGDS composite on PLA surface. The modified PLA demonstrated a marked increase in spreading of bovine aortic endothelial cells over unmodified PLA.

2.3.4.3 Growth factors

Growth factors could be incorporated with biomaterials either within the fabrication of scaffolds or after the fabrication as a method of the surface modification.

As described in section 2.2.4, bone morphogenetic proteins (BMPs) have the ability to induce bone formation when implanted in a variety of mammalian species (Sampath *et al.,* 1990; Urist *et al.,* 1983; Wang *et al.,* 1988; Wang *et al.,* 1990; Wozney *et al.,* 1988). By delivering BMP molecules directly to the biaomaterials or scaffolds surface, bone formation may be promoted.

Kokubo and coworkers (2003) impregnated PLGA-coated gelatin scaffold with various concentrations of rhBMP-2 and treated the bone defect in rabbits. The results showed that all defects treated with rhBMP-2 were repaired, while neither untreated nor implanted PLGA-coated gelatin scaffold alone showed radiographic union.

Gao and coworkers (Gao *et al.,* 1996) coated naturally occurring sheep bone morphogenetic protein (sBMP) and type IV collagen on a tricalcium phosphate cylinder (TCP). TCP cylinders coated with type IV collagen alone were used as control. The results from implant experiments showed a healing superiority of the segmental bone defects replaced by the implants in the group with sBMP/collagen coating.

Besides BMPs, other growth factors were also used in the surface modification. For example, TGF-β1 was loaded on collagen scaffolds to promote repair in skull defects of rabbits (Ueda *et al.,* 2002).

Park and coworkers (2000) coated platelet-derived growth factor-BB (PDGF-BB) on chitosan scaffolds by soaking chitosan sponges into the PDGF-BB solution. The results showed that PDGF-BB-coated chitosan sponge induced significantly high cell attachment and proliferation level, which demonstrated rapid calcification and marked increase in new bone formation, and indicated good cellular adaptability.

2.3.4.4 Other polymers

Some natural polymer have been also investigated with regard to the effects on surface modification. Researchers (Cai *et al.,* 2002a&2002b; Yohko *et al.,* 1998; Gotoh *et al.,* 1997) reported that silk fibroin could benefit fibroblasts cell viability, growth and functions.

Chitosan is a biodegradable natural polymer, widely used in biomedical fields. Cai and coworkers (2002c) used it to modify the surface of poly (D,L-lactic acid)

(PDLLA). The results showed that the ALP activity and osteoblasts proliferation on modified PDLLA films were significantly higher than those found on the control.

Yokota and coworkers (2001) coated a gelatin scaffold with poly(D,L-lactic-co-glycolic acid) to mechanically reinforce the gelatin framework.

2.3.5 Combined methods

Each surface modification approach has its advantages and drawbacks. For example, increased surface energy could improve the cell adhesion. However, it may increase also the adhesion of other unnecessary cells. Just like composite materials could combine the best characteristics of each component material, combination of various surface modification methods may also achieve better effectiveness than either method alone.

Yang and coworkers (2002b) modified the surface of poly (D,L-lactide) (PDLLA) by combining plasma treatment and collagen modification. The results showed that cell affinity of PDLLA modified by combining treatments was greatly improved. They believed that plasma pre-treatment could improve the roughness and incorporated polar groups and positively charged groups onto the sample surface, so the plasma pre-treated surface would benefit in anchoring more collagen tightly.

Even with the above surface modification methods, there are still much room for improvement. In this thesis research, surface modification is the focus. We endeavor to improve the efficiency of some of the existing surface modification methods and to integrate various surface modification methods to combine their

advantages. For example, we carry out the biomimetic process in the flowing condition. We also combined a physicochemical method with a biochemical method, namely, apatite coating with collagen immobilization.

CHAPTER 3

EXPERIMENTAL AND METHODS

3.1 Materials

PLLA with an inherent viscosity of approximately 7.11 dl/g was purchased from PURAC (PURAC, Netherlands). Chloroform and dioxane used for dissolving PLLA, and all the analytical grade chemicals for making SBF were purchased from Acros (Acros Organics, Belgium). Phosphate buffer saline (PBS) tablets were supplied by Zymed (Zymed Laboratories Inc, CA). Collagen was obtained from Tsinghua University (Tsinghua University, China). The osteoblast-like cells, Saos-2 cells, were supplied by American Type Culture Collection (ATCC, USA).

The sheet of fibrous nonwoven PGA scaffold with a nominal bulk density of 60.4mg/cc (a porosity of about 95%) was commercially available (US Surgical, USA). PGA scaffold were cored out into small discs of 6mm diameter and 2mm in thickness.

3.2 Fabrication of PLLA films and scaffolds

3.2.1 Fabrication of PLLA films (Figure 3.1):

It is relatively easier to examine the coating on flat substrate than that within the porous scaffold. PLLA films were fabricated and used as the substrate for the coating studies. The results of the coating on film could give some instructive cues for our later study of coating onto scaffold.

To make PLLA films, PLLA particles (1g) were dissolved in 40 ml of chloroform. The mixture was stirred at 50℃ for at least 4h to obtain a homogeneous polymer solution. This solution was transferred to a 90mm-diameter glass plate to form a film by evaporation in air at 24℃ in a fume hood. PLLA films with an even thickness (~0.1mm) were finally obtained. PLLA films were cut using a blade into rectangular specimens with dimensions of 15mm×10mm.

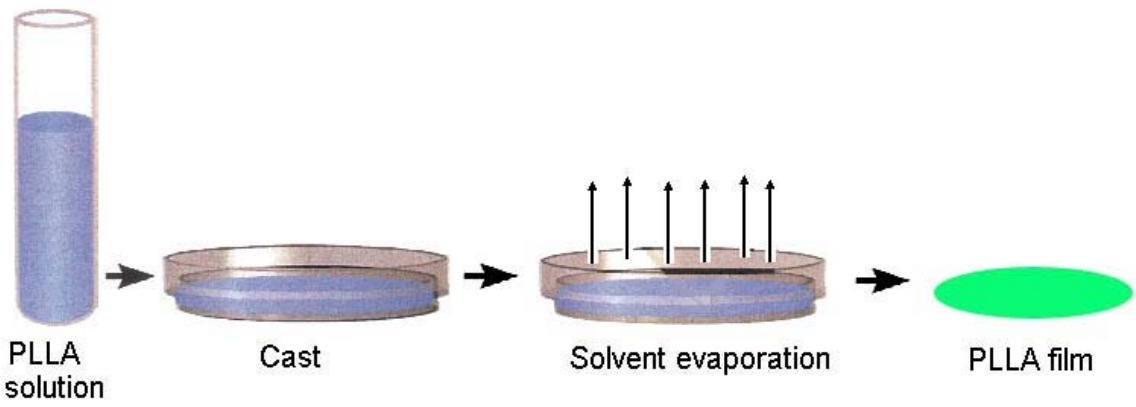

Figure 3.1 *Schematic illustrating the fabrication of PLLA films*

3.2.2 Fabrication of PLLA scaffolds (Figure 3.2)

PLLA scaffold was prepared by solid-liquid phase separation of polymer solutions and subsequent sublimation of solvent. PLLA granules were dissolved in dioxane to make a solution with the concentration of 2.5% or 5%. The mixture was stirred at 50℃ for at least 4h to obtain a homogeneous polymer solution. The beaker containing the solution was rapidly transferred into a freeze dry system (Labconco corporation, USA) at a preset temperature(-20℃) to solidify the solvent and induce solid-liquid phase separation. The solidified mixture was maintained at that temperature for 2h. Then the temperature was adjusted to -8℃ and vacuum pump was

started. The samples were freeze dried at about 20Pa for at least 3 days to remove the solvent.

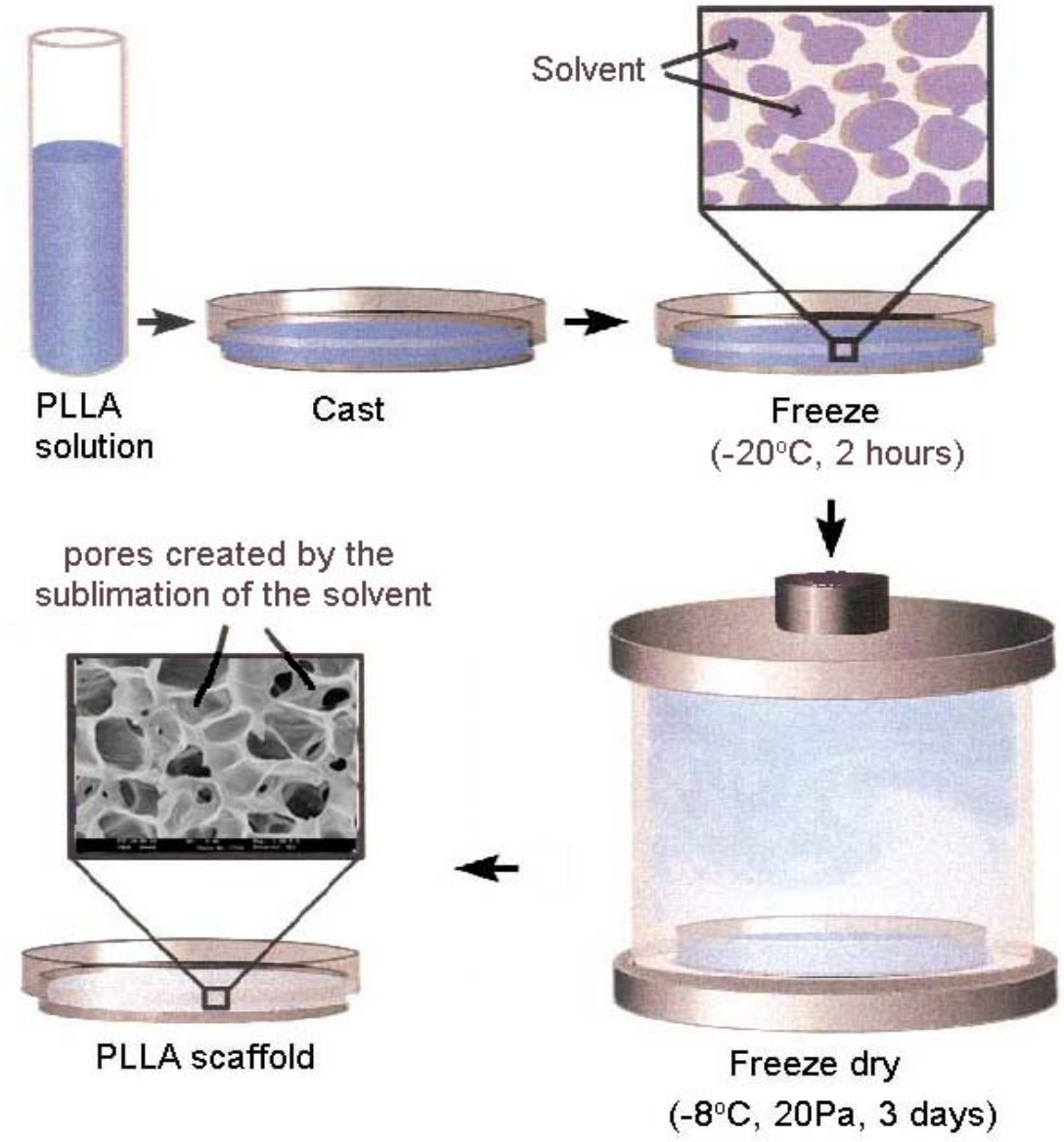

Figure 3.2 *Schematic of fabrication of PLLA scaffolds*

3.3 Surface modification of PLLA films and scaffolds

3.3.1 Plasma treatment

The N_2 gas plasma treatment was carried out on Samco Plasma Deposition (Model PD-2, 13.56 MHz). PLLA film (15mm×10mm×0.1mm) was placed over the electrode in the plasma chamber. After the pressure in the chamber had equilibrated at an appropriate value, a glow discharge plasma was generated for a predetermined duration.

3.3.2 Apatite coating by an accelerated biomimetic process

5 times simulated body fluid (5SBF): SBF with nearly 5 times of the inorganic ion concentrations of human blood plasma was prepared by dissolving NaCl, $NaHCO_3$, Na_2SO_4, KCl, K_2HPO_4, $MgCl_2{\cdot}6H_2O$, and $CaCl_2{\cdot}2H_2O$ in distilled deionized water. Solution pH value was adjusted to 6.4 with HCl and Tris to increase the solubility of chemicals. The concentration of the ions were 710.0 mM Na^+, 25.0 mM K^+, 12.7 mM Ca^{2+}, 7.7 mM Mg^{2+}, 739.7 mM Cl^-, 21.0 mM HCO_3^-, 5.0 mM HPO_4^{2-} and 2.5 mM SO_4^{2-}, respectively.

Reference Solutions: Reference Solution-1 was distilled deionized water. Its pH value was adjusted to 6.4, the same as the 5SBF solution, with HCl and Tris. SBF with 1.5 times of the inorganic ion concentration of human blood plasma was prepared as Reference Solution-2. The solution was buffered at a pH value of 7.4 with HCl and Tris. The concentration of the ions were 213.0 mM Na^+, 7.5 mM K^+, 3.8 mM

Ca^{2+}, 2.3 mM Mg^{2+},221.9 mM Cl^-, 6.3 mM HCO_3^-, 1.5 mM HPO_4^{2-} and 0.75 mM SO_4^{2-}, respectively.

Phosphate Buffered Saline (PBS) solution: The PBS solution was prepared by dissolving PBS tablet with distilled deionized water. The PBS solution contained 10mM phosphate, 150mM sodium chloride, pH 7.2 to 7.3.

Incubation in test solutions: Three rectangular PLLA film specimens with dimensions of 15mm×10mm×0.1mm were immersed in 50mL 5SBF in a plastic bottle in a shaker bath set at 60rpm with the temperature maintained at 37^{o}C. After being incubated for various periods of time, the specimens were removed from the 5SBF solution, washed carefully with distilled deionized water to remove the soluble inorganic ions, and dried in air. The rectangular PLLA scaffold specimens (7mm×5mm×2.2mm) and the PGA scaffold specimens (6mm diameter, 2mm thickness) were treated in the same process (three specimens in 50mL 5SBF) except for being dried at -10^{o}C under a vacuum. Incubation of PLLA films, PLLA scaffolds, and PGA scaffolds in the reference solutions was also conducted in the same way.

3.3.3 Apatite/collagen composite coating

5SBF with collagen (5SBFC): Collagen (Type I) was dissolved in malonic acid solution with stirring for at least 2 hours to achieve a homogeneous solution. It was then mixed with SBF solution. Solution pH value was also adjusted to 6.4 with HCl and Tris. The chemical compositions of 5SBF and 5SBFC were summarized in table 3.1.

Table 3.1 *Compositions and ion concentrations (mM) of 5SBF and 5SBFC*

	Na^+	K^+	Ca^{2+}	Mg^{2+}	Cl^-	HCO_3^-	HPO_4^{2-}	SO_4^{2-}	malonic acid	collagen
5SBF	710.0	25.0	12.7	7.7	739.7	21.0	5.0	2.5	/	/
5SBFC	710.0	25.0	12.7	7.7	739.7	21.0	5.0	2.5	3g/L	1g/L

Incubation: Three rectangular PLLA films (15mm×10mm×0.1mm) were immersed in 50mL 5SBF or 5SBFC in a plastic bottle in a shaker bath set at 60rpm with the temperature maintained at 37℃. After 24 hours of incubation, the specimens were taken out, washed carefully with distilled deionized water to remove the soluble inorganic ions, and dried in air. The rectangular PLLA scaffold specimens (7mm×5mm×2.2mm) were treated in the same process except for being dried at -10℃ under a vacuum.

3.3.4 Apatite coating in the flowing condition

Two discs of PLLA scaffolds with 10mm diameter and 10mm thickness were placed in a flow system [Figure 3.3]. Five hundred milliliters of 5SBF were added into the system. All of the system was kept at 37℃. The flow rate of the 5SBF solution passing through one PLLA scaffold was about 0.1625 mL/min. After incubation for 24 hours, PLLA scaffolds were removed from the system, washed carefully with distilled deionized, and dried at -10℃ under a vacuum.

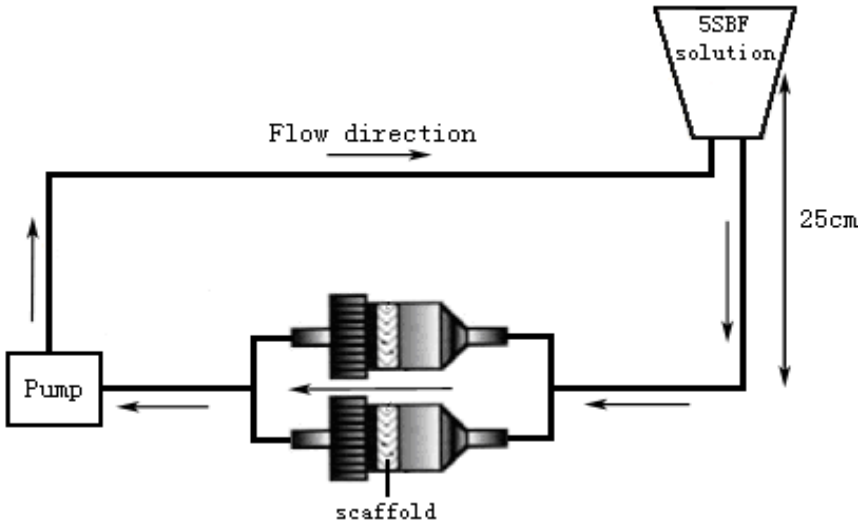

Figure 3.3 *Schematic illustrating the accelerated biomimetic coating process in the flowing condition.*

3.4 Cell seeding

Saos-2 osteoblast-like cells were cultured at 37^{o}C in a humidified atmosphere of 5% CO_2 in air, in flasks (90cm diameter) containing 10ml Dulbecco's modified Eagle's medium (DMEM; Gibco), 5% fetal bovine serum (FBS; Gibco) and 1% penicillin/streptomycin. The medium was changed every third day. After 7-day culture, the Saos-2 cells were removed from the culture dish using trypsin, centrifuged and resuspended in DMEM medium to adjust cell density to 4×10^5 cells/ml. 100ul (about 4×10^4 cells) of the cell suspensions were placed on the samples and cultured for 4h before 0.9 ml culture medium was added into each well. The plate was incubated at a temperature of 37^{o}C in a 5% CO_2 atmosphere. The medium was changed every 2 days. After incubation, any non-adherent cells on the samples were removed by aspirating the medium and washing with PBS solution.

3.5 Characterization

3.5.1 Characterization of samples without cell

3.5.1.1 Contact angles of films

To investigate the wettabilities of the PLLA film without and with coating, contact angles were measured using the sessile drop method and an image analysis system. The water droplet was about 1uL. Each determination was obtained by averaging the results of three measurements.

3.5.1.2 Porosity of scaffolds

The porosity was measured by liquid displacement using a mercury intrusion porosimeter. The morphology of scaffolds was viewed under a LEICA scanning electron microscope (Model Stereoscan 440) after being coated with gold.

3.5.1.3 Mechanical properties

Biomechanical tests of PLLA scaffolds were preformed using the Instron 5569 Table Mounted Materials Testing System (Instron Corp., USA) with a 500N load cell. The PLLA scaffolds samples were all soaked in the PBS solution during testing. The crosshead speed was 0.5mm/min. A fixed small tare-deformation was applied to each of the samples to ensure the scaffold surfaces were in contact with the load cell at the

beginning of test. The compressive modulus was defined as the initial linear modulus. Six specimens were tested for each group.

Biomechanical tests of PGA scaffolds were performed in a MTS 858 Mini Bionix (MTS System Corporation, USA) with a 5N load cell. The PGA scaffold samples were all soaked in the PBS solution during testing. The crosshead speed was 0.5 mm/min. A fixed small tare deformation was applied to each of the samples to ensure the scaffold surfaces were in contact with the load cell at the beginning of the test. The compressive modulus was defined as the linear modulus for the initial 10% strain. Six specimens were tested for each group.

3.5.1.4 Scanning electron microscopy (SEM)

The apatite formed on the PLLA film and PLLA scaffold were viewed under a LEICA scanning electron microscope (Model Stereoscan 440) after being coated with gold.

3.5.1.5 Energy dispersive X-ray spectroscopy (EDX)

EDX was obtained without gold coating. Randomly selected areas of about 1mm×1mm on the surface were examined for different incubation conditions.

3.5.1.6 X-ray diffraction (XRD)

XRD spectra were obtained using a Philips X-ray diffractometer with a fixed incidence of 1^{o} in the range of $10\text{-}40^{o}$ using 0.06^{o} step and 1s/step scan speed.

3.5.1.7 Fourier transform infrared spectroscopy (FTIR)

The transmission spectra of the samples were measured with a Perkin-Elmer FTIR Spectrometer. A small amount of coating was scratched from the substrate surface. It was then milled with potassium bromide (KBr) and pressed into a transparent film for FTIR analysis. PLLA films were cut into fine particles. Small amount of them were also milled with KBr and pressed into thin film for FTIR analysis.

3.5.1.8 pH value

pH measurements of the 5SBF solution were conducted at equal intervals during the incubation period. Three readings were taken each time.

3.5.1.9 Mass changes

The mass changes of the samples after incubation in 5SBF and reference solutions were measured using an analytical balance (accuracy: 0.1mg). Six specimens were measured for each incubation condition to obtain an averaged result.

3.5.2 Characterization of samples with cell

3.5.2.1 Cell morphology

The samples, after having been cultured for a predetermined period, were taken out of the culture plates and washed with PBS three times. Thereafter, the

samples were fixed with 3% glutaraldehyde in PBS for 24 hours at 4^{o}C. After being thoroughly washed with PBS, samples were dehydrated sequentially in 30,50,70,80,90,95,100% ethanol. Samples were dehydrated twice in ethanol, each for about 15 min. The fixed samples were freeze-dried, sputter-coated with gold, and examined under a LEICA scanning electron microscope (Model Stereoscan 440).

3.5.2.2 Cell attachment and proliferating assay

In the quantitative assay, the adherent cells after being cultured for a predetermined period were removed from the samples by trypsinization. The viable cells were counted using a hemocytometer. For each type of the substrates, 3 samples were used to obtain a mean value and standard deviation of the number of adherent cells.

3.5.2.3 The 3-(4,5-dimethylthiazol-2-yl)-2,5-diphenyltetrasodium bromide (MTT) assay

The MTT assay was used as a relative measure of cell viability. After the Saos-2 cells were cultured on films or scaffolds in 96-wells for 8 days, cell viability was evaluated using the MTT assay (Acros, Belgium), in which 20μL of MTT (5mg/L) was added to each well and incubated at 37^{o}C for 4h. The blue formazan reaction product was then dissolved by adding 150μL DMSO. The absorbance was measured using a microplate reader.

3.5.2.4 Alkaline phosphatase assay

Alkaline phosphatase activity was measured using an alkaline phosphatase assay kit (ZHONGSHENG BEIKONG, China). Cells were incubated on films in a 24-wells plate or on scaffolds in a 96-well plate for 8 days. After removing the culture medium, the cell layers were washed with PBS and then detached using trypsin/EDTA. After centrifugation, the cell pellets were washed with PBS and resuspended by vortexing them in 0.1ml (for films) or 0.025ml (for scaffolds) of deionized water with 0.1% Triton X-100. The cell pellets were disrupted via a cyclic freezing/thawing process. The prepared cell lysates were used to determine ALP activity according the manufacturer's instruction.

3.5.2.5 Statistical analysis

Experiments were run in triplicate per sample. All data were expressed as mean±standard deviation (SD) for n=3. Single factor analysis of variance (ANOVA) technique and post-hoc multiple comparison test were used to assess statistical significance of results. P values <0.05 were considered significant.

CHAPTER 4

RESULTS

4.1 Surface modification of PLLA films and scaffolds

4.1.1 Plasma treatment

A comparison of surface contact angles to water between the untreated and plasma-treated PLLA samples were listed in Table 4.1. It could be seen that the surface hydrophilicity of the PLLA films was improved by plasma treatment and the improvement was closely related to the treating parameters such as power, pressure and treating time.

Table 4.1 *Contact angle of PLLA films after plasma treatment*

gas	Condition			Contact angle θ H_2O (deg)
	Pressure(Pa)	Power(W)	Time(s)	(average of three samples)
control	-	-	-	62.4±2.6
N_2	15	400	30	28.9±1.8
N_2	15	400	120	23.9±2.5
N_2	15	200	30	21.4±1.3
N_2	15	200	120	12.4±1.9

The SEM micrographs of PLLA films before and after plasma treatment are shown in Figure 4.1. It could be seen that the surface of the control was almost smooth [Figure 4.1 (a)] and that of the sample treated with plasma [Figure 4.1 (b)] showed distinctly rough surface.

(a)

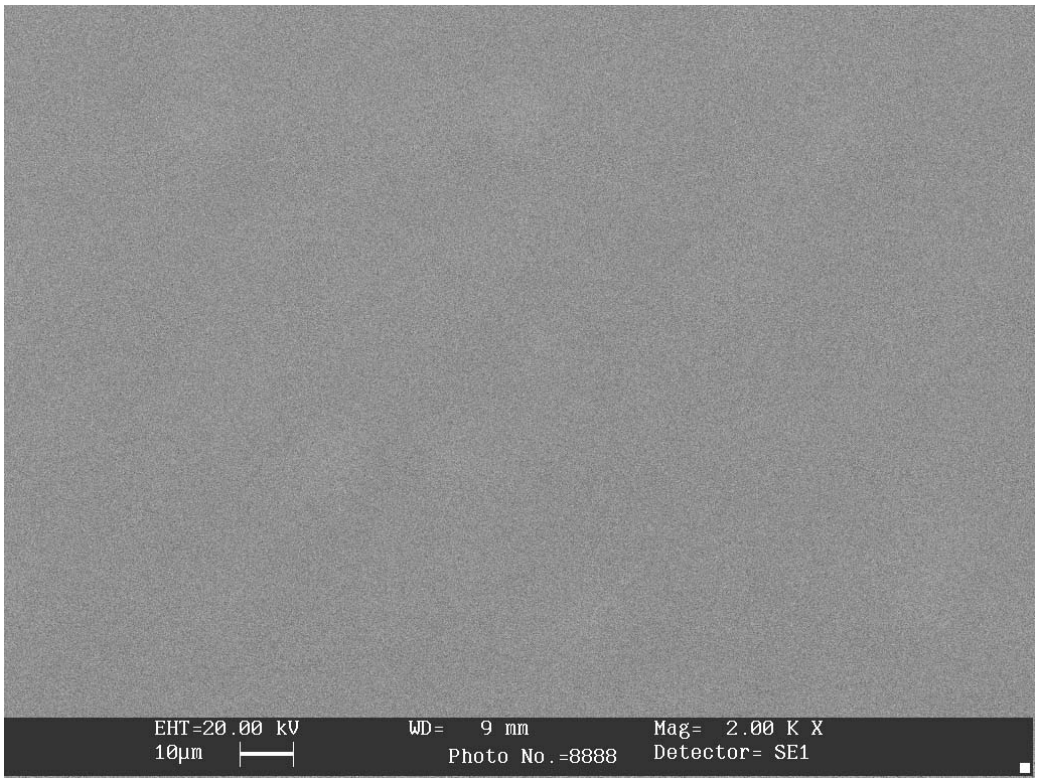

(b)

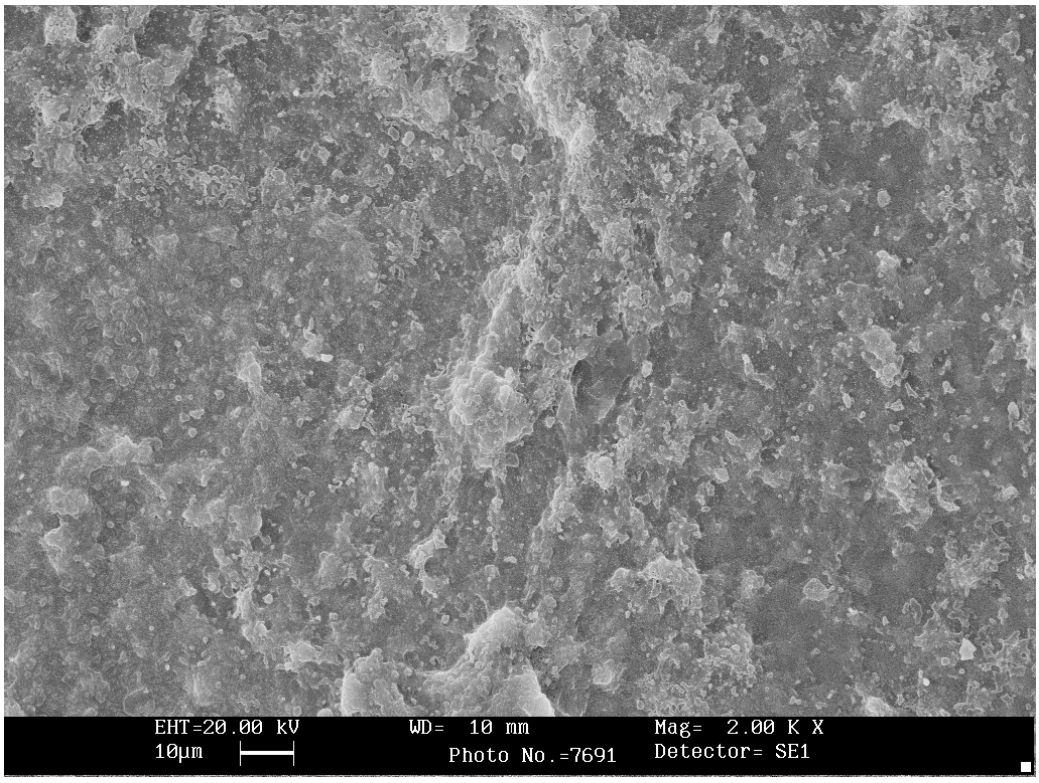

Figure 4.1 *SEM micrographs (original magnification 2000×) of PLLA films (a) control (b) after plasma treatment (Power: 400W; Time: 30s).*

4.1.2 Apatite coating by an accelerated biomimetic process

4.1.2.1 Morphology of apatite coating

I. Apatite coating on PLLA films

The PLLA films were incubated in 5SBF at 37^{o}C for 6, 12, 18, and 24 hours, respectively. The SEM micrographs of PLLA films before and after incubation are shown in Figure 4.2 and Figure 4.3.

The coating could be clearly seen on the films (Figure 4.2(b)-(e)) and it is obvious that its amount increased with incubation time. The whole surface of film was covered with microparticles after 24 hours of incubation time. However, in the classical biomimetic process (1.5SBF solution), little apatite deposition was observed on the surface of the PLLA film incubated for 24 hours (Figure 4.2(f)).

SEM micrographs at larger magnifications (Figure 4.3) exhibited clear apatite particles which assembled in small flake-like pieces. Few apatite microparticles were observed on the surface of PLLA films after 6 hours of incubation. Scattered particles with the size of less than 200nm were observed at 12 hours. After 18 hours of incubation, there were more particles, some of which joined together. At 24 hours, particles almost grew to a continuous layer with slightly bigger particle size (200–600nm). Because nucleation could occur during the whole process, there were some particles located on the former apatite particles after 18 hours of incubation (Figure 4.3(c)(d)).

(a)

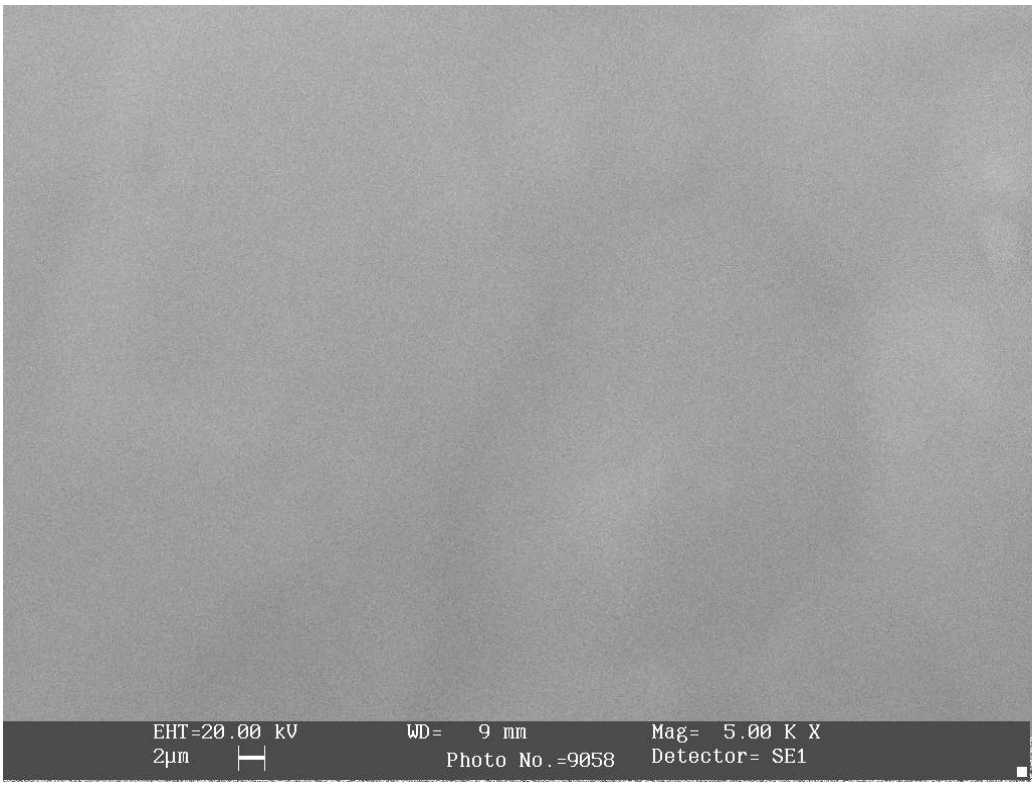

(b)

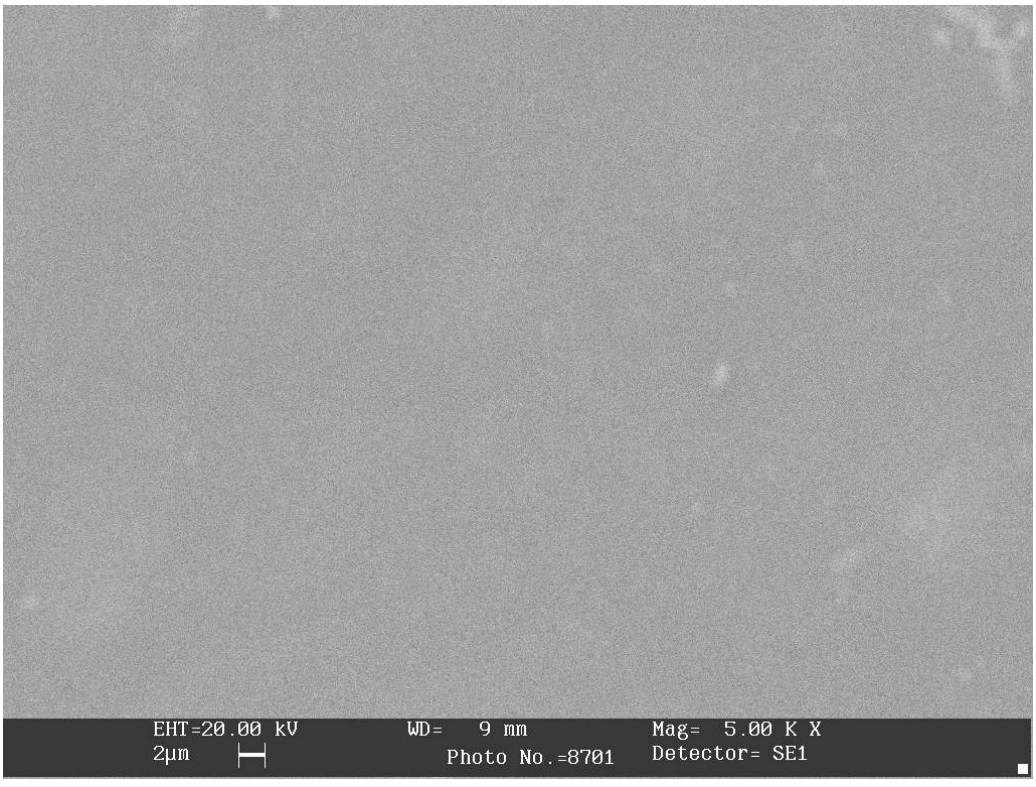

Figure 4.2 *SEM micrographs (original magnification 5000×) of PLLA films incubated in 5SBF for (a) 0 hour, (b) 6 hours. (c) 12 hours, (d) 18 hours, (e) 24 hours; and (f) in 1.5SBF for 24 hours.*

(c)

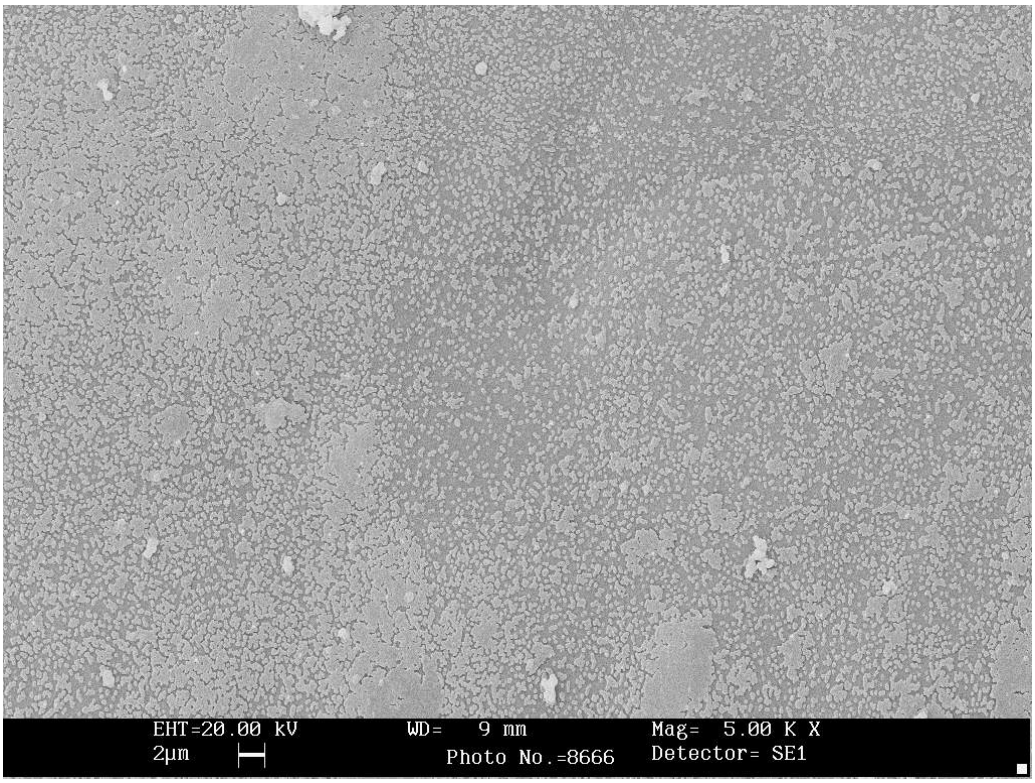

(d)

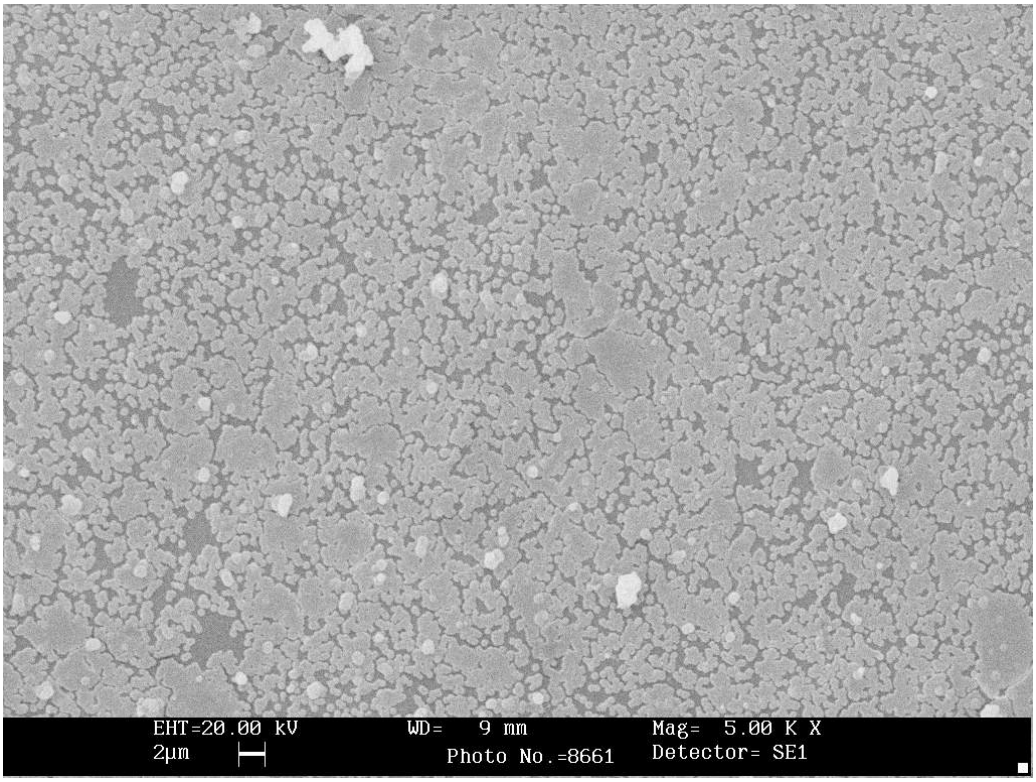

Figure 4.2 *(continued)*

(e)

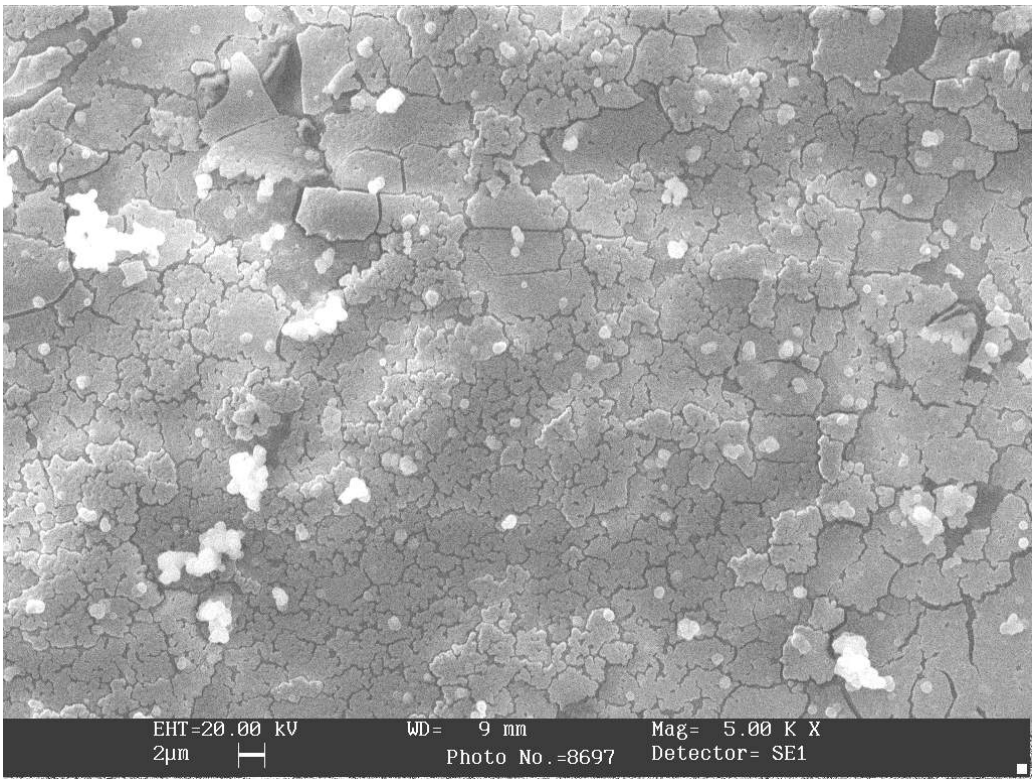

(f)

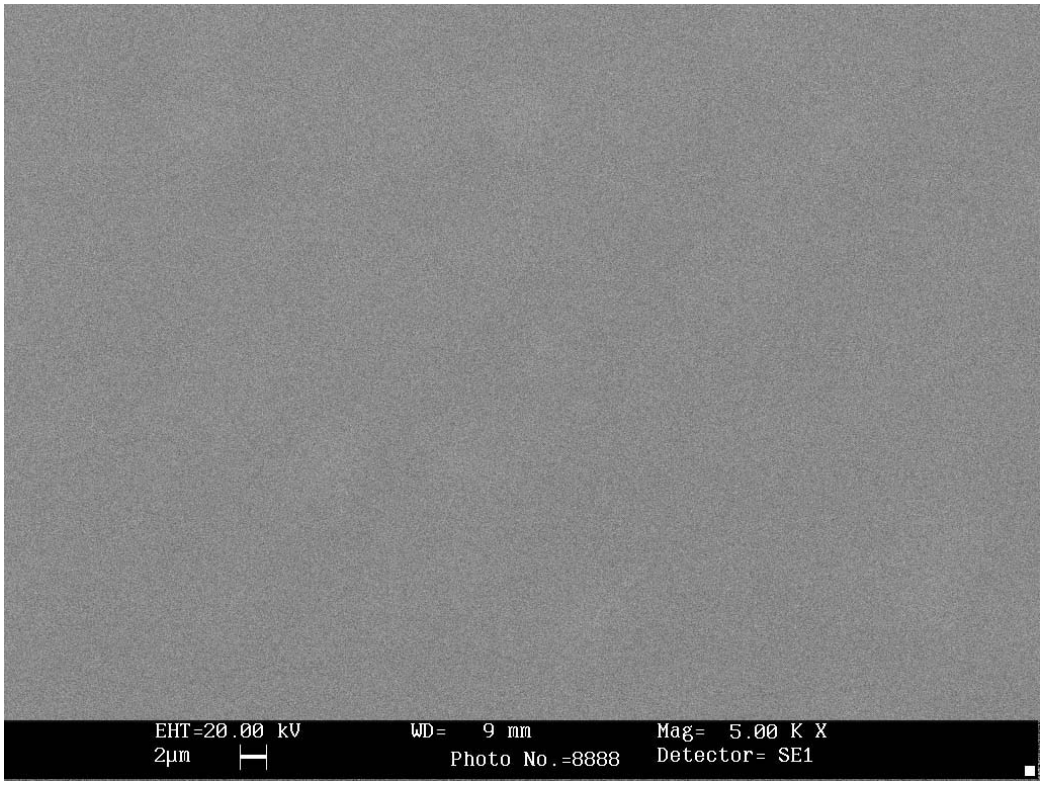

Figure 4.2 *(continued)*

(a)

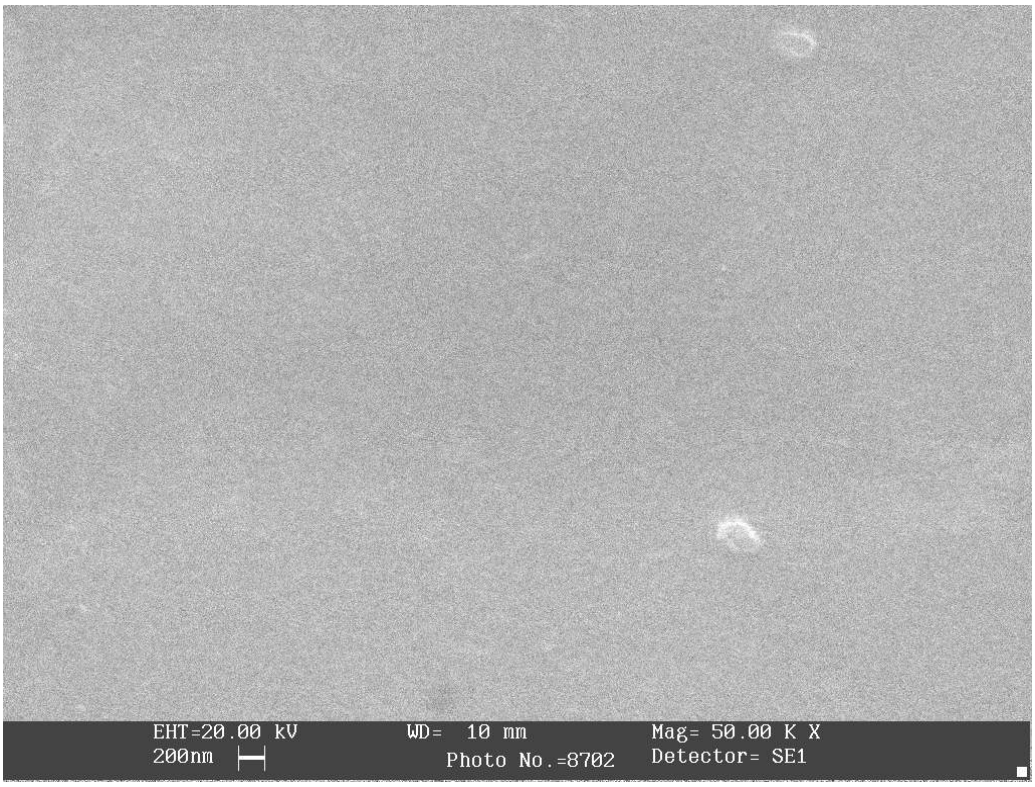

(b)

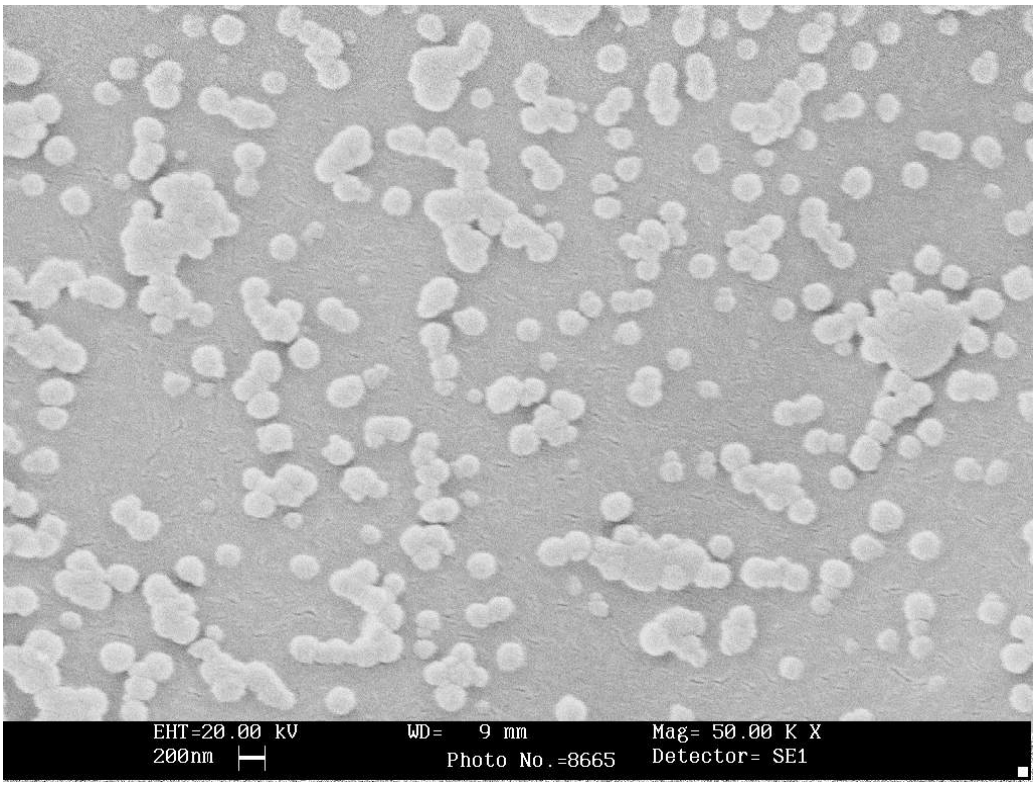

Figure 4.3 *SEM micrographs (original magnification 50,000×) of PLLA films incubated in 5SBF for various periods of time. (a) 6 hours; (b) 12 hours; (c) 18 hours; (d) 24 hours.*

(c)

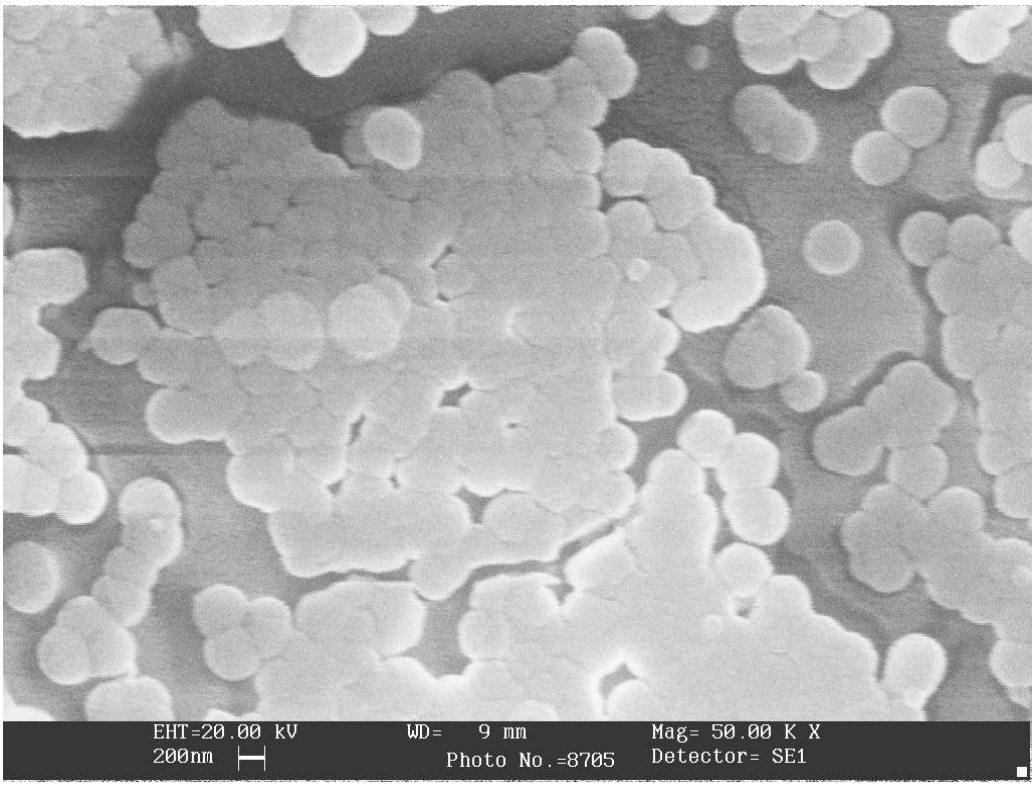

(d)

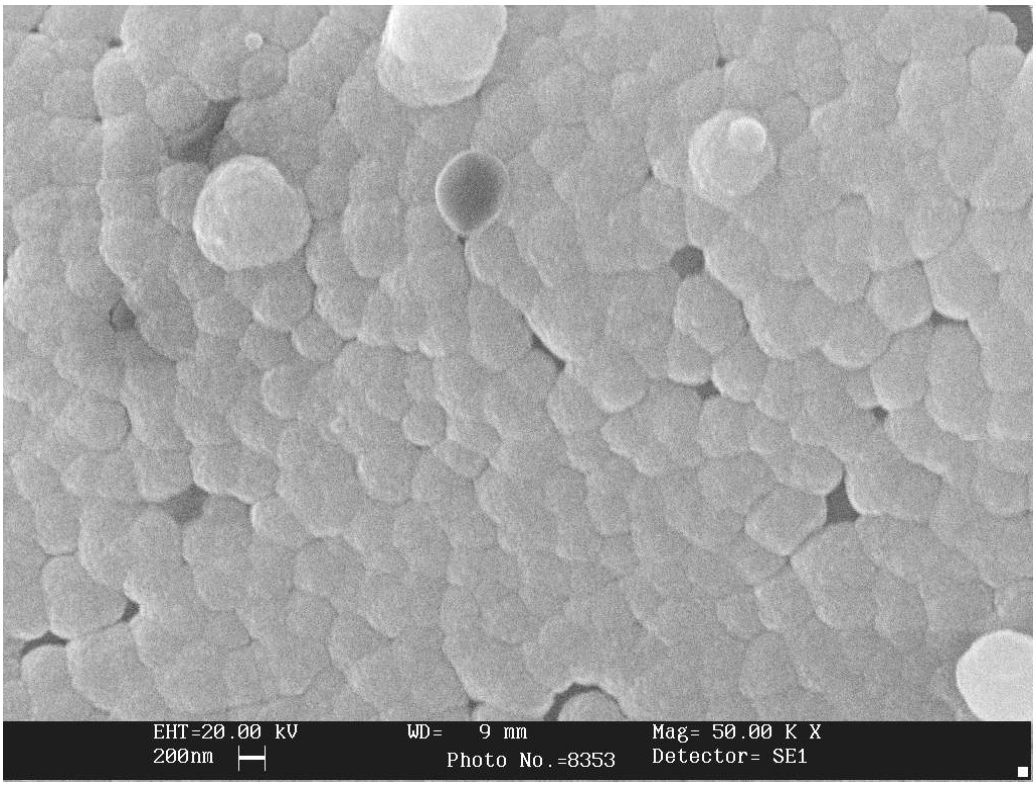

Figure 4.3 *(continued)*

II. Apatite coating on the PLLA scaffolds

PLLA scaffolds prepared from solid-liquid phase separation of the PLLA/dioxane solution were highly porous with an interconnected pore network (Figure 4.4(a), Figure 4.5(a)). For PLLA scaffolds with small pore size (20-30um), after 24 hours incubation, the coating could also be clearly seen on the pore walls near the surface. (Figure 4.4(b)-(d)). SEM micrographs at larger magnifications (Figure 4.4(d)) exhibited clear apatite particles which almost grew to a continuous layer with nano-scaled particle size (200–600nm). For PLLA scaffolds with big pore size (100-320um), apatite coating was also formed in 24 hours (Figure 4.5).

The microstructure of the coating formed on PLLA films and scaffolds in this accelerated biomimetic process was similar to those deposited on the surface of PLLA fibers (Yuan *et al.*, 2001), which our group have reported earlier and on PLLA films (Zhang and Ma, 1999a) reported by others using a classical biomimetic process.

III. Apatite coating on the PGA scaffolds

A large number of microparticles also formed on PGA non-woven fibrous scaffolds in 5SBF (Figure 4.6). However, the surfaces of scaffold fibers [Figure 4.6(b)(c)] were not completely covered after 24 hours of incubation. Inside the PGA scaffold [Figure 4.6(d)] relatively less particles were observed than near the surface [Figure 4.6(b)].

(a)

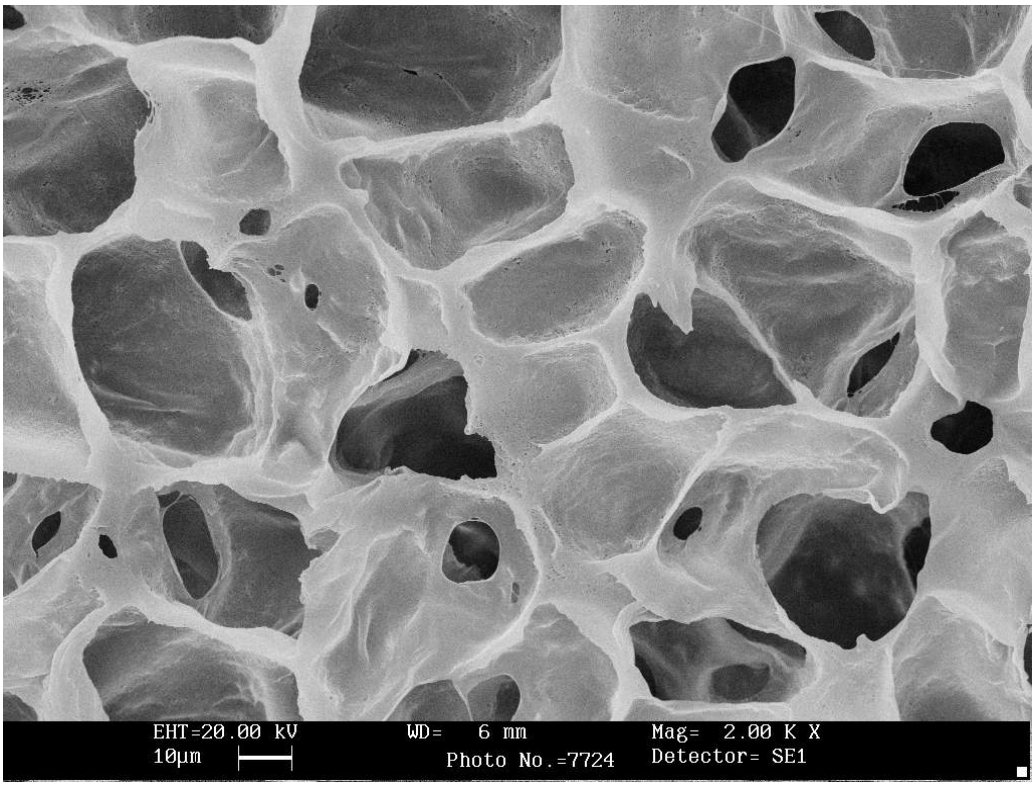

(b)

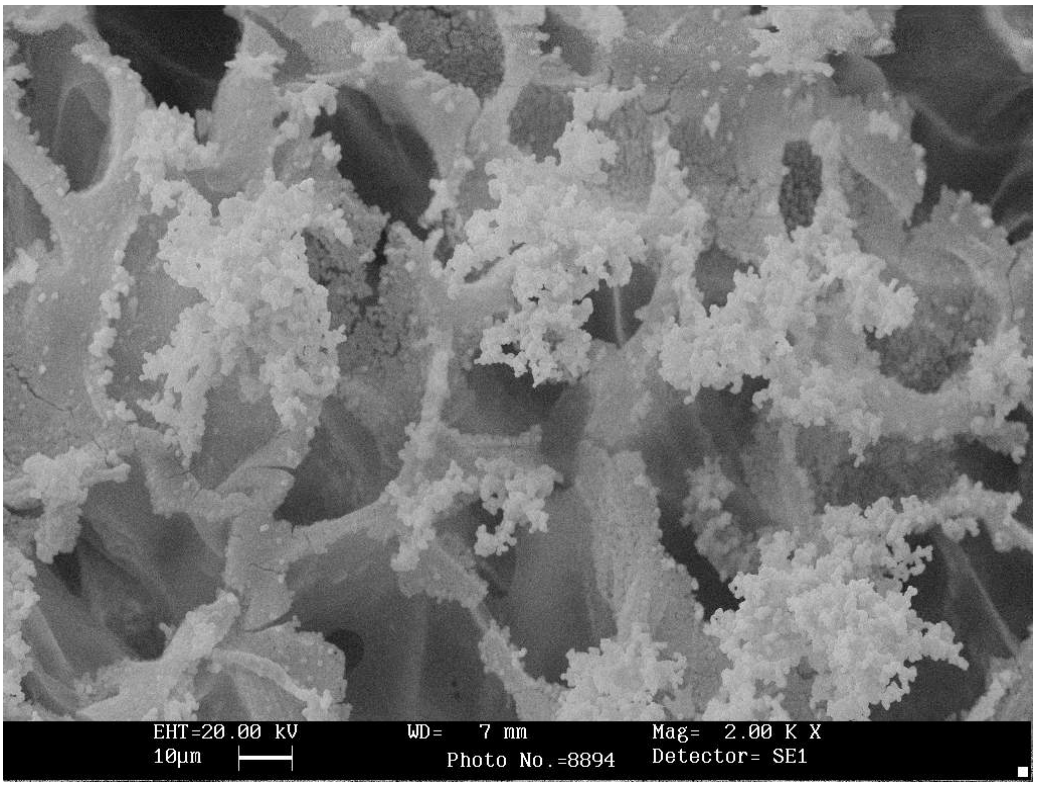

Figure 4.4 *SEM micrographs of the pore walls near the surface before and after incubating in 5SBF for (a) 0 hour, magnification 2000×; (b) 24 hours, magnification 2000×; (c) 24 hours, magnification 5000×; (d) 24 hours, magnification 20,000×.*

(c)

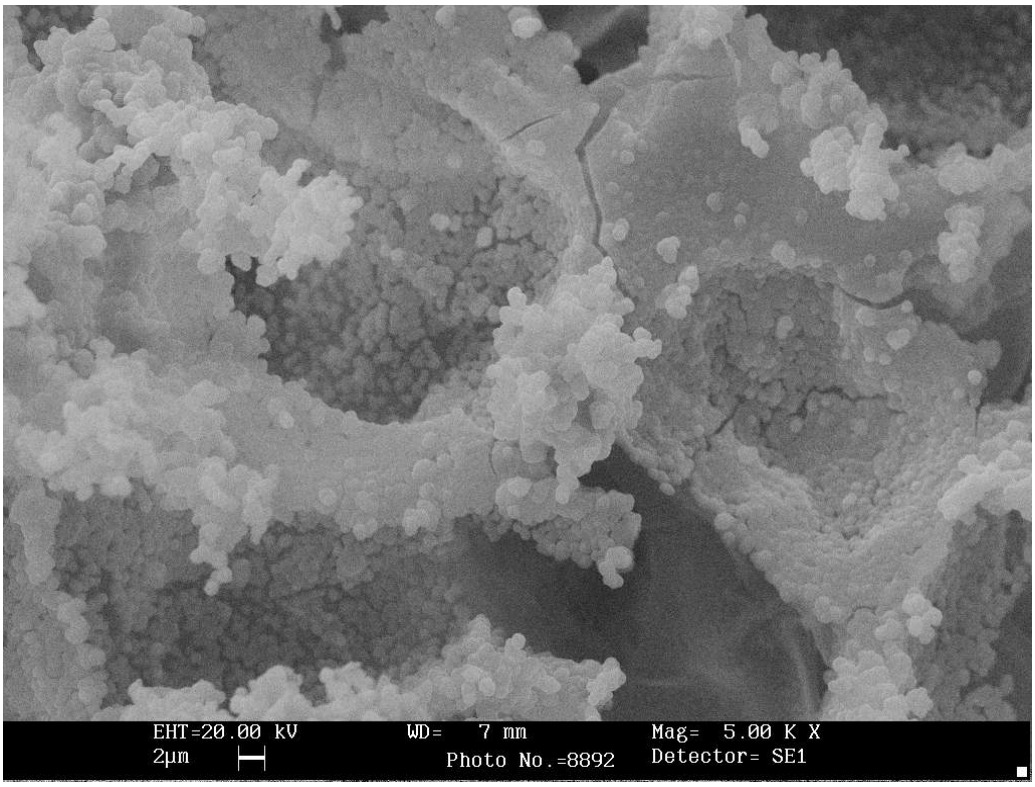

(d)

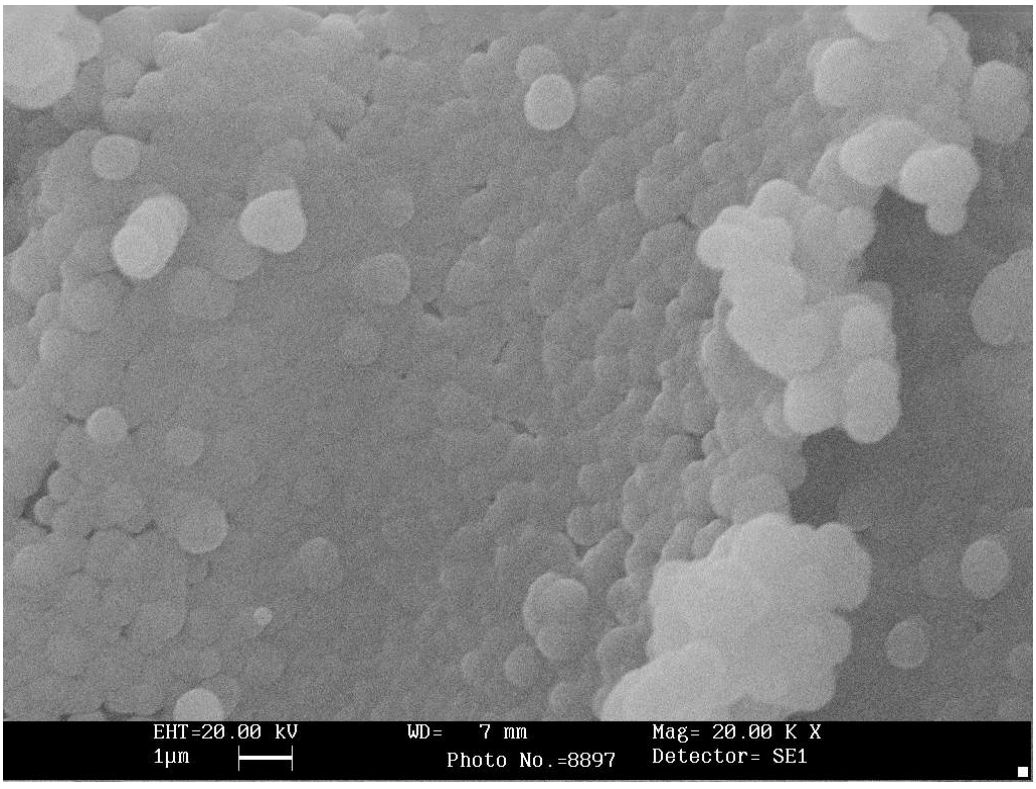

Figure 4.4 *(continued)*

(a)

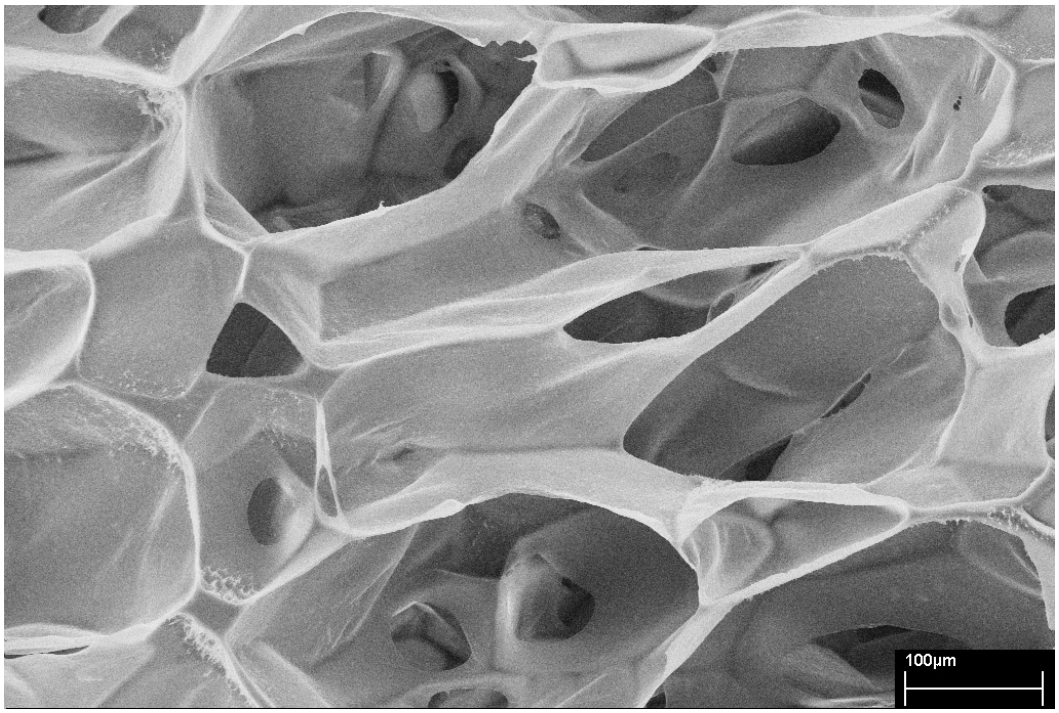

(b)

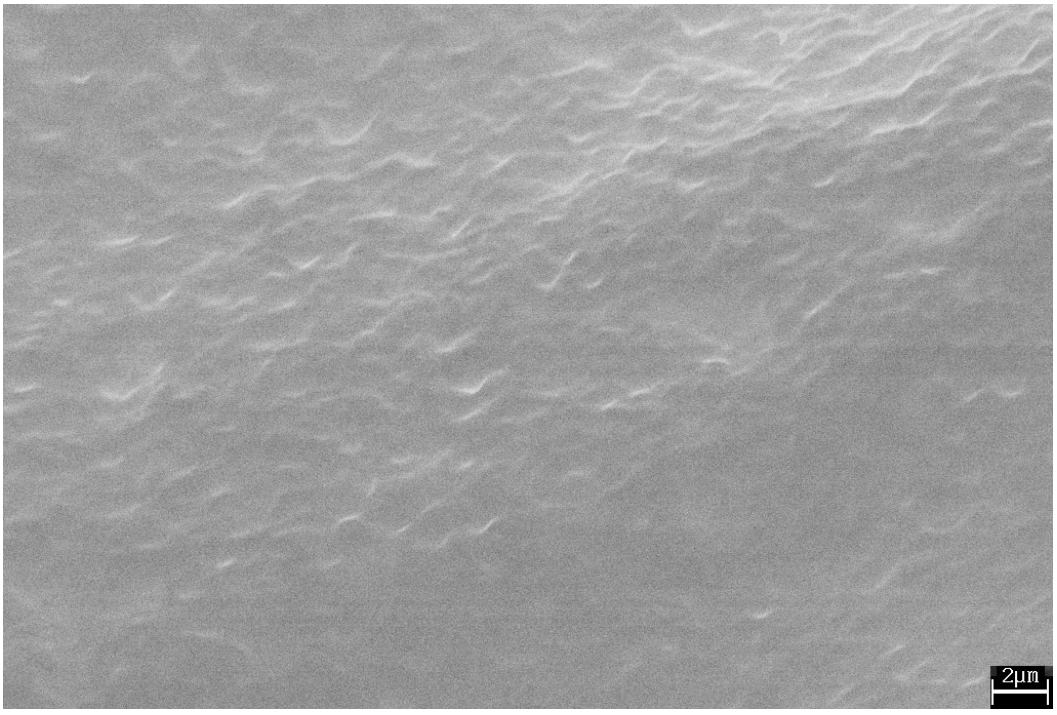

Figure 4.5 *SEM micrographs of PLLA scaffolds with big pore size (a) control, magnification 500×; (b) control, magnification 10,000×; (c) after incubating in 5SBF for 24h, 500×; (d) after incubating in 5SBF for 24h, magnification 10,000×;*

(c)

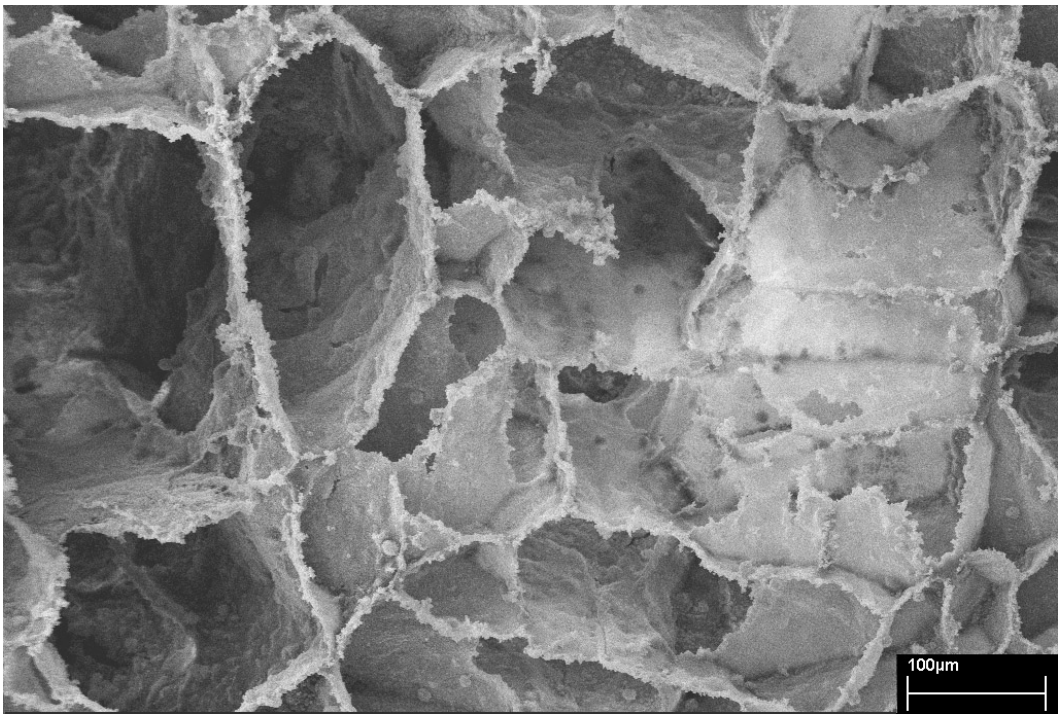

(d)

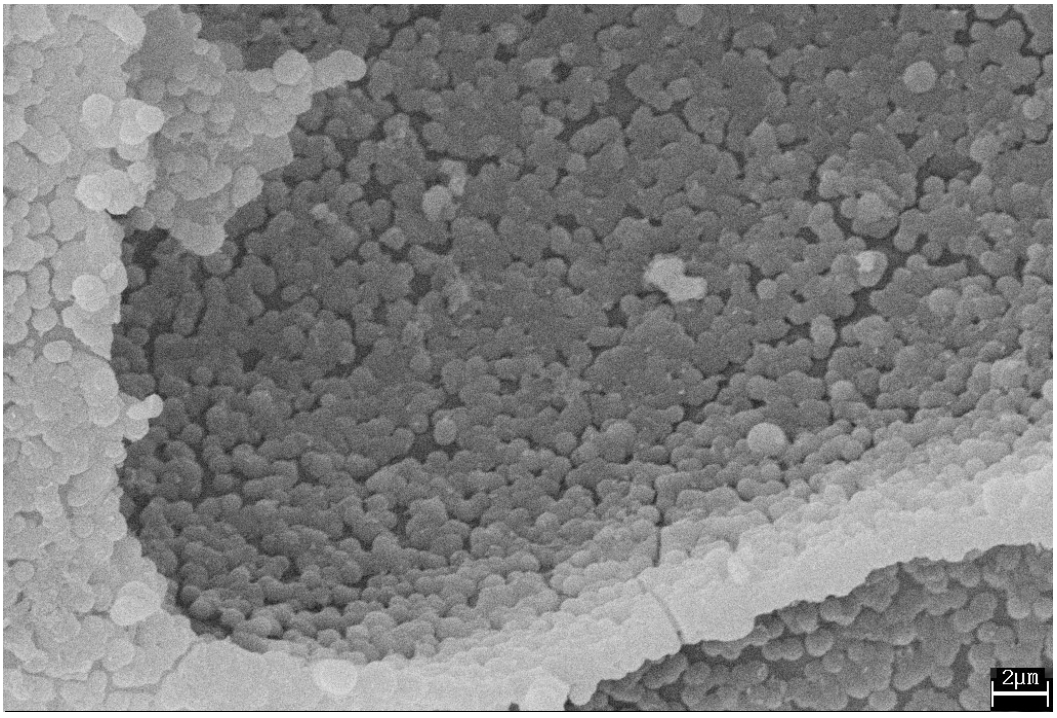

Figure 4.5 *(continued)*

(a)

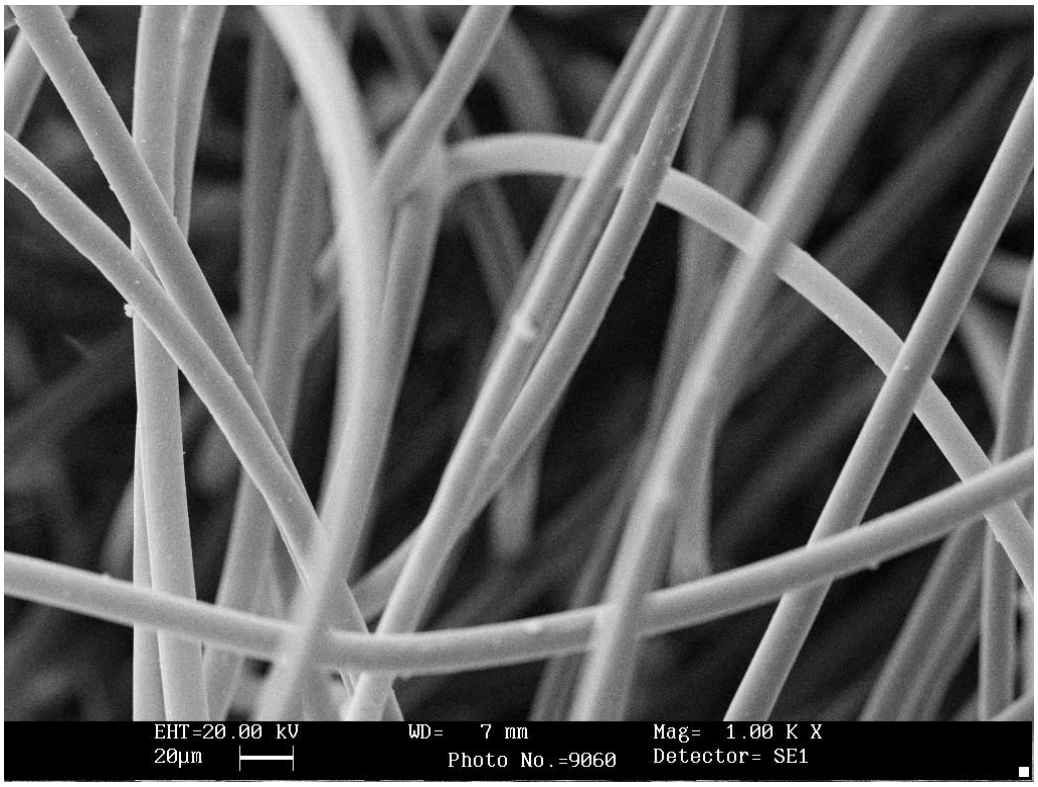

(b)

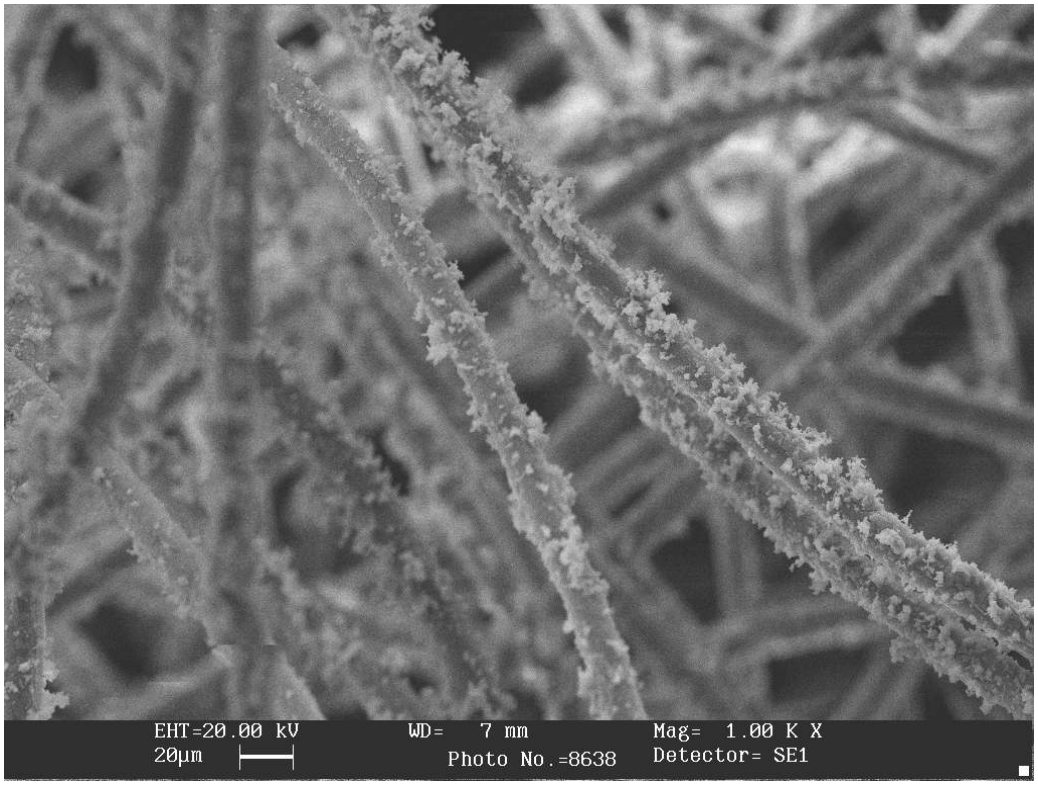

Figure 4.6 *SEM of none-woven fibrous PGA scaffolds before and after incubating in 5SBF for (a) 0 hour, surface, magnification 1000×; (b) 24 hours, surface, 1000×; (c) 24 hours, surface, 20,000×; (d) 24 hours, internal midsection, 1000×.*

(c)

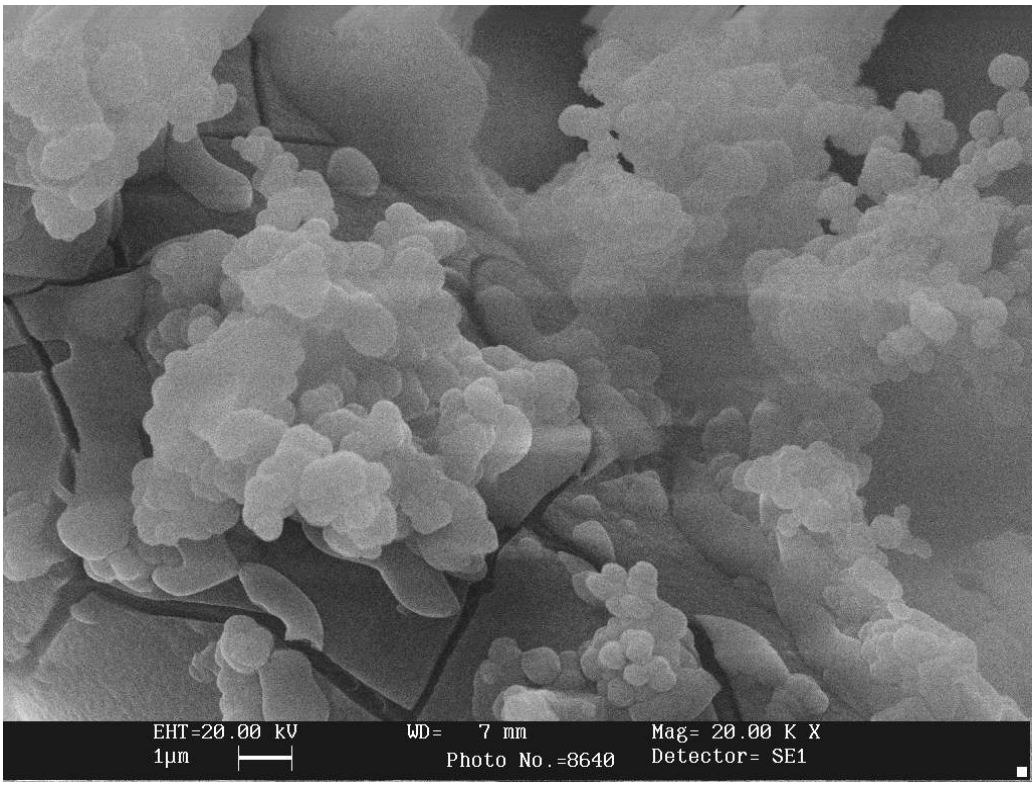

(d)

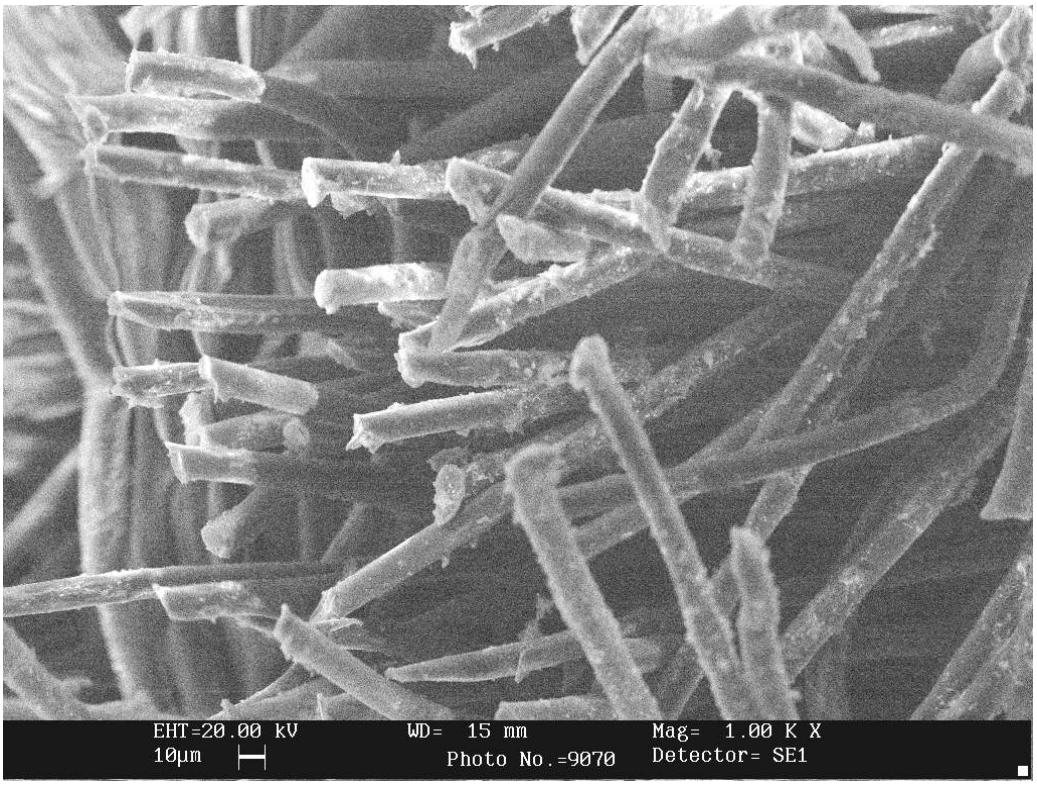

Figure 4.6 *(continued)*

4.1.2.2 EDX

EDX spectra of PLLA films with variable incubation time were shown in Figure 4.7 (a)-(e). It was shown that carbon and oxygen were the main elements of the PLLA film before incubation [Figure 4.7 (a)]. After incubation, the main elements were carbon, oxygen, calcium, and phosphorus [Figure 4.7 (b)-(e)]. Calcium and phosphorus could only be from the coating. EDX analysis also demonstrated that the calcium and phosphate contents increased with incubation time [Figure 4.7 (b)-(e)]. The Ca/P ratio was 1.06, 1.65, 1.31, and 1.32, respectively, after incubation for 6, 12, 18, and 24 hours. PLLA scaffolds and PGA scaffolds after 24 hours incubation was shown in Figure 4.8. The elements of calcium and phosphorus were also indicated after incubation. The calcium and phosphorus shown could only be from the coating.

4.1.2.3 XRD

The XRD patterns of PLLA film before and after incubation in 5SBF for 24 hours were shown in Figure 4.9. PLLA films [Figure 4.9 (A)] showed the characteristic peaks of PLLA (Brizzolara *et al.,* 1996). Besides the characteristic peaks of PLLA, PLLA films after incubation [Figure 4.9 (B)] also revealed the two characteristic peaks (25.9^{o}, $31.8\text{-}32.2^{o}$) of apatite. These peaks correspond to the (002) plane and (211)(112) planes of apatite, respectively (Abe et al., 1990). The XRD patterns of PLLA scaffolds before and after incubation in 5SBF (Figure 4.10) also revealed these differences. The XRD patterns of PGA scaffolds with coating (Figure 4.11(B)) also showed the characteristic peak ($31.8\text{-}32.2^{o}$) of apatite compared with PGA scaffolds control (Figure 4.11(A)). The 25.9^{o} peak of apatite was not obvious in the XRD patterns of PGA with coating. This may be because the broad peak (about $25\text{-}30^{o}$) of pure PGA covered this weak peak.

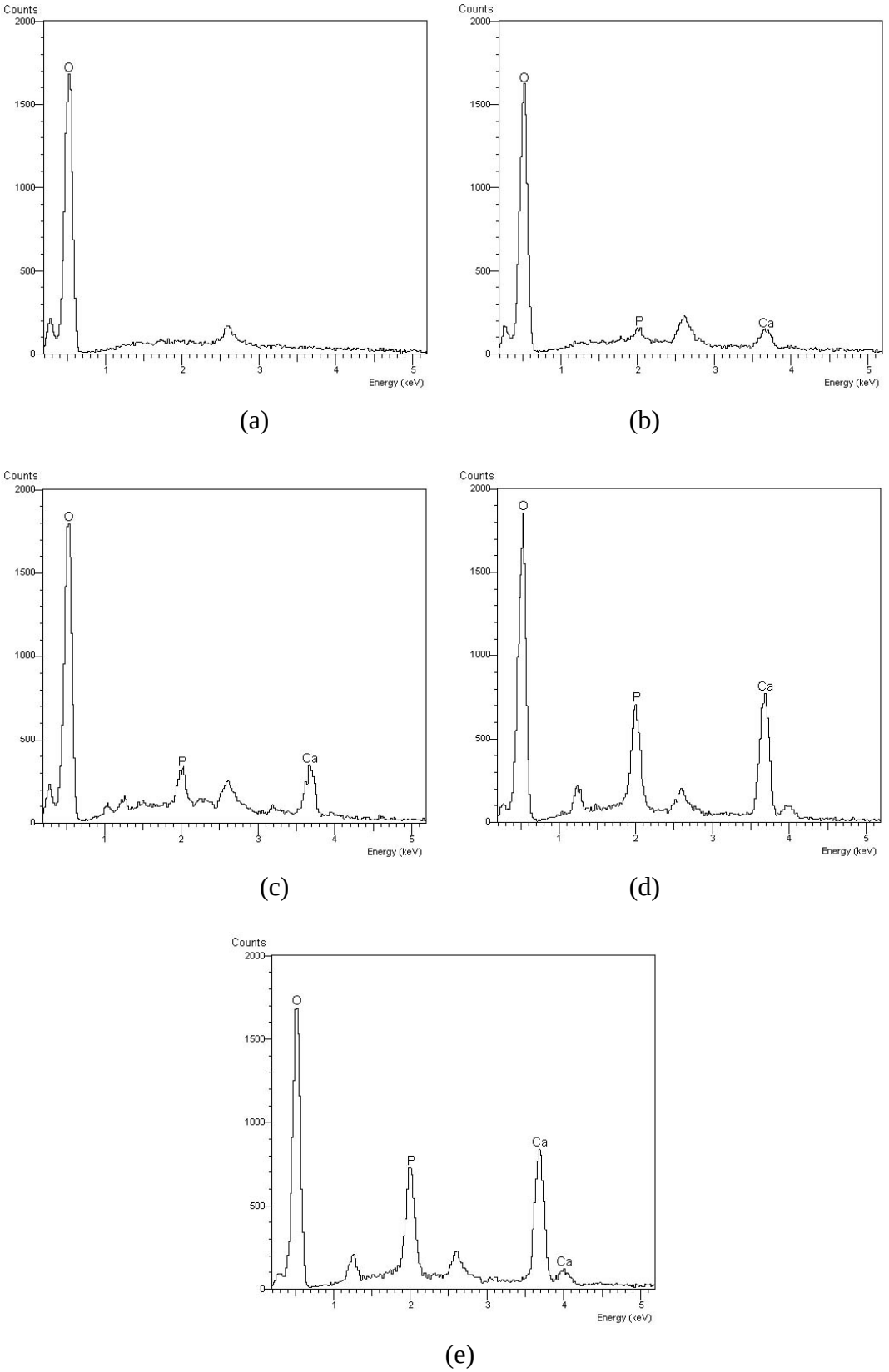

Figure 4.7 *EDX spectra of PLLA film incubated in 5SBF for (a) 0 hour, (b) 6 hours, (c) 12 hours, (d) 18 hours, (e) 24 hours.*

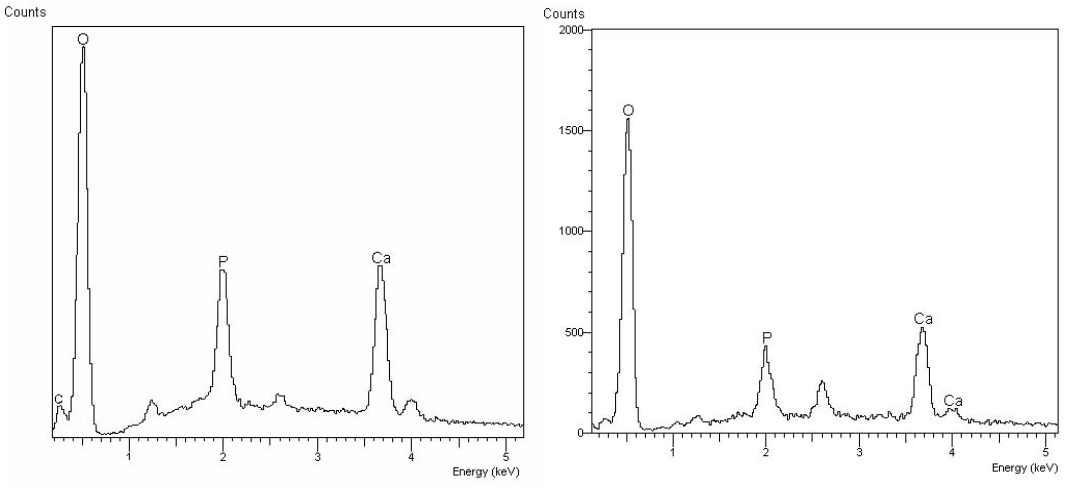

(a) (b)

Figure 4.8 *(a) PLLA scaffold with incubation time of 24 hours; (b) PGA scaffold with incubation time of 24 hours.*

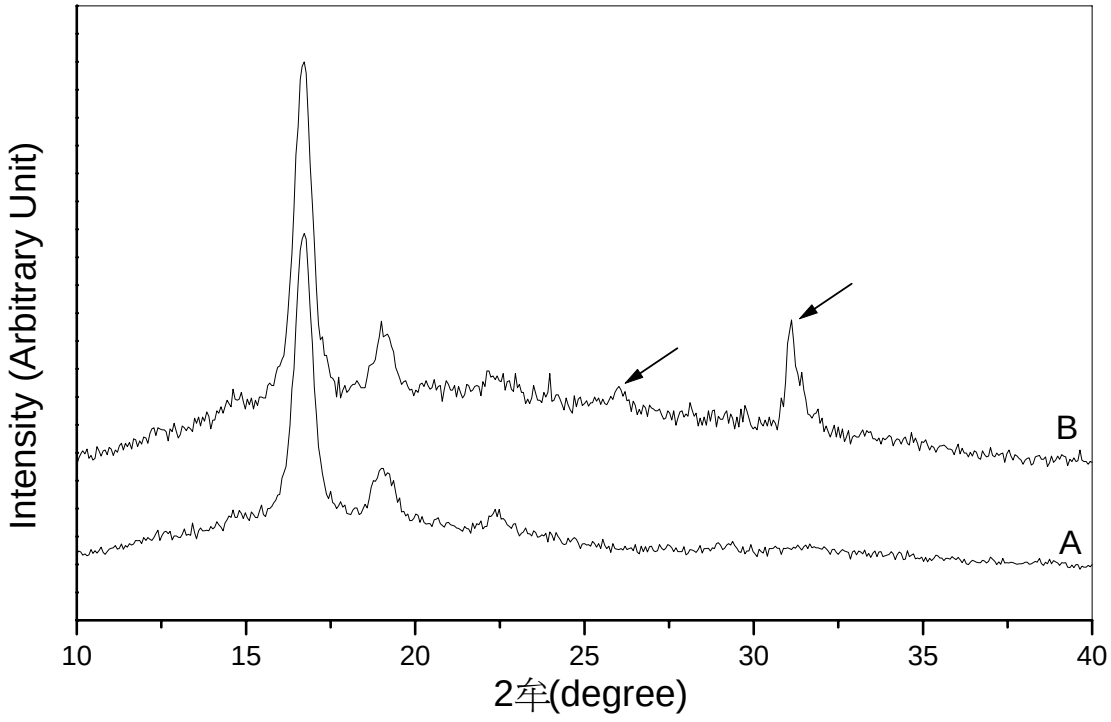

Figure 4.9 *X-ray diffraction patterns of (A) PLLA film (B) PLLA film incubated in 5SBF for 24 hours. The arrows indicate the characteristic peaks of apatite.*

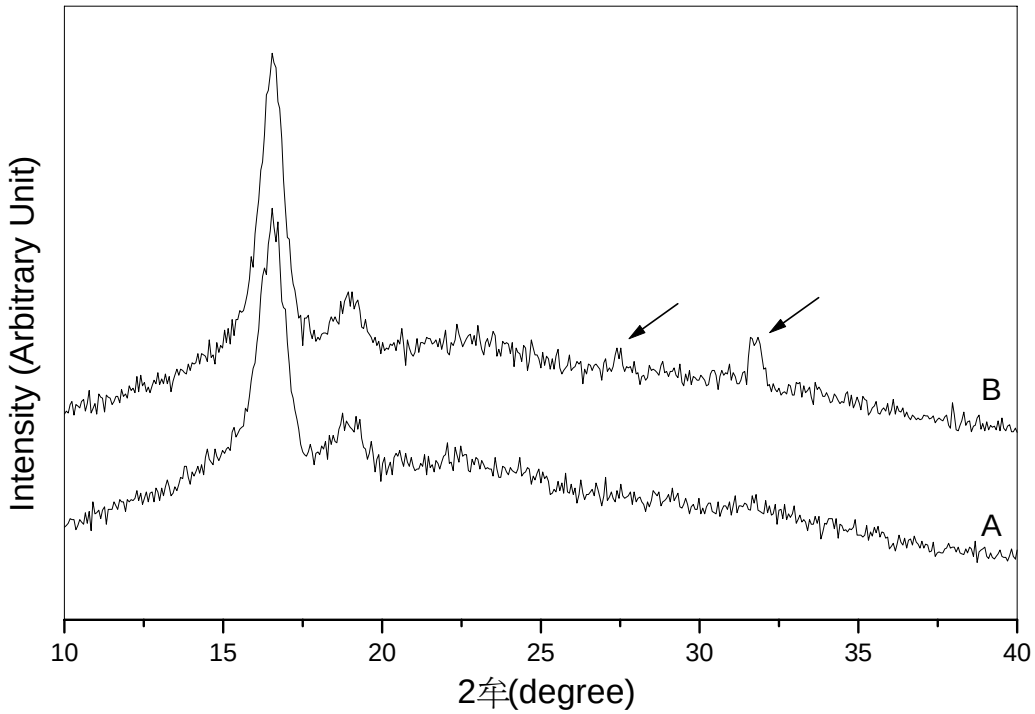

Figure 4.10 *X-ray diffraction spectra of (A) PLLA scaffold (B) PLLA scaffold incubated in 5SBF for 24 hours.*

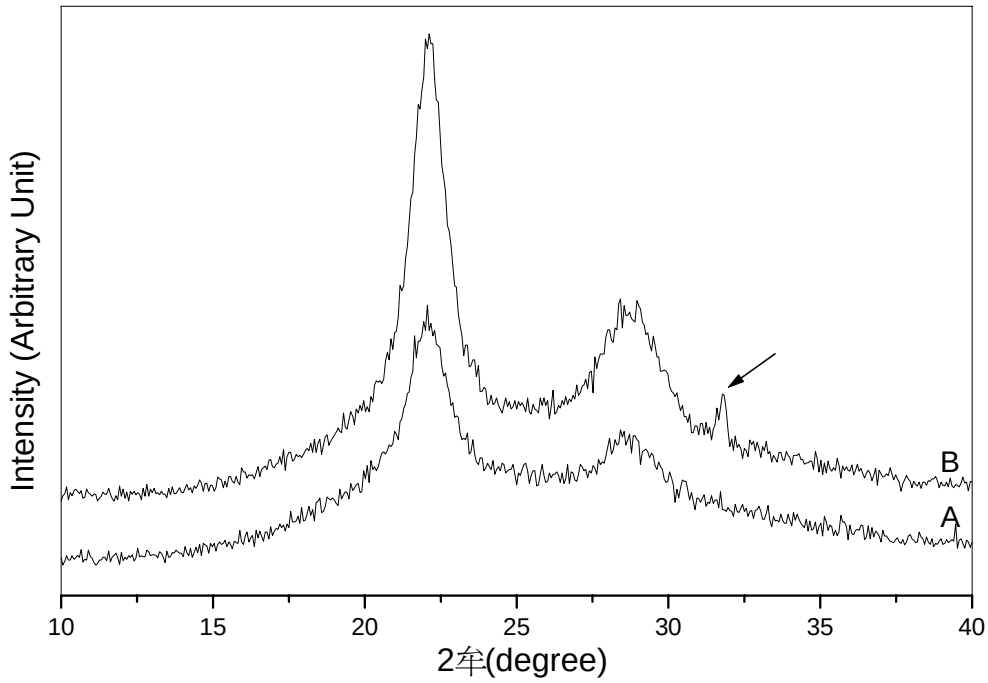

Figure 4.11 *X-ray diffraction patterns of (A) PGA scaffold (B) PGA scaffold incubated in 5SBF for 24 hours. The arrow indicates the characteristic peak of apatite.*

4.1.2.4 FTIR

FTIR spectroscopy was used to gain additional information on the chemical structure of the coating. In the FTIR spectroscopy of coating formed on PLLA film incubated in 5SBF for 24 hours (Figure 4.12(B)), strong absorptions at 1031 cm^{-1} and 563 cm^{-1}, which were designated to the ν_3 and ν_4 vibration of PO_4^{3-} respectively (Rehman and Bonfield, 1997), were observed. The peak around 1640 cm^{-1} was assigned to the ν_3 absorption of CO_3^{2-} as shown in the coating spectra. Spectra also exhibited broad bands for OH stretching at 3570cm^{-1}. A weak absorption peak at 2826-2998 cm^{-1}, the same as PLLA (Figure 4.12(A)), was attributed to the vibrations of C-H bend in PLLA (Silverstein and Webster, 1998), which could be scratched off with the apatite particles and pressed together into the KBr film prepared for FTIR analysis. FTIR spectrum revealed that the coating contained OH, PO_4^{3-} and CO_3^{2-} functional groups. Results of FTIR spectrum (Figure 4.13) also indicated that the coating on PLLA scaffolds included OH, PO_4^{3-} and CO_3^{2-} functional groups.

4.1.2.5 Mass changes of samples in incubation

The mass of PLLA films in 5SBF increased with incubation time, and showed a significant ($p<0.05$) increase (29.84±2.36%) after 24 hours of incubation (Figure 4.14 (C)). In contrast, the films in the distilled water (pH=6.4) (Figure 4.14(A)) and in 1.5SBF (Figure 4.14(B)) did not change significantly in their mass within 24 hours of incubation. The mass of PLLA scaffolds in 5SBF showed a significant ($p<0.05$) increase, 18.94±10.19%, after 24 hours incubation.

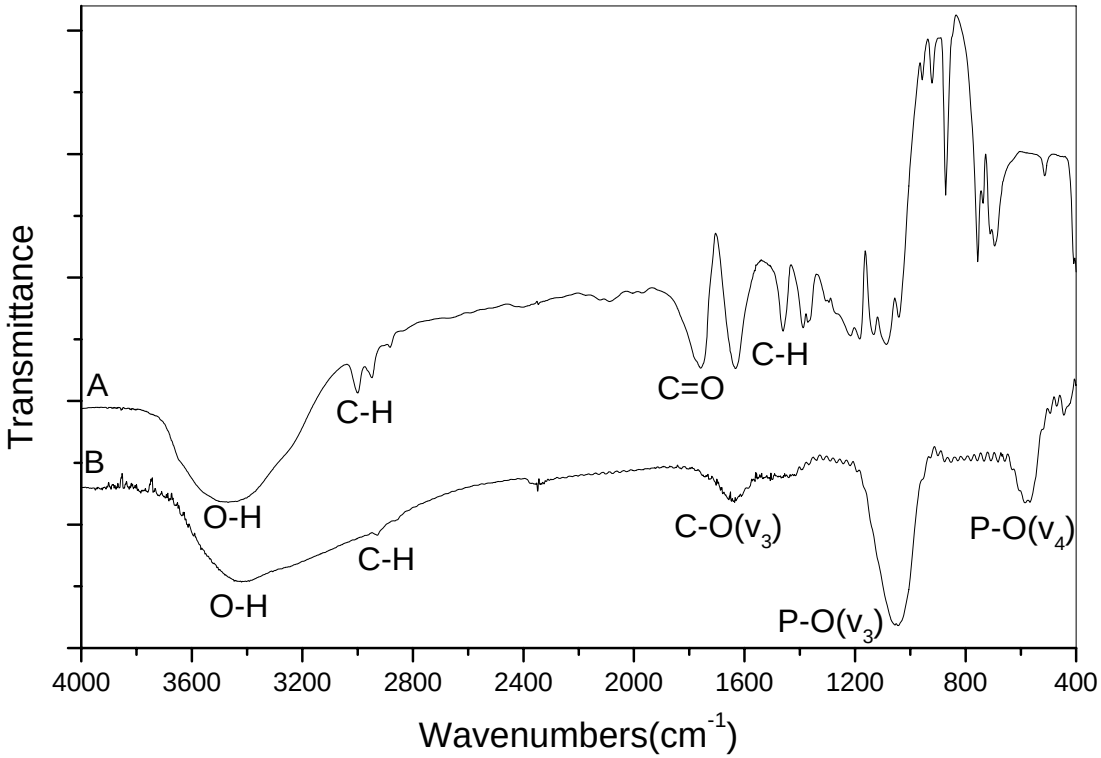

Figure 4.12 *FTIR spectra of PLLA(A) and coating formed in 5SBF for 24 hours(B).*

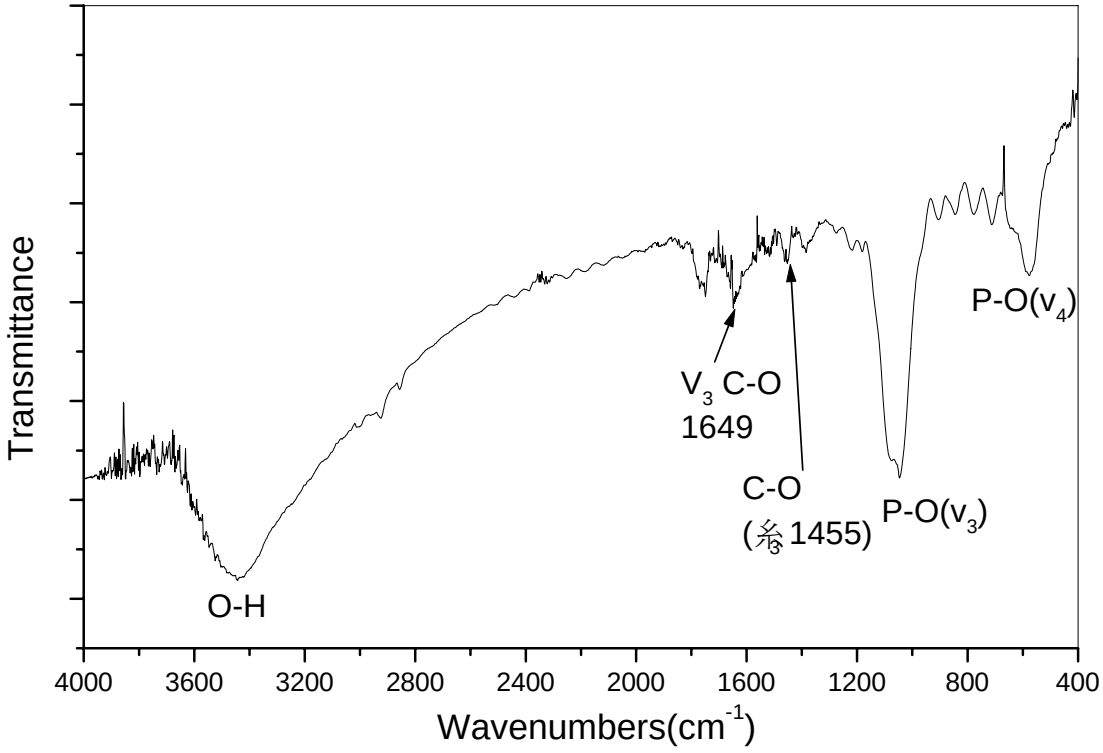

Figure 4.13 *FTIR spectrum of PLLA scaffolds incubated in 5SBF for 24 hours.*

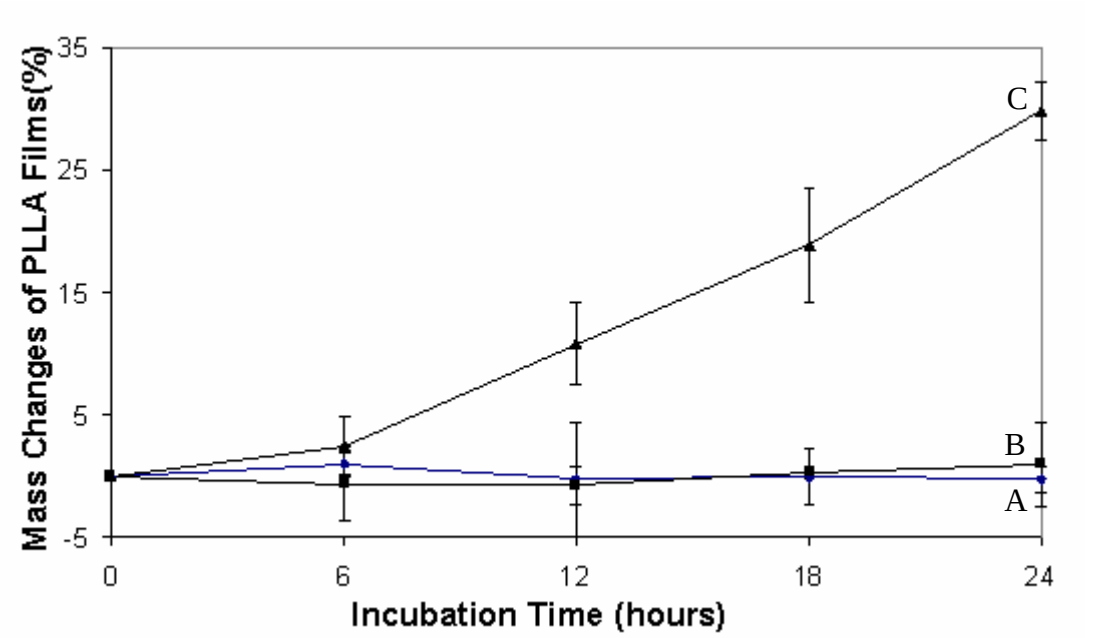

Figure 4.14 *Mass changes of PLLA films in (A) distilled water (pH=6.4), (B) 1.5SBF, and (C) 5SBF.*

The mass of PGA scaffolds increased by 48.28±8.83% in 5SBF for 24 hours. This high increase might be due to the high ratio of surface area/mass of scaffold compared with film, leading to high ratio of coating mass/substrate mass. There was no significant change in mass in the distilled water (pH=6.4) and in 1.5SBF after 24 hours.

4.1.2.6 pH value change in the incubation

Figure 4.15 exhibited the pH value versus time for the 5SBF during the incubation of PLLA films. The pH progressively increased with time and reached 7.4 after 24 hours. During the first 6 hours, the pH increased by 0.4 pH-unit. Later on, the pH increased more slowly than the beginning.

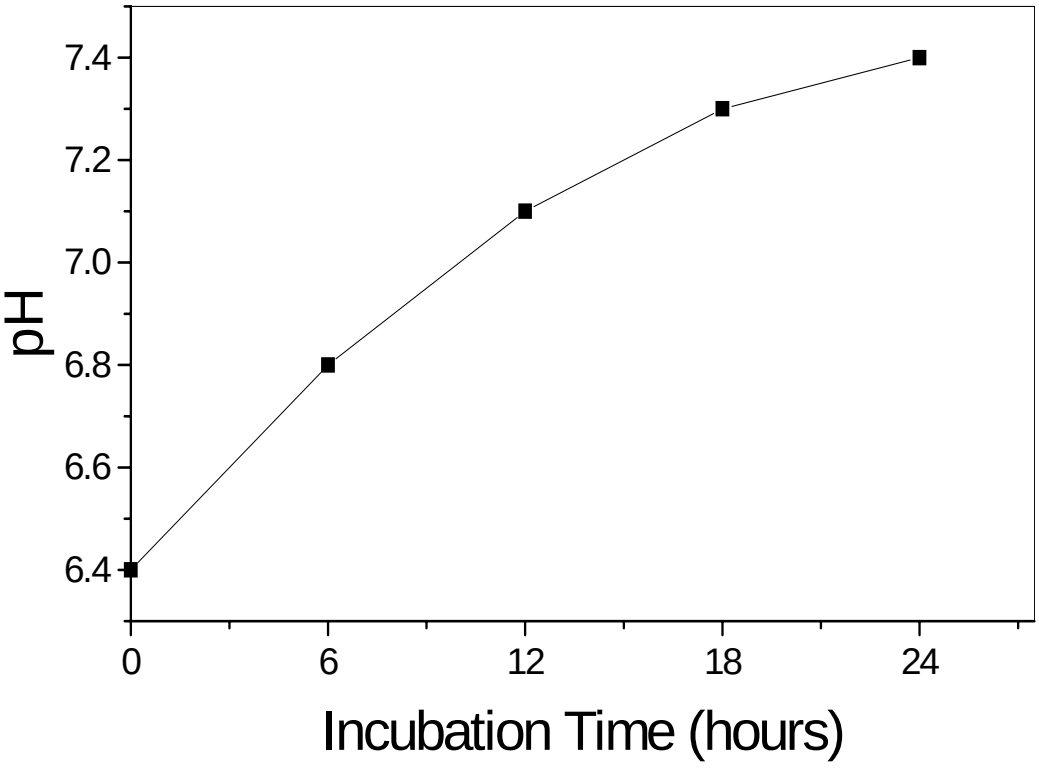

Figure 4.15 *pH change of the 5SBF solution during the incubation of PLLA films.*

4.1.2.7 Mechanical properties

Figure 4.16 exhibited the compressive stress/strain curve of a PLLA sample. As described in Chapter 3, the compressive modulus was defined as the initial linear modulus.

Figure 4.17 compared the compression modulus of PLLA scaffold before and after 24 hours incubation in water (pH=6.4) or in 5SBF (pH=6.4). There was no significant difference ($p>0.05$) between the modulus of PLLA scaffolds before and after the incubation in distilled water (PH=6.4) for 24h, while modulus of PLLA scaffold in 5*SBF (PH=6.4) for 24h was significantly higher ($p<0.05$) than that of control.

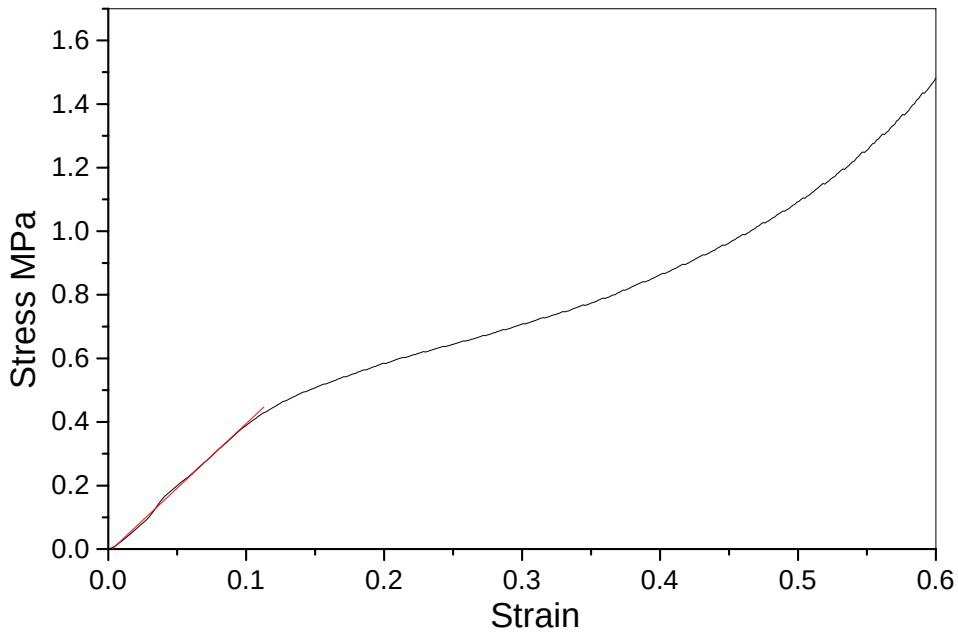

Figure 4.16 *Compression stress/strain curve of one PLLA sample*

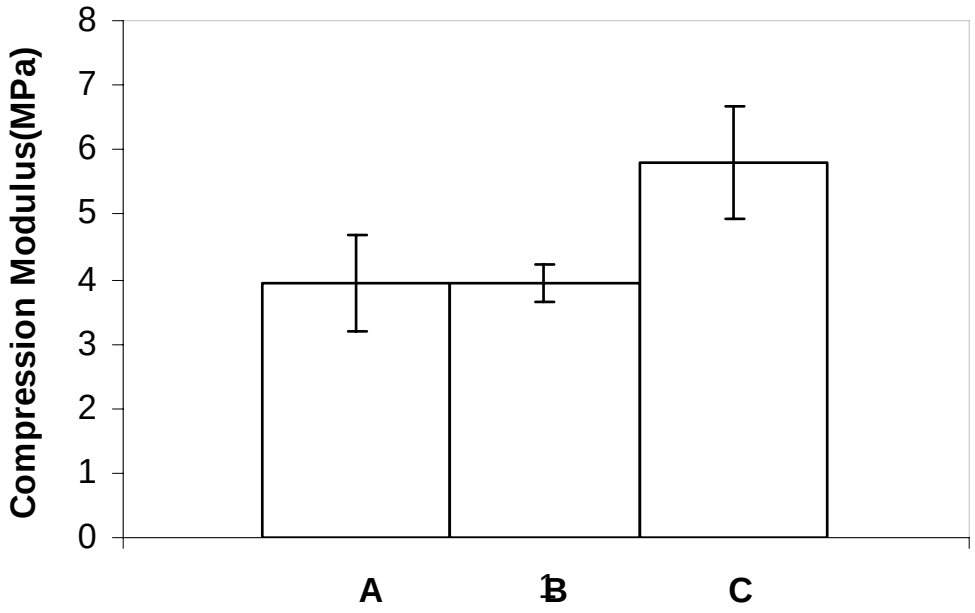

Figure 4.17 *Compressive modulus of PLLA scaffolds. (A) non-incubated samples (B) samples after incubation in distilled water (pH=6.4) for 24 hours (C) Samples after incubation in 5SBF for 24 hours.*

The compressive modulus of PGA scaffolds with apatite coating was also significantly higher than that of the PGA scaffold [Figure 4.18]. The compressive modulus of PGA scaffolds after incubation in distilled water (pH=6.4) for 24 hours was slightly, but not significantly ($p>0.05$), lower than that before incubation. This indicated that apatite particles coated on PGA scaffolds enhanced the mechanical properties of the scaffold.

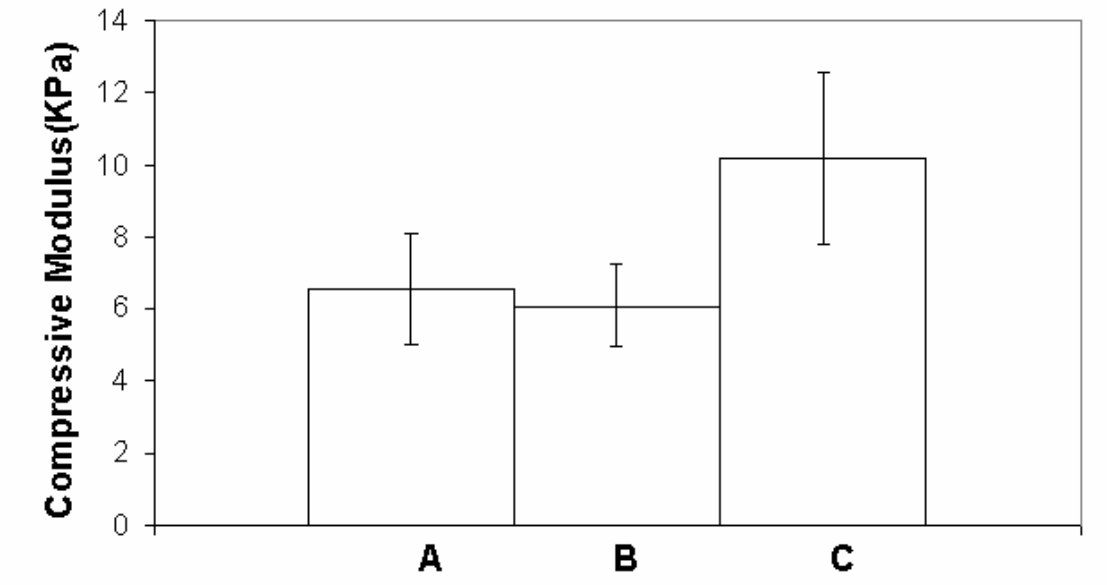

Figure 4.18 *The compressive moduli of PGA scaffolds. (A) non-incubated samples (B) samples after incubation in distilled water (pH=6.4) for 24 hours (C) Samples after incubation in 5SBF for 24 hours.*

4.1.3 Apatite/collagen composite coating

4.1.3.1 Morphology of apatite/collagen coating

The SEM micrograph in Figure 4.19 showed the surface morphologies of the PLLA films before and after incubation in 5SBF and 5SBFC for 24 hours. Compared with PLLA films before incubation, the films immersed for 24 hours in 5SBF and

5SBFC [Figure 4.19(b),(c)] showed an apatite coating and an apatite/collagen composite coating, respectively. The SEM micrograph of PLLA films with apatite coating at larger magnifications [Figure 4.20(a)] exhibited clearly the submicron apatite particles (200–600nm) which assembled in small flake-like pieces. In the SEM micrograph of PLLA films with apatite/collagen composite coating [Figure 4.20(b)], some submicron apatite particles (100-200nm) were observed on the collagen fibers, as well as on the PLLA surface. The diameters of fibers were also submicron. Finer porosity was formed with deposited fibers interlapping randomly with each other. The composite coating was not homogeneous. This combined apatite/collagen coprecipitation in 5SBFC allowed the formation of a nano-scaled biocomposite of collagen and apatite in a manner more similar to natural bone.

(a)

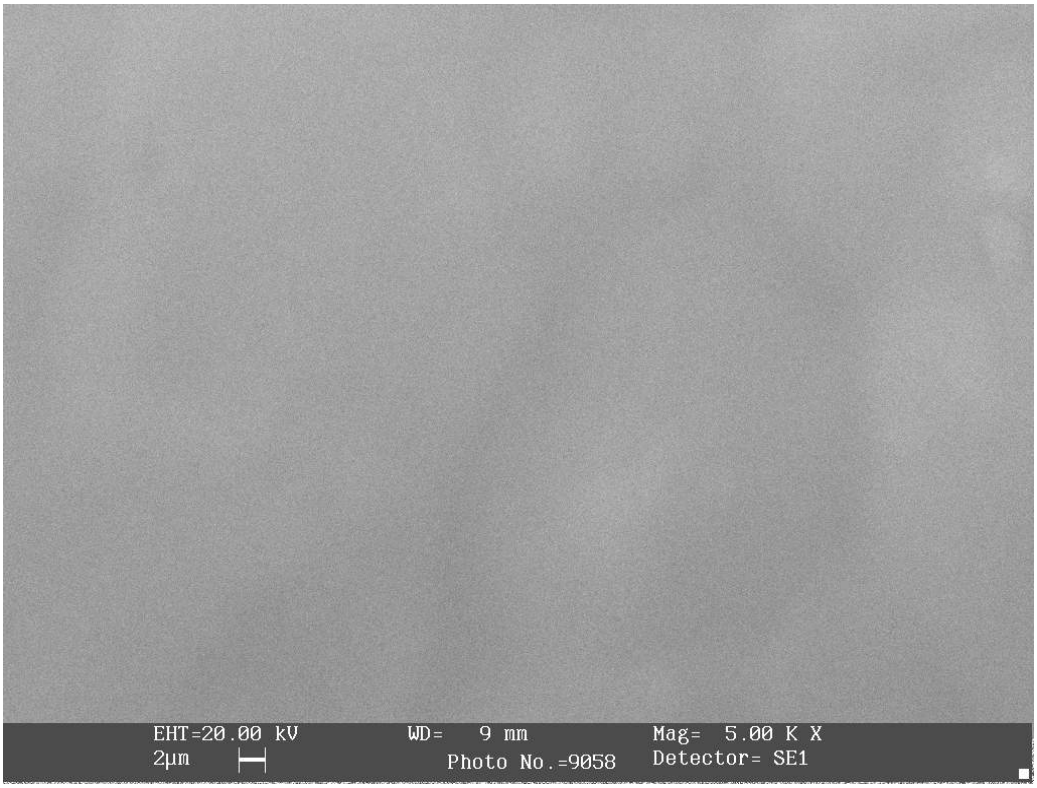

Figure 4.19 *SEM micrographs (magnification 5,000×) of PLLA films (a) without treatment; (b) incubated in 5SBF for 24 hours (the same as Figure 4.2(e), reproduced here for easy comparison); (c) incubated in 5SBFC for 24 hours.*

(b)

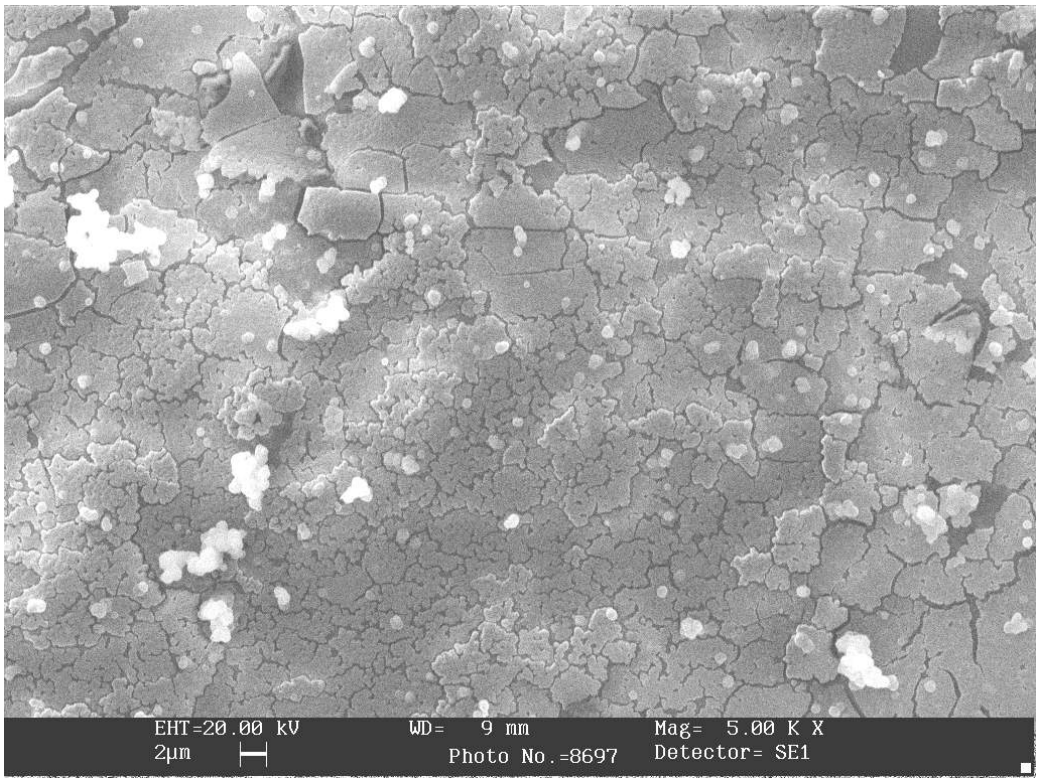

(c)

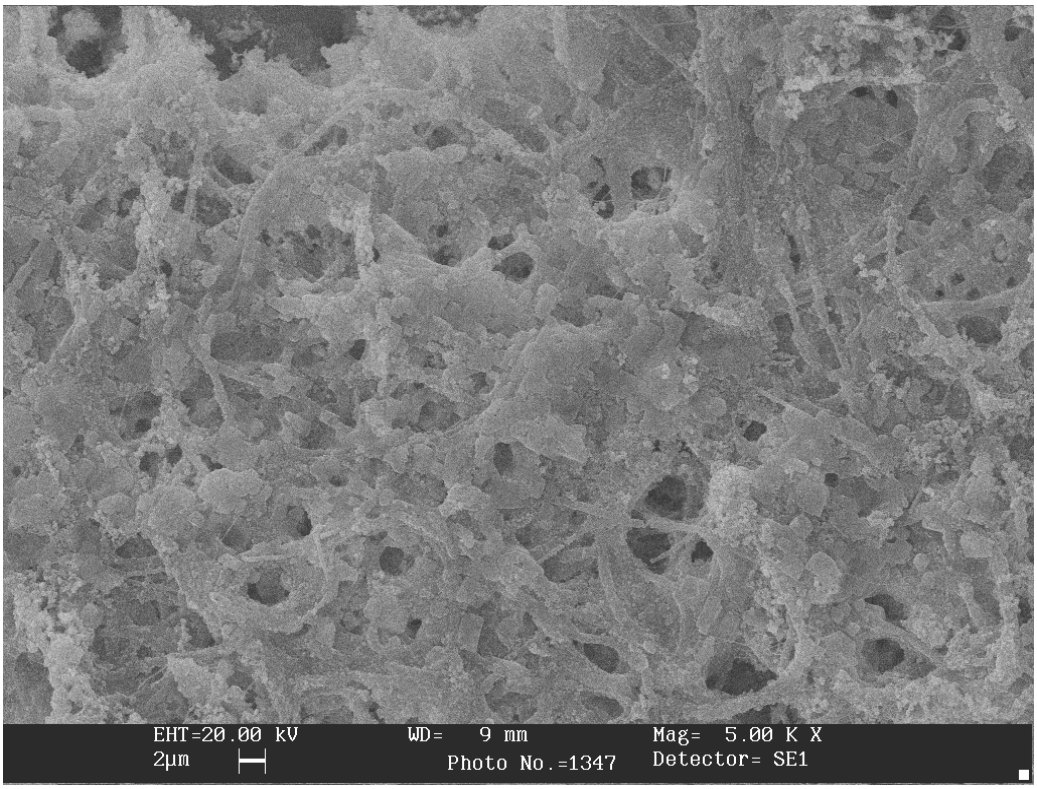

Figure 4.19 *(continued)*

(a)

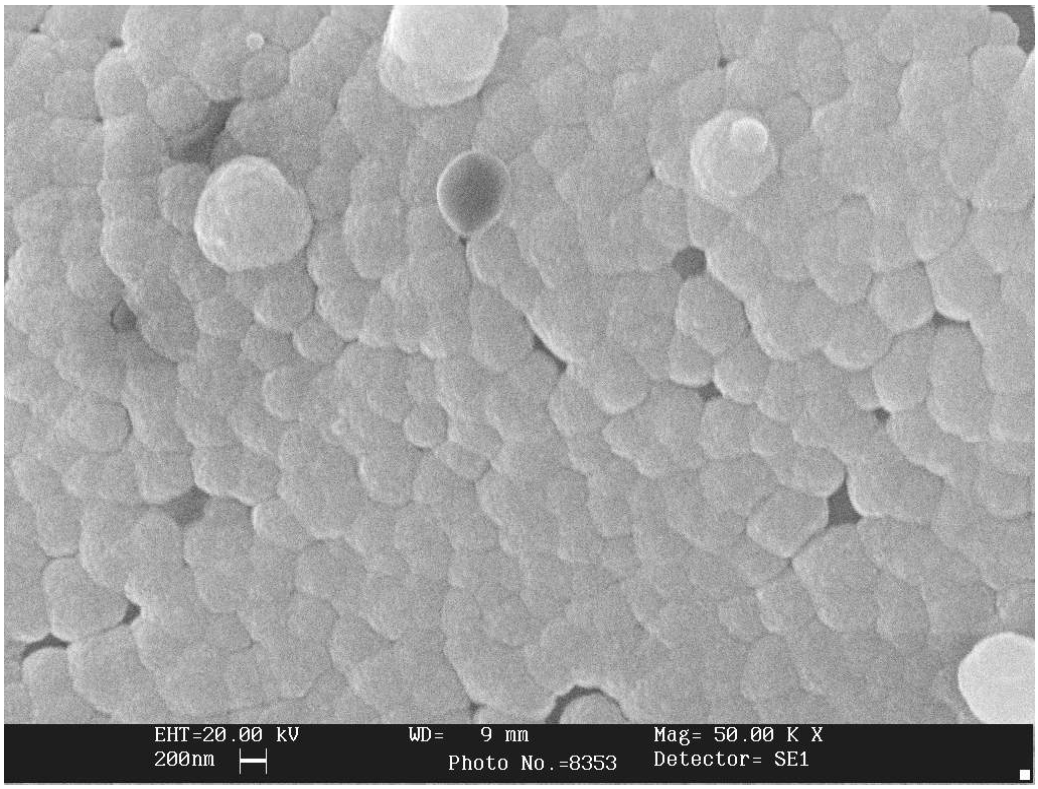

(b)

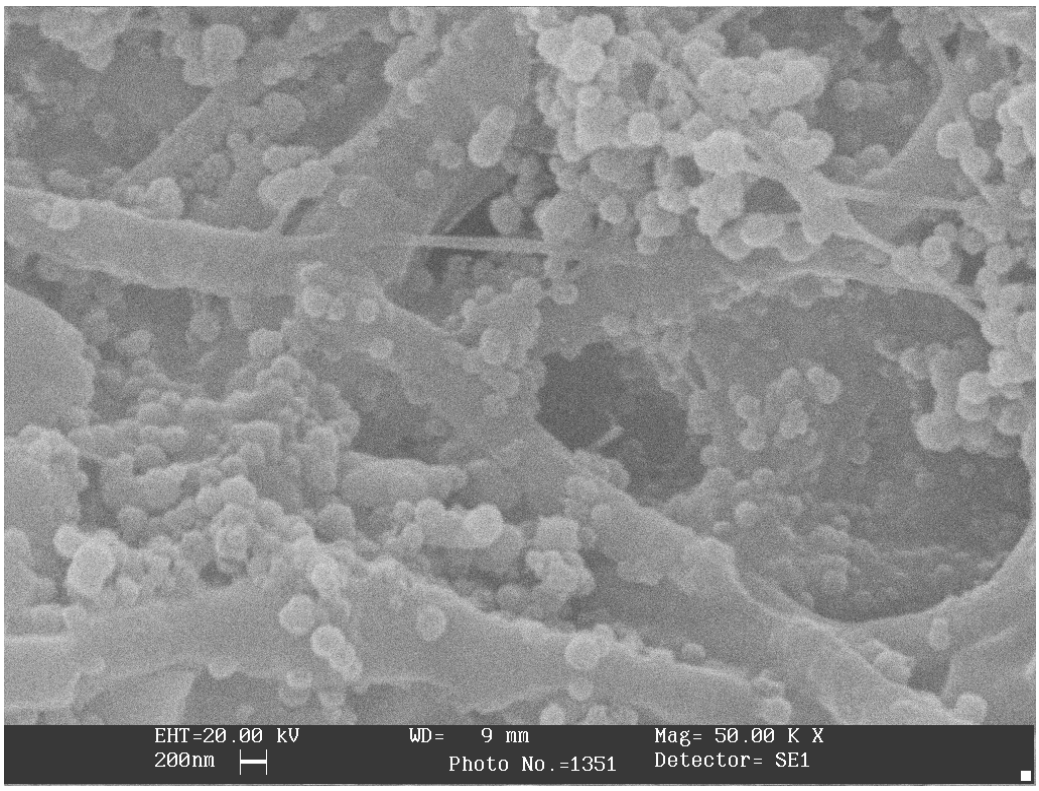

Figure 4.20 *SEM micrographs (magnification 50,000×) of PLLA films (a) incubated in 5SBF for 24 hours (the same as Figure 4.3(d), reproduced here for easy comparison); (b) incubated in 5SBFC for 24 hours.*

Figure 4.21 and Figure 4.22 showed the SEM photographs of PLLA scaffolds before and after incubation in 5SBF and 5SBFC for 24 hours. From Figure 4.21(b) and Figure 4.22(a), only apatite particles were deposited on the PLLA scaffold incubated in 5SBF. For the PLLA scaffolds incubated in 5SBFC (Figure 4.21(c), Figure 4.22(b)), both particles and fibers were observed. Collagen fibrils were formed in the pores of PLLA scaffolds, and apatite particulates were deposited on the surface of PLLA and collagen.

(a) 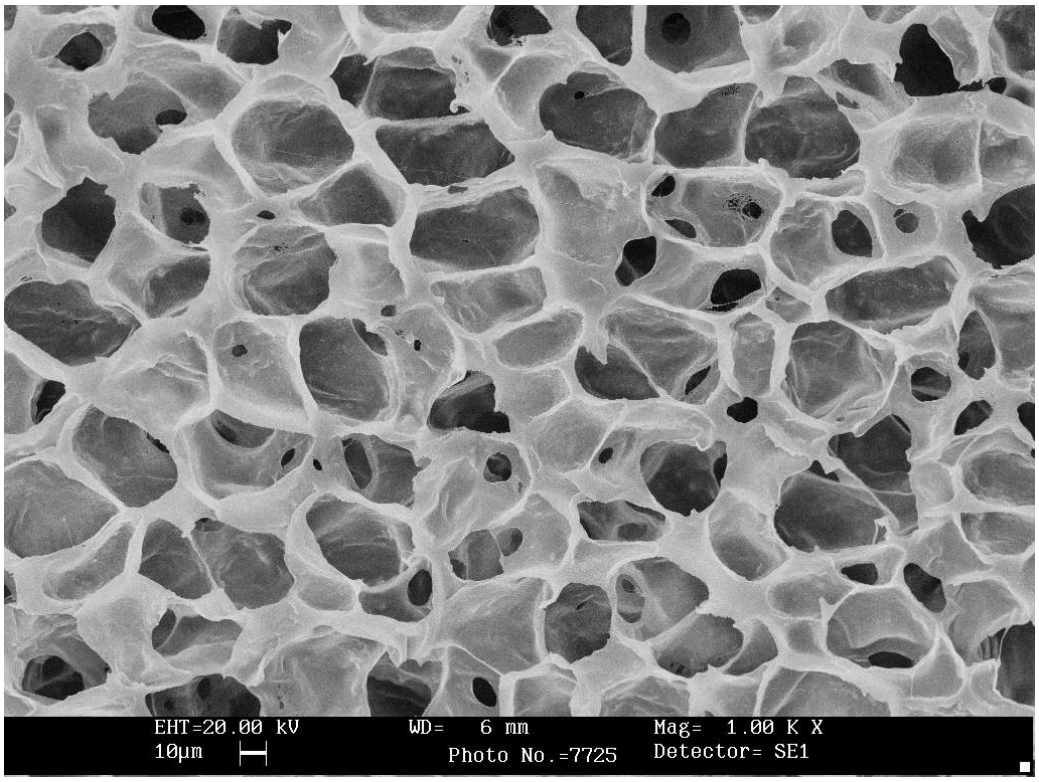

Figure 4.21 *SEM micrographs (magnification 1,000×) of PLLA scaffolds (a) without treatment; (b) incubated in 5SBF for 24 hours; (c) incubated in 5SBFC for 24 hours.*

(b)

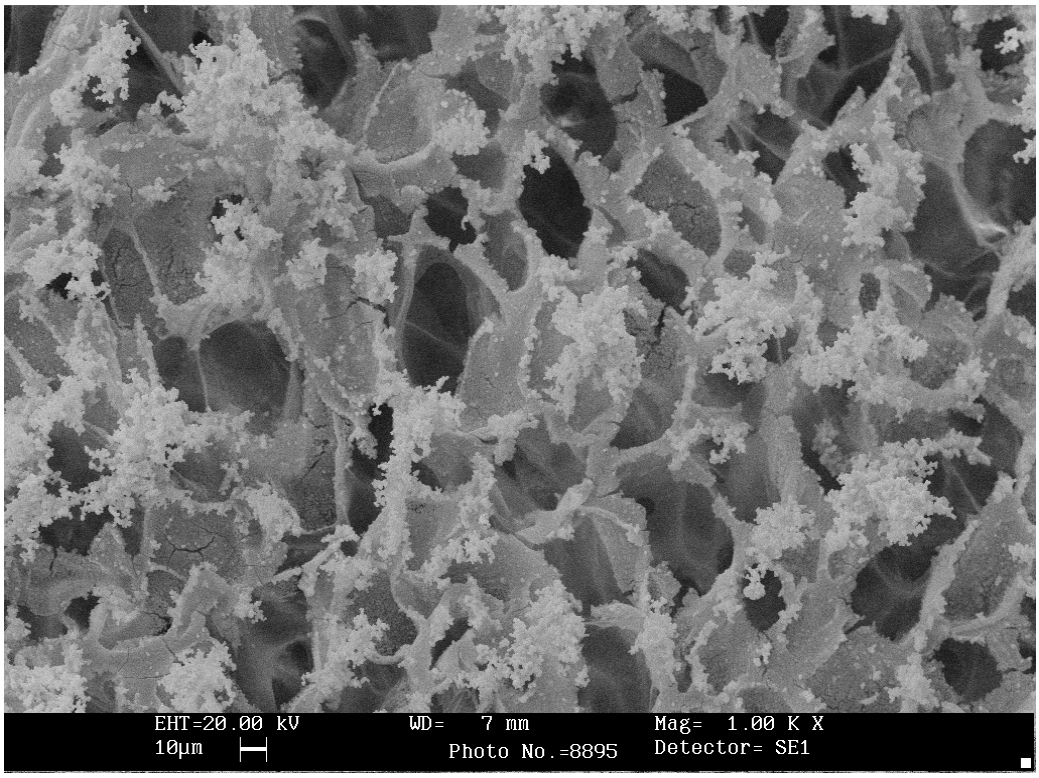

(c)

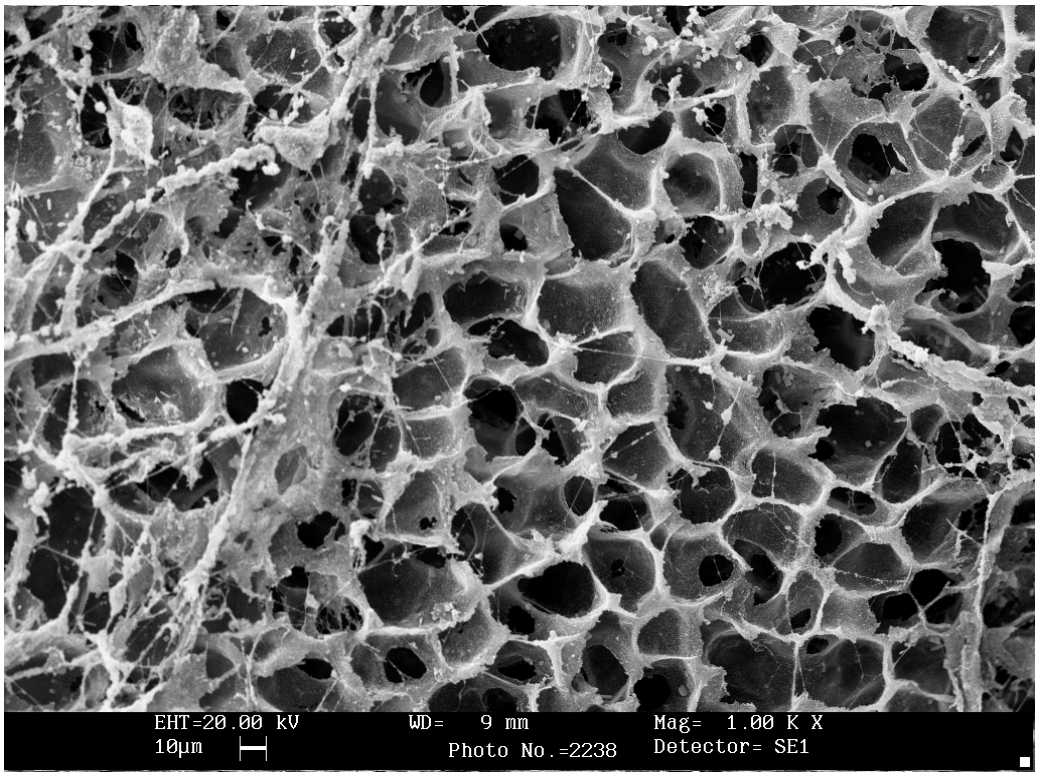

Figure 4.21 *(continued)*

(a)

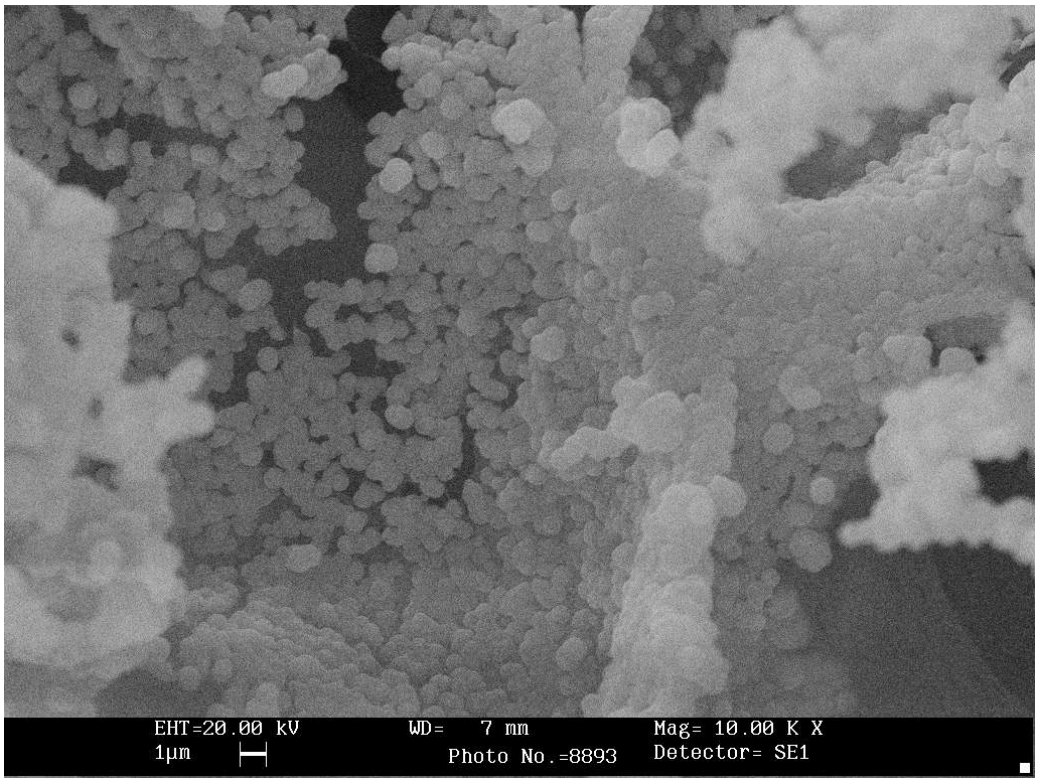

(b)

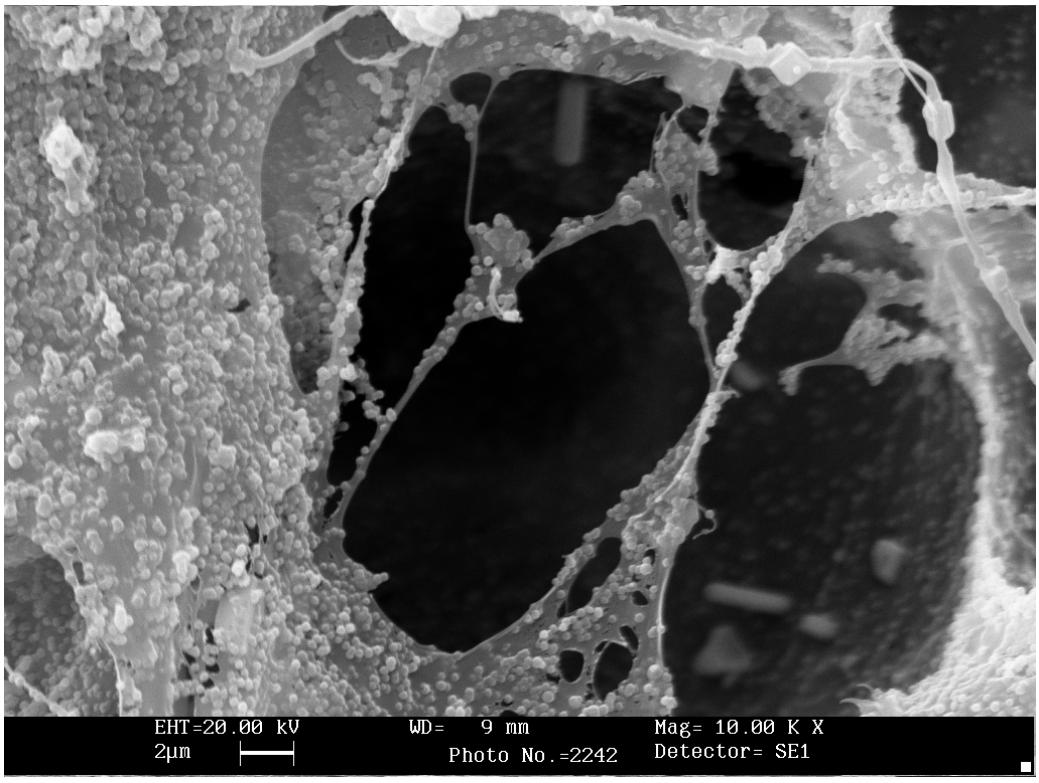

Figure 4.22 *SEM micrographs (magnification 10,000×) of PLLA scaffolds (a) incubated in 5SBF for 24 hours; (b) incubated in 5SBFC for 24 hours.*

4.1.3.2 EDX

EDX results shown in Figure 4.23 indicated that calcium and phosphorus elements existed in both types of coatings formed on PLLA films. It was also noticed that the calcium and phosphate contents formed in 5SBFC were relatively lower than those formed in 5SBF. This may be because of the incorporation of collagen in the coating formed in 5SBFC. The nitrogen, the only element that is in collagen and not in PLLA and apatite, could not be identified from the EDX spectrum of the coating formed in 5SBFC because nitrogen is a light element and its peak is quite near to that of oxygen. The Ca/P atomic ratio of the coating formed in 5SBF and 5SBFC for 24 hours were 1.32 and 1.17, respectively.

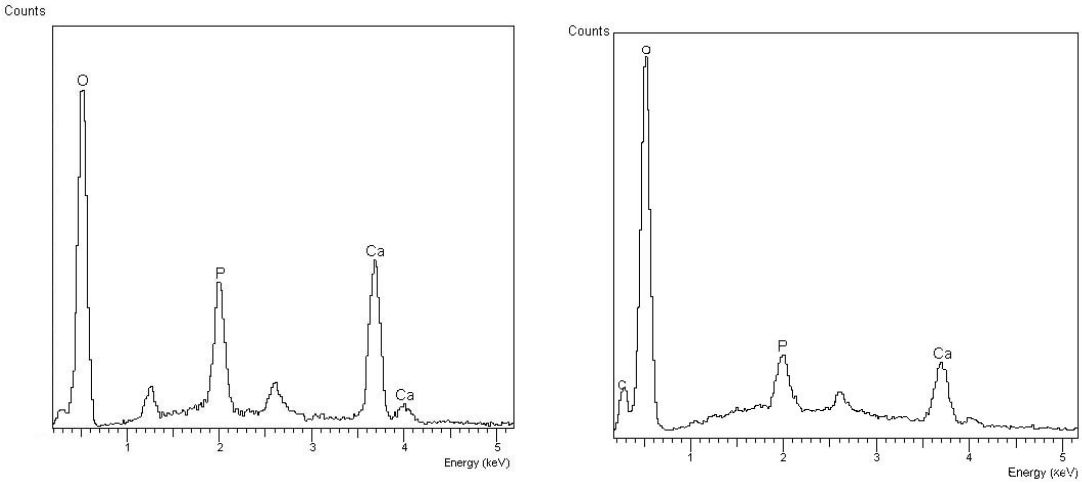

(a) (b)

Figure 4.23 *EDX spectra of PLLA films incubated for 24 hours (a) in 5SBF (b) 5SBFC.*

4.1.3.3 XRD

In the XRD pattern [Figure 4.24], compared with pure PLLA films (A), PLLA films after incubation in both 5SBF(B) and 5SBFC (C) showed the characteristic peak (31.8-32.2^{o}) of apatite.

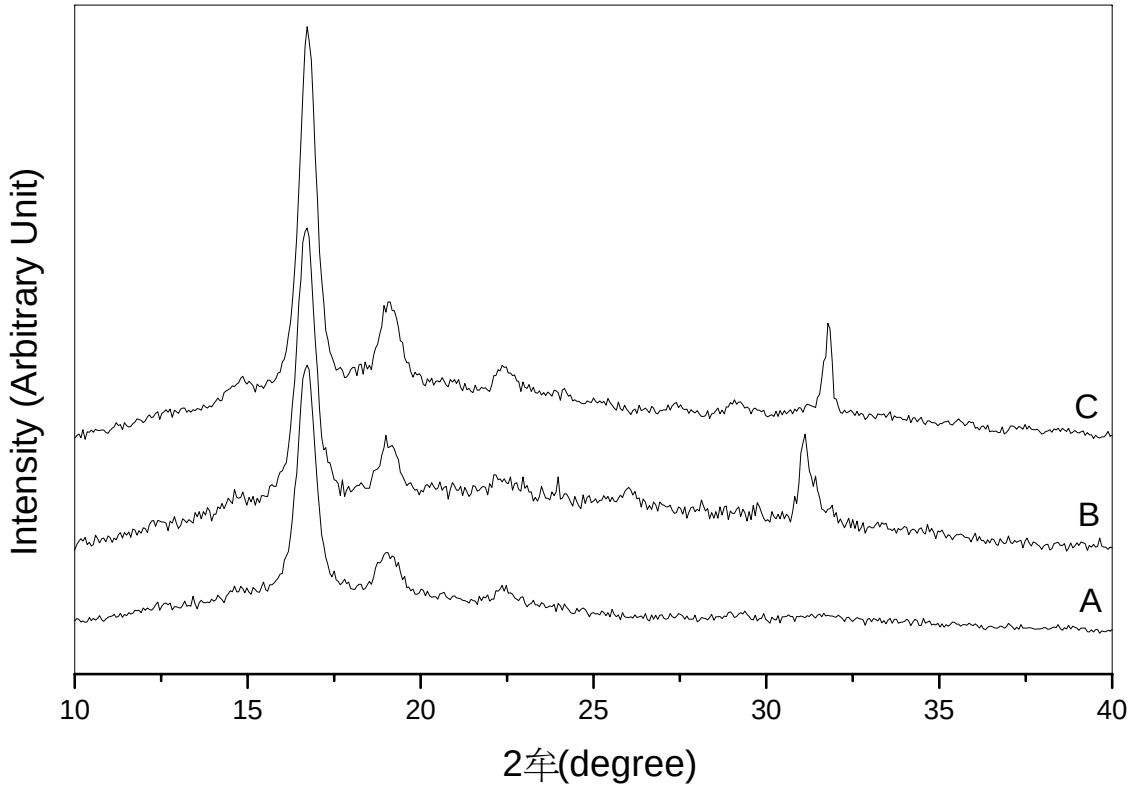

Figure 4.24 *X-ray diffraction patterns of PLLA film (A) without treatment (B) incubated in 5SBF for 24 hours (C) incubated in 5SBFC for 24 hours.*

4.1.3.4 FTIR

The FTIR spectra acquired from the coating formed in 5SBF and 5SBFC were displayed in Figure 4.25. In the FTIR spectrum of coating formed by the accelerated biomimetic coprecipitation process in 5SBFC (B), besides the same functional groups,

PO_4^{3-}, CO_3^{2-}, and OH^-, as in 5SBF(A), amide peaks are also revealed (Camacho *et al.*, 2001).

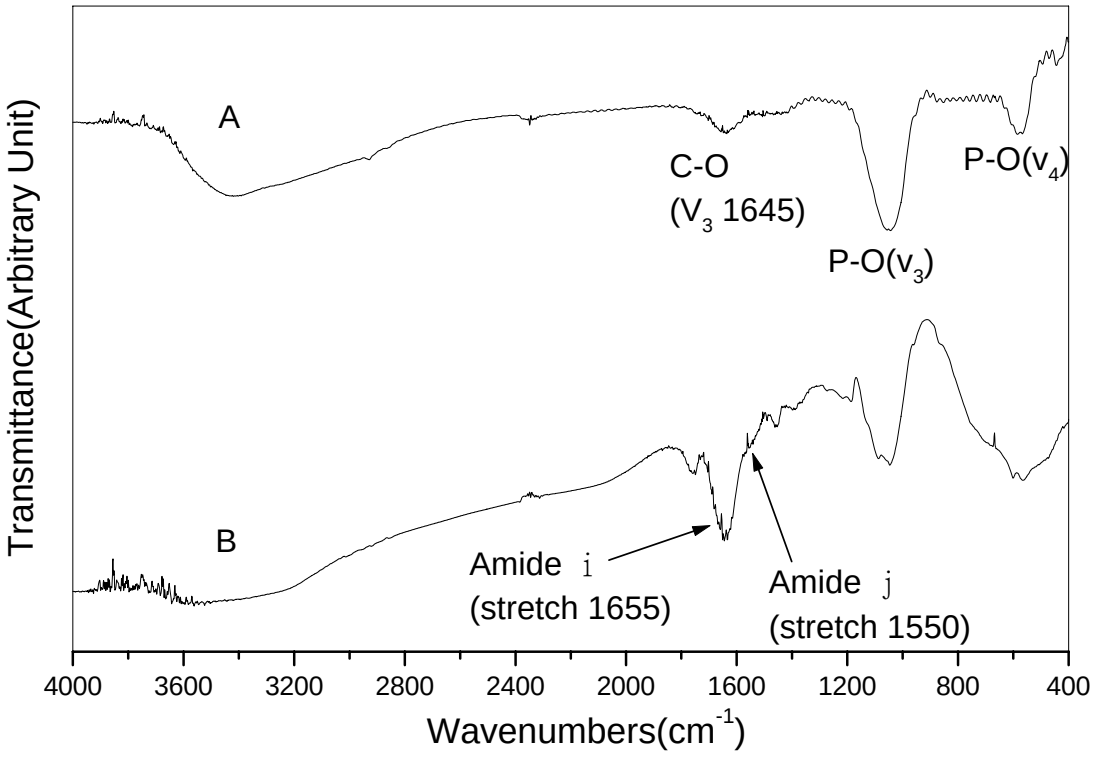

Figure 4.25 *FTIR spectrum of PLLA films incubated for 24 hours (A) in 5SBF (B) in 5SBFC.*

4.1.3.5 Wettability

The wettability of PLLA films with or without coating, as determined by measuring the contact angles, showed differences among the three surfaces [Table 4.2]. The PLLA substrate without coating seemed to be more hydrophobic than those with apatite coating and apatite/collagen composite coating. As seen in SEM pictures (Fig. 1), the PLLA substrate was composed of a dense nonporous material. In contrast, the apatite layer was an aggregate of tiny apatite particulates forming pores at the

boundary of tiny apatite particulates, whereas the apatite/collagen layer consisted of fibers and particles interlapping randomly with each other forming much larger pores.

Table 4.2 *Wettability of PLLA film with and without coating as determined by water contact angle*

Samples	Contact angle (deg)
Control PLLA films	71±1
Apatite coated PLLA films	29±3
Apatite/collagen coated PLLA films	22±3

4.1.4 Apatite coating in the flowing condition

After 24 hours of incubation in the flow system, apatite coating could also be clearly observed on the pore of PLLA scaffolds (pore size:100-320um; porosity: 96.15%) . Figure 4.26 and Figure 4.27 compared the coating formed on the flow-in surface, the internal section and the flow-out surface of the scaffold. In the flowing condition, there was no much difference in the density of apatite particles on the pore walls among the different sites. Almost all of the surfaces were covered by apatite.

(a)

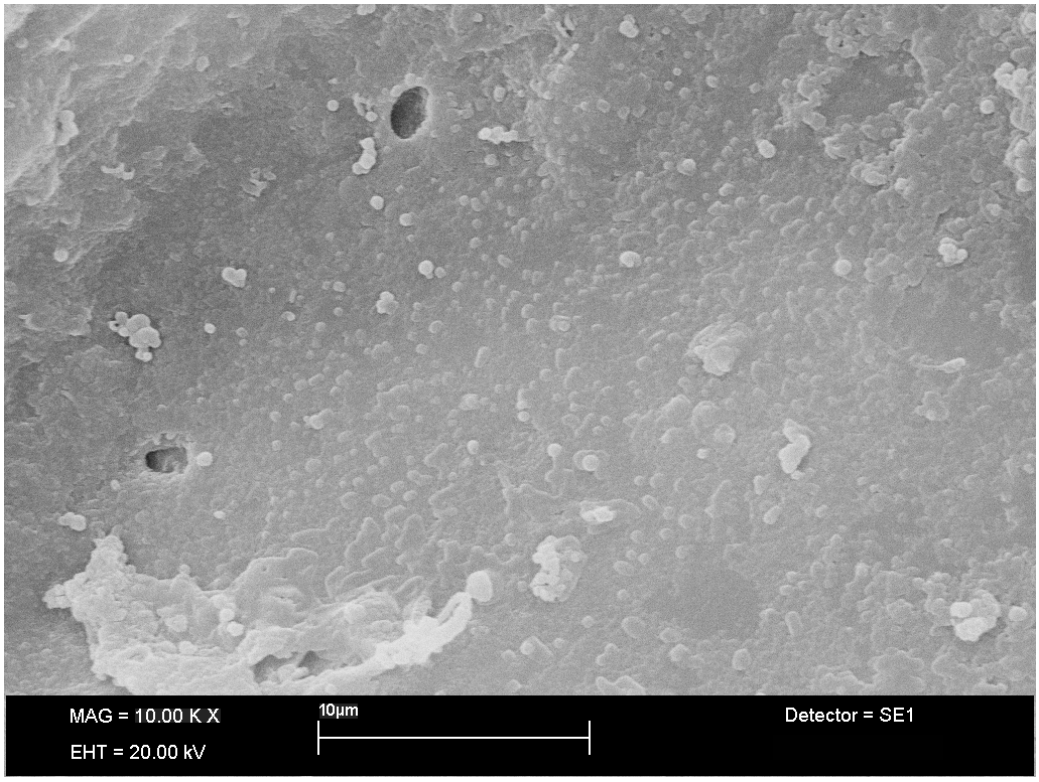
MAG = 10.00 K X
EHT = 20.00 kV
10µm
Detector = SE1

(b)

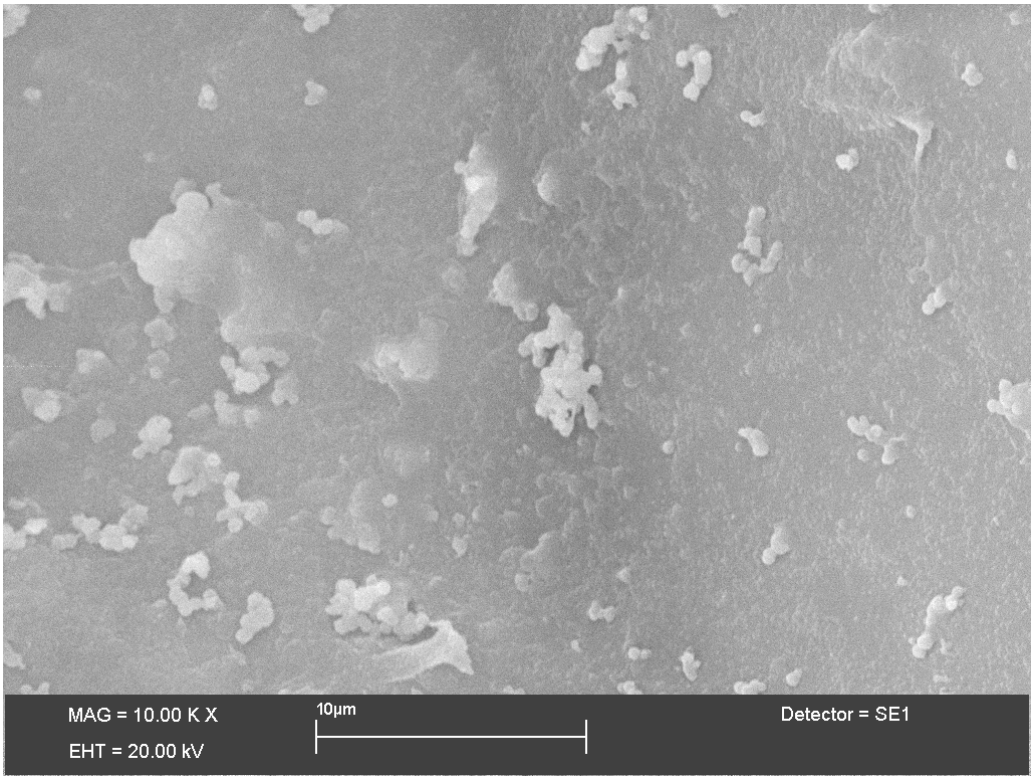
MAG = 10.00 K X
EHT = 20.00 kV
10µm
Detector = SE1

Figure 4.26 *SEM micrographs of PLLA scaffold after incubation in 5SBF in the flowing condition for 24 hours (a) flow-in surface (b) internal section (c) flow-out surface of specimens. (original magnification ×10,000)*

(c)

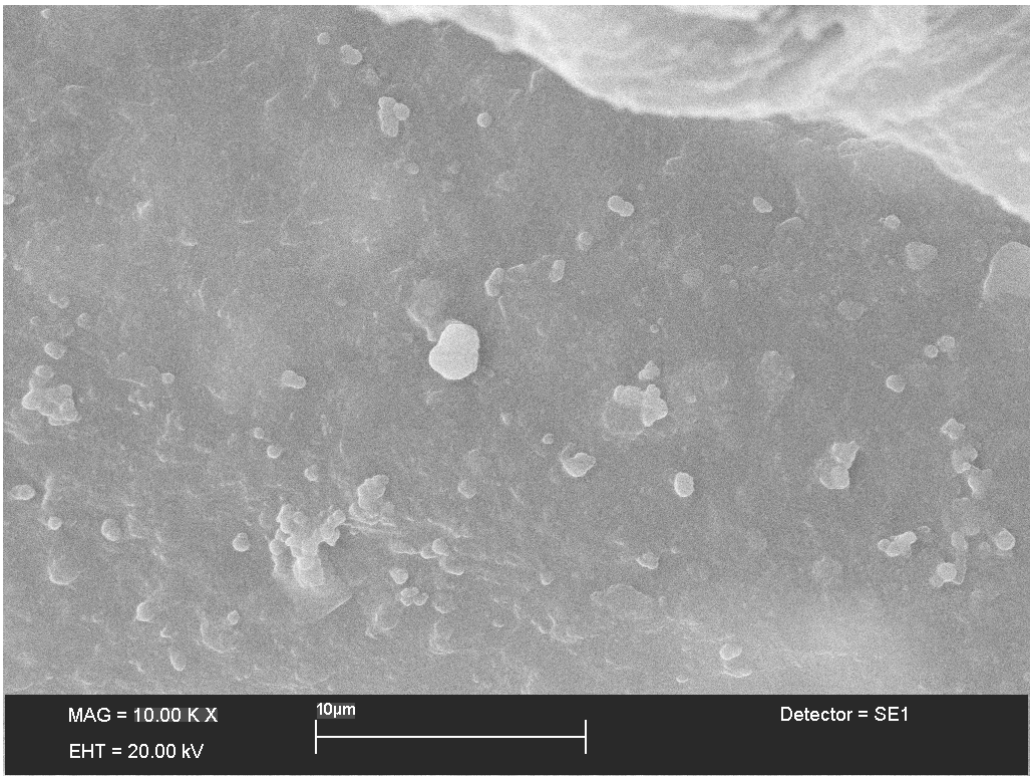

Figure 4.26*(continued)*

(a)

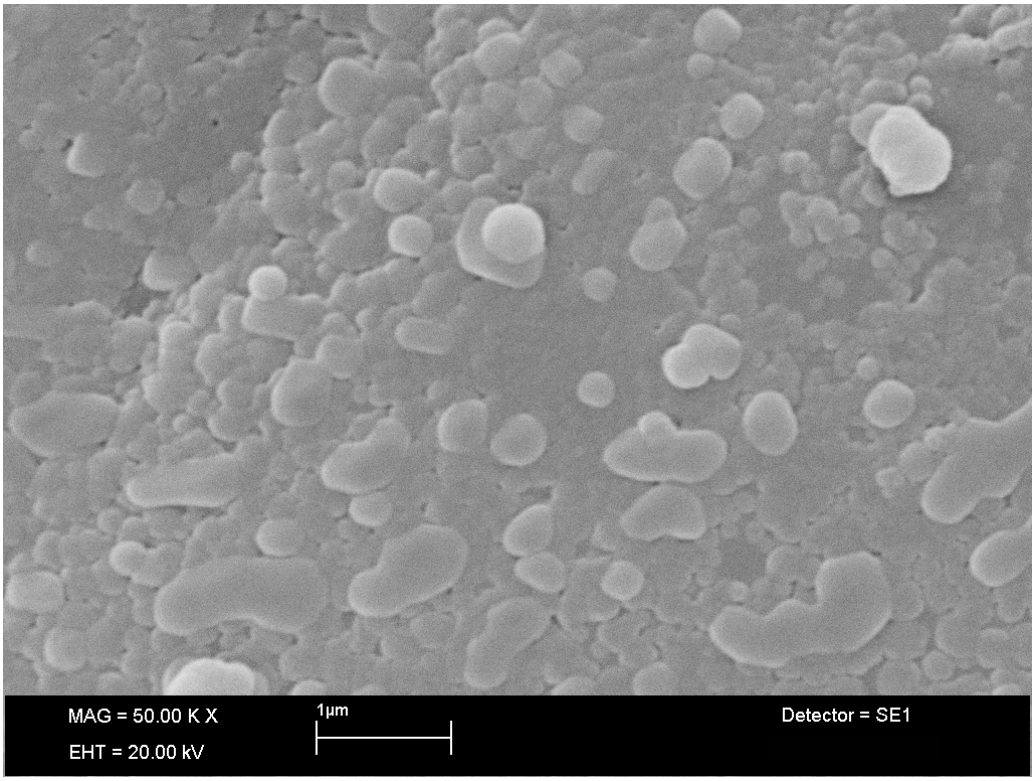

(b)

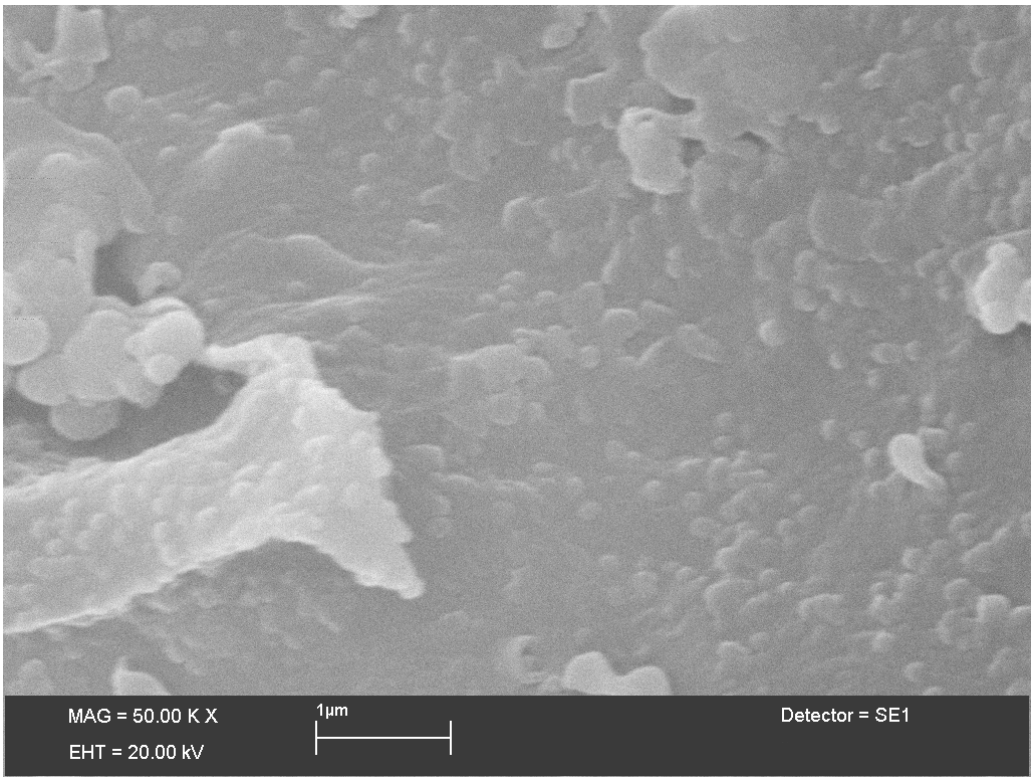

Figure 4.27 *SEM micrographs of PLLA scaffold after incubation in 5SBF in the flowing condition for 24 hours (a) flow-in surface (b) internal section (c) flow-out surface of specimens. (original magnification ×50,000)*

(c) 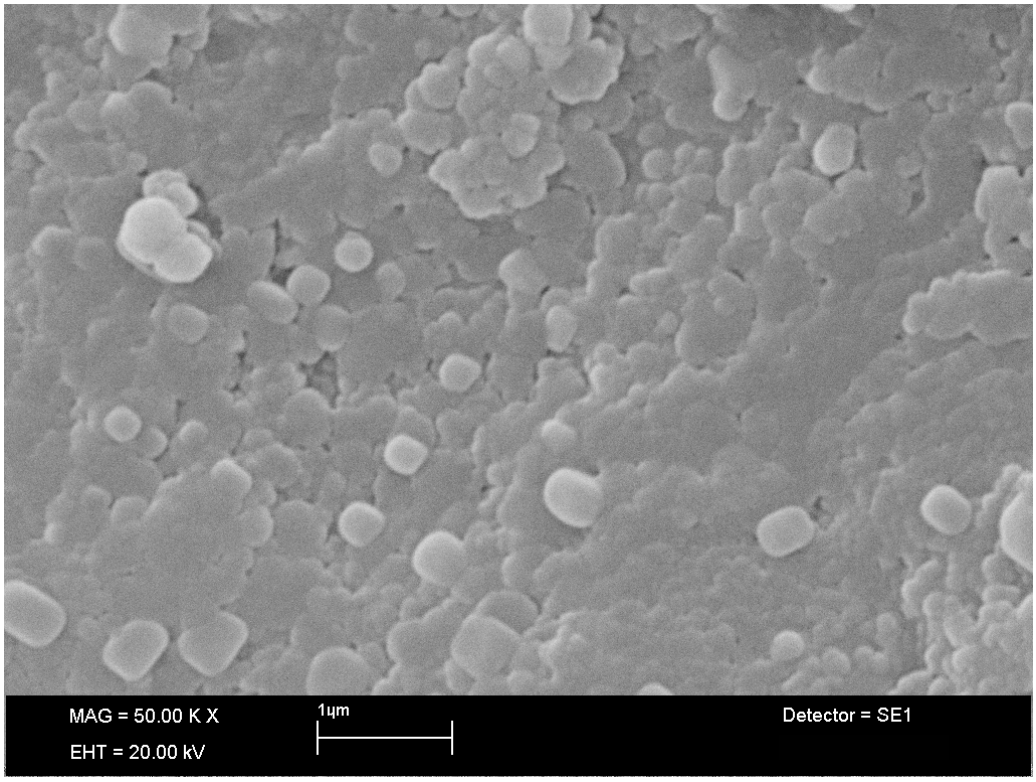

Figure 4.27 *(continued)*

In the agitated condition in the shaking table, fewer apatite particles were formed on the pore walls in the internal regions than near the surface [Figure 4.28]. These could be explained that the formation of apatite nuclei consumed calcium and phosphate ions from the surrounding fluid and it was more difficult for the central region than the surface region of scaffolds to exchange ions with outer fluid. Lower ion concentration in the central region induced the formation of fewer apatite particles.

(a)

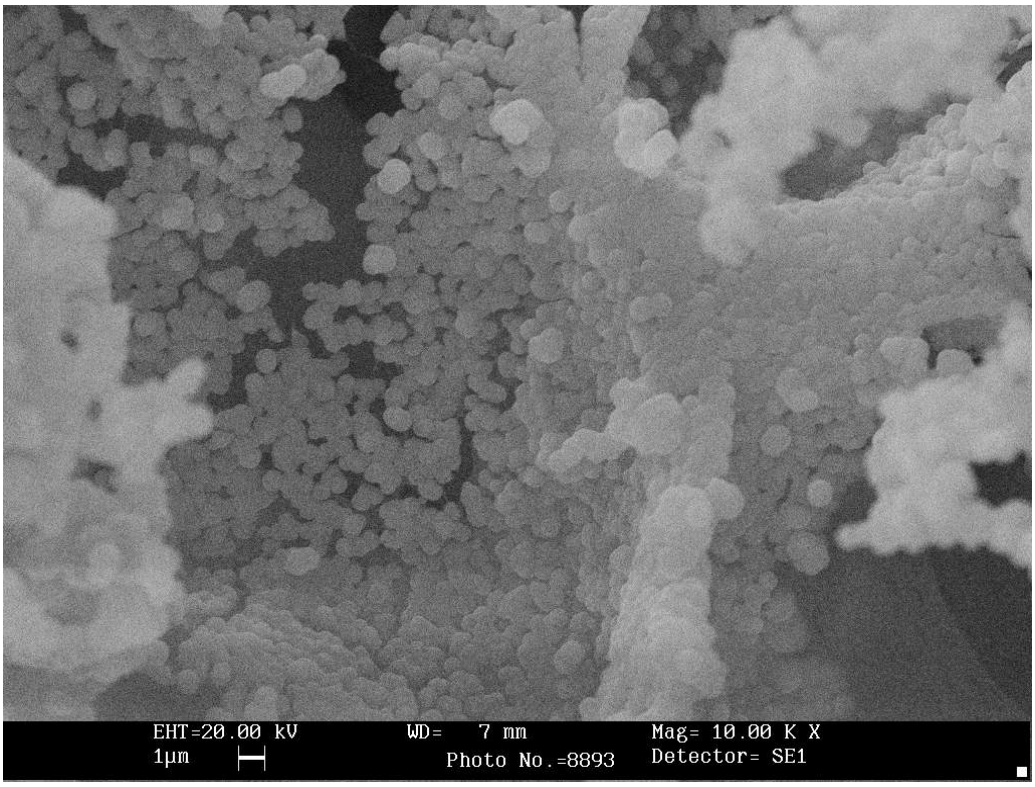

(b)

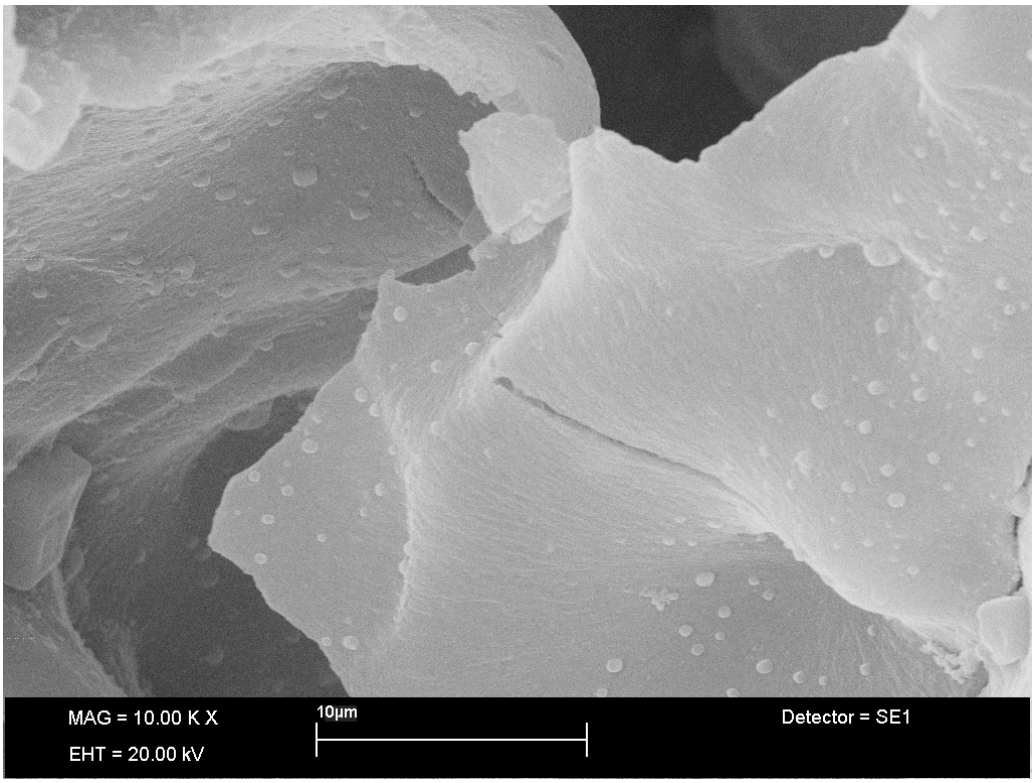

Figure 4.28 *SEM micrographs of PLLA scaffold after incubation in 5SBF in the shaking table for 24 hours (a) pores walls near the surface(×10,000); (b) pores walls in the internal mid-section (×10,000).*

4.2 cell seeding

4.2.1 cell seeding on films

4.2.1.1 Cell morphology

From the SEM [Figure 4.29], it could be observed that after 2 hours of culture more cells were found attached on the composite coating and they had stretched their pseudopodia well, whereas fewer cells were observed on the PLLA substrate and their pseudopodia were less obvious. Cell number and morphology on the apatite coating were somewhat between that on PLLA substrate and composite coating.

SEM observations of Saos-2 cultures at day 6 showed that osteoblast-like cells had proliferated and formed a 100% confluent cell layer on the 3 substrates [Figure 4.30]. No obvious differences in morphology were observed among the cells grown on PLLA films with and without coating. At a higher magnification, the cells were found anchored to the surface by discrete filopodia exhibiting numerous microvilli on its dorsal surface.

(a)

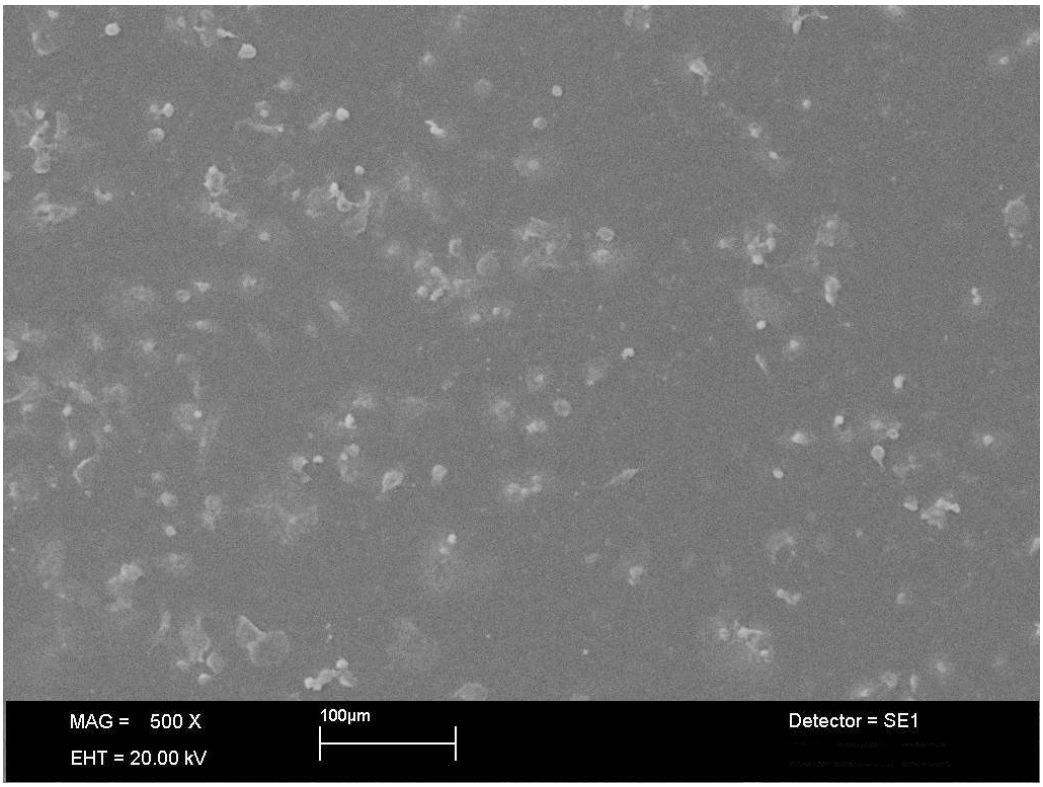

(b)

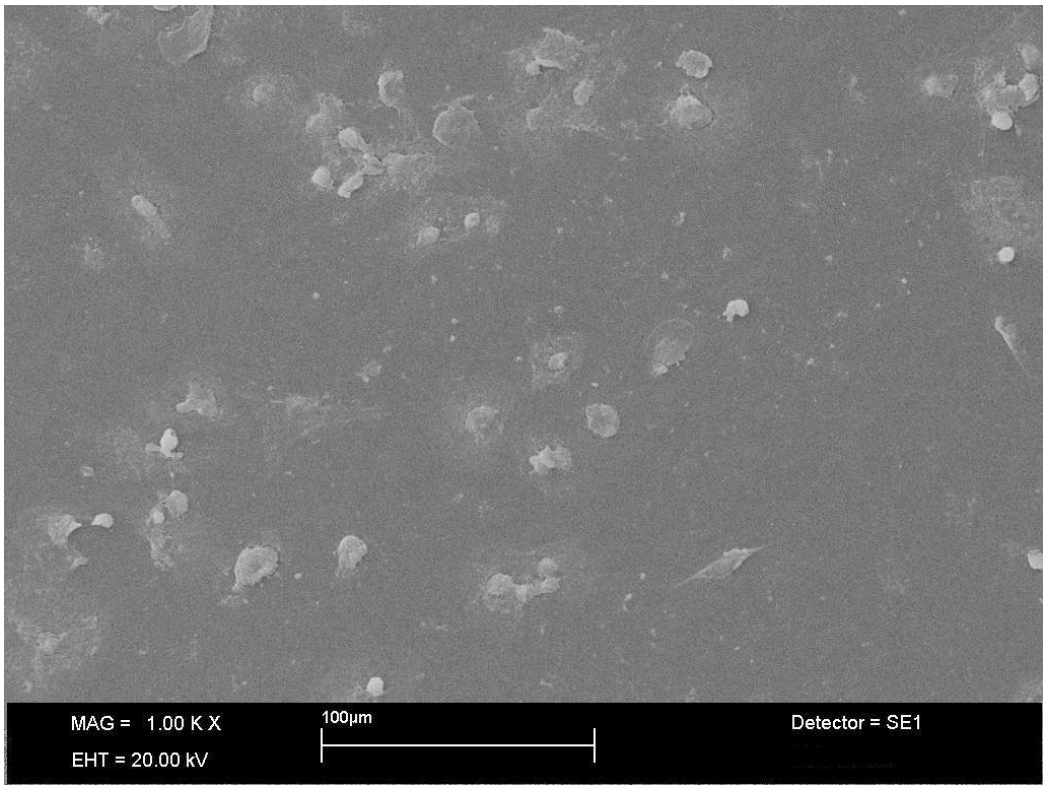

Figure 4.29 *SEM image of Saos-2 cells after 2h culture on PLLA film (a)(b) without coating, (c)(d) with apatite coating, (e)(f) with apatite/collagen composite coating.*

(c)

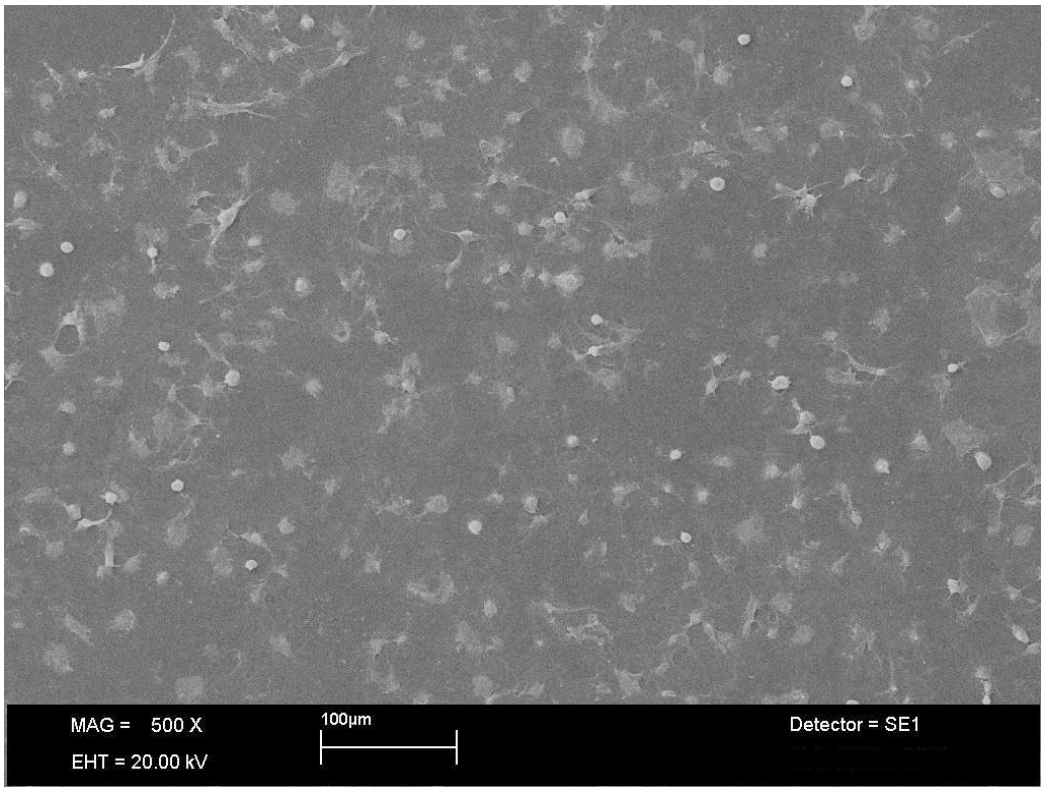

(d)

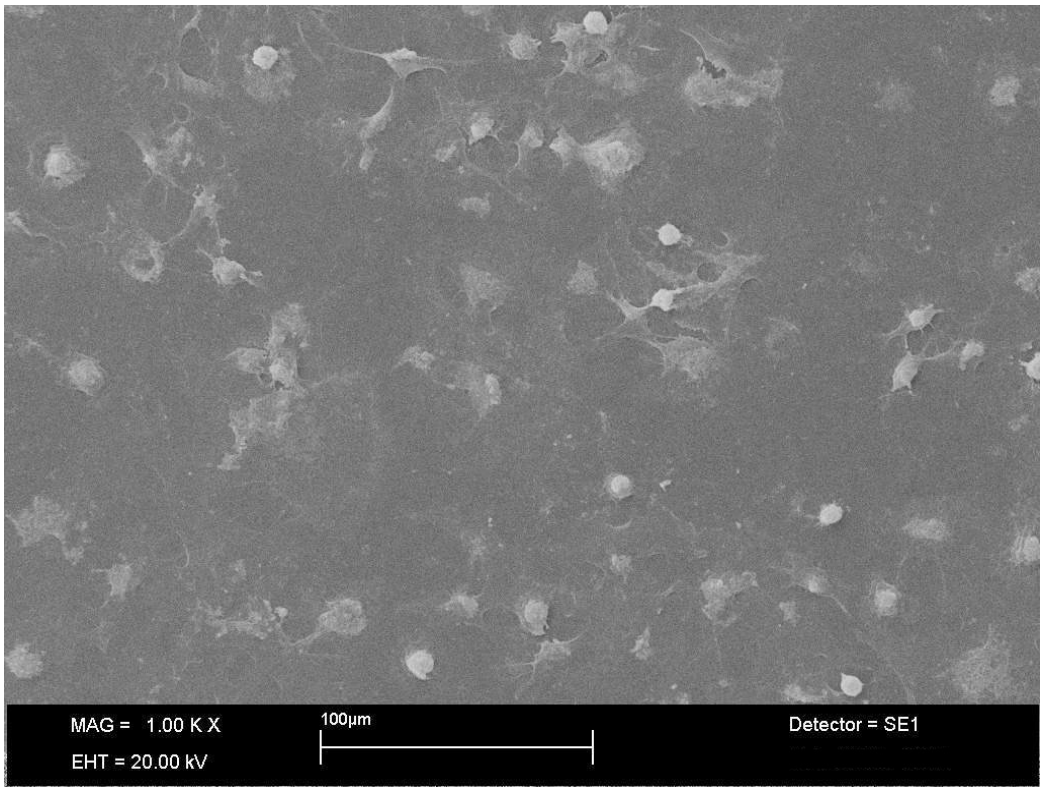

Figure 4.29 *(continued)*

(e)

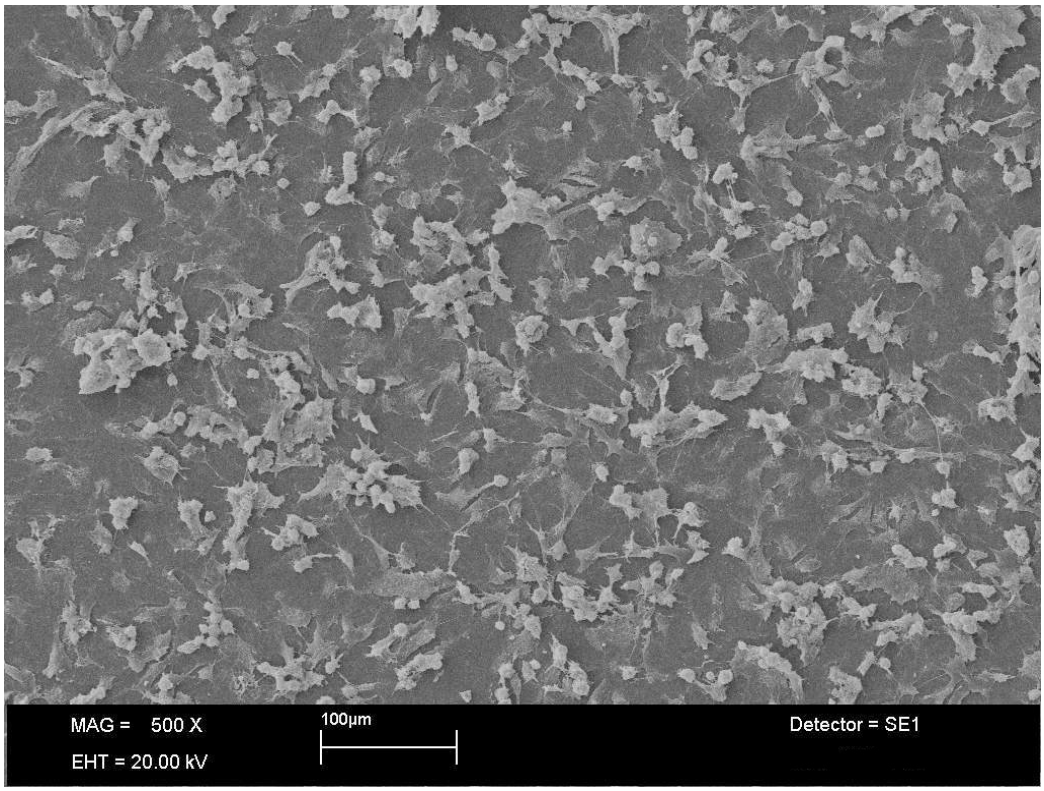

(f)

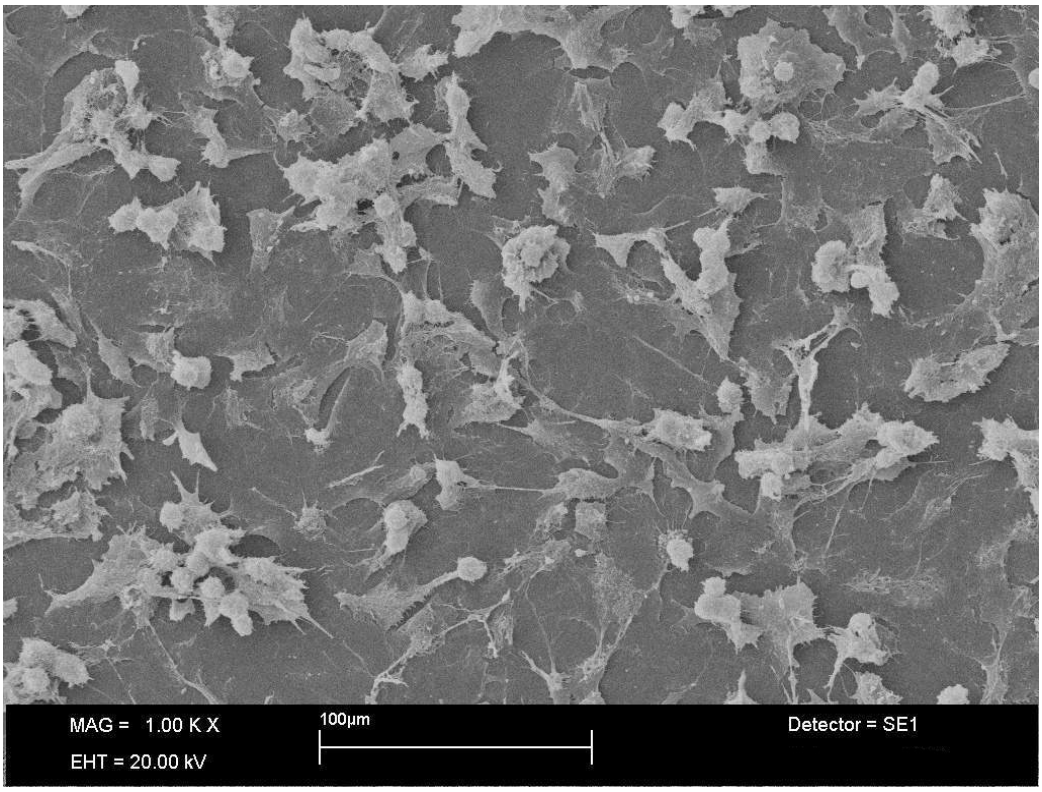

Figure 4.29 *(continued)*

(a)

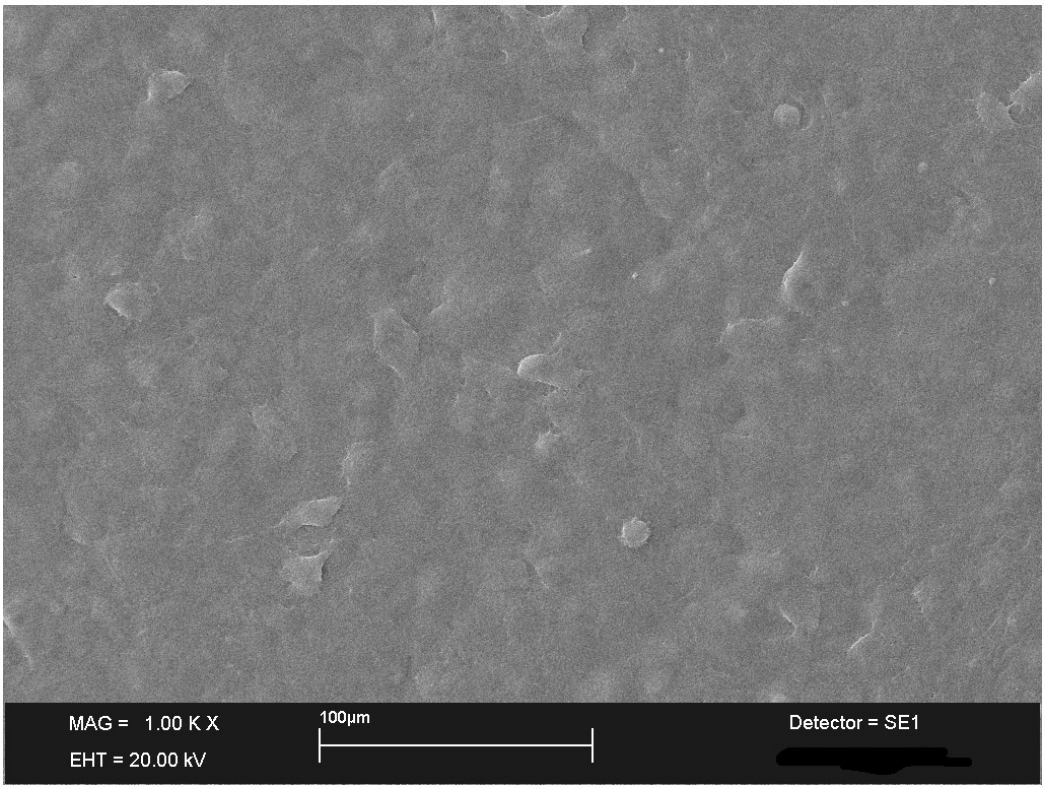

(b)

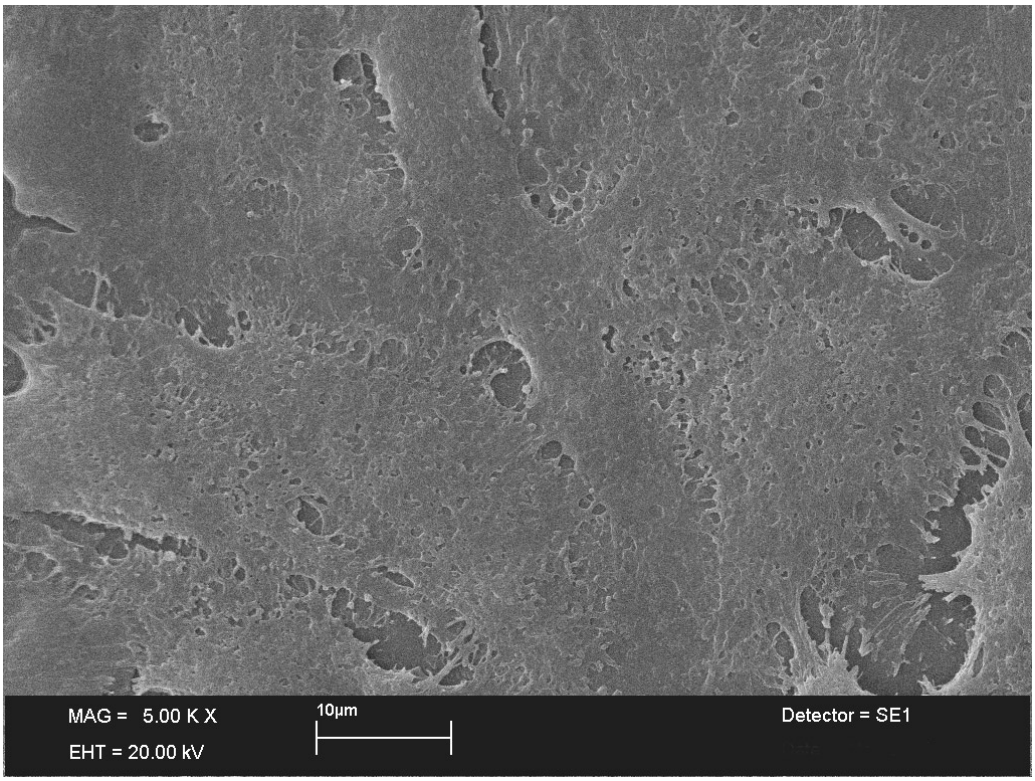

Figure 4.30 *SEM image of Saos-2 cells after 6 days culture on PLLA film (a)(b) without coating, (c)(d) with apatite coating, (e)(f) with apatite/collagen composite coating*

(c)

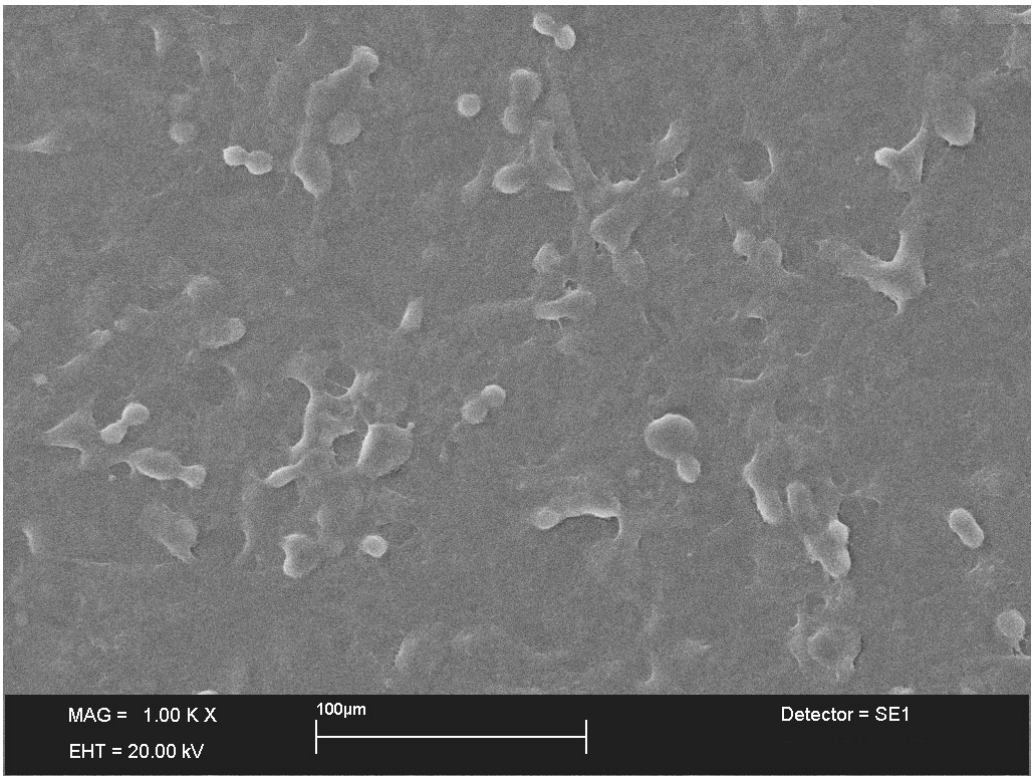

(d)

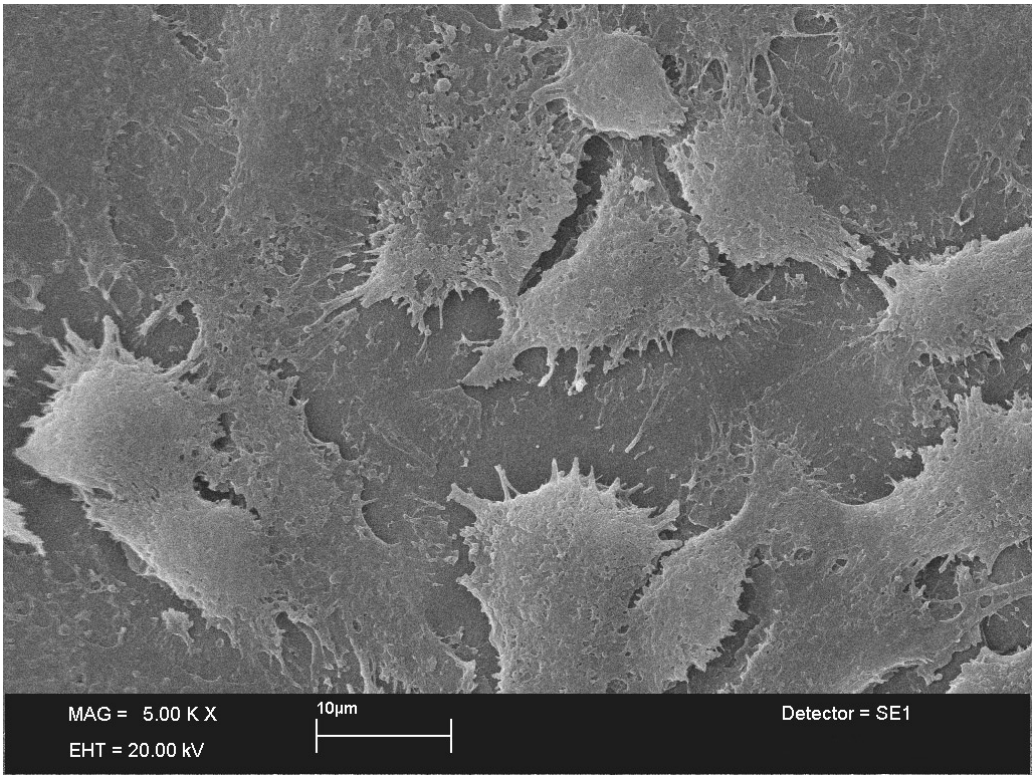

Figure 4.30 *(continued)*

(e)

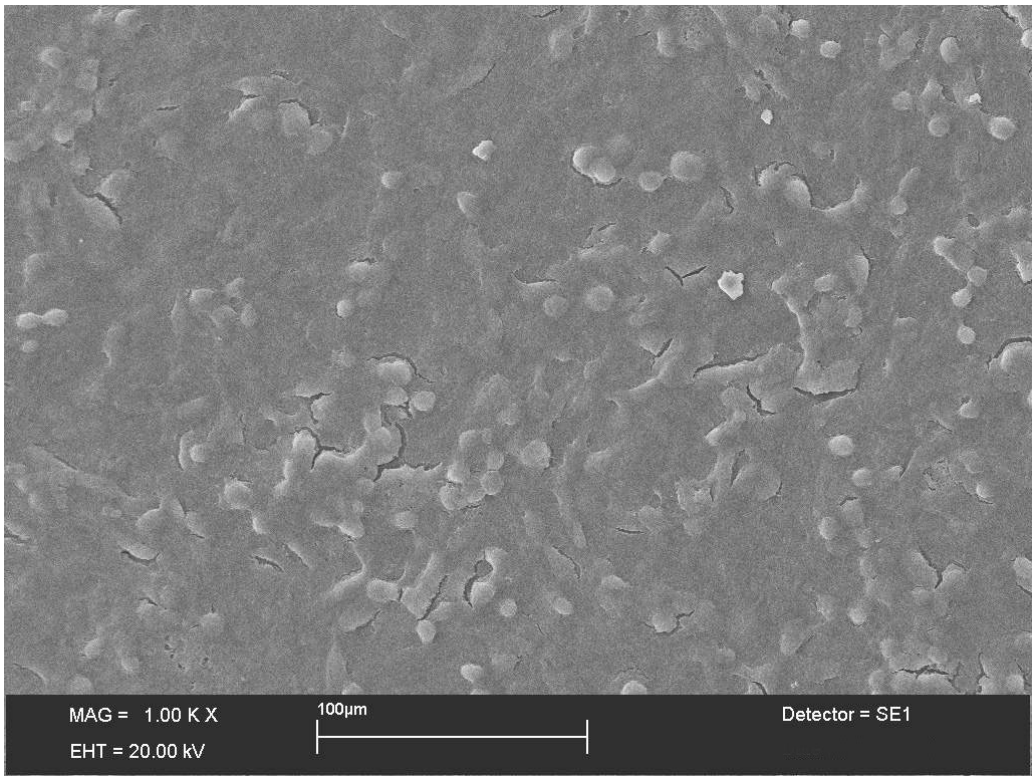

(f)

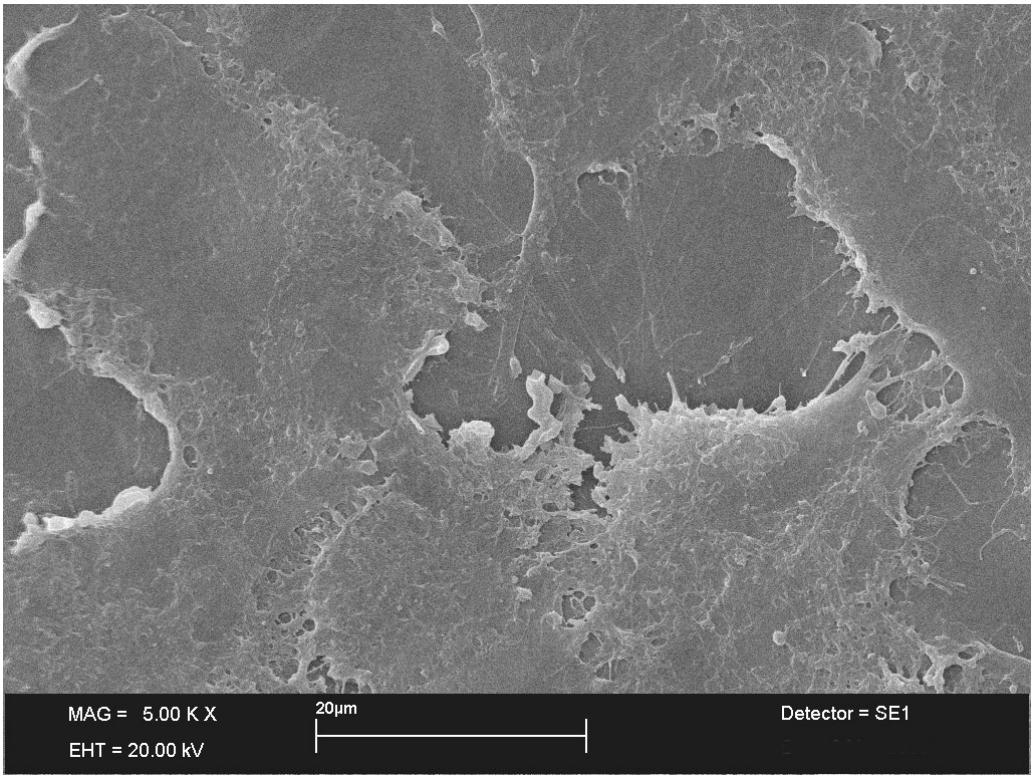

Figure 4.30 *(continued)*

4.2.1.2 Cell attachment

Cell attachment is the basis of cell migration, proliferation, and differentiation. After 2 hours (6 hours if including the 4 hours before the 0.9 ml medium was added), the number of cells attached to composite coating was significantly different as compared with that on the PLLA control film($p<0.01$) and apatite coating($p<0.05$) [Figure 4.31]. The number of cells attached to the apatite coating was apparently higher than that on the PLLA control film, though such difference was not statistically significant.

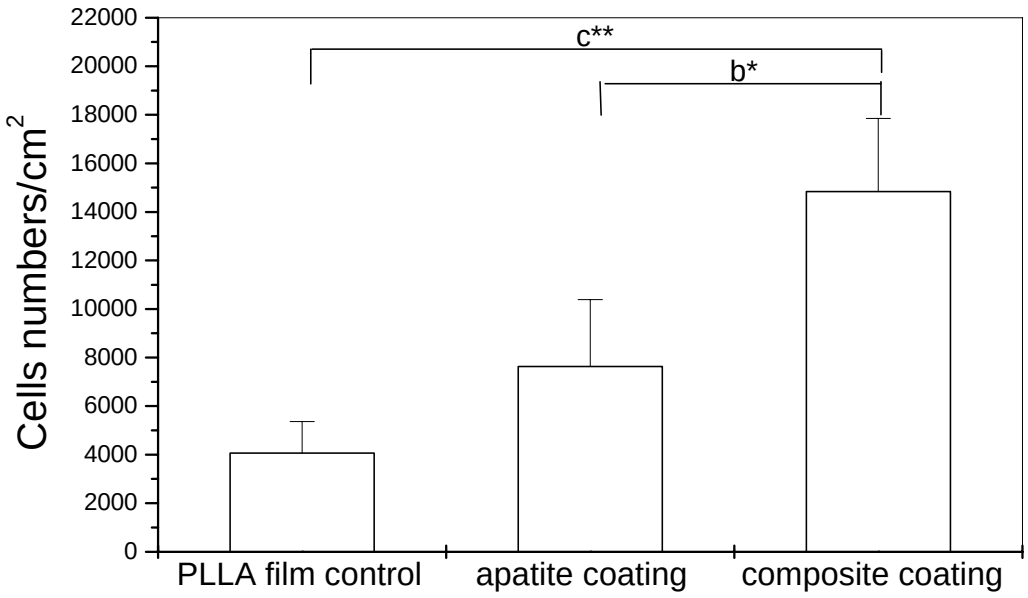

Figure 4.31 *The attachment of osteoblast-like cells cultured on PLLA film without and with coating. Error bars represent means±SD for n=3. (*P<0.05; **P<0.01. (b) composite coating compared to apatite coating; (c) composite coating compared to control).*

4.2.1.3 Cell proliferation

Compared to control films, osteoblast-like cells proliferated faster on apatite coating ($p<.0.05$) and apatite/collagen composite coating ($p<0.01$) than on PLLA films throughout the culture period (Figure 4.32). The number of osteoblast-like cells on composite coating was higher than that of the apatite coating. This differences were significant after 5 ($p<0.05$) and 7 ($p<0.01$) days culture.

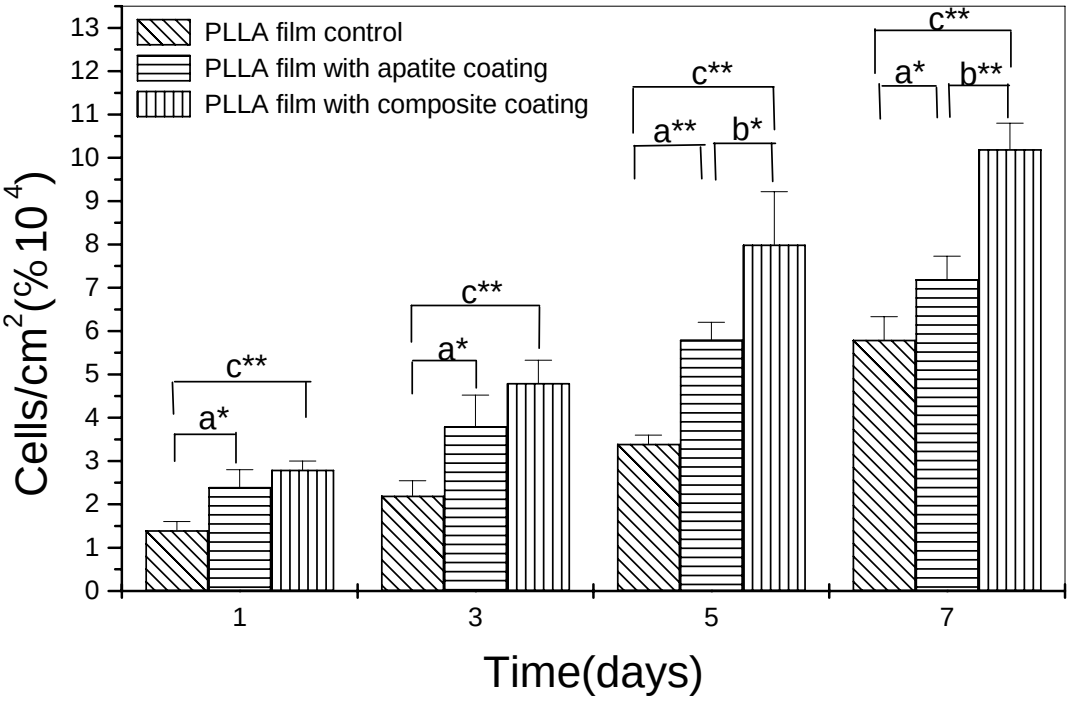

Figure 4.32 *Proliferation kinetics of osteoblast-like cells cultured on PLLA film without and with coating. Error bars represent means±SD for n=3. (*P<0.05; **P<0.01. (a) apatite coating compared to control; (b) composite coating compared to apatite coating; (c) composite coating compared to control).*

4.2.1.4 Cell viability

MTT [3-(4,5-dimethylthiazol-2-yl)-2,5-diphenyltetrasodium bromide] reagent is a pale yellow substrate that is reduced by living cells to a dark blue formosan product. This process requires active mitochondria, and the absorbance of formazan indirectly reflected the level of cell metabolism. Thus this process is taken as an accurate measure of the viability of cells in culture. After 8 days of culture [Figure 4.33], the viability of Saos-2 cultured on composite coating was significantly higher than that of control($p<0.05$) and apatite coating($p<0.05$). Although the cell viability of saos-2 on apatite coating was higher than that of the control, the results failed to demonstrate a significant difference($p>0.05$).

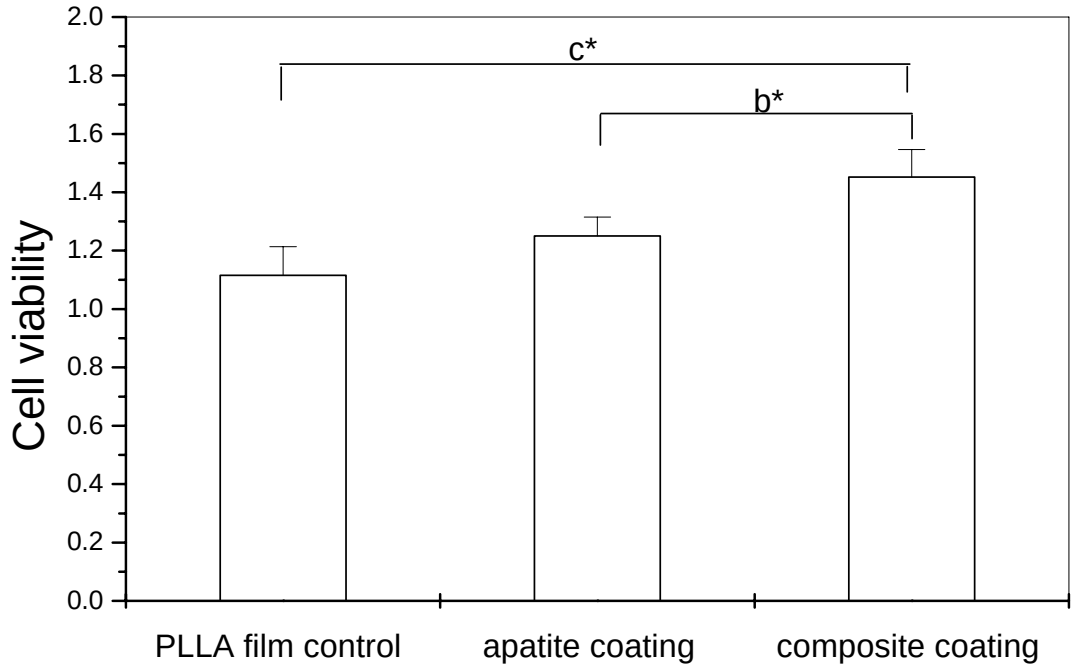

Figure 4.33 *MTT assay, Formosan aborbance expressed as a measure of cell viability from osteoblast-like cells seeded onto PLLA films with and without coating. Error bars represent means±SD for n=3. (*P<0.05;. (b) composite coating compared to apatite coating; (c) composite coating compared to control).*

4.2.1.5 Alkaline phosphatase (ALP) activity

Alkaline phosphatase activity, one of the markers of differentiated osteoblast functions, was assessed after 8 days of culture. Figure 4.34 shows the ALP activity of osteoblast-like cells cultured on PLLA films and on PLLA films with apatite or composite coating. The ALP activity of saos-2 cultured on PLLA films with apatite coating and composite coating were significantly higher than that on the PLLA films control with $p<0.05$ and $p<0.01$, respectively. Compared to the apatite coating, the ALP activity of Saos-2 cultured on PLLA films with composite coating was significantly higher ($p<0.05$). The present study shows that the apatite coating and composite coating have positive effects on the growth of osteoblast-like cells and on the upregulating of the osteoblastic phenotype, as shown by an increased ALP activity.

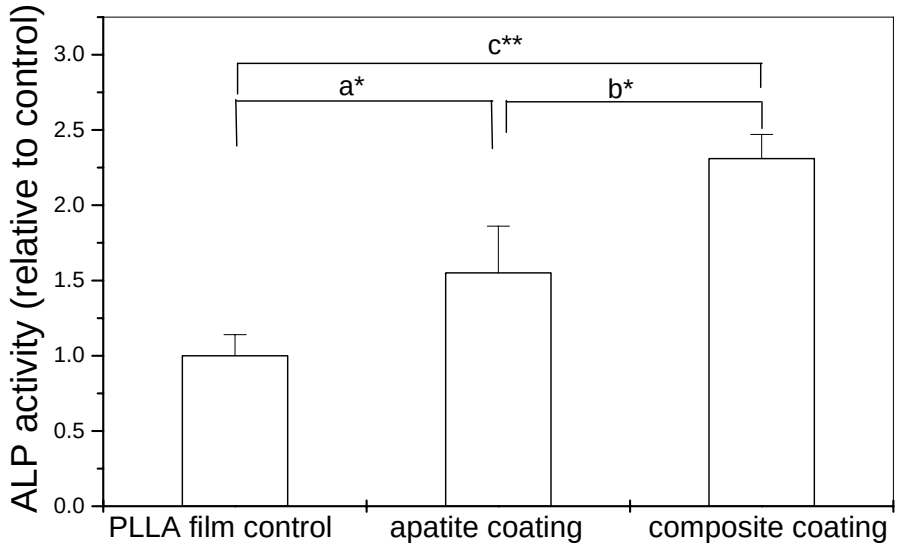

Figure 4.34 *The ALP activity of osteoblast-like cells seeded on PLLA film without and with coating. Error bars represent means±SD for n=3. (*P<0.05; **P<0.01. (a) apatite coating compared to control; (b) composite coating compared to apatite coating; (c)composite coating compared to control).*

4.2.2 Cell seeding on scaffolds

4.2.2.1 Cells morphology

Figure 4.35 shows the surface around the center of one arbitrary side of the rectangular scaffold following 2-day incubation. In the control PLLA scaffold, the cells tended to aggregate, did not spread well, and remained round in shape; while in the apatite-coated and apatite/collagen coated PLLA scaffolds, the cells tended to spread more and exhibited filopodia.

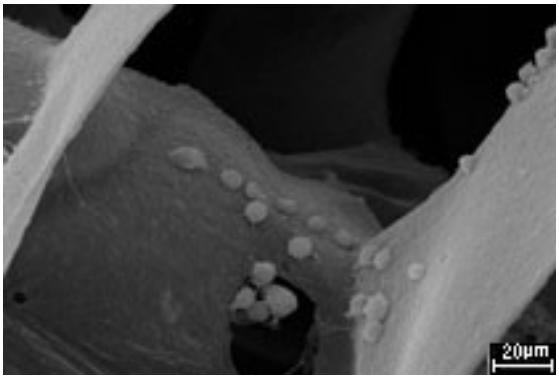

(a)

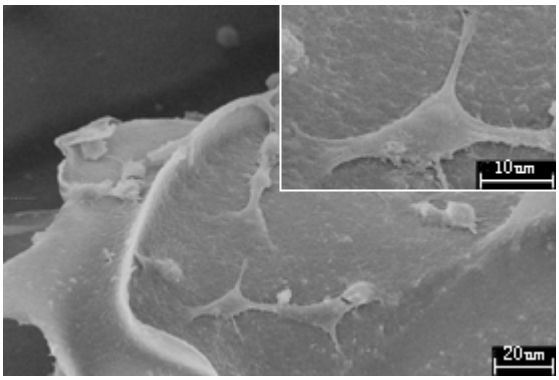

(b)

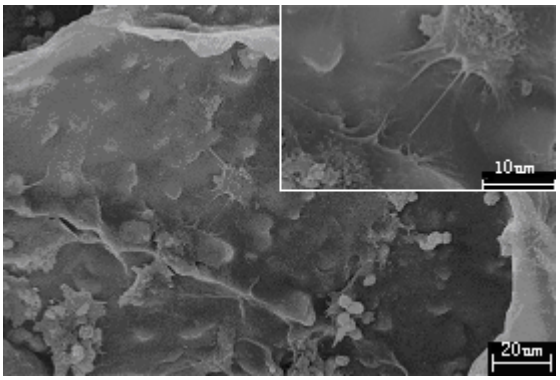

(c)

Figure 4.35 *SEM image of Saos-2 cells after 2 day culture on PLLA scaffold (a) without coating, (b) with apatite coating, (c) with apatite/collagen composite coating.*

4.2.2.2 Cell viability

Figure 4.36 showed the absorbance of formazan produced by cells on the PLLA scaffolds with and without coating after 8 days culture. Compared to the control, higher absorbance was obtained when the scaffolds were coated with apatite and apatite/collagen with $p<0.05$ and $p<0.01$, respectively. Compared to the apatite coating, the viability of saos-2 cultured on apatite/collagen composite coating was significantly higher ($p<0.05$).

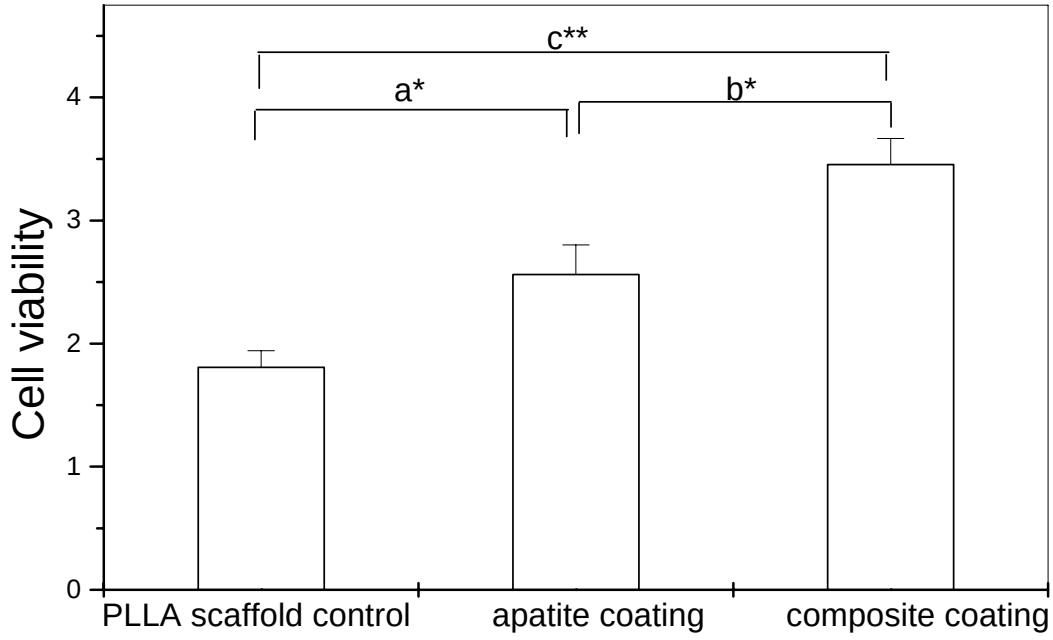

Figure 4.36 *MTT assay, Formosan aborbance expressed as a measure of cell viability from osteoblast-like cells seeded onto PLLA scaffolds with and without coating. Error bars represent means±SD for n = 3. (*P<0.05, **P<0.01;. (a) apatite coating compared to control; (b) composite coating compared to apatite coating; (c) composite coating compared to control).*

4.2.2.3 Alkaline phosphatase (ALP) activity

Alkaline phosphatase activity was measured to assess the differentiated osteogenic activity of the cell constructs. Figure 4.37 shows the ALP activity of osteoblast-like cells cultured on PLLA scaffolds and on PLLA scaffolds with apatite or apatite/collagen composite coating. The ALP activity of saos-2 cultured on PLLA scaffolds with composite coating were significantly higher than that on the PLLA scaffolds control ($p<0.05$) and apatite coating ($p<0.05$). Although the ALP activity of saos-2 cells on apatite coating was higher than that of the control, the results failed to demonstrate a significant difference ($p>0.05$).

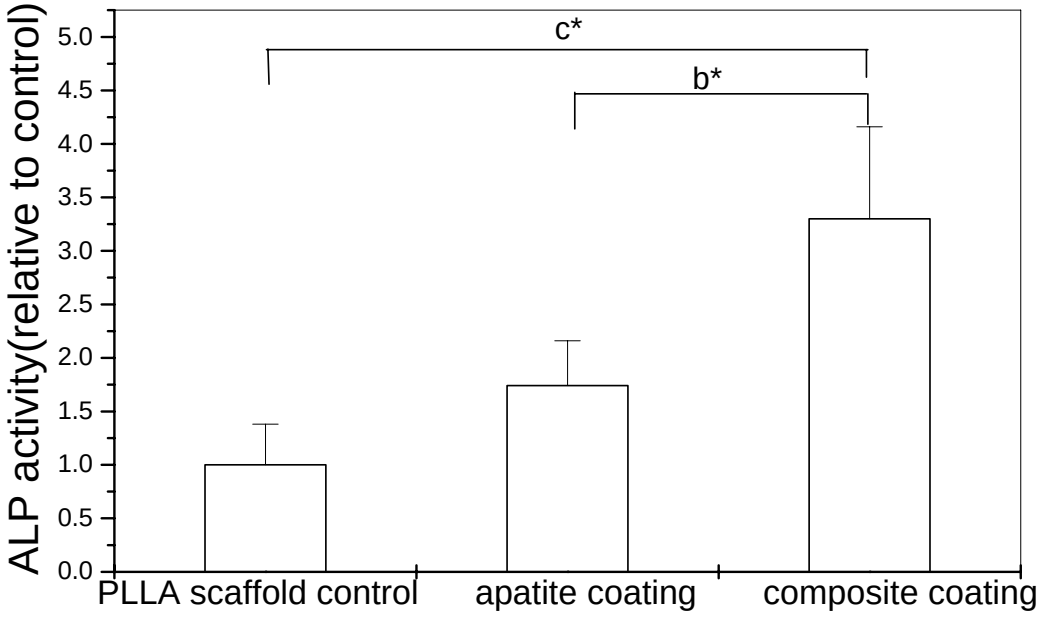

Figure 4.37 *The ALP activity of osteoblast-like cells seeded on PLLA scaffolds without and with coating. Error bars represent means±SD for n=3. (*P<0.05. (b) composite coating compared to apatite coating; (c) composite coating compared to control).*

CHAPTER 5

DISCUSSIONS

5.1 Surface modification of PLLA films and scaffolds

5.1.1 Apatite coating by an accelerated biomimetic process

From the analyses of SEM, EDX, XRD, FTIR, it was confirmed that the coating formed on the PLLA films, PLLA scaffolds and PGA scaffolds in the accelerated biomimetic process was carbonated apatite, which was similar in composition and structure to the natural apatite in human and animal hard tissues.

It was reported that PLLA film was completely covered with apatite after incubation in the SBF for 15 days (Zhang and Ma, 1999a). In the accelerated biomimetic process (5SBF), this period was shortened to 24 hours. It has also been reported that bone-like apatite particles were formed on PLLA scaffolds in the classical biomiemtic process (Zhang and Ma, 1999a). However, even after the incubation of 30 days in the classical biomimetic process, the scaffold pore walls near the surface were not completely covered with apatite. In the accelerated biomimetic process (5SBF), after 24 hours incubation, the pore walls near the surface were almost completely covered with apatite.

5.1.1.1 Morphology and composition of apatite coating

The morphology and composition of apatite on PLLA films by the accelerated and classical biomimetic processes were quite similar. However, apatite particles by this accelerated biomimetic process were much smaller (200-400nm vs.2-6μm) than those by a classical biomimetic process (Yuan *et al.*, 2001; Zhang and Ma, 1999a) when the whole surface of the PLLA film was covered by the apatite coating. That may be because more nuclei were available in 5SBF. A large number of nuclei grew competitively, leading to a smaller average size. These submicron apatite particles are closer to that in the natural bone (Wang M., 2003) in dimension than the micro-sized apatite particles formed in the classical process.

One concern of apatite coating by a biomimetic process is weak adhesive strength between the substrate and apatite layer. Researchers have tried to increase the adhesive strength using various methods, such as acid or alkali pretreatment (Tanahashi *et al.*, 1994&1995a), ultraviolet irradiation pretreatment (Liu *et al.*, 1998), and glow discharge pretreatment of the substrate (Tanahashi *et al.*, 1995b). Increase of adhesive strength by these methods could be attributed to the increase of the surface roughness or the increase of the amount of polar groups which could bond with apatite. The size of apatite microparticles should also influence the physical adhesive strength between apatite coating layer and substrate. If coating is composed of larger particles, it might be easier for the coating layer to detach from the substrate. The submicron apatite particles formed on Poly(a-hydroxy acid) are assumed to possess higher adhesive strength with the substrate than the micro-sized particles formed using the classical methods (SBF or 1.5SBF). Such assumption, however, would require further study and confirmation.

5.1.1.2 Possible reasons for the accelerated process

The shortened coating period is believed to be due to the high ion concentration and low pH value in 5SBF. High concentrations of calcium and phosphate ion enhance the condition of supersaturation near the substrate, thus avail more nuclei of apatite on the substrate. The process of nuclei growing consumes more calcium and phosphate ions from the surrounding fluid. High ion concentrations could provide fast supply to the area surrounding the nuclei, leading to an accelerated growing of the layer. Hence, the time to cover the whole surface can be remarkably shortened.

Low pH value of 5SBF may be another reason for the accelerated process. The hydrolysis of polymer substrate was demonstrated to be important in the formation apatite nucleation (Yuan *et al.*, 2001; Zhang and Ma, 1999a). Zhang and Ma (1999a) proposed that weak acidic group COOH generated by PLLA hydrolysis may transfer to COO^- and provide a negatively charged surface to adsorb positive Ca^{2+} and induce apatite nucleation. In the accelerated biomimetic process, the pH value of 5SBF solution was adjusted lower than that of the classic SBF(6.4 vs. 7.4) to obtain stable highly concentrated solution because the solubility of Ca-P salts increased with the decrease of pH (Elliot, 1994). The weak acidic condition may contribute to the formation of more apatite nuclei by promoting the hydrolysis of PLLA and producing more COO^- or other polar groups.

5.1.1.3 Ca/P ratio

It was also noticed that Ca/P ratio changed during the incubation of PLLA film. This could be explained by the nucleation mechanism above. The surface

registered more calcium when many such ($COO^- + Ca^{2+}$) nuclei formed by 12 hours of incubation. With the nuclei growing, more PO_4^{3-} might combine with the nuclei. This might explain why Ca/P ratio decreased to 1.31-1.32 at hour-16 and hour-24. The resultant Ca/P ratio after 24 hours was below the value of 1.71 for human bone. This may be because some PO_4^{3-} sites are substituted by HPO_4^{2-}. Other researchers have also reported that the apatite formed by the classical (Gu *et al.,* 2004; Guo *et al.,* 2001) or accelerated (Chou *et al.,* 2004) biomimetic process was comparatively calcium deficient.

5.1.1.4 pH value of 5SBF

Because the solubility of Ca-P salts increased with the decrease of pH (Elliot, 1994), the pH value of 5SBF solution was adjusted lower than the classic 1.5SBF(6.4 vs. 7.4) to obtain a highly concentrated yet stable solution. Barrere and coworkers (2002b) used bubbling carbon dioxide (CO_2) to attain this aim. They pointed out that once the CO_2 supply was stopped at the beginning of incubation, dissolved CO_2 would be released out of the solution to air, leading to a rise in pH. Progressively, the solution reached its supersaturation point, leading to the precipitation and formation of coating. In this study, even though HCl was used to lower the pH, it is believed that the release of CO_2 during apatite formation is still the cause for the increase of pH. In the solution of 5SBF, the following chemical reactions took place:

$$HCO_3^- + H_2O \leftrightarrow H_2CO_3 + OH^- \qquad pK_2=7.64 \qquad (1)$$

$$HCO_3^- + H_2O \leftrightarrow CO_3^{2-} + H_3O^+ \qquad pK_2=10.25 \qquad (2)$$

$$H_2CO_3 \leftrightarrow CO_2 + H_2O \qquad (3)$$

When HCl was added, reactions (1) and (3) proceeded in the right direction, more CO_2 was produced and dissolved in the solution. During the incubation period in a shaker bath, the dissolved CO_2 could be released from the solution. Bubbles were indeed observed on the substrate during the incubation experiments. With being CO_2 released from the solution, reaction (3) proceeded right, resulting in the right trend of reaction (1) and the left trend of reaction (2). Hence, the pH value of solution increased with incubation time. With the accumulation of concentration of OH^-, the right trend rate of reaction (1) was slowed down. Hence, the increase rate of pH value became slower with incubation time.

5.1.1.5 Significance of the accelerated biomimetic process

Besides time-saving, fast coating by this accelerated biomimetic process shows great significance for biodegradable polymers. PLLA degrades in humid environments via hydrolysis. In the classical biomimetic process in the SBF or 1.5SBF, after 4 weeks incubation, the properties of PLLA substrates, such as weight, average molecular weight, crystallinity and melting temperature, and the structure of scaffolds, such as porosity, median pore diameter, and surface/volume ratio, changed to some extent (Lu *et al.*, 2000; Yuan *et al.*, 2002). In the accelerated biomimetic process, one day incubation could reduce such degradative influences. The mechanical analysis in Figure 4.16 and Figure 4.17 suggested that hydrolysis for one day in water (pH=6.4) did not reduce the scaffold stiffness, while apatite formed enhanced the scaffold stiffness. For example, the compressive modulus of PGA scaffolds in the aqueous condition with pH=6.4 for 24 hours decreased by about 6% [Figure 4.17], while that of PGA scaffolds in the aqueous condition with pH=7.4 for 14 days decreased by about 50% (Shum and Mak, 2003).

This work has demonstrated how the ion concentration significantly influences the rate of apatite formation on polymer substrates in a biomimetic solution. Although only the PLLA films and PLLA scaffolds were studied in this investigation, this method could be applied to grow apatite rapidly on other biodegradable polymeric substrates, dense or porous.

5.1.1.6 PGA scaffolds with apatite coating

It was reported that the composites of PGA and carbonated apatite as bone substitutes showed slower degradation rate than pure PGA (Linhart *et al.*, 2001). In that study, the carbonated apatite was prepared by mixing a solution of $NH_4H_2PO_4$ and K_2CO_3 with a solution of $Ca(NO_3)_2$. In this study, these PGA scaffolds with bone-like carbonated apatite formed by the accelerated biomimetic method is expected to show comparatively slower degradation rate. This may enhance the use of apatite-coated PGA in the orthopaedic application where slightly longer service life might often be preferred. To our knowledge, this work represented the first time that bone-like apatite was successfully grown on the PGA substrate. Because PGA has a fast degradation rate and will disintegrate after 4 weeks (Shum and Mak, 2003), it is difficult to coat a substantial layer of apatite on PGA in SBF or 1.5SBF within a period of 2-4 weeks. Using this accelerated coating process in 5SBF, apatite could be coated on PGA in 24 hours. The short immersion time for coating apatite minimizes the extent of PGA hydrolysis, and therefore minimizes the degradation effects on the properties of the substrate.

PGA scaffolds were not completely covered with apatite particles in 24 hours. This was presumably due to a much lager surface area of the fibrous scaffold and thus a smaller density of apatite nuclei on the scaffold substrate. The internal section had fewer apatite particles than near the scaffold surface, probably because the transport of ions between the scaffold internal and the surrounding solution was not as efficient as that between the scaffold surface and the surrounding solution, leading to lower ion concentration and fewer nuclei on the internal substrate.

The compressive modulus of PGA scaffolds with apatite coating was significantly higher than that of the PGA scaffold. The compressive modulus of PGA scaffolds after incubation in distilled water (pH=6.4) for 24 hours was slightly, but not significantly ($p>0.05$), lower than that before incubation. This indicated that apatite particles coated on PGA scaffolds enhanced the mechanical properties of the scaffold.

5.1.1.7 “Bone-like apatite”

Kokubo and coworkers named the layer formed in SBF as “bone-like apatite” (Abe *et al.*, 1990). They used the characterization of thin-film XRD, EDX, FTIR, SEM and TEM to demonstrate the coating is “bone-like apatite”. The characterizations could be summarized as follows:

Table 5.1 *Characterizations for the demonstration of "bone-like apatite"*

Characterizations	Descriptions
EDX	Ca peak and P peak
XRD	The peak at 26 ^{o} was assigned to the 002 diffraction of apatite. The range of 31-33^{o} was assigned to the 211, 112, and 300 diffractions of apatite.
FTIR	PO_4^{3-} (604 and 563 cm^{-1} were assigned to the v_4 vibration, 1031cm^{-1} was designated as associated with the v_3 vibration, 959 and 465 cm^{-1} were designated as associated with the v_1 and v_2 vibration)
TEM	Electron diffraction patterns were ascribed to the (002) (211) (222) (213) planes of crystalline apatite

Since then, numerous studies on the formation of "bone-like apatite" were published using the same characterization methods (Tanahashi *et al.,* 1994b; Barrere *et al.,* 2001; Murphy *et al.,* 1999; Rhee and Tanaka, 1998; Yokogawa *et al.,* 1999; Yuan *et al.,* 2001; Zhang and Ma, 1999a). In this thesis, the word of "bone-like apatite" was also used in this sense.

Recently Leng and coworkers (Leng et al., 2003; Lu and Leng, 2004; Xin et al., 2005&2006) proposed that more characterization should be needed to identify whether the coating is apatite. They believed that conventional XRD could not distinguish octacalcium phosphate (OCP) from apatite, because the two main diffraction peak positions associated with OCP and apatite in the XRD spectra (20 ^{o}-40 ^{o}) are very close. The main differences between apatite and OCP in the XRD

spectra are in low 2θ range. However, low-angle peaks are difficult to detect. Furthermore, they believe that the OCP and apatite could not be identified from the ring pattern of electron diffraction in TEM because OCP rings of (100) and (110) are too close to the central beam spot and the high brightness of the central spot makes those invisible. Meanwhile, they demonstrated that the diffraction patterns of single crystals obtained in TEM could distinguish OCP and apatite. They studied the coatings formed on hydroxyapatite/β-tricalcium phosphate (HA/TCP) ceramics (Leng et al., 2003) and titanium metals (Lu and Leng, 2004) using TEM and demonstrated that the coatings formed in SBF were octacalcium phosphate (OCP) instead of apatite.

In this thesis, the word of “bone-like apatite” was used in the traditional way in which Kokubo and many researchers have used it. The work of Leng and coworkers should be considered when the word of “bone-like apatite” is to be used in the future.

5.1.2 Apatite/collagen composite coating

These analyses of SEM, EDX, XRD and FTIR showed that the coating formed in the accelerated biomimetic coprecipitation process contained not only carbonated apatite but also collagen, which is more similar in composition to natural bone.

5.1.2.1 Possible mechanism of accelerated formation of apatite/collagen composite coating

The hydrolysis of polymer substrate was demonstrated to be important in the formation apatite nucleation (Yuan *et al.*, 2001; Zhang and Ma, 1999a). The reactive group of –COOH was also important for collagen adsorption (Ma *et al.*, 2002; Bisson *et al.*, 2002). In the accelerated biomimetic coprecipitation process in 5SBFC, we believed that the hydrolysis of PLLA was important to induce the deposition of collagen and apatite complex composite coating. The mechanism of apatite and collagen formation on the PLLA in 5SBFC was schematically illustrated in Figure 5.1 The sequence was from (a) to (f). PLLA hydrolysis may generate acidic groups –COOH on the surface [Figure 5.1(b)], which may facilitate collagen absorption [Figure 5.1(c)]. The groups of –COOH may also further change to $–COO^-$ [Figure 5.1(d)], providing a negatively charged surface to adsorb positive Ca^{2+} and induce apatite nucleation [Figure 5.1(e)]. The functional groups existing on the surface of collagen, such as –COOH and $–NH_2$ [Figure 5.1(c)], may also become charged groups, such as $–COO^-$ and $–NH_3^+$ [Figure 5.1(d)], which again could absorb positive Ca^{2+} and negative HPO_4^{2-} to form apatite nuclei [Figure 5.1(e)]. Hence apatite particulates could form on the surface of collagen and PLLA [Figure 5.1(f)]. Because both apatite nucleation and collagen deposition could occur during the whole coprecipitation process, it was possible that additional collagen fibrils and apatite particulates can be deposited on top of the former apatite particles and collagen fibrils. This roughly explain how a complex composite of collagen fibrils and apatite particulates could be formed on PLLA surface in this accelerated biomimetic coprecipitation process [Figure 4.19 (b), Figure 4.21 (b)].

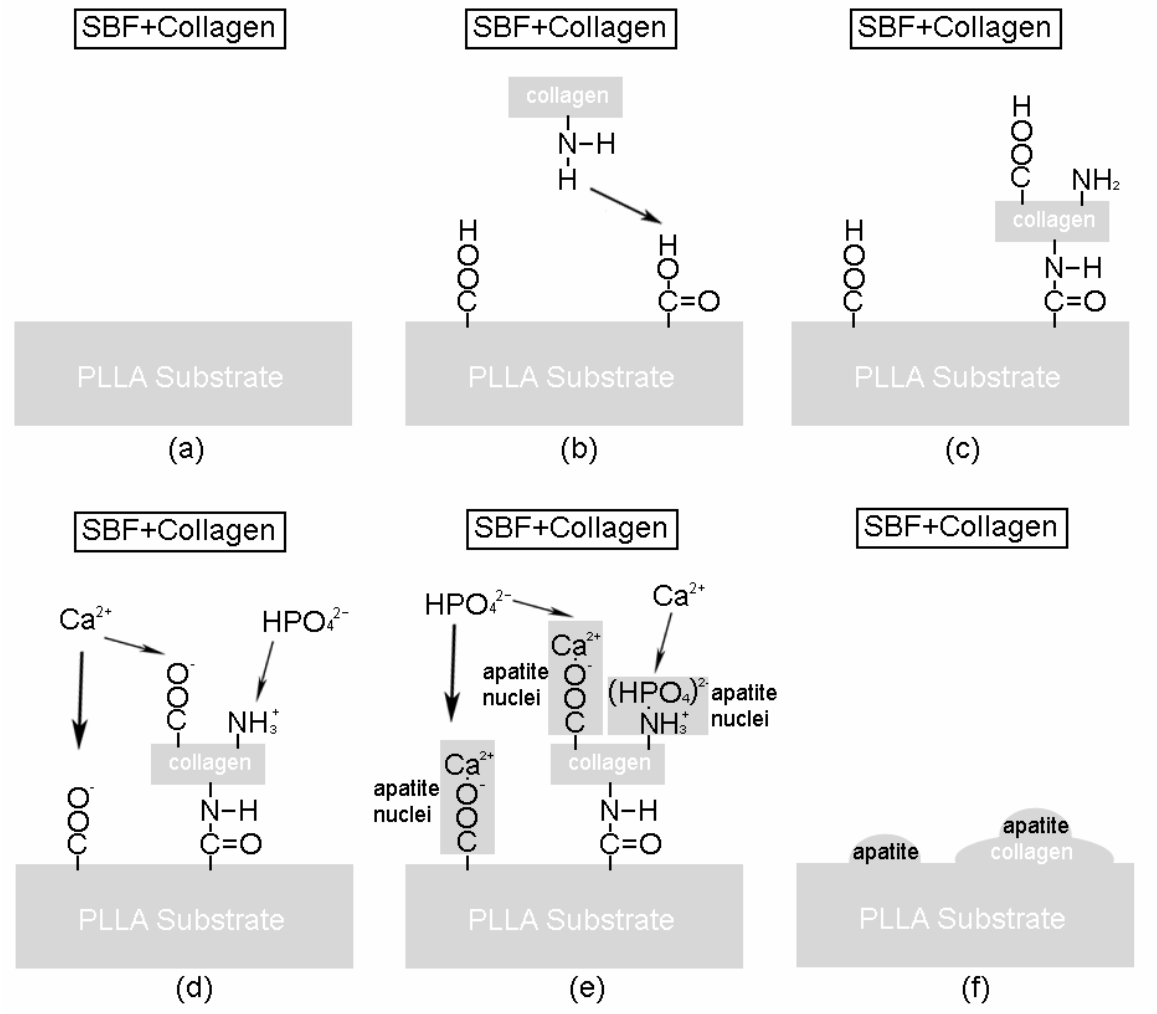

Figure 5.1 *Schematic diagram of apatite and collagen formation on the PLLA in 5SBFC with the sequence of (a)-(f).*

As described in the section of 5.1.1, compared with the classical bimimetic process, the accelerate biomimetic process has some advantages, such as time-saving, applicable to some polymers which degrade too fast to be coated with apatite in the classical biomimetic process, forming submicron apatite particles closer in dimension to the apatite in natural bone. The accelerated biomimetic process also facilitated the biomimetic coprecipitation process. The usual period for the classical biomimetic apatite coating process was 1-4 weeks, while that for the collagen coating was 2-24 hours. The difference in time scale could coprecipitation difficult. The period for the

accelerated biomimetic process was reduced to 24 hours, which matched the collagen adsorption period, making the coprecipitation and composite coating possible.

It was noticed that the size of apatite particles formed in 5SBFC is less than that of particles formed in 5SBF for 24 hours [Fig.5(a) vs. (b), Fig. 7(a) vs. (b)]. This may be explained by the incorporation of collagen into the biomimetic precipitation process. During the coprecipitation of apatite and collagen in 5SBFC, the apatite particles formed earlier may be covered by a later deposition of collagen fibers. Since the new apatite nuclei formed on the surface of these later collagen fibers had less time to grow, apatite particulates observed on the outer surface tended to be smaller.

5.1.2.2 pH value of 5SBFC

In the section of 5.1.1.4, we have proposed that the release of CO_2 during apatite formation resulted in the increase of pH progressively, making the solution reach its supersaturation point and leading to the precipitation and formation of apatite coating. In the accelerated biomimetic coprecipitation process in 5SBFC, the pH value also increased after 24 hours incubation (8.5 for PLLA films, 8.4 for PLLA scaffolds). It was also believed that the release of CO_2 during coating formation resulted in the increase of pH. With the increasing pH value, collagen and the ions of SBF reach their supersaturation point, leading to the coprecipitation and formation of apatite/collagen composite coating.

5.1.2.3 Significance of the apatite/collagen composite coating

Collagen and apatite are the two primary components of extracellular bone matrix (ECM), and have demonstrated good osteoconductivity. However, by themselves, mechanical properties of apatite or collagen are quite limiting in many applications. Therefore, coating them on other biomaterials, such as Poly(α-hydroxy acid) scaffolds, may hopefully synthesize their advantages to provide three-dimensional scaffolds with appropriate mechanical properties and excellent cell recognition receptors for cell attachment. Poly(a-hydroxy acids) matrix coated with collagen (Suh *et al.,* 2001; Ma *et al.,* 2002; Yang *et al.*, 2002) or apatite (Yuan *et al.,* 2001; Zhang and Ma, 1999a) have separately been attempted. From a biomimic point of view, collage/apatite composite coating may be more beneficial for cell attachment, proliferation, and differentiation.

Some researchers indeed have made efforts to fabricate the apatite/collagen composite coating (Doi *et al.,* 1996; Chen *et al.,* 2001; Shibutani *et al.,* 2000). Usually, collagen was coated on the substrate first. Then apatite was deposited on the surfaces of collagen. The procedure was comparatively complex. And the method to deposit apatite in the second step was not a bimimetic process. So the apatite formed was not bone-like. Li and coworkers (Li et al., 1998) also developed an apatite/collagen coating on the 3D carbon/carbon composite in a bioactivating medium with collagen. Howerver, the structure of apatite particulates aligning on collagen fibrils was not reported. In this work, collagen and apatite were combined into the accelerated biomimetic coating process. A composite coating of bone-like submicron apatite particulates and collagen fibrils was formed on PLLA films and scaffolds in 24 hours.

Natural bone is a composite in which apatite particulates are aligned on the collagen fibers at the nm to μm scale. The submicron composite coating formed on the PLLA surface may provide better cell interaction and osteoconductivity.

Although only PLLA was used here as an example of substrates, other biomaterials, metal or polymer, dense or porous, also could be coated with this composite coating of bone-like sumbmicron apatite combined with collagen fibers using the accelerated biomimetic coprecipitation process.

5.1.3 Apatite coating formed in the flowing condition

For scaffold substrates treated in the biomimetic process, besides the incubation period, another concern is the spatial distribution of apatite. Fewer apatite particles usually found in the internal regions than the periphery region because of easier ions exchange between periphery regions and the surrounding fluid (Zhang and Ma, 2004). Inspired by the application of perfusion bioreactors in the cell seeding and culture which could yield a highly uniform cell distribution and high mass transfer not only at the periphery but also within internal pores of scaffolds (Wendt *et al.*, 2003), we hypothesize that if the SBF solution flows directly through the scaffold, high transport of ion will be achieved between the internal regions and flowing solution, therefore, more apatite particles will be formed in the internal pore walls of scaffolds. In this study, a flowing condition was introduced into the biomimetic process to make 5SBF solution flow directly through scaffolds.

The formation of apatite nuclei consumes calcium and phosphate ions from the surrounding fluid. In the static condition, it is more difficult for the central region than the surface region of scaffolds to exchange ions with outer fluid. It was believed that lower ion concentration in the central region induced the formation of fewer apatite particles. In the agitated condition in a shaking table, the ion exchange between the central region and outer solution was strengthened, however, still weaker than that between surface region and outer solution [Figure 5.2]. In the flowing condition, the 5SBF solution flew directly through the pores of scaffolds, yielding high ions transfer at the periphery and the internal regions. Hence, more uniform spatial distribution of apatite particles was achieved [Figure 5.3].

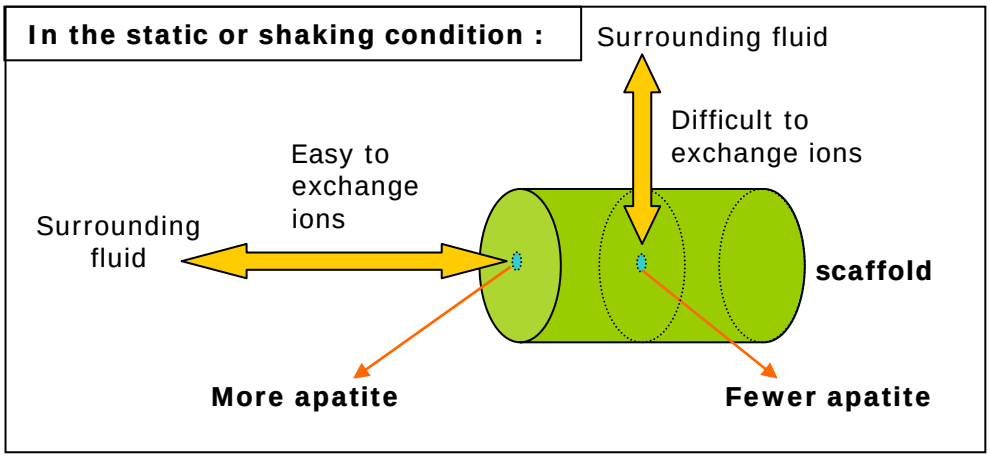

Figure 5.2 *Schematic of the ion exchange in the static or shaking condition*

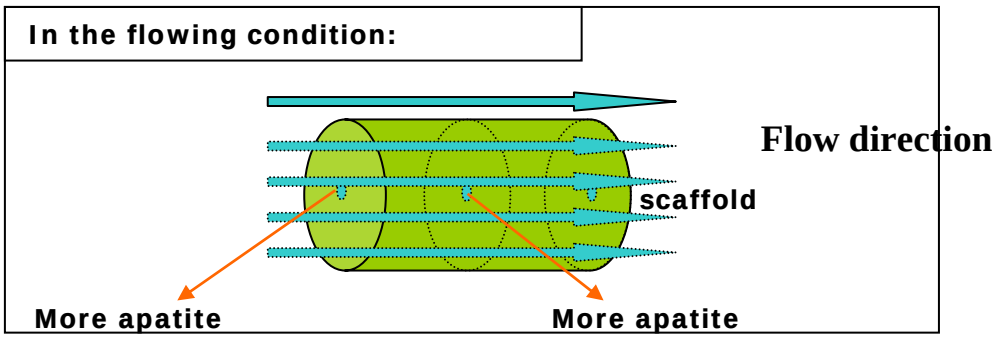

Figure 5.3 *Schematic of the ion exchange in flowing condition*

5.2 Cell seeding

We have analyzed the effect of the apatite layer and apatite/collagen layer on the PLLA films and scaffolds, formed in 5SBF and 5SBFC wthin 24 hours, on the attachment efficiency and proliferative behavior of osteoblastic cells. It was found that none of the three surfaces (PLLA, apatite, and apatite/collagen composite) appeared to elicit any major deleterious or cytotoxic responses. However, PLLA with apatite or apatite/collagen coating, especially with composite coating, were obviously more suitable for osteoblast-like cells attachment and proliferation than pure PLLA.

.

The physical and chemical properties of biomaterial surfaces, such as hydrophilicity and chemical composition, could affect cell-biomaterials interactions (Lincks *et al.*, 1998; Chesmel *et al.*, 1995). Surface properties have a major impact on the viability and functional activity of anchorage-dependent cells, such as osteoblasts. In this study, wettability results obtained from static contact angles showed that apatite coated and apatite/collagen coated surface are more hydrophilic than PLLA control surface [Table 4.2]. The chemical composition of PLLA, apatite, and apatite/collagen composite are not identical. It is likely that these factors are all involved in causing the different biologic behaviors of osteoblast-like cells.

The apatite/collagen composite coating has most “bone-like” chemical composition among the three surfaces, namely the uncoated PLLA surface, PLLA surface with apatite coating and PLLA surface with composite coating. This may be one reason that explains the highest cell proliferation degree detected on cells growing

on the composite coating. Another possible reason is the surface topography. Apatite/collagen coated surface are most hydrophilic among the three surfaces. Researchers have reported that cell attachment was better on the rougher surfaces as compared to the smoother ones (Boyan *et al.,* 1996).

From the cell seeding study, it was shown that bone-like carbonated apatite coating formed in 5SBF for 24h stimulated osteoblast-like cells differentiation *in vitro*. The enhancement of the osteoblastic activity on prefabricated apatite also was reported by other researchers (Loty *et al.,* 2000; Olmo *et al.,* 2003). Loty and coworkers (Loty et al., 2000) formed a carbonated apatite layer on a bioactive apatite-wollastonite (AW) glass-ceramic by a biomimetic process. After 23 days culture of fetal rat osteoblasts, the ALP activity was about 30% greater on AW with apatite coating compared with AW disks. Olmo and coworkers (Olmo *et al.,* 2003) cultured rat osteoblasts on bioactive glasses with and without apatite coating prefabricated by soaking in SBF for 7d. They reported that cell attachment shows a higher efficiency on the apatite layer and the biocompatibility of glass is greatly enhanced after induction of the formation of an apatite layer.

Collagen is an adhesion protein, which could facilitate cell attachment (Bisson *et al.,* 2002; Becker *et al.,* 2002; Ma *et al.,* 2005). Suh and coworkers (Suh *et al.,* 2001) grafted collagen onto ozone oxidized PLLA surface and found that the grafted type I collagen provided a favorable matrix for cell attachment and growth. Ma and coworkers (Ma *et al.,* 2005) cultured chondrocyte on the collagen immobilized PLLA surfaces and found collagen showed significantly improved cell spreading and growth. Yang and coworkers (Yang et al., 2004) immobilized type I collagen on particulate

microporous hydroxyapatite and found that collagen increased ALP activity and bone morphogenetic protein 2 (BMP-2) gene expression of human bone marrow stromal cells after 1 and 5 days compared with pure hydroxyapatite. In this study, collagen was also found to facilitate cell attachment and proliferation when it was combined with apatite particles.

The cell culture model used in our study is the human osteosarcoma cell line Saos-2. These cells are widely used in studies on bone cell differentiation, proliferation and metabolism and are known to be capable of bone production (Anderson *et al.,* 1995; Hunt *et al.,* 1996). *in vitro* studies with these osteoblast-like cells have offered insights into the biological performance of bone implant materials. A set of properties associated with the osteoblast phenotype has been established, including alkaline phosphatase (ALP) activity, type I collagen synthesis, secretion of osteocalcin and production of a mineralized matrix (Rea *et al.*, 2004; Skojdt and Russell, 1992). Of these properties, ALP is a widely recognized marker of osteoblastic differentiation. In this study, the ALP activity of the osteoblastic cells on apatite/collagen composite coating was significantly higher than that on apatite coating and PLLA. It could be explained that collagen has a positive effect on ALP activity of osteoblasts. This is in agreement with findings of increased ALP activity of osetoblastic cells on collagen matrices (Celic et al., 1998; Andrianarivo et al., 1992; Masi et al., 1992; Lynch et al., 1995). This also showed that the collagen after the process of incorporation in 5SBF and coprecipitation with apatite particles still maintain its biological activation.

In surface coating, signal recognition ligands and sequence are usually incorporated into the coating to mediate the response of anchorage-dependent cells such as bone osteoblasts and osteoclasts. Matrix proteins such as laminin (Uchida *et al.*, 2004), fibronectin (Golbus et al., 1998; Moursi *et al.*, 1997), and bone morphogenetic proteins (BMPs) (Sampath *et al.*, 1990; Wang EA *et al.*, 1990), have shown to play important roles in enhancing osteoblastic functions. In the accelerated biomimetic process, these proteins may be also incorporated into the 5SBF and into the protein-containing apatite coating.

CHAPTER 6

CONCLUTIONS AND FUTURE STUDIES

6.1 Conclusions

Continuous bonelike apatite coating was formed on PLLA films, PLLA scaffolds and PGA scaffolds within 24 hours by an accelerated biomimetic process (5SBF). Based on SEM, EDX, XRD and FTIR analyses, the coating was similar in morphology and composition to that formed in the classical biomimetic process (SBF or 1.5SBF). This indicated that an accelerated biomimetic apatite coating formation could be achieved by immersing biodegradable polymer substrates into a concentrated simulated body fluid, 5SBF, at 37^{o}C. Besides time-saving, this accelerated biomimetic process has another two main advantages. Firstly, some polymers which degrade too fast to be coated with apatite in a classical biomimetic process could be coated with bone-like apatite by this accelerated biomimetic process. Secondly, the particle dimension of apatite by this accelerated biomimetic process was submicron which was closer to the dimension of apatite in natural bone.

Composite coating of bone-like submicron apatite particles combined with collagen fibers was formed on PLLA films and scaffolds within 24 hours by an accelerated biomimetic coprecipitation process. This coating showed a composition more relevant to that of natural bone than apatite coating or collagen coating alone. This work provided an efficient process to obtain bone-like apatite/collagen composite coating, which is potentially useful for bone tissue engineering.

The present two biomimetic coatings, that is bone-like apatite coating and apatite/collagen composite coating, fabricated through the accelerated biomimetic process were found to be effective in improving the interactions between osteoblasts and PLLA. The apatite/collagen composite coating was more effective than purely apatite coating. The reason of this superiority may be attributed to the similarity of such composite coating with natural bone in composition and scale and its hydrophilicity. These results reflect that the apatite/collagen composite coating is a promising choice for surface modification in bone tissue engineering. The PLLA scaffolds coated with collagen submicron fibrils and apatite submicron paticulates are expected to be useful as a novel 3D template for bone tissue engineering.

The accelerated biomimetic process performed in the flowing condition yielded more uniform spatial distribution of apatite particles. This work provides a novel condition for obtaining uniform spatial distribution of bone-like apatite within the scaffolds quickly, which is expected to facilitate uniform distribution of attached cells within the scaffolds *in vitro* or *in vivo*.

6.2 Future work

In this work, we applied the accelerated biomimetic process on the polymeric substrate, introduced the flowing condition into the biomimetic process, and incorporated the collagen into the biomimetic process. The chemical characterization and cell seeding results demonstrated the improvement caused by these novel methods. There are still many related issues worthy of further study. They are briefly introduced as follows:

6.2.1 Animal model experiments

The development of a tissue engineering construct requires the evaluation of its performance on preclinical studies prior to evaluation in human subjects. The next step following this research work may be to implant PLLA scaffolds with bimimetic apatite/collagen coating in smaller animals to perform preclinical trials. If the results are positive the preclinical studies will proceed to larger animals.

6.2.2 Incorporating other components into the accelerated biomimetic process

Growth factors and signal recognition ligands, such as BMP and RGD, may also be incorporated into the accelerated biomimetic process. They could be involved solely, or all together with collagen. More complicated composite coatings are expected to be produced with the incorporation of these components.

6.2.3 Combination of plasma treatment and coating

Plasma treatment is a convenient method to improve the hydrophilicity and increase the surface energy of the polymer. Combining plasma treatment with collagen coating has been reported (Yang *et al.*, 2002). It was pointed out that plasma pre-treated surface would benefit in anchoring more collagen tightly. Therefore, the plasma treatment could be also combined with our coating methods. Plasma pre-treatment and after-treatment may be used. The routine is described as following:

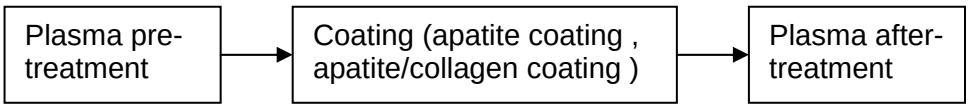

Plasma pre-treatment is expected to improve the substrate absorption ability to the apatite and collagen. The adhesion strength of plasma pretreated coating is expected to be stronger than that of control. Plasma after-treatment is expected to further improve the hydrophilicity of the coating surface and thus to further enhance cell attachment.

6.2.4 Apatite and apatite-containing coating in the flowing condition

The flow rate could be varied to determine the optimum parameter, and to study how the parameter influence the morphology and structure of the resultant coating. Furthermore, apatite/collagen or other apatite-contained composite coating may also be formed in the flowing condition to obtain a uniform distribution in the scaffolds.

Furthermore, the flowing condition may change the morphology of apatite/collagen composite coating. In the condition that 5SBFC flows through the substrates, collagen fibers may align along the flow direction and apatite may locate along the collagen fibers (Figure 6.1). At the nm to mm scale, the bone apatite reinforced collagen formed individual lamella (Figure 2.1). Thus apatite/collagen coating formed in the flowing condition may be more similar in morphology to that of natural bone.

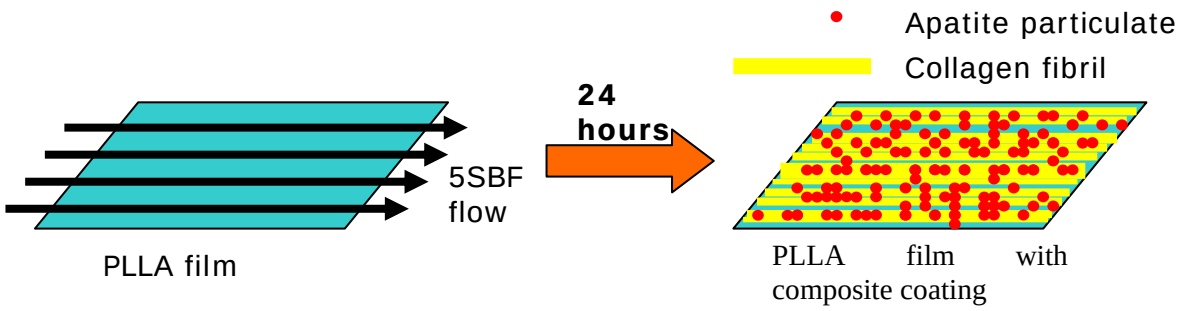

Figure 6.1 *Schematic of the morphology of apatite/collagen composite coating in the flowing condition*

6.2.5 Controlling the apatite/collagen ratio in the composite coating

The apatite/collagen ratio may be controlled to be more similar to that of natural bone by varying the collagen concentration of 5SBFC.

REFERENCES

Abe Y, Kokubo T, Yamamuro T. Apatite coating on ceramics, metals and polymers utilizing a biological process. J Mat Sci Mater Med 1990; 1:233–238.

Agarwala MK, Jamalabad VR, Langrana NA, Safari A, Whalen PJ, Danforth SC. Structural quality of parts processed by fused deposition. Rapid Prototyping J 1996; 2(4):4-19.

Agrawal CM, Ray RB. Bioderadable polymeric scaffolds for musculoskeletal tissue engineering. J Biomed Mater Res 2001; 55:141-150.

Akao M, Sakatsume M, Aoki H, Takagi T, Sasaki S. *in vitro* mineralization in bovine tooth germ cell cultured with sintered hydroxyapatite. J Mater Sci Mater Med 1993; 4(6):569-574.

Amstein CF, Hartman PA. Adaptation of plastic surfaces for tissue culture by glow discharge. J Clin Microbiol 1975; 2(1):46-54.

Anderson HC, Hsu HHT, Raval P. The mechanism of bone induction and bone healing byhuman osteosarcoma cell extracts. Clin Orthop 1995; 313:129-134.

Andrianarivo AG, Robinson JA, Mann KG, Tracy RP. Growth on type I collagen promotes expression of the osteoblastic phenotype in human osteosarcoma MG-63 cells. J Cell Physiol 1992; 153:256–265.

Andriano KP, Tabata Y, Ikada Y, Heller J. *In vitro* and *in vivo* comparison of bulk andsurface hydrolysis in absorbable polymer scaffolds for tissue engineering. J Biomed Mater Res 1999; 48:602-612.

Asahina I, Seto I, Oda M, Marukawa E, Imranul AM, Enomoto S. Bone Engineering. Em squared, Toronto, 1999:526.

Asahina I, Watanabe M, Sakurai N, Mori M, Enomoto S. Repair of bone defect in primate mandible using a bone morphogenetic protein (BMP)-hydroxyapatite-collagen composite. J Med Dent Sci 1997; 44:63-70.

Baksh D, Davies JE. Design strategies for 3-dimensional *in vitro* bone growth in tissue engineering scaffolds. In: Davies JE, editor. Bone Engineering. Em squared, Toronto, 2000:488-495.

Bansil R, Liao G. Kinetics of spinodal decomposition in homopolymer solutions andgels. Trends Polym Sci 1997; 5(5):146-154.

Baier RE, Meyer AE. Implant surface preparation. Int J Oral Maxillofac Implants 1988; 3:9-20.

Baron R. Primer on the Metabolic Bone Diseases and Disorders of Mineral Metabolism. Raven Press, New York, 1993:3.

Barrera DA, Zylstra E, Lansbury PT, Langer R. Synthesis and RGD peptide modification of a new biodegradable copolymer (polylactic acid-co-lysine). J Am Chem Soc 1993; 115:11010-11011.

Barrere F, Layrolle P, van Blitterswijk CA, de Groot K. Biomimetic coatings on titanium: a crystal growth study of octacalcium phosphate. J Mater Sci Mater Med 2001; 12:529–534.

Barrere F, Blitterswijk CA, Groot K, Layrolle P. Influence of ionic strength and carbonate on the Ca–P coating formation from SBF×5 solution. Biomaterials 2002(a); 23(9):1921–1930.

Barrere F, Blitterswijk CA, Groot K, Layrolle P. Nucleation of biomimetic Ca–P coatings on Ti6Al4V from a SBF×5 solution: influence of magnesium. Biomaterials 2002(b); 23(10):2211–2220.

Barrere F, van der Valk CM, Meijer G, Dalmeijer RA, de Groot K, Layrolle P. Osteointegration of biomimetic apatite coating applied onto dense and porous metal implants in femurs of goats. J Biomed Mater Res 2003; 67B:655-665.

Beaman JJ. Backround and definitions. In: Beamann JJ, Barlow JW, Bourell DL, Crawford RH, Marcus HL, McAlea KP, editors. Solid Free-form Fabrication: a New Direction in Manufacturing. Kluwer Academic Publishers, Boston (USA), 1997:1-20.

Becker D, Geißler U, Hempel U, Bierbaum S, Scharnweber D, Worch H., Wenzel KW. Proliferation and differentiation of rat calvarial osteoblasts on type I collagen-coated titanium alloy. J Biomed Mater Res 2002; 59(3):516-527.

Begley CM, Kleis SJ. The fluid dynamic and shear environment in the NASA/JSC rotating-wall perfused-vessel bioreactor. Biotechnol Bioeng 2000; 70:32–40.

Behravesh E, Yasko AW, Engel PS, Mikos AG. Synthetic biodegradable polymers for orthopaedic applications. Clin Orthop Relat Res 1999; 367 Suppl:S118-129.

Behravesh E, Jo S, Zygourakis K, Mikos AG. Synthesis of in situ cross-linkable macroporous biodegradable poly(propylene fumarate-co-ethylene glycol) hydrogels. Biomacromolecules 2002; 3:374-381.

Bisson I, Kosinski M, Ruault S, Gupta B, Hilborn J, Wurm F, Frey P. Acrylic acid grafting and collagen immobilization on poly(ethylene terephthalate) surfaces for adherence and growth of human bladder smooth muscle cells. Biomaterials 2002; 23(15):3149-3158.

Black J, Hastings G. Handbook of Biomaterial Properties. Chapman & Hall, London, 1998.

Blau HM, Brazelton TR, Weimann JM. The evolving concept of a stem cell: entity or function? Cell 2001; 105:829-841.

Boo JS, Yoichi Y, Yasuhiro O, Yoshitaka H, Kunihiko O, Ken-Ichiro H, Takafumi Y; Yasuo S, Minoru U. Tissue-engineered bone using mesenchymal stem cells and a biodegradable scaffold. J Craniofacial Surg 2002; 13:231-239.

Bostrom MPG, Lane JM, Berberian WS, Missri AAE, Tomin E, Weiland A. Immunolocalization and expression of bone morphogenetic proteins 2 and 4 in fracture healing. J Orthop Res 1995; 13:357-367.

Bostrom MP, Camacho NP. Potential role of bone morphogenetic proteins in fracture healing. Clin Orthop Rel Res 1998; 355 Suppl:S274-282.

Bostrom MP, Saleh KJ, Einhorn TA. Osteoinductive growth factors in preclinical fracture and long bone defects models. Orthop Clin North Am 1999; 30:647–58.

Botchwey EA, Pollack SR, Levine EM, Laurencin CT. Bone tissue engineering in a rotating bioreactor using a microcarrier matrix system. J Biomed Mater Res 2001; 55:242–253.

Boyan BD, Hummert TW, Dean DD, Schwartz Z. Role of material surfaces in regulating bone and cartilage cell response. Biomaterials 1996; 17:137–146.

Brizzolara D, Cantow HJ, Diederichs K, Keller E, Domb AJ. Mechanism of the stereocomplex formation between enantiomeric poly(lactide)s. Macromolecules 1996; 29:191–197.

Burg KJ, Porter S, Kellam JF. Biomaterial developments for bone tissue engineering. Biomaterials 2000; 21:2347-2359.

Burkersroda F v, Schedl L, Gopferich A. Why degradable polymers undergo surface erosion or bulk erosion. Biomaterials 2002; 23:4221-4231.

Cai KY, Yao KD, Lin SB, Yang Z, Li X, Xie H, Qing T, Gao L. Poly(D,L-lactic acid) surfaces modified by silk fibroin: effects on the culture of osteoblast *in vitro*. Biomaterials 2002(a); 23: 1153-1160.

Cai KY, Yao KD, Cui YL, Yang ZM, Li XQ, Xie.HQ, Qing TW, Gao LB. Influence of different surface modification treatments on poly(D,L-lactic acid) with silk fibroin and their effects on the culture of osteoblast *in vitro*. Biomaterials 2002(b); 23:1603-1611.

Cai KY, Yao KD, Cui YL, Lin SB, Yang ZM,. Li XQ, Xie HQ, Qing TW, Luo J. Surface modification of poly (D,L-lactic acid) with chitosan and its effects on the culture of osteoblasts *in vitro*. J Biomed Mater Res 2002(c); 60:398-404.

Camacho NP, West P, Torzilli PA, Mendelsohn R. FTIR microscopic imaging of collagen and proteoglycan in bovine cartilage. Biopolymers 2001; 62(1):1-8.

Canalis E, Agnusdei D. Insulin-like growth factors and their role in osteoporosis. Calcif Tissue Int 1996; 58:133-134.

Caplan AI. The mesengenic process. Clin Plast Surg 1994; 21:429-435.

Carrier RL, Papadaki M, Rupnick M, Schoen FJ, Bursac N, Langer R, Freed LE, Vunjak-Novakovic G. Cardiac tissue engineering: cell seeding, cultivation parameters, and tissue construct characterization. Biotechnol Bioeng 1999; 64:580–589.

Celic S, Katayama Y, Chilco PJ, Martin TJ, Findlay DM. Type I collagen influence on gene expression in UMR 106-06 osteoblast-like cells is inhibited by genistein. J Endocrinol 1998; 158:377–388.

Chapekar MS. Tissue engineering: challenges and opportunities. J Biomed Mater Res 2000; 53:617-620.

Chen D, Chen H, Feng JQ, Windle JJ, Koop BA, Harris MA, Bonewald LF, Boyce BF, Wozney JM, Mundy GR, Harris SE. Osteoblast cell lines derived from a transgenic mouse containing the osteocalcin promoter driving SV40T-antigen. Mol Cell Differ 1995; 3:193-212.

Chen G, Ushida T, Tateishi T. A biodegradable hybrid sponge nested with collagen microsponges. J Biomed Mater Res 2000; 51:273-279.

Chen G, Ushida T, Tateishi T. Poly(DL-lactic-co-glycolic acid) sponge hybridized with collagen microsponges and deposited apatite particulates. J Biomed Mater Res 2001; 57(1):8-14.

Chen CC, Chueh JY, Tseng H, Huang HM, Lee SY. Preparation and characterization ofbiodegradable PLA polymeric blends. Biomaterials 2003; 24:1167-1173.

Chesmel KD, Clark CC, Brighton CT, Black J. Cellular response to chemical and morphologic aspects of biomaterial surfaces. II. The biosynthetic and migratory response of bone cell population. J Biomed Mater Res 1995; 29:1101-1110.

Chim H, Ong JL, Schantz JT, Hutmacher DW, Agrawal CM. Efficacy of glow discharge gas plasma treatment as a surface modification process for three-dimensional poly(D,L-lactide) scaffolds. J Biomed Mater Res(Part A) 2003; 65:327-335.

Choi YS, Hong SR, Lee YM, Song KW, Park MH, Nam YS. Studies on gelatin-containing artificial skin: II. Preparation and characterization of cross-linked gelatin-hyaluronate sponge. J Biomed Mater Res 1999; 48:631-639.

Chou YF, Chiou WA, Xu YH, Dunn JCY, Wu BM. The effect of pH on the structural evolution of accelerated biomimetic apatite. Biomaterials 2004; 25(22):5323-5331.

Choueka J, Charvet JL, Koval KJ, Alexander H, James KS, Hooper KA, Kohn J. Canine bone response to tyrosine-derived polycarbonates and poly(L-lactic acid). J Biomed Mater Res 1996; 31:35-41.

Cima LG, Vacanti JP, Vacanti C, Ingber D, Mooney D, Langer R. Tissue engineering by cell transplantation using degradable polymer substrates. J Biom Eng 1991; 113:143-151.

Clemens JAM, Wolke JGC, Klein CPAT, de Groot K. Fatigue behavior of calcium phosphate coatings with different stability under dry and wet conditions. J Biomed Mater Res 1999; 48:741–748.

Cohen S, Bano MC, Cima LG, Allcock HR, Vacanti JP, Vacanti CA, Langer R. Design of synthetic polymeric structures for cell transplantation and tissue engineering. Clin Mater 1993; 13:3-10.

Cook AD, Hrkach JS, Gao NN, Johnson IM, Pajvani UB, Cannizzaro SM, Langer R. Characterization and development of RGD-peptide-modified poly(lactic acid-co-lysine) as an interactive, resorbable biomaterial. J Biomed Mater Res 1997; 35:513-523.

Cooke MN, Fisher JP, Dean D, Rimnac C, Mikos AG. Use of stereolithography to manufacture critical-sized 3D biodegradable scaffolds for bone ingrowth. J Biomed Mater Res 2003; 64B:65-69.

Cowin SC. Mechanics of Materials. In: Cowins SC, editor. Bone Mechanics. CRC Press, Boca Raton, 1989:15-42.

Croteau S, Rauch F, Silvestri A, Hamdy RC. Bone morphogenetic proteins in orthopaedics: from basic science to clinical practice. Orthopaedics 1999; 22:686-695.

Curtis AS, Forrester JV, McInnes C, Lawrie F. Adhesion of cells to polystyrene surfaces. J Cell Biol 1983; 97:1500-1506.

Curtis AS, McMurray H. Conditions for fibroblast adhesion without fibronectin. J Cell Sci 1986; 86:25-33.

Dhert WJ. Retrieval studies on calcium phosphate-coated implants. Med Prog Technol 1994; 20:143-154.

Doi Y, Horiguchi T, Moriwaki Y, Kitago T, Kajimoto T, Iwayama Y. Formation of apatite–collagen complexes. J Biomed Mater Res 1996; 31:43–49.

Ducheyne P. Bioactive ceramics. J Bone Joint Surg 1994; 76B:861-862.

El-Hadi A, Schnabel R, Straube E, Uller GM, Henning S. Correlation between degree of crystallinity, morphology, mechanical properties and biodegradation of poly(3-hydroxyalkanoate) PHAs and their blends. Polym Test 2002; 21:665-674.

Elliot JC. Structure and chemistry of the apatite and other calcium orthophosphates. Elsevier, Amsterdam(The Netherlands), 1994.

Felicity RAJR, Richard OCO. Bone tissue engineering: hope vs hype. Biochem Biophys Res Commun 2002; 292(1):1-7.

Fisher JP, Holland TA, Dean D, Engel PS, Mikos AG. Synthesis and properties of photocrosslinked poly(propylene fumarate) scaffolds. J Biomater Sci Polym Ed 2001; 12:673-687.

Fisher JP, Vehof JW, Dean D, van der Waerden JP, Holland TA, Mikos AG, Jansen JA. Soft and hard tissue response to photocrosslinked poly(propylene fumarate) scaffolds in a rabbit model. J Biomed Mater Res 2002; 59:547-556.

Franceschi RT, Xiao G. Regulation of the osteoblast-specific transcription factor, Runx2: responsiveness to multiple signal transduction pathways. J Cell Biochem 2003; 88:446-454.

Freed LE, Vunjak-Novakovic G. Culture of organized cell communities. Adv Drug Deliv Rev 1998; 33:15-30.

Friedman CD, Costantino PD, Takagi S, Chow LC. BoneSource hydroxyapatite cement: a novel biomaterial for craniofacial skeletal tissue engineering and reconstruction. J Biomed Mater Res (Appl Biomater) 1998; 43:428-432.

Fung YC. Biomechanics: Mechanical Properties of Living Tissues. Springer, New York, 1994.

Fujibayashi S, Neo M, Kim HM, Kokubo T, Nakamura T. A comparative study between *in vivo* bone ingrowth and *in vitro* apatite formation on $Na_2O–CaO–SiO_2$ glasses. Biomaterials 2003; 24(8):1349-1356.

Furumatsu T, Shen ZN, Kawai A, Nishida K, Manabe H, Oohashi T, Inoue H, Ninomiya Y. Vscular endothelial growth factor principally works as the main angiogenic factor in the early stage of human osteoblastogenesis. J Biochem 2003; 133:633-639.

Gao TJ, Lindholm TS, Kommonen B, Ragni P, Paronzini A, Lindholm TC. Enhanced healing of segmental tibial defects in sheep by a composite bone substitute composed of tricalcium phosphate cylinder, bone morphogenetic protein, and type IV collagen. J Biomed Mater Res 1996; 32:505-512.

Gao T, Aro HT, Ylänen H, Vuorio E. Silica-based bioactive glasses modulate expression of bone morphogenetic protein-2 mRNA in Saos-2 osteoblasts *in vitro.* Biomaterials 2001; 22(12):1475-1483.

Geissler U, Hempel U, Wolf C, Scharnweber D, Worch H, Wenzel KW. Collagen type I coating of Ti6Al4V promotes adhesion of osteoblasts. J Biomed Mater Res 2000; 51:752-760.

Gibbons D. Tissue response to resorbable synthetic polymers. In: Plank H, Dauner M, Renardy M, editors. Degradation Phenomena on Polymeric Biomaterials. Springer-Verlag, New York, 1992:97-104.

Giordano RA, Wu BM, Borland SW, Cima LG, Sachs EM, Cima MJ. Mechanical properties of dense polylactic acid structures fabricated by three dimensional printing. J Biomater Sci Polym Ed 1996; 8:63-75.

Gitelman SE, Kobrin MS, Ye JQ, Lopez AR, Lee A, Derynck R. Recombinant Vgr-1/BMP-6 expressing tumors induce fibrosis and endochrondral bone formation *in vivo*. J Cell Biol 1994; 126:1595-1609.

Golbus RK, Doty SB, Lull JC, Holmuhamedov E, Humphries MJ, Damsky CH. Fibronectin is a survival factor for differentiated osteoblasts. J Cell Sci 1998; 111: 1385-1393.

Goldstein AS, Juarez TM, Helmke CD, Gustin MC, Mikos AG. Effect of convection on osteoblastic cell growth and function in biodegradable polymer foam scaffolds. Biomaterials 2001; 22:1279-1288.

Goodman I, Rhys J. Polycarbonates. In: Rhys JA, Goodman I, editors. Polyesters. Elsevier, New York, 1965:141-153.

Gotoh Y, Tsukada M, Minoura N, Imai Y. Synthesis of poly(ethylene glycol)–silk fibroin conjugates and surface interaction between L-929 cells and the conjugates. Biomaterials 1997; 18:267-71.

Govinden R, Bhoola KD. Genealogy, expression, and cellular function of transforming growth factor-β. Pharmacol Ther 2003; 98:257-265.

Gu YW, Khor KA, Cheang P. Bone-like apatite layer formation on hydroxyapatite prepared by spark plasma sintering (SPS). Biomaterials 2004; 25(18):4127-4134.

Guo L, Huang M, Heng Y, Davie JE, Zhang X. Structure and composition comparison of bone mineral and apatite layers formed *in vitro*. Key Eng Mater 2001; 192-195:187-190.

Hammerle CH, Olah AJ, Schmid J, Fluckiger L, Gogolewski S, Winkler JR. The biological effect of natural bone mineral on bone neoformation on the rabbit skull. Clin Oral Implants Res 1997; 8:198-207.

Harris LD, Kim BS, Mooney DJ. Open pore biodegradable matrices formed with gas foaming. J Biomed Mater Res 1998; 42:396-402.

Heath CA. Cells for tissue engineering. Trends Biotech 2000; 18:17-19.

Hench LL. Bioceramics: from concept to clinic. J Am Ceram Soc 1991; 74:1487-1510.

Hench LL. Bioceramics: From concept to clinic. Am Ceram SOC Bull 1993; 72:93-98.

Hench LL, Wilson J. An introduction to bioceramics. World Scientific, Singapore, 1993.

Hesby RM, Haganman CR, Stanford CM. Effects of radiofrequency glow discharge on impression material surface wettability. J Prosthet Dent 1997; 77:414–422.

Hill PA, Orth M. Bone remodeling. Brit J Orthod 1998; 25:101-107.

Hollahan JR,Stafford BB,Falb RD,Payne ST. Attachment of amino groups to polymers surfaces by radiofrequency plasmas. J Appl Polym Sci 1969; 13:807-816.

Hollinger JO, Battistone GC. Biodegradable bone repair materials. Clin Orthop Rel Res 1986; 207:290-305.

Hu YH, Winn SR, Krajbich I, Hollinger JO, Porous polymer scaffolds surface-modified with arginine-glycine-aspartic acid enhance bone cell attachment and differentiation *in vitro.* J Biomed Mater Res 2003; 64A:583-590.

Hubbell JA. Principles of Tissue Engineering. Academic press, USA, 1997.

Hubbell JA, Bioactive biomaterials. Curr Opin Biotechnol 1999; 10:123-129.

Hull D, Clyne TW. An introduction to composite materials. Cambridge University Press, Cambridge, 1996.

Hunt TR, Schwappach JR, Anderson HC. Healing of segmental defect in the rat femur with use of an extract from a cultured human osteosarcoma cell-line (Saos-2). J Bone Jt Surg [Am] 1996; 78:41-48.

Hutmacher DW. Scaffolds in tissue engineering bone and cartilage. Biomaterials 2000; 21:2529-2543.

Ibim SE, Uhrich KE, Attawia M, Shastri VR, El-Amin SF, Bronson R, Langer R, Laurencin CT. Preliminary *in vivo* report on the osteocompatibility of poly(anhydride-co-imides) evaluated in a tibial model. J Biomed Mater Res 1998(a); 43:374–379.

Ibim SM, Uhrich KE, Bronson R, El-Amin SF, Langer RS, Laurencin CT. Poly(anhydride-co-imides): *in vivo* biocompatibility in a rat model. Biomaterials 1998(b); 19:941–951.

Ikada Y, Shikinami Y, Hara Y, Tagawa M, Fukada E. Enhancement of bone formation by drawn poly(L-lactide). J Biomed Mater Res 1996; 30:553-558.

Jadlowiec JA, Celil AB, Hollinger JO. Bone tissue engineering: recent advances and promising therapeutic agents. Expert Opin Biol Ther 2003; 3:409-423.

Jeschke B, Meyer J, Jonczyk A, Kessler H, Adamietz P, Meenen NM, Kantlehner M, Goepfert C, Nies B. RGD-peptides for tissue engineering of articular cartilage. Biomaterials 2002; 23:3455-3463.

Johnson EE, Urist MR, Finerman GA. Repair of segmental defects of the tibia with cancellous bone grafts augmented with human bone morphogenetic protein. A preliminary report. Clin Orthop Relat Res 1988; 236:249-257.

Juni K, Nakano M. Poly(hydroxy acids) in drug delivery. Crit Rev Ther Drug Carrier Syst 1987; 3(3):209-232.

Karp JM, Shoichet MS, Davies JE. Bone formation on two-dimensional poly(DL-lactide-coglycolide) (PLGA) films and three-dimensional PLGA tissue engineering scaffolds *in vitro*. J Biomed Mater Res 2003; 64A:388-396.

Kasemo B, Lausmaa J. Surface science aspects on inorganic biomaterials. CRC Crit Rev Biocomp 1986; 2:335-380.

Katti DS, Lakshmi S, Langer R, Laurencin CT. Toxicity, biodegradation and elimination of polyanhydrides. Advanced Drug Delivery Reviews 2002; 54:933-961.

Kikuchi M, Suetsugu Y, Tanaka J. Preparation and mechanical properties of calcium phosphate/copoly-L-lactide composites. J Mater Sci Mater Med 1997; 8:361-364.

Kirker-Head CA, Gerhart TN, Armstrong R, Schelling SH, Carmel LA. Healing bone using recombinant human bone morphogenetic protein 2 and copolymer. Clin Orthop Rel Res 1998; 349:205-217.

Koempel JA, Patt BS, O'Grady K, Wozney J, Toriumi DM. The effect of recombinant human bone morphogenetic protein-2 on the integration of porous hydroxyapatite implants with bone. J Biomed Mater Res 1998; 41:359-363.

Kohn J, Langer R. Poly(iminocarbonates) as potential biomaterials. Biomaterials 1986; 7:146–182.

Kokubo T. Formation of biologically active bone-like apatite on metals and polymers by a biomimetic process. Thermochim Acta 1996; 280-281:479-490.

Kokubo S, Fujimotob R, Yokotac S, Fukushimaa S, Nozakia K, Takahashia K, Miyataa K. Bone regeneration by recombinant human bone morphogenetic protein-2 and a novel biodegradable carrier in a rabbit ulnar defect model. Biomaterials 2003; 24:1643-1651.

Kruyt MC, JD de Bruijn, CE Wilson, FC Oner,. CA van Blitterswijk, A. J. Verbout, WJ Dhert. Viable osteogenic cells are obligatory for tissue-engineered ectopic bone formation in goats. Tissue Eng 2003; 9:327-336.

Kweh SWK, Khor KA, Cheang P. Plasma-sprayed hydroxyapatite (HA) coatings with flame-spheroidized feedstock: microstructure and mechanical properties Biomaterials 2000; 21:1223-1234.

Langer R, Vacanti JP. Tissue engineering. Science 1993; 260:920-926.

Lappa M. Organic tissue in rotating bioreactors: fluid-mechanical aspects, dynamic growth models, and morphological evolution. Biotechnol Bioeng 2003; 84:518-532.

Laurencin CT, Attawia MA, Lu LQ, Borden MD, Lu HH, Gorum WJ, Lieberman JR. Poly(lactide-co-glycolide)/hydroxyapatite delivery of BMP-2-producing cells: a regional gene therapy approach to bone regeneration. Biomaterials 2001; 22(11): 1271-1277.

Lee SJ, Lim GJ, Lee JW, Atala A, Yoo JJ. *In vitro* evaluation of a poly(lactide-co-glycolide)–collagen composite scaffold for bone regeneration. Biomaterials 2006; 27:3466-3472.

LeGeros RZ. Properties of Osteoconductive Biomaterials: Calcium Phosphates. Clin Orthop Rel Res 2002; 395:81-98.

Leng Y, Chen J, Qu S. TEM study of calcium phosphate precipitation on HA/TCP ceramics. Biomaterials 2003; 24:2125-2131.

Leong KF, Cheah CM, Chua CK, Biomaterials Solid freeform fabrication of three-dimensional scaffolds for engineering replacement tissues and organs 2003; 24: 2363-2378.

Levine JP, Bradley J, Turk AE, Ricci JL, Benedict JJ, Steiner G. Bone morphogenetic protein promotes vascularization and osteoinduction in preformed hydroxyapatite in the rabbit. Ann Plastic Surg 1997; 39:158-68.

Li C, Kohn J. Synthesis of poly(iminocarbonates): Degradable polymers with potential applications as disposable plastics and as biomaterials. Macromolecules 1989; 22:2029–2036.

Li S, Zheng Z, Liu Q, de Wijn JR, de Groot K. Collagen/apatite coating on 3-dimensional carbon/carbon composite J Biomed Mater Res 1998; 40(4):520-529.

Li Y, Ma T, Kniss DA, Lasky LC, Yang ST. Effects of filtration seeding on cell density, spatial distribution, and proliferation in nonwoven fibrous matrices. Biotechnol Prog 2001; 17:935–944.

Li JZ, Hankins GR, Kao C, Li H, Kammauff J, Helm GA. Osteogenesis in rats induced by a novel recombinant helper-dependent bone morphogenetic protein-9 (BMP-9) adenovirus. The Journal of Gene Medicine 2003(a); 5(9):748-756.

Li P. Biomimetic nano-apatite coatingcapable of promoting bone ingrowth. J Biomed Mater Res (Part A) 2003; 66:79-85.

Li S, de Wijn JR, Li J, Layrolle P, de Groot K. Macroporous Biphasic Calcium Phosphate Scaffold with High Permeability/Porosity Ratio. Tissue Eng 2003; 9:535-548.

Liefeith K, Sauberlich S, Frant M, Klee D, Richter EJ, Hocker H, Spiekermann H. Characterization of the properties of differently modified titanium surfaces for dental implantology. 1: Methods for surface analysis. Biomed Tech 1998; 43(11):330-335.

Lincks J, Boyan BD, Blanchard CR, Lohmann CH, Liu Y. Response of MG63 osteoblast-like cells to titanium and titanium alloy is dependent on surface roughness and composition. Biomaterials 1998; 19:2219–2232.

Linhart W, Peters F, Lehmann W, Schwarz K, Schilling AF, Amling M, Rueger JM, Epple M. Biologically and chemically optimized composites of carbonated apatite and polyglycolide as bone substitution materials. J Biomed Mater Res 2001; 54(2):162-171.

Liu GJ, Miyaji F, Kokubo T, Takadama H, Nakamura T, Murakami A. Apatite-organic polymer composites prepared by a biomimetic process: Improvement in adhesion of the apatite layer to the substrate by ultraviolet irradiation. J Mater Sci Mater Med 1998; 9:285–290.

Liu X, Smith L, Wei G, Won Y, Ma PX. Surface Engineering of Nano-Fibrous Poly(L-Lactic Acid) Scaffolds via Self-Assembly Technique for Bone Tissue Engineering. J Biomed Nanotech 2005; 1:54–60.

Lo H, Ponticiello MS, Leong KW. Fabrication of controlled release biodegradable foams by phase separation. Tissue Eng 1995; 1:15–28.

Lo H, Kadiyala S, Guggino E, Leong KW. Poly(L-lactic acid) foams with cell seeding and controlled-release capacity. J Biomed Mater Res 1996; 30:475–484.

Loty C, Sautier JM, Boulekbache H, Kokubo T, Kim HM, Forest N. *In vitro* bone formation on a bone-like apatite layer prepared by a biomimetic process on a bioactive glass-ceramic. J Biomed Mater Res 2000; 49(4):423-434.

Lovell TP, Dawson EG, Nilsson OS, Urist MR. Augmentation of spinal fusion with bone morphogenetic protein in dogs. Clin Orthop 1989; 243:266-274.

Lowe C. Polymers of high melting lactide. US patent 2, 668, 162, 1954.

Lu HH, Kofron MD, El-Amin SF, Attawia MA, Laurencin CT. *In vitro* bone formation using muscle-derived cells: a new paradigm for bone tissue engineering using polymer–bone morphogenetic protein matrices. Biochem Biophys Res Commun 2003; 305:882-889

Lu L, Peter SJ, Lyman MD, Lai HL, Leite SM, Tamada JA, Vacanti JP, Langer R, Mikos AG. *In vitro* degradation of porous poly(L-lactic acid) foams. Biomaterials 2000; 21(15):1595-1605.

Lu X, Leng Y. TEM study of calcium phosphate precipitation on bioactive titanium surfaces. Biomaterials 2004; 25:1779-1786.

Lynch MP, Stein JL, Stein GS, Lian JB. The influence of type I collagen on the development and maintenance of the osteoblast phenotype in primary and passaged rat calvarial osteoblasts: Modification of expression of genes supporting cell growth, adhesion, and extracellular matrix mineralization. Exp Cell Res 1995; 216:35–45.

Mackay AM, Beck SC, Murphy JM, Barry FP, Chichester CO, Pittenger MF. Chondrogenic differentiation of cultured human mesenchymal stem cells from marrow. Tissue Eng 1998; 4:415-428.

Ma PX, Langer R. Fabrication of biodegradable polymer foams for cell transplantation and tissue engineering. In: Yarmush M, Morgan J, editors. Tissue engineering. Humana Press, New Jersey, 1998.

Ma PX, Zhang R. Synthetic nano-scale fibrous extracellular matrix. J Biomed Mater Res 1999; 46(1): 60-72.

Ma PX, Zhang R, Xiao G, Franceschi R. Engineering new bone tissue *in vitro* on highly porous poly(alpha-hydroxyl acids)/hydroxyapatite composite scaffolds. J Biomed Mater Res 2001; 54:284-93.

Ma PX, Zhang R. Microtubular architecture of biodegradable polymer scaffolds J Biomed Mater Res 2001; 56:469-477.

Ma WH. The analysis and application of the mechanism of BMP induction of bone formation in bone rehabilitation. Orthop J Chin 2001; 8(2):167-170.

Ma Z, Gao C, Ji J, Shen J. Protein immobilization on the surface of poly-L-lactic acid films for improvement of cellular interactions. European Polymer Journal 2002; 38:2279-2284.

Ma Z, Gao C, Gong Y, Shen J. Cartilage tissue engineering PLLA scaffold with surface immobilized collagen and basic fibroblast growth factor. Biomaterials 2005; 26:1253-1259.

Madihally SV, Matthew HWT. Porous chitosan scaffolds for tissue engineering. Biomaterials 1999; 20(12):1133-1142.

Maeda H, Kasuga T, Nogami M, Ueda M. Preparation of bonelike apatite composite for tissue engineering scaffold. Sci Tech Adv Mater 2005; 6:48–53.

Malafaya PB, Silva GA, Baran ET, Reis RL. Drug delivery. therapies: General trends and its importance on bone tissue engineering applications. Curr Opin Solid State Mater Sci 2002; 6:283-295.

Maquet V, Jerome R. Design of macroporous biodegradable. polymer scaffolds for cell transplantation. Mater Sci Forum 1997; 250:15-42.

Marchand-Brynaert J, Detrait E, Noiset O, Boxus T, Schneider YJ, Remacle C. Biological evaluation of RGD peptidomimetics, designed for the covalent derivatization of cell culture substrata, as potential promotors of cellular adhesion. Biomaterials 1999; 20:1773-1782.

Marra KG, Szem JW, Kumta PN, DiMilla PA, Weiss LE. *In vitro* analysis of biodegradable polymer blend/hydroxyapatite composites for bone tissue engineering. J Biomed Mater Res 1999; 47:324-35.

Martin I, Padera RF, Langer R, Vunjak-Novakovic G, Freed LE. *In vitro* differentiation of chick embryo bone marrow stromal cells into cartilaginous and bone-like tissues. J Orthop Res 1998; 16:181–189.

Martin I, Wendt D, Heberer M. the role of bioreactors in tissue engineering. TRENDS in Biotechnology 2004; 22:80-86.

Masi L, Franchi A, Santucci M, Danielli D, Arganini L, Giannone V, Formigli L, Benvenuti S, Tanini A, Beghe F, Mian M, Brandi M. Adhesion, growth, and matrix production by osteoblasts on collagen substrata. Calcif Tissue Int 1992; 51:202–212.

Mayr-Wohlfart U, Fiedler J, Günther KP, Puhl W, Kessler S. Proliferation and differentiation rates of a human osteoblast-like cell line (SaOS-2) in contact with different bone substitute materials. J Biomed Mater Res 2001; 57(1):132-139.

Mazariegos GV, Patzer JF 2nd, Lopez RC, Giraldo M, Devera ME, Grogan TA, Zhu Y, Fulmer ML, Amiot BP, Kramer DJ. First clinical use of a novel bioartificial liver support system (BLSS). Am J Transplant 2002; 2:260–266.

Mikos AG, Sarakinos G, Leite SM, Vacanti JP, Langer R. Laminated three-dimensional biodegradable foams for use in tissue engineering. Biomaterials 1993; 14:323–330.

Mikos AG, Thorsen AJ, Czerwonka LA, Bao Y, Langer R, Winslow DN, Vacanti JP. Preparation and characterization of poly(L-lactic acid) foams. Polymer 1994; 35:1068–1077.

Miyaji F, Kim HM, Handa S, Kokubo T, Nakamura T. Bonelike apatite coating on organic polymers: novel nucleation process using sodium silicate solution. Biomaterials 1999; 20:913-919.

Miyamoto S, Takaoka K, Okada T, Yoshikawa H, Hashimoto J, Suzuki S. Evaluation of polylactic acid homopolymers as carriers for bone morphogenetic protein. Clin Orthop Rel Res 1992; 278:274-285.

Miyamoto S, Takaoka K, Okada T, Yoshikawa H, Hashimoto J, Suzuki S. Polylactic acid-polyethylene glycol block copolymer. A new biodegradable synthetic carrier for bone morphogenetic protein. Clin Orthop Relat Res 1993; 294:333-343.

Mooney DJ, Baldwin DF, Suh NP, Vacanti JP, Langer R. Novel approach to fabricate porous sponges of poly(D, L-lactic-coglycolic acid) without the use of organic solvents. Biomaterials 1996; 17:1417–1422.

Morra M, Cassinelli C, Cascardo G, Cahalan P, Cahalan L, Fini M, Giardino R. Surface engineering of titanium by collagen immobilization. Surface characterization and *in vitro* and *in vivo* studies. Biomaterials 2003; 24(25):4639-4654.

Moursi AM, Globus RK, Damsky CH. Interactions between integrin receptors and fibronectin are required for calvarial osteoblast differentiation *in vitro*. J Cell Sci 1997; 110:2187-2196.

Mueller SM, Shortkroff S,Schneider TO, Breinan HA, Yannas IV, Spector M. Meniscus cells seeded in type I and type II collagen–GAG matrices *in vitro*. Biomaterials 1999; 20(8):701-709.

Muggli DS, Burkoth AK, Anseth KS. Crosslinked polyanhydrides for use in orthopedic applications: degradation behavior and mechanics. J Biomed Mater Res 1999; 46:271-278.

Murakami N, Saito N, Takahashi J, Ota H, Horiuchi H, Nawata M, Okada T, Nozaki K, Takaoka K. Repair of a proximal femoral bone defect in dogs using a porous surfaced prosthesis in combination with recombinant BMP-2 and a synthetic polymer carrier. Biomaterials 2003; 24:2153-2159.

Murphy WL, Kohn DH, Mooney DJ. Growth of continuous bonelike mineral within porous poly(lactide-*co*-glycolide) scaffolds *in vitro*. J Biomed Mater Res 1999; 50:50-58.

Murphy WL, Peters MC, Kohn DH, Mooney DJ. Sustained release of vascular endothelial growth factor from mineralized poly(lactide-co-glycolide) scaffolds for tissue engineering. Biomaterials 2000; 21:2521-2527.

Murphy WL, Dennis RG, Kileney JL, Mooney DJ. Salt Fusion: An Approach to Improve Pore Interconnectivity within Tissue Engineering Scaffolds. Tissue Eng 2002; 8:43-52.

Murry E, Provvedini D, Curran D, Catherwood B, Sussman H, Manolagas S. Characterization ofa human osteoblastic osteosarcoma cell line(Saos-2) with high bone alkaline phosphatase activity. J Bone Miner Res 1987; 2:231-238.

Nagano M, Kitsugi T, Nakamura T, Kokubo T, Tanahashi M. Bone bondingability of an apatite-coated polymer produced usinga biomimetic method: a mechanical and histological study *in vivo*. J Biomed Mater Res 1996; 31(4):487-94.

Nam YS, Park TG. Porous biodegradable polymeric scaffolds prepared by thermally induced phase separation. J Biomed Mater Res 1999(a); 47(1):8-17.

Nam YS, Park TG. Biodegradable polymeric microcellular foams by modified thermally induced phase separation method. Biomaterials 1999(b); 20:1783-1790.

Neff JA, Tresco PA, Caldwell KD, Surface modification for controlled studies of cell-ligand interactions. Biomaterials 1999; 20:2377-2393.

Nishizaki K, Tsujigiwa H, Takeda Y, Yoshino T, Maeta M, Fukushima K, Nagatsuka H, Nagai N. Mastoid obliteration by BMP-2/collagen composites: An experimental study using tissue engineering. Am J Otolaryngol 2003; 24:14-18.

Obradovic B, Carrier RL, Vunjak-Novakovic G, Freed LE. Gas Exchange is Essential for Bioreactor Cultivation of Tissue Engineered Cartilage. Biotechnol Bioeng 1999; 63(2):197-205.

Obradovic B, Meldon JH, Freed LE, Vunjak-Novakovic G. Glycosaminoglycan deposition in engineered cartilage: Experiments and mathematical model. AIChE J 2000; 46:1860–1871.

Ohgushi H, Caplan AI. Stem cell technology and bioceramics: from cell to gene engineering. J Biomed Mater Res 1999; 48(6):913-927.

Olmo N, Martín AI, Salinas AJ, Turnay J, Vallet-Regí M, Lizarbe MA. Bioactive sol–gel glasses with and without a hydroxycarbonate apatite layer as substrates for osteoblast cell adhesion and proliferation. Biomaterials 2003; 24:3383-3393.

Ong JL, Lucas LC, Prince CW, Raikar GN. Characterization of ion beam sputter deposited calcium phosphate coatings. In: Wise DL, Trantolo DJ, Altobelli DE, Yaszemski MJ, Gresser JD, Schwartz ER, editors. Encyclopedic Handbook of

Biomaterials and Bioengineering, Part A: Materials. Marcel Dekker, New York, 1995:1565-1581.

Ong JL, Lucas LC. Auger electron spectroscopy and its use for the characterization of titanium and hydroxyapatite surfaces. Biomaterials 1998; 19:455- 464.

Park A, Wu B, Griffith LG. Integration of surface modification and 3D fabrication techniques to prepare patterned poly(Llactide) substrates allowing regionally selective cell adhesion. J Biomater Sci Polym Ed 1998; 9:89-110.

Park JB, Lakes RS. Biomaterials: an Introduction. Plenum Press, New York, 1992.

Park JB, Bronzino JD. Biomaterials Principles and Applications. CRC press, Florida, 2003.

Park YJ, Lee YM, Park SN, Sheen SY, Chung CP, Lee SJ. Platelet derived growth factor releasing chitosan sponge for periodontal bone regeneration. Biomaterials 2000; 21:153-159.

Partridge K, Yang X, Clarke NM, Okubo Y, Bessho K, Sebald W, Howdle SM, Shakesheff KM, Oreffo RO. Adenoviral BMP-2 gene transfer in mesenchymal stem cells: *in vitro* and *in vivo* bone formation on biodegradable polymer scaffolds. Biochem Biophys Res Commun 2002; 292:144-152.

Petite H, Viateau V, Bensaid W, Meunier A, de Pollak C, Bourguignon M, Oudina K, Sedel L, Guillemin G. Tissue-engineered bone regeneration. Nat Biotechnol 2000; 18:959-963.

Peter SJ, Yaszemski MJ, Suggs LJ, Payne RG, Langer R, Hayes WC, Unroe MR, Alemany LB, Engel PS, Mikos AG. Characterization of partially saturated poly(propylene fumarate) for orthopaedic application. J Biomater Sci Polym Ed 1997; 8:893-904.

Peter SJ, Miller MJ, Yasko AW, Yaszemski MJ, Mikos AG. Polymer concepts in tissue engineering. J Biomed Mater Res 1998; 43:422-427.

Pignataro B, Conte E, Scandurra A, Marletta G. Improved cell adhesion to ion beam-irradiated polymer surfaces. Biomaterials 1997; 18:1461-1470.

Pittenger MF. When The Body Can't Heal Itself. Nature 2001; 414:132.

Pouton CW, Akhtar S. Biosynthetic polyhydroxyalkanoates and their potential in drug delivery. Adv Drug Del Rev 1996; 18:133-162.

Pulapura S, Li C, Kohn J. Structure–property relationships for the design of polyiminocarbonates. Biomaterials 1990; 11:666–678.

Puleo DA, Holleran LA, Doremus RH, Bizios R. Osteoblast responses to orthopedic implant materials *in vitro*. J Biomed Mater Res 1991; 25(6):711-723.

Qiu QQ, Ducheyne P, Ayyaswamy PS. Fabrication, characterization and evaluation of bioceramic hollow microspheres used as microcarriers for 3-D bone tissue formation in rotating bioreactors. Biomaterials 1999; 20:989-1001.

Quirk RA, Chan WC, Davies MC, Tendler SJB, Shakesheff KM. Poly(L-lysine)-GRGDS as a biomimetic surface modifier for poly(lactic acid). Biomaterials 2001; 22:865-872.

Ramsey WS, Hertl W, Nowlan ED, Binkowski NJ. Surface treatments and cell attachment. In Vitro 1984; 20(10):802-808.

Rasubala L, Yoshikawa H, Nagata K, Ijima T, Ohishi M. Platelet-derived growth factor and bone morphogenetic protein in the healing of mandibular fractures in rats. Br J Oral Maxillofac Surg 2003; 41:173-178.

Rea SM, Brooks RA, Best SM, Kokubo T, Bonfield W. Proliferation and differentiation of osteoblast-like cells on apatite-wollastonite/polyethylene composites. Biomaterials 2004; 25(18):4503-4512.

Reddi AH. Role of morphogenetic proteins in skeletal tissue engineering and regeneration. Nat Biotechnol 1998a; 16:247-252.

Reddi AH. Initiation of fracture repair by bone morphogenetic proteins. Clin Orthop Relat Res 1998b; 355:66-72.

Rehman I, Bonfield W. Characterization of hydroxyapatite and carbonated apatite by photo acoustic FTIR spectroscopy. J Mater Sci Mater Med 1997; 8:1–4.

Rengachary SS. Bone Morphogenetic Proteins: Basic Concepts. Neurosurg Focus 2002; 13:1-6.

Reusch RN. Low molecular weight complexed poly(3-hydroxybutyrate): a dynamic and versatile molecule *in vivo*. Can J Microbiol 1995; 41:50-54.

Rhee SH, Tanaka J. Hydroxyapatite coating on a collagen membrane by a biomimetic method. J Am Ceram Soc 1998; 81(11):3029-3031.

Ripamonti U, Duneas N. Tissue morphogenesis and regeneration by bone morphogenetic proteins. Plast Reconstr Surg 1998; 101:227-239.

Rivard CH, Chaput C, Rhalmi S, Selmani A. Bio-absorbable synthetic polyesters and tissue regeneration. A study of threedimensional proliferation of ovine chondrocytes and osteoblasts. Ann Chir 1996; 50:651-658.

Rizzi SC, Heath DJ, Coombes AGA, Bock N, Textor M, Downes S. Biodegradable polymer/hydroxyapatite composites: Surface analysis and initial attachment of human osteoblasts. J Biomed Mater Res 2001; 55:475-486.

Robinson BP, Hollinger JO, Szachowicz EH, Brekke J. Calvarial bone repair with porous D,L polylactide. Otolaryngol Head Neck Surg 1995; 112:707-713.

Rocha LB, Goissis G, Rossi MA. Biocompatibility of anionic collagen matrix as scaffold for bone healing. Biomaterials 2002; 23:449-456

Rose FR, Oreffo RO. Bone tissue engineering : hope vs hype. Biochem Biophys Res Commun 2002; 292:1-7.

Ruoslahti E. RGD and other recognition sequences for integrins. Ann Rev Cell Dev Biol 1996; 12:697-723.

Sachs E, Cima M, Williams P, Brancazio D, Cornie J. Threedimensional printing: rapid tooling and prototypes directly from a CAD model. J Eng Industry 1992; 114:481-488.

Sampath TK, Coughlin JE, Whetstone RM, Banach D, Corbett C, Ridge RJ, Ozkaynak E, Oppermann H, Rueger DC. Bovine osteogenic protein is composed of dimers of OP-1 and BMP-2A, two members of the transforming growth factor-beta superfamily. J Biol Chem 1990; 265:13198-13205.

Sampath TK, Maliakal JC, Hauschka PV, Jones WK, Sasak H, Tucker RF. Recombinant human osteogenic protein-1 (hOP-1) induces new bone formation *in vivo* with a specific activity comparable with natural bovine osteogenic protein and stimulates osteoblast proliferation and differentiation *in vitro*. J Biol Chem 1992; 267:20352-20362.

Schakenraad JM, Busscher HJ, Wildevuur CR, Arends J. The influence of substratum surface free energy on growth and spreading of human fibroblasts in the presence and absence of serum proteins. J Biomed Mat Res 1986; 20:773-784.

Schneider AK. Preparation of high molecular weight polyhydroxyacetic ester. US patent 2, 703, 316, 1955.

Schugens C, Maguet V, Grandfils C, Jerome R, Teyssie P. Polylactide macroporous biodegradable implants for cell transplantation. 2. Preparation of polylactide foams by liquid–liquid phase separation. J Biomed Mater Res 1996; 30:449–461.

Schwarz RP, Goodwin TJ, Wolf DA. Cell culture for threedimensional modeling in rotating-wall vessels: an application of simulated microgravity. J Tissue Cult Methods 1992; 14:51-58.

Shapiro L, Cohen S. Novel alginate sponges for cell culture and transplantation. Biomaterials 1997; 18(8):583-590.

Shibutani T, Iwanaga H, Imai K, Kitago M, Doi Y, Iwayama Y. Use of glass slides coated with apatite-collagen complexes for measurement of osteoclastic resorption activity. J Biomed Mater Res 2000; 50(2):153-159.

Shin H, Jo S, Mikos AG. Modulation of marrow stromal osteoblast adhesion on biomimetic oligo[poly(ethylene glycol) fumarate] hydrogels modified with Arg-Gly-Asp peptides and a poly(ethyleneglycol) spacer. J Biomed Mater Res 2002; 61:169-179.

Shinoka T, Ma PX, Shum-Tim D, Breuer CK, Cusick RA, Zund G, Langer R, Vacanti JP, Mayer JE Jr. Tissue-engineered heart valves. Autologous valve leaflet replacement study in a lamb model. Circulation 1996; 94(9):164-168.

Shipman P, Walker A, Bichell D. The Human Skeleton. Harvard University Press, USA, 1985.

Shum AWT, Mak AFT. Morphological and biomechanical characterization of poly(glycolic acid) scaffolds after *in vitro* degradation. Polymer Degradation and Stability 2003; 81:141-149.

Sikavitsas VI, Temenoff JS, Mikos AG. Biomaterials and bone mechanotransduction. Biomaterials 2001; 22:2581-2593.

Sikavitsas VI, Bancroft GN, Mikos AG. Formation of three-dimensional cell/polymer constructs for bone tissue engineering in a spinner flask and a rotating wall vessel bioreactor. J Biomed Mater Res 2002; 62:136-148.

Silverstein RM, Webster FX. Spectrometric Identification of Organic Compounds. John Wiley & Sons Inc., New York, 1998:79–99.

Simon GC, Khatri CA, Wight SA, Wang FW. Preliminary report on the biocompatibility of a moldable, resorbable, composite bone graft consisting of calcium phosphate cement and poly(lactide-co-glycolide) microspheres. J Orthop Res 2002; 20:473-482.

Sittinger M, Bujia J, Rotter N, Reitzel D, Minuth WW, Burmester GR. Tissue engineering and autologous transplant formation: Practical approaches with resorbable biomaterials and new cell culture techniques. Biomaterials 1996; 17:237-242.

Skojdt M, Russell G. Bone cell biology and the regulation of bone turnover. In: Gowen M, editor. Cytokines and Bone Metabolism. CRC Press, Boca Raton, 1992:1-70.

Solchaga LA., Gao J, Dennis JE, Awadallah A, Lundberg M, Caplan AI, Goldberg VM. Treatment of Osteochondral Defects with Autologous Bone Marrow in a Hyaluronan-Based Delivery Vehicle. Tissue Engineering 2002; 8(2):333-347.

Song SW, Torkelson JM. Coarsening effects on microstructure formation in isopycnic polymer solutions and membrane produced via thermally induced phase separation. Macromolecules 1994; 27:6389-6397.

Spector M, Michno MJ, Smarook WH, Kwiakowski GT. A high-modulus polymer for porous orthopedic implants: Biomechanical compatibility of porous implants. J Biomed Mater Res 1978; 12:655-677.

Spitzer R, Perka C, Lindenhayn K, Zippel H. Matrix engineering for osteogenic differentiation of rabbit periosteal cells using α-tricalcium phosphate particles in a three-dimensional fibrin culture. J Biomed Mater Res 2002; 59:690-696.

Suchanek W, Yoshimura M. Processing and properties of hydroxyapatite-based biomaterials for use as hard tissue replacement implants. J Mater Res 1998; 13: 94-117.

Suh H, Hwang YS, Lee JE, Han CD, Park JC. Behavior of osteoblasts on a type I atelocollagen grafted ozone oxidized poly L-lactic acid membrane. Biomaterials 2001; 22:219–230.

Sun JS, Wu SYH, Lin FH. The role of muscle-derived stem cells in bone tissue engineering. Biomaterials 2005; 26: 3953-3960.

Szabo G, Kovacs L, Vargha K, Barabas J, Nemeth ZJ. A new advanced surface modification technique – titanium oxide ceramic surface implants: the background and long−term results. J Long-Term Effects Med Implant 1999; 9 (3):247-259.

Takagi K, Urist MR. The role of bone marrow in bone morphogenetic protein-induced repair of femoral massive diaphyseal defects. Clin Orthop Rel Res 1982:224-231.

Tanahashi M, Yao T, Kokubo T, Minoda M, Miyamoto T, Nakamura T, Yamauro T. Apatite coated on organic polymers by biomimetic process: Improvement in its adhesion to substrate by NaOH treatment. J Appl Biomater 1994(a); 5:339–347.

Tanahashi M, Yao T, Kokubo T, Minoda M, Miyamoto T, Nakamura T, Yamamuro T. Apatite coating on organic polymers by a biomimetic process. J Am Ceram Soc 1994(b); 77:2805–2808.

Tanahashi M, Yao T, Kokubo T, Minoda M, Miyamoto T, Nakamura T, Yamauro T. Apatite coated on organic polymers by biomimetic process: Improvement in adhesion to substrate by HCl treatment. J Mater Sci Mater Med 1995(a); 6:319–326.

Tanahashi M, Yao T, Kokubo T, Minoda M, Miyamoto T, Nakamura T, Yamamuro T. Apatite coated on organic polymers by biomimetic process: Improvement in its adhesion to substrate by glow-discharge treatment. J Biomed Mater Res 1995(b); 29:349-357.

Tancred DC, McCormack BAO, Carr AJ. A synthetic bone implant macroscopically identical to cancellous bone. Biomaterials 1998; 19:2303-2311.

Takahashi T, Tominaga T, Watabe N, Yokobori Jr. AT, Sasada H, Yoshimoto T. Use of porous hydroxyapatite graft containing recombinant human bone morphogenetic protein-2 for cervical fusion in a caprine model. J Neurosurg 1999; 90:224-30.

Tangpasuthadol V, Pendharkar SM, Kohn J. Hydrolytic degradation of tyrosine-derived polycarbonates, a class of new biomaterials. Part I: Study of model compounds. Biomaterials 2000(a); 21:2371-2378.

Tangpasuthadol V, Pendharkar SM, Peterson RC, Kohn J. Hydrolytic degradation of tyrosine-derived polycarbonates, a class of new biomaterials. Part II: 3-yr study of polymeric devices. Biomaterials 2000(b); 21:2379-2387.

Temenoff JS, Lu L, Mikos AG. Bone Engineering. Em squared, Toronto, 1999:454.

Temenoff JS, Mikos AG. Review: Tissue engineering for regeneration of articular cartilage. Biomaterials 2000; 21:431-440.

Teófilo JM, Brentegani LG, Lamano-Carvalho TL. Bone healing in osteoporotic female rats following intra-alveolar grafting of bioactive glass. Archives of Oral Biology 2004; 49:755-762.

Tiselius A, Hjerten S, Levin O. Protein chromatography on calcium phosphate columns. Arch Biochem Biophys 1956; 56:132–155.

Thomson RC, Mikos AG, Beahm E, Lemon JC, Satterfield WC, Aufdemorte TB, Miller MJ. Guided tissue fabrication from periosteum using preformed biodegradable polymer scaffolds. Biomaterials 1999; 20:2007-2018.

Uchida M, Oyane A, Kim HM, Kokubo T, Ito A. Biomimetic coating of laminin-apatite comoposite on titanium metal and its excellent cell-adhesive properties. Adv Mater 2004; 16;1071-1074.

Ueda H, Hong L, Yamamoto M, Shigeno K, Inoue M, Toba T, Yoshitani M, Nakamura T, Tabata Y, Shimizu Y. Use of collagen sponge incorporating transforming growth factor-β1 to promote bone repair in skull defects in rabbits. Biomaterials 2002; 23:1003-1010.

Unsworth BR, Lelkes PI. Growing tissues in microgravity. Nat Med 1998; 4:901–907.

Urist MR, DeLange RJ, Finerman GAM. Bone cell differentiation and growth factors. Science 1983; 220: 680-686.

van de Witte P, Dijkstra PJ, van den Berg JWA, Feijen J. Phase separation processes in polymer solutions in relation to membrane formation. J Membr Sci 1996; 117:1-31.

van Wachem PB, Hendriks M, Blaauw EH, Dijk F, Verhoeven MLPM, Cahalan PT, van Luyn MJA. (Electron) microscopic observations on tissue integration of collagen-immobilized polyurethane. Biomaterials 2002; 23(6):1401-1409.

Varma HK, Yokogawa Y, Espinosa FF, Kawamoto Y, Nishizawa K, Nagata F, Kameyama T. Porous calcium phosphate coating over phosphorylated chitosan film by a biomimetic method. Biomaterials 1999; 20:879-884.

Vunjak-Novakovic G, Obradovic B, Martin I, Bursac PM, Langer R, Freed LE. Dynamic cell seeding of polymer scaffolds for cartilage tissue engineering. Biotechnol Prog 1998; 14:193–202.

Wan YQ, Yang J, Yang JL, Bei JZ, Wang SG. Cell adhesion on gaseous plasma modified poly (l-lactide) surface under shear stress field. Biomaterials 2003; 24:3757-64.

Wan Y, Qu X, Lu J, Zhu C, Wan L, Yang J, Bei J, Wang S. Characterization of surface property of poly(lactide-co-glycolide) after oxygen plasma treatment. Biomaterials 2004; 25(23):4777-4783.

Wang EA, Rosen V, Cordes P, Hewick RM, Kriz MJ, Luxenberg DP, Sibley BS, Wozney JM. Purification and characterization of other distinct bone-inducing factors. Proc Natl Acad Sci USA 1988; 85: 9484-9488.

Wang EA, Rosen V, D'Alessandro JS, Bauduy M, Cordes P, Harada T, Israel DI, Hewick RM, Kerns KM, LaPan P, Luxenberg DH, McQuid D, Moutsatsos IK, Nove J, Wozney JM**.** Recombinant human bone morphogenetic protein induces bone formation. Proc Natl Acad Sci USA 1990; 87:2220-2224.

Wang M. Developing bioactive composite materials for tissue replacement. Biomaterials 2003; 24:2133-2151.

Weinand C, Pomerantseva I, Neville CM, Gupta R, Weinberg E, Madisch I, Shapiro F, Abukawa H, Troulis MJ and Vacanti JP. Hydrogel-β-TCP scaffolds and stem cells for tissue engineering bone. Bone 2006; 38:555-563

Wendt D, Marsano A, Jakob M, Heberer M, Martin I. Oscillating perfusion of cell suspensions through three-dimensional scaffolds enhances cell seeding efficiency and uniformity. Biotechnol Bioeng 2003; 84:205–214.

Whang K, Thomas CH, Healy KE, Nuber GA. A novel method to fabricate bioabsorbable scaffolds. Polymer 1995; 36:837–842.

Wiesmann HP, Nazer N, Klatt C, Szuwart T, Meyer U. Bone tissue engineering by primary osteoblast-like cells in a monolayer system and 3-dimensional collagen gel. J Oral Maxillofac Surg 2003; 61:1455-1462.

Williams DF. Bone Engineering. Em squared, Toronto, 1999:577.

Williams SF, Martin DP, Horowitz DM, Peoples OP. PHA applications: addressing the price performance issue I. Tissue Engineering. Int J Biol Macromol 1999; 25:111-121.

Wozney JM, Rosen V, Celeste AJ, Mitsock LM, Whitters MJ, Kriz RW, Hewick RM, Wang EA. Novel regulators of bone formation: Molecular clones and activities. Science 1988; 242:1528-1534.

Xin R, Leng Y, Chen J, Zhang Q. A comparative study of calcium phosphate formation on bioceramics in vitro and in vivo. Biomaterials 2005; 26:6477-6486.

Xin R, Leng Y, Wang N. In situ TEM examinations of octacalcium phosphate to hydroxyapatite transformation. Journal of crystal growth. 2006; 289:339-344.

Yan WQ, Nakamura T, Kawanabe K, Nishigochi S, Oka M, Kokubo T. Apatite layer-coated titanium for use as bone bonding implants. Biomaterials 1997; 18(17):1185-1190.

Yang J, Bei JZ, Wang SG. Improving cell affinity of poly(d,llactide) film modified by an hydrous ammonia plasma treatment. Polym Adv Technol 2002(a); 13:220-226.

Yang J, Bei JZ, Wang SG. Enhanced cell affinity of poly (D,L-lactide) by combining plasma treatment with collagen anchorage. Biomaterials 2002(b); 23:2607-2614.

Yang S, Leong KF, Du Z, Chua CK. The design of scaffolds for use in tissue engineering. Part I. Traditional factors. Tissue Eng 2001; 7:679-689.

Yang S, Leong KF, Du Z, Chua CK. The design of scaffolds for use in tissue engineering. Part II. Rapid prototyping techniques. Tissue Eng 2002; 8:1-11.

Yang Y, Magnay JL, Cooling L, El HA. Development of a 'mechano-active' scaffold for tissue engineering. Biomaterials 2002; 23:2119-2126.

Yang Y, Porté MC, Marmey P, El Haj AJ, Amédée J, Baquey C. Covalent bonding of collagen on poly(L-lactic acid) by gamma irradiation. Nuclear instruments and methods B 2003; 207:165-174.

Yang XB, Bhatnagar RS, Li S, Oreffo ROC. Biomimetic collagen scaffolds for human bone cell growth and differentiation. Tissue Eng 2004; 10:1148-1159.

Yang SH, Hsu CK, Wang KC, Hou SM, Lin FH. Tricalcium phosphate and glutaraldehyde crosslinked gelatin incorporating bone morphogenetic protein - A viable scaffold for bone tissue engineering. J Biomed Mater Res(Appl Biomater) 2005; 74B:468-475

Yasko AW, Lane JM, Fellinger EJ, Rosen V, Wozney JM, Wang EA. The healing of segmental bone defects, induced by recombinant human bone morphogenetic protein (rhBMP-2). A radiographic, histological, and biomechanical study in rats [published erratum appears in J Bone Jt Surg Am 1992; 74(7):1111]. J Bone Jt Surg Am 1992; 74:659-670.

Yaszemski MJ, Oldham J. B., Lu L, Currier BL. Bone Engineering. Em squared, Toronto, 1994:541.

Yeh LC, Tsai AD, Lee JC. Osteogenic protein-1 (OP-1, BMP-7) induces osteoblastic cell differentiation of the pluripotent mesenchymal cell line C2C12. J Cell Biochem 2002; 87(3):292-304.

Yohko G, Masuhiro T, Norihiko M. Effect of the chemical modification of the arginyl residue in Bombyx mori silk fibroin on the attachment and growth of fibroblasts cells. J Biomed Mater Res 1998; 39:351-357.

Yokogawa Y, Nagata F, Toriyama M. Calcium phosphate formation on highly-oriented collagen fibrils. Chem Lett 1999; 6:527-528.

Yokota S, Sonohara R, Yoshida M, Murai M, Shimokawa S, Fujimoto R, Fukushima S, Kokubo S, Nozaki K, Takahashi K, Uchida T, Yokohama S, Sonobe T. A new recombinant human bone morphogenetic protein-2 carrier for bone regeneration. Int J Pharm 2001; 223:69-79.

Yoon JJ, Park TG. Degradation behaviors of biodegradable macroporous scaffolds prepared by gas foaming of effervescent salts. J Biomed Mater Res 2001; 55:401-408.

Yuan XY, Mak AFT, Li JL. Formation of bone-like apatite on poly(L-lactic acid) fibers by a biomimetic process. J Biomed Mater Res 2001; 57:140-150.

Yuan XY, Mak AFT, Yao K. Comparative observation of accelerated degradation of poly(L-lactic acid) fibres in phosphate buffered saline and a dilute alkaline solution. Poly Degrad Stabil 2002; 75(1):45-53.

Zhang K, Wang Y, Hillmyerb MA, Francisa LF. Processing and properties of porous poly(L-lactide)/bioactive glass composites. Biomaterials 2004; 25(13):2489-2500.

Zhang RY, Ma PX. Porous poly(L-lactic acid)/apatite composites created by biomimetic process. J Biomed Mater Res 1999(a); 45:285-293.

Zhang R, Ma PX. Poly(α-hydroxyl acids)/hydroxyapatite porous composites for bone-tissue engineering. I. Preparation and morphology. J Biomed Mater Res 1999(b); 44:446-455.

Zhang R, Ma PX. Synthetic nano-fibrillar extracellular matrices with predesigned macroporous architectures. J Biomed Mater Res 2000; 52(2):430-438.

Zhang R, Ma PX. Biomimetic polymer/apatite composite scaffolds for mineralized tissue engineering. Macromol Biosci 2004; 4:100-111.

Zhang Y, Ni M, Zhang M, Ratner B. Calcium Phosphate—Chitosan Composite Scaffolds for Bone Tissue Engineering. Tissue Engineering 2003; 9(2):337-345.

Zhao Q, Zhai GJ, Zhao F, Yin Y, Lu WW, Leong JC, Zhang W, Zhang J, Zhang M, Yao K. Preparation and histological evaluation of biomimetic three-dimensional hydroxyapatite/chitosan-gelatin network composite scaffolds. Biomaterials 2002; 23(15): 3227-3234.

Zhao Q, Zhai GJ, Ng DHL, Zhang XZ, Chen ZQ. Surface modification of Al_2O_3 bioceramic by NH^+_2 ion implantation.Biomaterials 1999; 20:595-599.